UNIVERSITY OF CALIFORNIA, SAN DIEGO

# Molecular Mechanisms of B Cell Tolerance, Proliferation and Motility

A dissertation submitted in partial satisfaction of the requirements for the degree of Doctor of Philosophy

in

Molecular Pathology

by

Cecille D. Browne

Committee in charge:

Professor Ananda Goldrath, Chair
Professor Daniel Donoghue, Co-Chair
Professor Jack Bui
Professor Michael David
Professor Elena Pasquale
Professor Robert Rickert

2010

The Dissertation of Cecille D. Browne is approved, and it is acceptable in quality and form for publication on microfilm and electronically:

Co-Chair

Chair

University of California, San Diego

2010

## DEDICATION

This dissertation is first and foremost dedicated to my children, Jasmine and Jonathan. You are my inspiration in life and in my career in science. I wish that you will someday find yourself in a career that you can be passionate about as I am with scientific research. Follow your dreams with utmost integrity and humility.

This work is also dedicated to my husband, Ken, for his love and support throughout the years. Thank you for believing in me.

This work is also for my parents, Purita Dalanon and the late Cesar J. Dalanon for instilling in me the joy of learning and the passion for investigative work. This is also for my sister, Darlene, and brothers, Pierre and Cesar, with whom I shared the challenges we faced as young, new immigrants in this country as well as the joy of accomplishing our dreams despite the odds.



*The pursuit of science, in its purest sense, is soothing to the soul.*

## TABLE OF CONTENTS

## LIST OF FIGURES

## ACKNOWLEDGEMENTS

I thank Dr. Robert Rickert for his unparalleled mentoring style, wisdom, patience and understanding, which have made my graduate experience rich, rewarding and enjoyable. I also thank members of the Rickert lab for their scientific input, their support and friendship. The time I spent in the lab has been fun because of you.

I would like to thank my distinguished committee members, Dr. Elena Pasquale, Dr. Ananda Goldrath, Dr. Michael David, Dr. Daniel Donoghue, Dr. Jack Bui and Dr. Robert Rickert for all your input in my work that helped me bring my projects to fruition.

Chapter 1 of this dissertation is based on the manuscript that has been published in the journal, *Immunity* (Browne CD, Del Nagro CJ, Cato MH, Dengler HS, Rickert RC. Suppression of phosphatidylinositol 3,4,5-trisphosphate production is a key determinant of B cell anergy. Immunity. 2009 Nov 20;31(5):749-60). Contents of this chapter are presented as it may appear in the publication, but supplemented with unpublished figures. Cecille D. Browne is the primary author of this paper. Chris DelNagro is a co-first author of this paper and other contributing authors are Matthew Cato, Sarah Dengler and Robert Rickert.

Chapter 2 of this dissertation is based on the manuscript that has been published in the journal, *Nature Immunology* (Cantor J, Browne CD, Ruppert R, Féral CC, Fässler R, Rickert RC, Ginsberg MH. CD98hc facilitates B cell proliferation and adaptive humoral immunity. Nature Immunology. 2009 Apr;10(4):412-9). Contents of this chapter are presented as it may appear in the publication but supplemented with

unpublished figures. Cecille D. Browne is the second author of this paper. The primary author is Joseph Cantor and other contributing authors are Raphael Ruppert, Chloé Féral, Reinhard Fässler, Robert Rickert and Mark Ginsberg.

Chapter 3 of this dissertation includes work on the role of SHEP1 in B cell differentiation and function. Content of this chapter is being prepared for submission for publication. Cecille will be the primary author of this paper. Supporting authors include Yann Wallez, Melanie Hoefer, Suresh Chintalapati, Matthew Cato, Derek Ostertag, Elena Pasquale and Robert Rickert.

Chapter 4 of this dissertation includes the immune characterization of $\beta_1$integrin conditional mutant mice. Contents of this chapter can serve as a foundation for future investigations regarding the role of integrins in B cells.

Chapter 5 of this dissertation presents a proposal written during my Howard Hughes Med-into-Grad Clinical Training in the area of Rheumatology, Allergy and Immunology under the guidance of clinical mentors Gary S. Firestein, M.D. and Susan E. Sweeney, M.D.

## VITA

### Education

| | |
|---|---|
| 2010 | Ph.D. in Molecular Pathology<br>University of California San Diego, La Jolla, CA |
| 2002 | M.S. in Cell and Molecular Biology<br>San Diego State University, San Diego, CA |
| 1988 | B.S. in Biology<br>San Diego State University, San Diego, CA |

### Work Experience

| | |
|---|---|
| 09/2009 – 03/2010 | Graduate Student<br>Molecular Pathology/Biomedical Sciences Graduate Program, UCSD, La Jolla, CA<br>Laboratory of Dr. Robert Rickert at Sanford\|Burnham Medical Research Institute, La Jolla, CA |

Projects: 1) PTEN in B cell tolerance; 2) SHEP1 in B cell development, differentiation and function; 3) CD98 in B cell function; and 4) Integrin $\beta_1$ in B cell development, differentiation and function.

Completed Clinical Experience in Rheumatology as a *Med-Into-Grad Scholar* through the Howard Hughes Medical Institute-sponsored program from September 2008 to March 2009 under the mentorship of Dr. Gary Firestein, UCSD School of Medicine, Rheumatology Department: Fall Quarter – attended lecture course and Winter Quarter – attended outpatient clinics at UCSD Medical Center Hillcrest and VA Hospital La Jolla, inpatient rounds at UCSD Medical Center Hillcrest and Thornton, Medicine Grand Rounds, Rheumatology case conferences, Rheumatology Grand Rounds, Rheumatology Seminar Series and Immunology Journal Club.

Supervised an undergraduate research intern.
Research Support: NIH Supplemental Grant

| | |
|---|---|
| 01/2002 – 09/2005 | Research Associate/Laboratory Manager<br>Laboratory of Dr. Jeffrey Smith at Sanford\|Burnham Medical Research Institute, La Jolla, CA |

Worked independently on various projects in cancer research. Projects included endothelial cell signaling, the role of fatty acid synthase in breast cancer, prostate

cancer and angiogenesis (discovered the ability of the fatty synthase inhibitor, orlistat, to inhibit VEGFR signaling in endothelial cells), and characterization of enzymatic activities and sequence specificities of metalloproteinases and cathepsins using high throughput phage display. Monitored the financial aspects of the lab (grants and fellowships). Managed Smith laboratory; interafaced with various departments at Burnham Institute to address laboratory needs; monitored and purchased laboratory supplies, computers and equipment; trained new employees; coordinated lab move from one building to another; organized lab.

01/2003 – 12/2004 Adjunct Faculty
San Diego Mesa College, San Diego, CA

Taught the General Biology course (Lecture and Laboratory sessions).

08/1999 – 05/2002 Graduate Student and Teaching Assistant
Master's Program in Cell and Molecular Biology
Laboratory of Dr. Constantine Tsoukas
San Diego State University, San Diego, CA

Characterized the role of the pleckstrin homology domain of Emt/Itk in T cells. Taught Microbiology laboratory courses.

11/1997 – 09/1999 Technical Operations Scientist
Beckman-Coulter Inc. (Hybritech)
San Diego, CA

Responded to technical issues in the manufacture and quality control of medical diagnostics. Investigated and troubleshoot root causes of nonconforming products. Wrote technical reports summarizing investigations/recommendations and presented in weekly interdepartmental forum. Facilitated product transfers from Product Development to Manufacturing. Improved manufacturing processes and revised/wrote manufacturing protocols

08/1990 – 07/1994 Manufacturing Technical Support Analyst
Johnson and Johnson
(Ortho Diagnostics, Inc.), Carpinteria, CA

Responded to technical issues in the manufacture and quality control of medical diagnostics. Designed and conducted shelf-life assays, stress tests, bioburden tests on biologic components of diagnostic products for infectious diseases. Reviewed and revised manufacturing SOPs to improve manufacturing processes. Investigated

technical problems in manufacturing and presented technical reports. Wrote new manufacturing protocols for products transferred from R&D to manufacturing. Coordinated with various organizational teams such as Planning, Manufacturing and Quality Control. Maintained cell and viral stock cultures for manufacturing use. Purified and conjugated large-scale antibody stocks for manufacturing use.

07/1998 - 07/1990 Research Technician
Laboratory of Dr. John Griffin
The Scripps Research Institute, La Jolla, CA

Performed experiments to understand properties of anti-coagulative proteins, Protein C and Protein S, and their endogenous inhibitors in human plasma. Managed laboratory inventory and ordered laboratory supplies.

**Publications**

Browne CD, Wallez Y, Hoefer MM, Chintalapati SK, Cato MH, Ostertag D, Pasquale EB, Rickert RC. SHEP1/CasL signaling axis modulates B cell integrin signaling (in preparation, 2010).

Browne CD, DelNagro CJ, Cato MH, Dengler HS and Rickert RC. Suppression of PI(3,4,5)P3 production is a key determinant of B cell anergy. *Immunity.* 2009 Nov 20;31(5):749-60.

Cantor J, Browne CD, Ruppert R, Féral CC, Fässler R, Rickert RC, Ginsberg MH. CD98hc facilitates B cell proliferation and adaptive humoral immunity. *Nature Immunology,* 2009 Apr;10(4):412-9.

Tsoukas CD, Grasis JA, Browne CD and Ching KA. (2006). Inducible T cell tyrosine kinase (ITK): structural requirements and actin polymerization. *Adv Exp Med Biol*. 2006; 584:29-41.

Browne CD, Hindmarsh EJ and Smith JW. (2006). Inhibition of endothelial cell proliferation and angiogenesis by orlistat, a fatty acid synthase inhibitor. *FASEB J*. 2006 Oct;20(12):2027-35.

Knowles LM, Axelrod F, Browne CD and Smith JW. (2004). Connections Between Fatty Acid Synthase Blockade and Skp2 Regulation. *J Biol Chem* 279:30540-30545.

Grasis JA, Browne CD and Tsoukas CD. (2003). Inducible T cell Tyrosine Kinase Regulates Actin-dependent Cytoskeletal Events Induced by the T cell Antigen Receptor. *Journal of Immunology* 170:3971-3976.

*Acknowledgements* (for experiments I performed during my work as a Research Technician in the laboratory of Dr. John Griffin which appeared in the four manuscripts below):

Heeb MJ, Kojima Y, Rosing J, Tans G and Griffin JH. (1999). C-terminal Residues 621-635 of Protein S Are Essential for Binding to Factor Va. *J Biol Chem* 274:36187-36192.

Heeb MJ, Mesters RM, Tans G, Rosing J and Griffin JH. (1993). Binding of Protein S to Factor Va Associated with Inhibition of Prothrombinase That Is Independent of Activated Protein C. *J Biol Chem* 268:2872-2877.

Heeb MJ, Gruber A and Griffin JH. (1991). Identification of Divalent Metal Ion-dependent Inhibition of Activated Protein C by alpha-2-Macroglobulin and alpha-2-

Antiplasmin in Blood and Comparisons to Inhibition of Factor Xa, Thrombin and Plasmin. *J Biol Chem* 266:17606-17612.

Heeb MJ, Bischoff R, Courtney M and Griffin JH. (1990). Inhibition of Activated Protein C by Recombinant alpha-1-Antitrypsin Variants with Substitution of Arginine or Leucine for Methionine. *J Biol Chem* 265:2365-2369.

**Presentations/Awards/Other**

8th Annual Burnham Science Network Symposium (**poster presentation**), Catamaran Resort Hotel, San Diego, CA, November 2009
35th Annual La Jolla Immunology Conference (**poster presentation**), The Salk Institute, La Jolla, CA, October 2009
UCSD Biomedical Sciences Graduate Program Retreat (**poster presentation**), Warner Springs Ranch, CA, September 2009
Burnham Institute Signal Transduction Retreat (**Session Chair**), The Inn at Rancho Santa Fe, CA July 2009
B cell Club (Scripps, UCSD, Burnham laboratories) (**Speaker**), Scripps Research Institute, La Jolla, CA, July 2009
Inflammatory Group Seminar (Scripps, UCSD, Burnham laboratories) (**Speaker**), Burnham Institute for Medical Research, La Jolla, CA, May 2009
**Howard Hughes Medical Institute** ***Med-Into-Grad Scholar;*** Clinical Experience for graduate students, UCSD School of Medicine, Rheumatology, Allergy and Immunology Department, La Jolla, CA, September 2008 to March 2009
RO1 Program Grant Meeting (**Speaker**), BIMR, La Jolla, CA, November 2008
7th Annual Burnham Science Network Symposium; **Abstract Award Recipient** (**Speaker**), Hilton La Jolla Torrey Pines, La Jolla CA, November 2008
34thAnnual La Jolla Immunology Conference (**poster presentation**), The Salk Institute, La Jolla, CA, October 2008
UCSD Biomedical Sciences Graduate Program Recruitment (**poster presentation**), Burnham Institute for Medical Research, La Jolla, CA, September 2008
**Safety Award Recipient**, The Burnham Institute for Medical Research, August 2008
UCSD Biomedical Sciences Graduate Program Annual Retreat 2008 (**Speaker**), Bahia Hotel, San Diego, CA, May 2008
Completion of 10-week Stem Cell lecture course offered by the Stem Cell Research Consortium and UCSD, January 2008 to March 2008
6th Annual Burnham Science Network Symposium (**poster presentation**), Hilton La Jolla, La Jolla CA, November 2007
Science Olympiad Cell Biology Coach, Poway High School, Poway, CA, October 2007 to present
33rd Annual La Jolla Immunology Conference (**poster presentation**), The Salk Institute, La Jolla, CA, October 2007
The Burnham Institute Signal Transduction Program Retreat (**Speaker**), Bahia Hotel, San Diego, CA, July 2007
B cell Club Seminar (Scripps, UCSD, Burnham) (**Speaker**), The Research Institute of Scripps, La Jolla, CA, June 2007
UCSD Molecular Pathology Graduate Program Retreat 2007 (**poster presentation**), Scripps, La Jolla, CA, April 2007
MBRS/MARC Meeting (**Speaker**), San Diego State University, San Diego, CA, October 2006

Inflammatory Group Seminar (Scripps, UCSD, Burnham laboratories) (**Speaker**), BIMR, La Jolla, CA, March 2006

Consortium for Proteolytic Pathways Retreat (**Speaker**), Half Moon Bay, CA, April 2005

Angiogenesis Program Meeting (**Speaker**), The Burnham Institute, La Jolla, CA, January 2005

Angiogenesis Program Meeting (**Speaker**), The Burnham Institute, La Jolla, CA, December 2003

MBRS/MARC Symposium, San Diego State University (**Speaker**), San Diego, CA, October 2001

SDSU Annual Cell and Molecular Biology Symposium (**poster presentation**), San Diego, CA, May 2001

MBRS/MARC Symposium, San Diego State University (**Speaker**), San Diego, CA, September 2000

American Heart Association Undergraduate Research **Award Recipient**, June 1988

**Technical Skills**

*Biochemistry:* Western blotting; 1D and 2D gel electrophoresis; immunoprecipitation; mass spectrometry (training only); large-scale antibody and enzyme (MMPs) purification; FITC and Biotin antibody conjugation; FPLC; phage ELISA; kinetic assays of enzymatic reactions of proteases (fluorescence); high-throughput phage clone isolation; fatty acid purification and analysis by thin layer chromatography; dialysis; GTPase activity pulldown assay; serum Ig ELISA (high affinity and low affinity Ig).

*Cell:* Flow cytometric characterization of B and T cell compartments of mice; cell culture maintenance of Vero, Hep2, McCoy, MRC-5, MDA-435, ECV, A20, BAL17, HUVEC, Jurkat and WEHI cell lines; thymidine incorporation proliferation assay; $^{14}C$ radiolabeling of fatty acids in cancer cells; transient and stable transfections; BrdU incorporation and CFSE incorporation to assess cell division; cell death ELISA assay; actin polymerization assay, fluorescent microscopy; confocal microscopy; intracellular staining for microscopy and flow cytometry; surface cell staining for microscopy and flow cytometry; immunohistochemistry; hematopoietic stem cell purification and culture; calcium flux.

*Viral/bacterial/other:* RSV, CMV, VZV, HSVI and II, EBV, *Chlamydia*, *Toxoplasma* culture maintenance; MOI determination; viral stock purification; transduction (retroviral); bacteriology; mycoplasma detection assay; phage library screening and phage clone purification.

*Animal:* kidney harvest and fibroblast enrichment from rabbits; human placenta blood vessel isolation for *ex vivo* angiogenesis assay; isolation of lymphoid tissues from mice (bone marrow, blood, spleen, thymus, lymph nodes); (histology) tissue embedding, sectioning and staining; mice immunizations (with NP-KLH, NP-FICOLL, sheep red blood cells, *Streptococcus pneumoniae*); retroorbital bleeding; bone marrow transfers and the generation of bone marrow chimeric mice; *in vivo* BrdU labeling.

*Molecular Biology:* cloning, genotyping; PCR; RT-PCR; microarray assay and analysis; RNA/DNA purification; RNAse protection assay.

*Medical Diagnostics:* use of Beckman Coulter (Hybritech) diagnostic kits for prostate cancer, ferritin, HCG, AFP; use of Johnson and Johnson (Ortho Diagnostics) diagnostic kits for ANA, Chlamydia, HSV, VZV, CMV, RSV.

*Administrative/Others:* Experience in writing/filling out Institutional Review Board form, Animal Protocol Approval Forms, Safety Control Plan and GMP Manufacturing protocols. Familiar with ISO compliance. Competent user of Microsoft Office, FlowJo, ImageQuant, Prism, Genespring (microarray analysis), Adobe Photoshop and Adobe Illustrator.

## ABSTRACT OF THE DISSERTATION

Molecular Mechanisms of B Cell Tolerance, Proliferation and Motility

by

Cecille D. Browne

Doctor of Philosophy in Molecular Pathology

University of California, San Diego, 2010

Professor Ananda Goldrath, Chair

Professor Daniel Donoghue, Co-Chair

Chapter 1 presents our investigation on how BCR signaling is affected by self-reactivity and how the dysregulation of PIP3 generation via the loss of PTEN leads to a break in B cell tolerance. The proliferation of antigen-specific lymphocytes and resulting clonal expansion are essential for adaptive immunity. Chapter 2 discusses the impact of the loss of CD98 on immune responses, particularly on the expansion of antigen-activated B cells. B cells adhere and migrate in response to chemokines in order to function and to differentiate. The molecular events downstream of BCR, S1P and chemokine stimulation leading to integrin activation are not completely understood. In Chapters 3 and 4, the roles of SHEP1 and β1 integrin in B cells are investigated. Finally, Chapter 5 presents a research proposal on the role of the inflammasome in the pathogenesis of gout, which was written during my clinical experience in Rheumatology as a Howard Hughes Med-Into-Grad Scholar.

# GENERAL INTRODUCTION

The immune system is a coordination of multiple cellular functions whose mission is to protect the organism from disease by targeting pathogens, tumor cells or self-reactive immune cells. Hence, a dysfunctional immune system brings about a host of debilitating diseases, generally in the form of an immunodeficiency, or of autoimmunity. The multifaceted nature and the complexities of the immune system make it both a fascinating and perplexing field of study. Thus, I have chosen this field to join the collective efforts of immunology researchers to unfold the blueprint of the immune system and to tame or harness the power of the immune system to resolve immunopathologies, infectious diseases and cancer.

The immune system responds either through the innate immune system or the adaptive immune system. The innate immune response provides a rapid but non-specific response to pathogens. The adaptive immune response offers improved recognition of the pathogen, the ability to recall a pathogen profile, and a sophisticated pathogen-specific attack. Adaptive immune responses involve B and T lymphocytes and even though each cell type employs its own response strategies, these two cell types communicate with each other. T cells, depending on the subset, can recognize antigen presented on MHC molecules, secrete enzymes to neutralize infected or cancer cells, and secrete cytokines to activate B cells. B cells, on the other hand, are involved in the secretion of immunoglobulins, which bind pathogens and making them easier targets for neutralization. The overall goal of this dissertation is to understand cellular and molecular processes governing B cell function and differentiation.

B cells initiate their existence in the bone marrow in direct contact with bone marrow stromal cells. Progenitor B cells (pro-B cells) adhere to stromal cells via the interaction of integrins expressed on pro-B cells with ligands expressed on stromal cells. Pro-B cells differentiate into precursor B cells (pre-B), which express receptors for the cytokine IL7 produced by stromal cells. Proliferation of pre-B cells gives rise to immature B cells. Immature B cells exit the bone marrow and home as transitional B cells (T1/T2) to the spleen, where they undergo further maturation and differentiation.

Mature B cells can be divided into three different subtypes: B1 B cells, marginal zone B cells and follicular B cells. B1 B cells are predominantly found in the peritoneal and pleural cavities. They are self-renewing, produce high levels of low affinity IgM antibodies and respond mainly to carbohydrate antigens. Follicular B cells comprise the majority of the B cell population in secondary lymphoid organs. They are highly diverse in their recognition sites and can respond to both protein and carbohydrate antigens. Marginal zone B cells (MZB) are situated at the periphery of follicles in the spleen. They are similar to follicular B cells in that they do not express CD5, but are more akin to B1 cells in that they respond to carbohydrate antigens. The spleen is an organ that houses and organizes a large number of B cells, T cells, macrophages, and is therefore, a good source of B cells used in our studies. The spleen is divided into red and white pulps, where the white pulp, or follicle, is a highly organized structure containing mostly lymphocytes. A splenic follicle consists of a T cell zone, follicular B cell area and the marginal zone. A histological clue of an ongoing immune response is the appearance of a germinal center. Germinal centers are regions in which B cells undergo affinity maturation and somatic hypermutation. Follicular, marginal zone, transitional and

germinal center B cells, as well as the antibody-secreting plasma cells, display unique markers that we used to distinguish B cell subpopulations.

The first chapter of this dissertation studies the process of B cell tolerance, which is the regulation of self-reactive, therefore potentially pathogenic B cells. A break in B cell tolerance allows these self-reactive B cells to enter the periphery. Cellular and molecular strategies are in place to curtail these B cells. Negative selection is the process by which self-reactive immature B cells in the bone marrow are deleted. Cells that survive negative selection enter the periphery in the state of anergy characterized by low reactivity, low proliferation and low immunoglobulin secretion. The molecular signaling axis downstream of the B cell receptor (BCR) is therefore highly guarded so as not to provoke positive signaling. The engagement of the BCR with antigen leads to the phosphorylation of CD19, which in turn recruits PI3 kinase to the BCR signaling complex. PI3 kinase phosphorylates lipids at the inner leaflet of the plasma membrane to generate PIP3 lipids to which pleckstrin domain-containing molecules, such as Akt and Btk, bind leading to B cell activation. The inositol phosphatase, PTEN, opposes the action of PI3 kinase and is therefore a negative regulator of B cell signaling. The signaling milieu downstream of self-reactive BCRs is not fully understood. Therefore, the goal of this project was to investigate the cellular and molecular consequences of uncontrolled PIP3 generation. We hypothesized that PI3 kinase activity needs to be regulated in self-reactive B cells, and PTEN loss would lead to unmitigated receptor signaling and a subsequent break in B cell tolerance. We found that the loss of PTEN not only recovers proliferative intracellular signaling, but also permits unwanted autoreactive B cell activation in immature and mature compartments.

The second chapter of this dissertation discusses CD98, which is a component of the large neutral amino acid transporter (LAT) that also interacts with integrins. The goal of this project was to study the role of CD98 in B cell clonal expansion and in adaptive immunity. The B cell-specific deletion of the heavy chain of CD98 (CD98hc) resulted in reduced antibody responses due to suppression of B cell proliferation and subsequent plasma cell formation. We found that CD98 supports rapid integrin-dependent proliferation of B cells.

B cell motility is crucial to its function. Studies on B cell motility have steadily increased over the years, yet intracellular molecular events engendering B cell movement are not completely understood. The third chapter of this dissertation centers on the role of SHEP1 in chemokine-, lipid-, and BCR- triggered B cell adhesion and migration. SHEP1 is an adaptor protein that binds another adaptor protein, CasL, and has been implicated in integrin function. We hypothesized that SHEP1 may play a role in signaling processes leading to integrin activation and actin polymerization triggered by the BCR or chemokine receptor engagement. To investigate the role of SHEP1 in B cells, conditional SHEP1 mutants, $SHEP1^{flox/flox}$ CD19cre, were generated. Experimental results presented in this chapter indicate SHEP1 as a key signaling intermediate promoting proper B cell migration and adhesion. In parallel to our study on SHEP1, we also studied the immunological consequences of $\beta_1$ integrin deletion in B cells. Our initial characterization of $\beta_1$ integrin-conditional mutant mice revealed a normal phenotype with moderate perturbations in the transitional and germinal center B cell populations. The lack of a striking phenotype in the absence of $\beta_1$ underscores the plasticity and compensation among the integrin family members.

# CHAPTER 1

## Suppression of PIP3 production is a key determinant of B cell anergy

### 1.1 - Introduction

A large proportion of newly formed B cells express antigen receptors possessing some degree of self-specificity. Hence, the body is challenged with the necessity of providing an ample pool of naïve B cells capable of responding to diverse antigenic challenges, while preventing the release and/or activation of self-reactive B cells. The consequences of self-antigen encounter is governed by B cell receptor (BCR) signaling and can be influenced by additional microenvironmental factors such as T cell-derived factors, B cell-activating factor (BAFF) and Toll-like receptor (TLR) ligands. The nature of the BCR signal has been well described in terms of "signal strength" dictated by the avidity and affinity of the BCR-antigen interaction. However, a biochemical understanding of how these signals result in B cell nonresponsiveness (anergy), rapid apoptosis (deletion) or continued Ig rearrangement (receptor editing) is a subject of continuing investigation.

Chronic exposure to antigen results in BCR desensitization, which is associated with impaired proximal signaling via Syk and Src family kinases, as well as the activation of some, but not all, downstream pathways (1, 2). Similarly, ablation of genes encoding negative or positive regulators of BCR signaling affect threshold-based negative (and positive) selection of emergent B cells (3, 4). In addition to alterations in intracellular signaling, it is apparent that chronic engagement of the BCR also causes a redistribution of the BCR complex, first noted by the selective downregulation of surface IgM and more recently, by evidence for disengagement of Igα/β signaling moieties, as

well as a redistribution of BCR components in membrane microdomains (5,6,7). Importantly, anergy is a reversible process and thus, mechanisms need to be in place to sustain the anergic state (8,9). Anergic B cells exhibit low basal $Ca^{++}$ oscillations sufficient to activate calcineurin-dependent nuclear factor of activated T cells (NFAT), but are refractory to induced $Ca^{++}$ flux (10). ERK activity is also elevated in the basal state, but is poorly induced in anergic B cells (10). Autoantibody production by anergic B cells may be prevented by sustained ERK signaling, as this exerts an inhibitory effect on CpG/TLR9- and LPS/TLR4-dependent plasma cell differentiation (11,12). Activation of JNK and classical NF-κB are also impaired in anergic B cells, but experimental evidence is lacking as to the causative relationship of these pathways to the anergic state. Interestingly, PKCδ has emerged as an important regulator of B cell tolerance through the integration of signals via the BCR as well as BAFF-R (13,14). In particular, nuclear translocation of PKCδ appears to be a critical regulatory event in promoting apoptosis.

In recent years, PI3K signaling has moved to the forefront as a central pathway affecting peripheral B cell maturation. Class IA PI3K molecules are composed of regulatory (p85α, p55α, p50α and p85β) and catalytic (p110α, p110β and p110δ) subunits and phosphorylate $PI(4,5)P_2$ to generate the potent yet transient secondary messenger $PI(3,4,5)P_3$. Gene-targeting studies show similar defects in follicular, B-1 and marginal zone B cell subsets in $p110\delta^{-/-}$ and $p85\alpha^{-/-}$ animals, indicating that the p85α/p110δ heterodimer is the most crucial form in B cells (15). Recruitment of PI3K to the BCR complex requires adaptor proteins bearing YXXM motifs, which upon tyrosine phosphorylation, can bind the SH2 domain of p85. While cytosolic proteins such as the BCAP adaptors may participate, the transmembrane adaptor CD19 appears to be most

crucial in recruiting PI3K (16). In addition to serving as the signal transducing component of the C3d-binding complement receptor CD21 (17), CD19 interacts via noncovalent interactions with components of the BCR complex and thus is rapidly phosphorylated upon BCR crosslinking (18). Accordingly, B cell defects observed in CD19-deficient mice are similar in scope to that observed in $p85\alpha^{-/-}$ and $p110\delta^{-/-}$ mice (15).

PI3K activity is directly antagonized by the D3 inositol phosphatase and tumor suppressor PTEN which, although subject to regulation, is generally highly active and present at the plasma membrane in both resting and activated cells (19). Mice lacking PTEN in B cells possess enlarged marginal zone and B-1 cell compartments and present a "hyper-IgM" phenotype due to enhanced plasma cell differentiation and repressed class switch recombination (20,21,22). Conversely, most defects in peripheral B cell differentiation in mice lacking the PI3K adaptor CD19 are reverted by the dual loss of PTEN (20). Thus, the magnitude and duration of $PI(3,4,5)P_3$ –dependent signaling is tightly regulated to govern B cell growth, survival and differentiation.

We sought to determine if the PI3K pathway modifies tolerogenic signaling in B cells. Using the hen egg lysozyme (HEL) neo-self antigen mouse model, we found that $PI(3,4,5)P_3$ was poorly generated in anergic B cells, resulting in reduced Akt activation. This deficit is due at least in part to impaired tyrosine phosphorylation of CD19 and elevated expression of PTEN. Importantly, $PI(3,4,5)P_3$ repression directly contributes to tolerogenic signaling, as deletion of *Pten* results in failed B cell anergy and enhanced responsiveness to BCR signaling in newly formed B cells. These findings document the

importance of the PI3K pathway in B cell tolerance, which may interface with other BCR independent signaling pathways to govern the tolerogenic state.

## 1.2 - Results

### .1.2.1 - Reduced PI(3,4,5)$P_3$ induction in anergic B cells

Anergic B cells exhibit reduced activation of some BCR signaling pathways. We hypothesized that the restriction of PI(3,4,5)$P_3$ generation may also be a key component of the anergic state. To investigate this possibility, naïve splenic B cells were obtained from MD4 transgenic mice that express an HEL-specific BCR, and were compared with anergic B cells obtained from MD4ML5 mice, which express the MD4 Ig transgene, as well as the ML5 transgene that encodes soluble HEL. Splenocytes from each group were stimulated with anti-IgM F(ab')$_2$, fixed and permeabilized, and PI(3,4,5)$P_3$ levels were assessed in B cells ($B220^+$) by intracellular staining using PI(3,4,5)$P_3$-specific antibodies. Upon stimulation, the level of PI(3,4,5)$P_3$ increased in MD4 B cells, but not in MD4ML5 B cells (Figure 1-1A). The scarcity of PI(3,4,5)$P_3$ would prevent the PH domain-dependent docking and activation of Akt and other PH domain-bearing effectors. To determine if this is the case in MD4ML5 cells, MD4 and MD4ML5 B cells were stimulated, and Akt phosphorylation (S473) was assessed by Western blot. Akt phosphorylation was induced in MD4, but not in MD4ML5 B cells upon stimulation with anti-IgM F(ab')$_2$ (Figure 1-1B, upper panels). Consistent with previous findings (23), Erk activation was basally elevated in MD4ML5 B cells and induced in both MD4 and MD4ML5 B cells (Figure 1-1B, upper panels). Since surface IgM is selectively downmodulated in MD4ML5 B cells, stimulations were also performed with HEL

antigen or anti-Igκ to engage both IgM and IgD receptors. Measurements of $Ca^{++}$ flux or Akt (S473) phosphorylation was measured and found to be consistent with the anti-IgM $F(ab')_2$ data (Supplementary Figure 1-1). It is possible that dampened $PI(3,4,5)P_3$ signaling in splenic MD4ML5 B cells reflects the absence of marginal zone (MZ) B cells, which appear to be hyperresponsive to BCR signaling and are absent in MD4ML5 but present in MD4 mice (24,25). Accordingly, we found reduced BCR-induced Akt activation in MD4 splenic B cells depleted of MZ B cells (Supplementary Figure 1-1C and D). However, Akt activation was impaired in MD4ML5 B cells relative to the follicular B cells from MD4 mice (Supplementary Figure 1-1D). Altogether, these findings indicate that PI3K activity is inhibited and/or inositol phosphatase activity is enhanced in anergic B cells.

### 1.2.2 - CD19 function in B cell anergy

Since the phosphorylation of CD19 upon BCR stimulation leads to the recruitment and activation of PI3K, we assessed whether signaling through CD19 was intact in anergic B cells. MD4 and MD4ML5 B cells were stimulated with anti-IgM $F(ab')_2$, and cell lysates were immunoblotted with antisera specific for one of the phosphorylated tyrosine residues (Y513) required for p85 binding to CD19. CD19 phosphorylation was induced in MD4 B cells, but not in MD4ML5 B cells (Figure 1-1B, lower panels). Surface expression of CD19 was unaltered in MD4ML5 cells (data not shown). This result suggests that in anergic B cells, Src kinase activity or functional association of CD19 with the BCR complex may be impaired.

To determine if impaired CD19 signaling was a cause or a consequence of anergy, MD4 and MD4ML5 mice were crossed onto the $CD19^{-/-}$ background. It has been reported that CD19 promotes positive selection of newly formed Ig-positive B cells (26,27); however, the role of CD19 modulation of BCR signaling in mediating negative selection has not been addressed. Consistent with previous findings (26,27), the loss of CD19 in MD4 B cells resulted in a modest reduction in peripheral B cell numbers (Figure 1-1C). Assessment of HEL-specific antibody revealed that tolerance mechanisms to prevent autoantibody production were intact in the absence of CD19 (Figure 1-1D). Both MD4ML5 and MD4ML5$CD19^{-/-}$ B cells selectively downregulated IgM (Figure 1-1E) and were short-lived, resulting in an equally reduced splenic B cell compartment relative to their naïve counterparts (Figure 1-1C). Thus, altered BCR signaling thresholds in the absence of CD19 do not affect anergy induction.

**1.2.3 - PTEN function in B cell anergy**

$PI(3,4,5)P_3$ is rapidly hydrolyzed to $PI(4,5)P_2$ by the lipid phosphatase PTEN, which we hypothesize is another means by which $PI(3,4,5)P_3$ availability is regulated in autoreactive B cells. To assess PTEN protein levels in naïve and anergic B cells, whole cell lysates were prepared from MD4 and MD4ML5 B cells and immunoblotted for PTEN expression. Interestingly, PTEN protein expression was found to be higher in MD4ML5 B cells compared to MD4 B cells (Figure 1-2A). Flow cytometric analysis revealed similar levels of PTEN in the MZ and follicular B cell compartments of MD4 mice (data not shown). Given that modest changes in PTEN expression can have striking

effects on cellular responses, these results suggest that PTEN may be required to suppress signaling via the PI3K pathway in autoreactive B cells.

Since PI(3,4,5)$P_3$ induction is reduced in anergic B cells, we postulated that inactivation of PTEN in maturing B cells would result in elevated PI(3,4,5)$P_3$ levels and the unabated activation of downstream effector molecules would cause a break in B cell tolerance. To test this hypothesis, MD4 mice and MD4ML5 mice were crossed with PTEN$^{flox/flox}$/CD19*cre* mice to inactivate *Pten* specifically in B cells and to allow for the analysis of B cell anergy induction and maintenance. The MD4, MD4ML5, MD4PTEN$^{flox/flox}$ and MD4ML5PTEN$^{flox/flox}$ animals used were all heterozygous for CD19 and express Cre recombinase. BCR induced PI(3,4,5)$P_3$ generation was measured in splenic cells obtained from MD4PTEN$^{flox/flox}$ and MD4ML5PTEN$^{flox/flox}$ mice. Splenic cells were stimulated with anti-IgM F(ab')$_2$, intracellularly stained with anti-PI(3,4,5)$P_3$, and analyzed by flow cytometry (Figure 1-2B). In contrast to the inhibition of PI(3,4,5)$P_3$ induction seen in MD4ML5 B cells (Figure 1-1A), MD4ML5PTEN$^{flox/flox}$ B cells showed an increase in PI(3,4,5)$P_3$ upon stimulation (Figure 1-2B). Downstream signaling was assessed by measuring $Ca^{++}$ flux in MD4, MD4ML5, MD4PTEN$^{flox/flox}$ and MD4ML5PTEN$^{flox/flox}$ B cells stimulated with anti-IgM F(ab')$_2$ or HEL antigen. As expected, MD4 B cells mobilized $Ca^{++}$ efficiently when stimulated with either anti-IgM F(ab')$_2$ or HEL, while MD4ML5 B cells did not (Figure 1-2C, left panels). In contrast, MD4PTEN$^{flox/flox}$ and MD4ML5PTEN$^{flox/flox}$ B cells were both able to mobilize $Ca^{++}$ (Figure 1-2C, right panels), indicating the continued ability to induce productive BCR signaling. To further confirm the restoration of BCR signaling in MD4ML5PTEN$^{flox/flox}$ B cells, lysates were prepared from anti-IgM or anti-Igκ stimulated MD4ML5 and

MD4ML5PTEN$^{flox/flox}$ B cells and immunoblotted for activated Akt (Figures 1-2D and Supplementary Figure 1-2). While Akt was not activated in MD4ML5 B cells, MD4ML5PTEN$^{flox/flox}$ B cells efficiently activated Akt (Figure 1-2D and Supplementary Figure 1-2). Erk was basally phosphorylated in MD4ML5, but not MD4ML5PTEN$^{flox/flox}$ B cells, while inducible in both B cell types (Figure 1-2D, lower panels). These results suggest that the loss of *Pten* prevents B cells from acquiring a biochemical profile consistent with the anergic state.

The hallmarks of B cell anergy include the selective downregulation of surface IgM, as well as limited cell lifespan and proliferation and an inability to become immunoglobulin-secreting cells. Therefore, we sought to determine if the observed recovery of productive BCR signaling by autoreactive PTEN-deficient B cells translated into increased B cell numbers in the periphery and increased titers of serum autoantibody. While MD4ML5 mice had low splenic and lymph node B cell numbers compared to their naïve counterparts, the B cell compartment in MD4ML5PTEN$^{flox/flox}$ mice was comparable to their naïve counterparts (Figures 1-3A and Supplementary Figure 1-3). Interestingly, the MZ B cell compartment is restored in MD4ML5PTEN$^{flox/flox}$ mice, but is not expanded to the extent observed in MD4PTEN$^{flox/flox}$ mice (Supplementary Figure 1-4). The ability of B cells to secrete immunoglobulin was assessed by measuring HEL-specific serum IgM levels by ELISA. We found that while MD4 mice had significantly higher levels of serum IgM than MD4ML5 mice, MD4PTEN$^{flox/flox}$ mice and MD4ML5PTEN$^{flox/flox}$ mice both maintained high levels of serum IgM (Figure 1-3B). Furthermore, while MD4ML5 B cells dramatically downregulated surface IgM, MD4ML5PTEN$^{flox/flox}$ B cells do so to a lesser extent (Figure 1-3C). These results

demonstrate that the loss of PTEN leads to failed anergy and the production of abundant autoantibody.

### 1.2.4 - Effects of PTEN loss on self-antigen availability and receptor occupancy

Secretion of autoantibody or the expression of autoreactive B cell receptors can effectively sequester self-antigen and impact B cell tolerance, as continued B cell receptor occupancy is necessary for the maintenance of tolerance (8,28). Receptor occupancy, as defined by the level of HEL bound to the surface of B cells, was measured in MD4, MD4ML5 and MD4ML5PTEN$^{flox/flox}$ B cells by flow cytometry using a polyclonal anti-HEL antibody. We found that freshly isolated MD4ML5 PTEN$^{flox/flox}$ B cells had ~10-fold lower level of bound HEL than MD4ML5 B cells (Figure 1-4A). This finding suggests that receptor occupancy *in vivo* is reduced on autoreactive PTEN-deficient B cells, which may contribute to the inability to maintain tolerance. Low receptor occupancy resulting in the increased presence of autoreactive B cells may be more prominent in adult mice as serum IgM levels accumulate and deplete available HEL. To address this possibility, receptor occupancy was quantified in adult (>8 week old) and young (3 week old) mice by incubating splenic B cells with excess exogenous HEL to fully occupy surface receptors. The level of surface HEL on these cells was compared to the levels of surface HEL on cells treated with PBS alone; hence, the degree of receptor occupancy was determined as the ratio of the mean fluorescence intensities (MFI) of the PBS- and HEL-treated samples. In adult MD4ML5 mice, the level of surface HEL on PBS-treated B cells was 50% that of HEL-treated B cells (Figure 1-4B), which has been previously reported as sufficient MD4 receptor occupancy by

endogenous antigen to induce and maintain tolerance (28). Consistent with the hypothesized sequestration of HEL by secreted or membrane-bound IgM in adult MD4ML5PTEN$^{flox/flox}$ mice, only 10% of MD4 receptors were occupied by endogenous HEL (Figure 1-4B). Interestingly, in young mice, receptor occupancy on both MD4ML5 and MD4ML5PTEN$^{flox/flox}$ B cells was approximately equivalent (~60%) (Figure 1-4B), suggesting a cumulative effect of self-antigen sequestration in MD4ML5PTEN$^{flox/flox}$ mice.

To qualitatively assess HEL antigen levels in MD4ML5PTEN$^{flox/flox}$ mice, we introduced CFSE-labeled MD4 B cells into MD4ML5 and MD4ML5PTEN$^{flox/flox}$ mice by tail vein injection and measured the downregulation of surface IgM upon acute *in vivo* antigen encounter. We found that donor MD4 B cells downregulated surface IgM strongly when exposed for 24 hr to the adult MD4ML5 environment, suggesting a productive encounter with HEL antigen (Figure 1-4C). In contrast, when donor MD4 B cells were exposed to the adult MD4ML5PTEN$^{flox/flox}$ environment, surface IgM expression was downregulated to a lesser extent (Figure 1-4C). In both cases, the downregulation of surface IgM was antigen-dependent as donor MD4 B cells transferred into non-HEL expressing MD4 and MD4PTEN$^{flox/flox}$ environments maintained similarly high basal levels of surface IgM (Figure 1-4C). Thus, less HEL is available in adult MD4ML5PTEN$^{flox/flox}$ animals to induce and sustain anergy.

As previously reported (29), acute encounter with HEL leads to the elimination of antigen-specific MD4 B cells *in vivo*. MD4, MD4PTEN$^{flox/flox}$ and MD4ML5PTEN$^{flox/flox}$ mice were administered exogenous HEL (1 mg) or PBS, and splenocytes were harvested 48 hr later to assess splenic B cell numbers, surface IgM downregulation and

upregulation of CD86. The introduction of exogenous HEL induced a measurable decrease in surface IgM in all groups, while CD86 was only upregulated on MD4PTEN$^{flox/flox}$ B cells (data not shown). Importantly, MD4PTEN$^{flox/flox}$ and MD4ML5PTEN$^{flox/flox}$ B cells expanded or persisted in the presence of additional HEL, respectively (Figure 1-4D), while MD4 B cells were eliminated. These findings indicate that increasing the concentration of free self-antigen confers an anergic phenotype on MD4ML5PTEN$^{flox/flox}$ B cells, but they remain long-lived.

The frequency of autoreactive B cells in normal mice is relatively low, while the abundance of anti-HEL B cells in the MD4ML5 system affects the concentration of available HEL self-antigen. Therefore, bone marrow chimeras were generated to assess whether the ability of PTEN-deficient, self-reactive B cells to escape the induction of anergy was independent of their frequency within the B cell repertoire. Lethally irradiated ML5 mice were reconstituted with a donor population of lineage depleted hematopoietic stems cells comprised of a 20:80 mixture of either nonTg:MD4 or nonTg:MD4PTEN$^{flox/flox}$ cells. After 12 weeks of reconstitution, we found that despite similar seeding frequencies, MD4PTEN$^{flox/flox}$ B cells survived and produced abundant autoantibody, whereas MD4 B cells were present at a lower frequency and produced little autoantibody (Figure 1-5), consistent with previous findings (30). These results confirm that PTEN-deficiency in self-reactive B cells impairs the induction or maintenance of the anergic state.

### 1.2.5 - Immature PTEN-deficient B cells are less sensitive to tolerogenic signals

Negative selection takes place at the immature B cell stage during which engagement of the B cell receptor with self-antigen leads to B cell anergy or death. One of the cellular strategies to induce anergy is through intrinsic negative regulation of key signaling components. To determine the contribution of $PI(3,4,5)P_3$ signaling to negative selection of newly formed B cells expressing a normal diverse repertoire of B cell receptors, we measured the activation and proliferation in response to BCR engagement of cultured immature B cells from nontransgenic wildtype and $PTEN^{flox/flox}$ mice. Bone marrow from non-transgenic wildtype and $PTEN^{flox/flox}$ mice were harvested and cultured with IL-7 over a 6 day period to promote the selective expansion of pre-B cells. Cells were then labeled with CFSE and either returned to IL-7 or removed from IL-7 to permit their transition to immature IgM-expressing B cells. In the latter culture, B cells were treated with anti-IgM $F(ab')_2$ fragments (1 or 10 μg/ml) to engage the BCR on newly-formed IgM-positive cells. B cells ($B220^+$) were enumerated and examined for an activated profile ($CD86^+$, increased forward scatter), as well as proliferative capacity (CFSE partitioning) over a 3 day period. CD86 staining showed a ~7-fold enhancement in the frequency of activated immature $PTEN^{flox/flox}$ B cells relative to immature wildtype B cells (Figure 1-6A). Gating on activated B cells revealed that immature $PTEN^{flox/flox}$ B cells proliferated to a much greater extent than immature wildtype B cells (Figure 1-6B). These findings suggest that sustained $PI(3,4,5)P_3$ signaling converts what is normally a tolerogenic response into a mitogenic response during B cell development.

Neonatal B cells exhibit phenotypic and functional characteristics similar to that of immature B cells of adult bone marrow. To assess the effects of $PI(3,4,5)P_3$ signaling

on tolerance induction during this gestational stage, 5 day old neonatal littermates consisting of non-transgenic wildtype and nontransgenic $PTEN^{flox/flox}$ mice were analyzed. Interestingly, neonatal spleens were not markedly enlarged in $PTEN^{flox/flox}$ mice as we typically see in adult $PTEN^{flox/flox}$ mice (20). Moreover, surface IgM/IgD profiles of wildtype and $PTEN^{flox/flox}$ B cells from neonatal spleens revealed similarly high frequencies of IgM+/IgD- B cells compared to adult B cells, which are largely IgM+/IgD+ (Figure 1-6C, left panels). Using established protocols (31,32), B cells from neonatal and adult wildtype and $PTEN^{flox/flox}$ mice were harvested and cultured in media containing IL-4 alone, IL-4 plus LPS, or IL-4 plus anti-IgM $F(ab')_2$. Proliferation was assessed by $^3$H-thymidine incorporation (Figure 1-6C, right panel). Wildtype neonatal B cells proliferated modestly in response to LPS, but no proliferation was observed in response to anti-IgM $F(ab')_2$, confirming that BCR stimulation is inhibitory in wildtype neonatal B cells (Figure 1-6C). In contrast, neonatal $PTEN^{flox/flox}$ B cells proliferated strongly in response to both LPS and anti-IgM $F(ab')_2$ (Figure 1-6C). These findings corroborate the results of the bone marrow culture system (Figure 1-6A and B) and demonstrate that sustained $PI(3,4,5)P_3$ signaling leads to activation and proliferation rather than inhibition and anergy in immature B cells upon BCR engagement.

## 1.3 – Discussion

Despite the striking differences in responsiveness to antigen by immature and mature B cells, the underlying biochemical bases for these distinct responses are unclear. Since PI3K signaling is central to cellular growth control, proliferation and survival, the current work focused on the role of the PI3K pathway in the induction and maintenance

of B cell anergy. In mature B cells, BCR engagement leads to the rapid generation of $PI(3,4,5)P_3$ as a consequence of PI3K (p85/p110) recruitment to CD19 and membrane-proximal adaptor proteins. In anergic B cells, we found that $PI(3,4,5)P_3$ production was significantly reduced. Consistent with this observation, CD19 was expressed at normal levels, but was not efficiently phosphorylated on the tyrosine residues that mediate PI3K recruitment. This defect may be a consequence of impaired tyrosine kinase activity, as has been noted in anergic B cells (33). Alternatively, CD19 may be physically uncoupled from the BCR complex upon chronic engagement of the BCR; such a mechanism has been described for the redistribution of the Igα/β heterodimer (6), and recent data indicates that CD19 function is crucial in the formation of and signaling by antigen-bound BCR microclusters (34). Interestingly, overexpression of human CD19 has been shown to cause a break in tolerance (35), likely resulting from a preferential association of human CD19 with the BCR (since it interacts inefficiently with murine CD21 (36). Coengagement of the BCR and CD21/CD19 Complement Receptor 2 complex by C3d-bearing self-antigens can also overcome peripheral tolerance (37,38), suggesting that forced recruitment of CD19 into the BCR complex overcomes receptor desensitization to augment PI3K activation.

Given these findings, it is perhaps not surprising that anergy was not affected by the loss of CD19. By contrast, the loss of CD19 appears to impair positive selection of newly formed B cells in both immunoglobulin transgenic as well as non-transgenic $CD19^{-/-}$ mice (26,27). We have confirmed that this is the case for the HEL system as $CD19^{-/-}$ MD4 mice have reduced peripheral B cells relative to wildtype MD4 counterparts (Figure 1C). These findings suggest that BCR-associated CD19 is critical

for the propagation of weak signals during positive selection, but is dispensable for negative selection mediated by strong signals (such as binding of HEL by the MD4 receptor). Consistent with this view are our previous findings of reduced survival of follicular CD19-deficient B cells responding to sub-mitogenic "tonic" signaling, but intact antigen-driven responses to potent multivalent antigens (39, 40).

In addition to impaired CD19 signaling, we found elevated expression of PTEN in anergic B cells. While loss of PTEN expression is oncogenic in most cells, increased PTEN expression or stability can further suppress growth factor receptor signaling (19). Since PTEN loss leads to failed anergy, we conclude that reduced $PI(3,4,5)P_3$ is not only a novel hallmark of anergic B cells, but is a prerequisite for anergy induction and maintenance. Relatedly, PI3K has also been recently shown to negatively regulate receptor editing by modulating RAG expression (41). $PI(3,4,5)P_3$ is transiently induced upon cell activation and triggers multiple downstream pathways via the recruitment of pivotal PH domain-containing proteins. In addition to the BCR, signaling via costimulatory receptors and accessory molecules is also augmented in the absence of PTEN (20,22). Of particular interest is threshold-based signaling via the BAFF-R, which utilizes the PI3K pathway and regulates the fate of anergic B cells in concert with the BCR (42,43,44). Normal hyporesponsive PI3K signaling downstream of the BCR and BAFF-R in self-reactive B cells undergoing anergy could be overcome by a loss of PTEN, resulting in a breach in tolerance. This hypothesis predicts that haplo-insufficient or B cell-specific PTEN-deficient animals would be prone to autoantibody production and autoimmune disease. Indeed, while autoantibody production has been noted in *Pten* mutant mice (45,22), we postulate that autoantibody-associated disease is generally not

observed since elevated PI3K signaling negatively regulates class switch recombination and hence, the production of pathogenic IgG (46,21).

The strength of signaling via the BCR is the key determinant of B cell fate following self-antigen encounter. Weak signals induced by low affinity/avidity interactions induce the anergic state, which can lead to apoptosis in the short term, but this fate can be averted upon removal of antigen, change in BCR specificity or provision of costimulatory signals (33, 3, 8, 47, 23, 48). In immunoglobulin transgenic systems, the affinity of the BCR for self-antigen is fixed; however the strength of signal can be modulated by the relative amount or nature of the self-antigen (soluble versus membrane-bound). Given that membrane or secreted anti-HEL immunoglobulin can deplete self-antigen, under some circumstances local HEL may become subthreshold, resulting in the accumulation of HEL-specific B cells that are "indifferent' or "ignorant" of self-antigen. Early studies using the soluble HEL system showed that receptor occupancy of approximately 50% was sufficient to induce and maintain anergy (28). This threshold correlates with the *in vivo* positioning of anergic B cells in the outer PALS (49, 30, 50), and can be recapitulated with the transfer of naïve immature or mature Ig transgenic B cells into HEL transgenic recipients (50). Our B cell transfer and HEL infusion experiments indicate that PTEN-deficient B cells in adult animals are exposed to lower levels of HEL, and thus are less likely to adopt the phenotypic and functional characteristics of anergy. Nonetheless, we also demonstrate using mixed bone marrow chimeras that PTEN loss causes an intrinsic defect in B cell signaling, resulting in impaired induction of maintenance of B cell anergy. These findings are consistent with our studies of nontransgenic PTEN-deficient immature B cells isolated from adult bone

marrow or neonatal/adolescent mice, which were found to be responsive to BCR signaling, indicating a primary defect in tolerogenic signaling in newly formed B cells that lack PTEN. These findings establish $PI(3,4,5)P_3$ metabolism as a focal point for inducing and maintaining the tolerogenic state in B cells, setting the stage for future studies exploring the role of particular $PI(3,4,5)P_3$ effectors in this context.

In summary (Figure 1-7), we propose that elevated and sustained activation of the PI3K pathway in newly formed B cells results in altered negative selection and the egress of autoreactive B cells into the periphery. Once in the periphery, these cells also appear to be refractory to elimination by the continued presence of self-antigen. Interestingly, since elevated PI3K signaling favors MZ B cell formation (20, 22), selection into this compartment may promote the propagation and further differentiation of autoreactive B cells in response to BAFF, TLR ligands and T cell-derived factors, as others have suggested (51, 44). In addition to these intrinsic effects, the accumulation of autoreactive B cells and secreted autoantibody will gradually sequester HEL, leading to the release and maturation of additional "clonally ignorant" B cells as a secondary event. This effect is dramatically revealed using the monoclonal HEL system since self-reactive B cells are present in great abundance (even in a mixed bone marrow chimera) and express or secrete high-affinity immunoglobulin. However, the chronicity of autoimmune disease and long-lived nature of antigen-selected B cells supports the broad premise that self-antigen depletion by autoantibody may perpetuate autoimmunity through the continued release of self-reactive bone marrow B cells; some of which may persist and differentiate into autoantibody producing cells in the periphery.

## 1.4 - Methods

### 1.4.1 Mice

Mice expressing MD4 (HEL-Ig transgene) and ML5 (sHEL transgene) were obtained from Jackson Laboratories (5). These mice were bred to obtain double transgenic mice (MD4ML5). $PTEN^{flox/flox}$ mice (Lesche et al., 2002) were crossed with CD19*cre* mice (in which cre recombinase expression is driven by the CD19 promoter, (52)) to generate $PTEN^{flox/flox}$/CD19*cre* mice. Single (MD4) and double transgenic (MD4ML5) mice were subsequently bred with $PTEN^{flox/flox}$/CD19*cre* mice to obtain naïve (MD4) and autoreactive (MD4ML5) mice with a B cell specific PTEN deletion. All animals were maintained in an animal facility and experimental procedures approved by the IACUC committee at The Burnham Institute for Medical Research (La Jolla, CA).

### 1.4.2 - Western blotting

Splenic B cells were purified using MACS beads to negatively select B cells, according to the manufacturer's recommended procedure (Miltenyi Biotech, Auburn, CA). One to ten million B cells were washed with PBS and stimulated with 10 µg/mL goat anti-mouse IgM $F(ab')_2$ (Zymed Laboratories, S. San Francisco, CA) for the indicated times at 37°C. Cell pellets were lysed on ice for 30 min in either RIPA lysis buffer (50 mM Tris-HCl pH 7.4, 150 mM NaCl, 2 mM EDTA, 1% NP-40, 0.1% SDS) or NP-40 lysis buffer (20 mM Tris-HCl pH 7.5, 1% NP-40, 10% glycerol, 10 mM NaCl, 1 mM EDTA) plus protease inhibitors (2 µg/ml leupeptin, 2 mM PMSF, 2 µg/ml aprotinin and 1 mM sodium orthovanadate). Lysates were electrophoresed using 4-12% acrylamide SDS gels and blotted onto nitrocellulose paper. Antibodies against CD19,

phospho-CD19, Akt, phospho-Akt, Erk, phospho-Erk, and actin were from Cell Signaling Technology, Inc. (Danvers, MA). Proteins were revealed with HRP-labeled anti-rabbit antibodies and developed with SuperSignal West Pico Chemiluminescent Substrate (Thermo Scientific, Rockford, IL).

**1.4.3 - Flow cytometry**

Spleens were excised and red blood cells depleted from cell suspensions using hypotonic ammonium chloride. One million splenic cells were resuspended in FACS buffer (PBS, 1% FBS and 0.01% sodium azide) and incubated with the following conjugated antibodies: IgM-APC, IgD-PE, B220-APC-Cy7, and CD11b-PE-Cy7 (BD Bioscience or eBioscience). Samples were washed with FACS buffer and analyzed using a FACSCanto flow cytometer and FlowJo software (Treestar, Ashland, OR). For $PI(3,4,5)P_3$ staining, $5 \times 10^6$ splenic cells were resuspended in 100-200 µl PBS; preincubated at 37°C for 5 min followed by stimulation with anti-IgM $F(ab')_2$ at a final concentration of 10 µg/ml at 37°C for 5 min. Cells were fixed with 1.5% formaldehyde at RT for 10 min, washed with cold PBS and resuspended in 500 µl permeabilization buffer (PBS, 1% BSA and 0.2% saponin) on ice for 10 min. Cells were subsequently stained with biotinylated anti- $PI(3,4,5)P_3$ IgM antibody (Echelon Biosciences, Salt Lake City, UT) or biotinylated IgM isotype control (BD Biosciences Pharmingen) in permeabilization buffer on ice for 30 min. Cells were washed twice with permeabilization buffer, resuspended in the same buffer containing strepavidin-FITC and B220-APC-Cy7 and analyzed by flow cytometry. For receptor occupancy, cells were incubated in 20 µg/ml hen egg lysozyme (Sigma) or PBS on ice for 1 hr. Cells were

blocked with anti-mouse CD16/32 and stained with biotinylated anti-hen egg lysozyme (Rockland) followed by strepavidin-PE and anti-B220-APC-Cy7. Mean fluorescence intensities of PBS-treated cells were divided by the corresponding mean fluorescence intensities of HEL-treated cells and multiplied by 100 to obtain the percentage of receptor occupancy.

### 1.4.4 - Serum ELISA

Serum samples were collected by retroorbital bleeding. 96-well high binding capacity plates were coated with 10 μg/ml HEL or anti-mouse IgM for 24 hr at 4°C. Plates were blocked for 20 min at RT with blocking buffer (0.5% BSA in PBS). Serum samples were serially diluted in blocking buffer and incubated in coated wells for 2 hr at RT. Plates were washed and incubated with alkaline phosphatase-conjugated anti-mouse IgM or conjugated anti-mouse kappa (Southern Biotech) for 1 hr at RT. Phosphatase substrate (Sigma, St. Louis, MO) was added to wells and $A_{405}$ measured using a BioTek Elx808 colorimetric plate reader (BioTek Instruments, Winooski, VT).

### 1.4.5 - Cell transfer

Purified B cells were incubated at 1 x $10^7$ cells/ml for 10 min. at RT in PBS containing 5 μM CFDA-SE (Invitrogen, Carlsbad, CA). FCS was added to a final concentration of 10%, and cells were incubated for 15 min at RT. Cells were washed twice with PBS and were injected via tail vein into recipient mice. After 18-26 hr, mice were sacrificed and splenic cells were stained with antibodies against B220 and IgM, and CFSE+ cells were gated and analyzed by flow cytometry.

### 1.4.6 - HEL injection

Animals were immunized *via* i.p. injection with either 1 mg HEL in PBS followed 24 hr later with a second 1 mg HEL injection or with a single 5 mg injection. Control mice were injected with PBS alone. 48 hr after the initial injection, animals were sacrificed and spleen suspensions prepared. For flow cytometric analysis of cellular activation, non-specific binding was first blocked by pre-incubating cells with anti-mouse CD16/32 blocking antibodies (eBioscience). Cells were then stained with biotin-conjugated anti-mouse CD86 followed by strepavidin-PerCP/Cy5.5 (eBioscience), IgM-APC and B220-APC/AF750 (eBioscience).

### 1.4.7 - Calcium flux

Two million B cells were resuspended in 250 µl media (DMEM, 10 mM HEPES and 2.5% FBS). Four µl Fura Red, 2 µl Fluo-4 and 2 µl pluronic acid (Molecular Probes) were added to 1 ml of media. An equal volume of dye mix was added to each cell suspension. Cells were incubated for 45 min at 37ºC in the dark, washed with media and stained with B220-APC. Stained cells were read for 1 min to obtain a baseline on the flow cytometer, and then stimulated with either 10 µg/ml anti-IgM $F(ab')_2$ or 10 µg/ml hen egg lysozyme. Calcium flux was measured by Fluo-4 (530 nm)/Fura Red (685 nm) emission ratiometry for 5 min.

### 1.4.8 - $^3$H-thymidine incorporation

Purified B cells were cultured at 1-2 x $10^6$ cells/ml in round bottom 96-well plates in 100-200 µl/well of RPMI complete medium in the presence of IL-4 (5 ng/ml) plus LPS

(20 μg/ml) Serotype 0111:B4 (Sigma, St. Louis, MO) or anti-IgM F(ab')$_2$ (20 μg/ml). Cells were cultured for 48 hr after which $^3$H-thymidine was added for the last 12 hr at 1 μCi per well. Cells were harvested using a FilterMate Harvester (PerkinElmer, Inc., Waltham, MA) and the amount of incorporated $^3$H-thymidine was measured using a MicroBeta Trilux scintillation counter (PerkinElmer, Inc.).

### 1.4.9 - Bone marrow culture

Mixed femoral bone marrow cells were treated with hypotonic solution to deplete red blood cells for 5 min on ice. B cells were purified using anti-B220 MACS beads and cultured at 2 x $10^6$ cells/ml in 6-well plates in 15% fetal bovine serum in OptiMEM media containing 10 ng/ml each of rIL-7, SCF and Flt3-L. After 6 days, nonadherent cells were collected in fresh media, labelled with CFSE and re-cultured in media containing IL-7 alone, 10 μg/ml anti-IgM F(ab')$_2$ or 1 μg/ml anti-IgM F(ab')$_2$ and incubated for three days. Cells were harvested and stained with 7AAD and antibodies to CD86 and B220.

### 1.4.10 - Statistical method

Student's t test was used to determine statistically significant differences between samples.

**Acknowledgement**

Chapter 1 of this dissertation is based on the manuscript that has been published in the journal, *Immunity* (Browne CD, Del Nagro CJ, Cato MH, Dengler HS, Rickert RC. Suppression of phosphatidylinositol 3,4,5-trisphosphate production is a key determinant of B cell anergy. Immunity. 2009 Nov 20;31(5):749-60). Contents of this chapter are presented as it may appear in the publication, but supplemented with unpublished figures. Cecille D. Browne is the primary author of this paper. Chris DelNagro is a co-first author of this paper and the other contributing authors are Matthew Cato, Hart Dengler and Robert Rickert.

## 1.5 - References


1. Cambier, J.C., Gauld, S.B., Merrell, K.T., and Vilen, B.J. (2007). B-cell anergy: from transgenic models to naturally occurring anergic B cells? Nat Rev Immunol *7*, 633-643.

2. Jun, J.E., and Goodnow, C.C. (2003). Scaffolding of antigen receptors for immunogenic versus tolerogenic signaling. Nat Immunol *4*, 1057-1064.

3. Cornall, R.J., Cyster, J.G., Hibbs, M.L., Dunn, A.R., Otipoby, K.L., Clark, E.A., and Goodnow, C.C. (1998). Polygenic autoimmune traits: Lyn, CD22, and SHP-1 are limiting elements of a biochemical pathway regulating BCR signaling and selection. Immunity *8*, 497-508.

4. Cyster, J.G., Healy, J.I., Kishihara, K., Mak, T.W., Thomas, M.L., and Goodnow, C.C. (1996). Regulation of B-lymphocyte negative and positive selection by tyrosine phosphatase CD45. Nature *381*, 325-328.

5. Goodnow, C.C., Crosbie, J., Adelstein, S., Lavoie, T.B., Smith-Gill, S.J., Brink, R.A., Pritchard-Briscoe, H., Wotherspoon, J.S., Loblay, R.H., Raphael, K., and et al. (1988). Altered immunoglobulin expression and functional silencing of self-reactive B lymphocytes in transgenic mice. Nature *334*, 676-682.

6. Vilen, B.J., Nakamura, T., and Cambier, J.C. (1999). Antigen-stimulated dissociation of BCR mIg from Ig-alpha/Ig-beta: implications for receptor desensitization. Immunity *10*, 239-248.

7. Weintraub, B.C., Jun, J.E., Bishop, A.C., Shokat, K.M., Thomas, M.L., and Goodnow, C.C. (2000). Entry of B cell receptor into signaling domains is inhibited in tolerant B cells. J Exp Med *191*, 1443-1448.

8. Gauld, S.B., Benschop, R.J., Merrell, K.T., and Cambier, J.C. (2005). Maintenance of B cell anergy requires constant antigen receptor occupancy and signaling. Nat Immunol *6*, 1160-1167.

9. Goodnow, C.C., Brink, R., and Adams, E. (1991). Breakdown of self-tolerance in anergic B lymphocytes. Nature *352*, 532-536.

10. Healy, J.I., Dolmetsch, R.E., Timmerman, L.A., Cyster, J.G., Thomas, M.L., Crabtree, G.R., Lewis, R.S., and Goodnow, C.C. (1997). Different Nuclear Signals Are Activated by the B Cell Receptor during Positive Versus Negative Signaling. Immunity *6*, 419-428.

11. Rui, L., Healy, J.I., Blasioli, J., and Goodnow, C.C. (2006). ERK signaling is a molecular switch integrating opposing inputs from B cell receptor and T cell

cytokines to control TLR4-driven plasma cell differentiation. J Immunol *177*, 5337-5346.

12. Rui, L., Vinuesa, C.G., Blasioli, J., and Goodnow, C.C. (2003). Resistance to CpG DNA-induced autoimmunity through tolerogenic B cell antigen receptor ERK signaling. Nat Immunol *4*, 594-600.

13. Mecklenbrauker, I., Kalled, S.L., Leitges, M., Mackay, F., and Tarakhovsky, A. (2004). Regulation of B-cell survival by BAFF-dependent PKCdelta-mediated nuclear signalling. Nature *431*, 456-461.

14. Mecklenbrauker, I., Saijo, K., Zheng, N.Y., Leitges, M., and Tarakhovsky, A. (2002). Protein kinase Cdelta controls self-antigen-induced B-cell tolerance. Nature *416*, 860-865.

15. Fruman, D.A., and Bismuth, G. (2009). Fine tuning the immune response with PI3K. Immunological Reviews *228*, 253-272.

16. Aiba, Y., Kameyama, M., Yamazaki, T., Tedder, T.F., and Kurosaki, T. (2007). Regulation of B cell development by BCAP and CD19 through their binding to phosphoinositide 3-kinase. Blood, blood-2007-2008-109769.

17. Rickert, R.C. (2005). Regulation of B lymphocyte activation by complement C3 and the B cell coreceptor complex. Curr Opin Immunol *17*, 237-243.

18. Carter, R.H., Doody, G.M., Bolen, J.B., and Fearon, D.T. (1997). Membrane IgM-induced tyrosine phosphorylation of CD19 requires a CD19 domain that mediates association with components of the B cell antigen receptor complex. J Immunol *158*, 3062-3069.

19. Tamguney, T., and Stokoe, D. (2007). New insights into PTEN. J Cell Sci *120*, 4071-4079.

20. Anzelon, A.N., Wu, H., and Rickert, R.C. (2003). Pten inactivation alters peripheral B lymphocyte fate and reconstitutes CD19 function. Nat Immunol *4*, 287-294.

21. Omori, S.A., Cato, M.H., Anzelon-Mills, A., Puri, K.D., Shapiro-Shelef, M., Calame, K., and Rickert, R.C. (2006). Regulation of class-switch recombination and plasma cell differentiation by phosphatidylinositol 3-kinase signaling. Immunity *25*, 545-557.

22. Suzuki, A., Kaisho, T., Ohishi, M., Tsukio-Yamaguchi, M., Tsubata, T., Koni, P.A., Sasaki, T., Mak, T.W., and Nakano, T. (2003). Critical roles of Pten in B cell homeostasis and immunoglobulin class switch recombination. Journal of Experimental Medicine *197*, 657-667.

23. Healy, J.I., and Goodnow, C.C. (1998). Positive versus negative signaling by lymphocyte antigen receptors. Annu Rev Immunol *16*, 645-670.

24. Mason, D.Y., Jones, M., and Goodnow, C.C. (1992). Development and follicular localization of tolerant B lymphocytes in lysozyme/anti-lysozyme IgM/IgD transgenic mice. Int Immunol *4*, 163-175.

25. Oliver, A.M., Martin, F., Gartland, G.L., Carter, R.H., and Kearney, J.F. (1997). Marginal zone B cells exhibit unique activation, proliferative and immunoglobulin secretory responses. Eur J Immunol *27*, 2366-2374.

26. Buhl, A.M., Nemazee, D., Cambier, J.C., Rickert, R., and Hertz, M. (2000). B-cell antigen receptor competence regulates B-lymphocyte selection and survival. Immunol Rev *176*, 141-153.

27. Diamant, E., Keren, Z., and Melamed, D. (2005). CD19 regulates positive selection and maturation in B lymphopoiesis: lack of CD19 imposes developmental arrest of immature B cells and consequential stimulation of receptor editing. Blood *105*, 3247-3254.

28. Goodnow, C.C., Crosbie, J., Jorgensen, H., Brink, R.A., and Basten, A. (1989). Induction of self-tolerance in mature peripheral B lymphocytes. Nature *342*, 385-391.

29. Schmidt, K.N., and Cyster, J.G. (1999). Follicular exclusion and rapid elimination of hen egg lysozyme autoantigen-binding B cells are dependent on competitor B cells, but not on T cells. J Immunol *162*, 284-291.

30. Cyster, J.G., Hartley, S.B., and Goodnow, C.C. (1994). Competition for follicular niches excludes self-reactive cells from the recirculating B-cell repertoire. Nature *371*, 389-395.

31. Chang, T.L., Capraro, G., Kleinman, R.E., and Abbas, A.K. (1991). Anergy in immature B lymphocytes. Differential responses to receptor-mediated stimulation and T helper cells. J Immunol *147*, 750-756.

32. Yellen, A.J., Glenn, W., Sukhatme, V.P., Cao, X.M., and Monroe, J.G. (1991). Signaling through surface IgM in tolerance-susceptible immature murine B lymphocytes. Developmentally regulated differences in transmembrane signaling in splenic B cells from adult and neonatal mice. J Immunol *146*, 1446-1454.

33. Cooke, M.P., Heath, A.W., Shokat, K.M., Zeng, Y., Finkelman, F.D., Linsley, P.S., Howard, M., and Goodnow, C.C. (1994). Immunoglobulin signal transduction guides the specificity of B cell-T cell interactions and is blocked in tolerant self-reactive B cells. J Exp Med *179*, 425-438.

34. Depoil, D., Fleire, S., Treanor, B.L., Weber, M., Harwood, N.E., Marchbank, K.L., Tybulewicz, V.L., and Batista, F.D. (2008). CD19 is essential for B cell activation by promoting B cell receptor-antigen microcluster formation in response to membrane-bound ligand. Nat Immunol *9*, 63-72.

35. Inaoki, M., Sato, S., Weintraub, B.C., Goodnow, C.C., and Tedder, T.F. (1997). CD19-regulated signaling thresholds control peripheral tolerance and autoantibody production in B lymphocytes. J Exp Med *186*, 1923-1931.

36. Hasegawa, M., Fujimoto, M., Poe, J.C., Steeber, D.A., and Tedder, T.F. (2001). CD19 can regulate B lymphocyte signal transduction independent of complement activation. J Immunol *167*, 3190-3200.

37. Del Nagro, C.J., Kolla, R.V., and Rickert, R.C. (2005). A critical role for complement C3d and the B cell coreceptor (CD19/CD21) complex in the initiation of inflammatory arthritis. J Immunol *175*, 5379-5389.

38. Lyubchenko, T., Dal Porto, J.M., Holers, V.M., and Cambier, J.C. (2007). Cutting Edge: Complement (C3d)-Linked Antigens Break B Cell Anergy. The Journal of Immunology *179*, 2695-2699.

39. Otero, D.C., Anzelon, A.N., and Rickert, R.C. (2003). CD19 function in early and late B cell development: I. Maintenance of follicular and marginal zone B cells requires CD19-dependent survival signals. J Immunol *170*, 73-83.

40. Rickert, R.C., Rajewsky, K., and Roes, J. (1995). Impairment of T-cell-dependent B-cell responses and B-1 cell development in CD19-deficient mice. Nature *376*, 352-355.

41. Verkoczy, L., Duong, B., Skog, P., Ait-Azzouzene, D., Puri, K., Vela, J.L., and Nemazee, D. (2007). Basal B cell receptor-directed phosphatidylinositol 3-kinase signaling turns off RAGs and promotes B cell-positive selection. J Immunol *178*, 6332-6341.

42. Lesley, R., Xu, Y., Kalled, S.L., Hess, D.M., Schwab, S.R., Shu, H.-B., and Cyster, J.G. (2004). Reduced Competitiveness of Autoantigen-Engaged B Cells due to Increased Dependence on BAFF. Immunity *20*, 441-453.

43. Patke, A., Mecklenbrauker, I., Erdjument-Bromage, H., Tempst, P., and Tarakhovsky, A. (2006). BAFF controls B cell metabolic fitness through a PKC{beta}- and Akt-dependent mechanism. The Journal of Experimental Medicine *203*, 2551-2562.

44. Thien, M., Phan, T.G., Gardam, S., Amesbury, M., Basten, A., Mackay, F., and Brink, R. (2004). Excess BAFF rescues self-reactive B cells from peripheral deletion and allows them to enter forbidden follicular and marginal zone niches. Immunity *20*, 785-798.

45. Di Cristofano, A., Kotsi, P., Peng, Y.F., Cordon-Cardo, C., Elkon, K.B., and Pandolfi, P.P. (1999). Impaired Fas response and autoimmunity in Pten+/- mice. Science *285*, 2122-2125.

46. Dengler, H.S., Baracho, G.V., Omori, S.A., Bruckner, S., Arden, K.C., Castrillon, D.H., DePinho, R.A., and Rickert, R.C. (2008). Distinct functions for the transcription factor Foxo1 at various stages of B cell differentiation. Nat Immunol *9*, 1388-1398.

47. Halverson, R., Torres, R.M., and Pelanda, R. (2004). Receptor editing is the main mechanism of B cell tolerance toward membrane antigens. Nat Immunol *5*, 645-650.

48. Phan, T.G., Amesbury, M., Gardam, S., Crosbie, J., Hasbold, J., Hodgkin, P.D., Basten, A., and Brink, R. (2003). B cell receptor-independent stimuli trigger immunoglobulin (Ig) class switch recombination and production of IgG autoantibodies by anergic self-reactive B cells. J Exp Med *197*, 845-860.

49. Cook, M.C., Basten, A., and Groth, B.F.d.S. (1997). Outer Periarteriolar Lymphoid Sheath Arrest and Subsequent Differentiation of Both Naive and Tolerant Immunoglobulin Transgenic B Cells Is Determined by B Cell Receptor Occupancy. J. Exp. Med. *186*, 631-643.

50. Fulcher, D.A., Lyons, A.B., Korn, S.L., Cook, M.C., Koleda, C., Parish, C., Fazekas de St Groth, B., and Basten, A. (1996). The fate of self-reactive B cells depends primarily on the degree of antigen receptor engagement and availability of T cell help. J Exp Med *183*, 2313-2328.

51. Enzler, T., Bonizzi, G., Silverman, G.J., Otero, D.C., Widhopf, G.F., Anzelon-Mills, A., Rickert, R.C., and Karin, M. (2006). Alternative and classical NF-kappa B signaling retain autoreactive B cells in the splenic marginal zone and result in lupus-like disease. Immunity *25*, 403-415.

52. Rickert, R.C., Roes, J., and Rajewsky, K. (1997). B lymphocyte-specific, Cre-mediated mutagenesis in mice. Nucleic Acids Res *25*, 1317-1318.

53. Lesche, R., Groszer, M., Gao, J., Wang, Y., Messing, A., Sun, H., Liu, X., and Wu, H. (2002). Cre/loxP-mediated inactivation of the murine Pten tumor suppressor gene. Genesis *32*, 148-149.

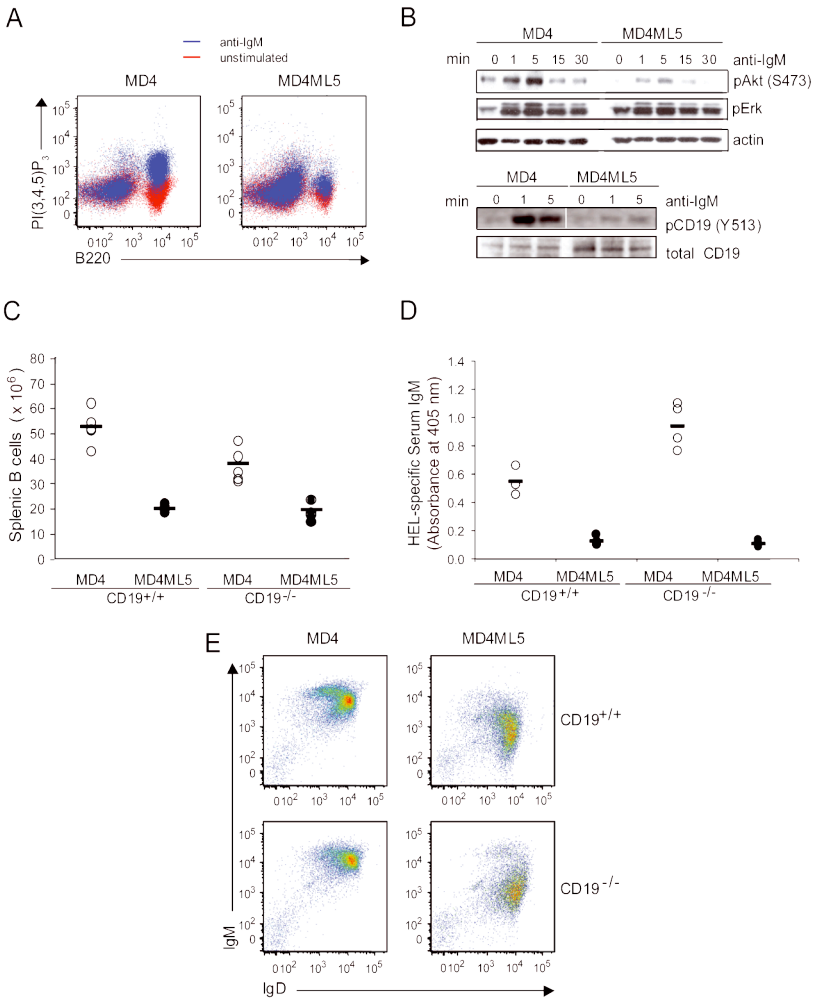


**Figure 1-1**: **PI3kinase signaling and CD19 activation are inhibited in anergic B cells.** A) Splenic cells from MD4 (left panel) and MD4ML5 (right panel) mice were stimulated with anti-IgM F(ab')$_2$ (blue) or left unstimulated (red) for 5 min. Cells were fixed, permeabilized, stained with antibodies against B220 and PI(3,4,5)$P_3$ and analyzed by flow cytometry. B) *Upper panel*, Purified MD4 and MD4ML5 B cells were stimulated with anti-IgM F(ab')$_2$ for the indicated times. Cell lysates were immunoblotted with anti-phosphorylated Akt (S473), anti-phosphorylated Erk and anti-actin. *Lower panels*, Purified MD4 and MD4ML5 B cells were stimulated with anti-IgM F(ab')$_2$ for the indicated times. Cell lysates were immunoblotted with anti-phosphorylated CD19 (Y513) and anti-CD19. C) Splenic B cells of MD4CD19$^{+/+}$, MD4ML5CD19$^{+/+}$, MD4CD19$^{-/-}$ and MD4ML5CD19$^{-/-}$ mice were enumerated. D) HEL-specificerum IgM levels from MD4CD19$^{+/+}$, MD4ML5CD19$^{+/+}$, MD4CD19$^{-/-}$ and MD4ML5CD19$^{-/-}$ mice were determined by ELISA. E) IgM/IgD profiles of B cells from MD4CD19$^{+/+}$, MD4ML5CD19$^{+/+}$, MD4CD19$^{-/-}$ and MD4ML5CD19$^{-/-}$ mice were determined by flow cytometry.

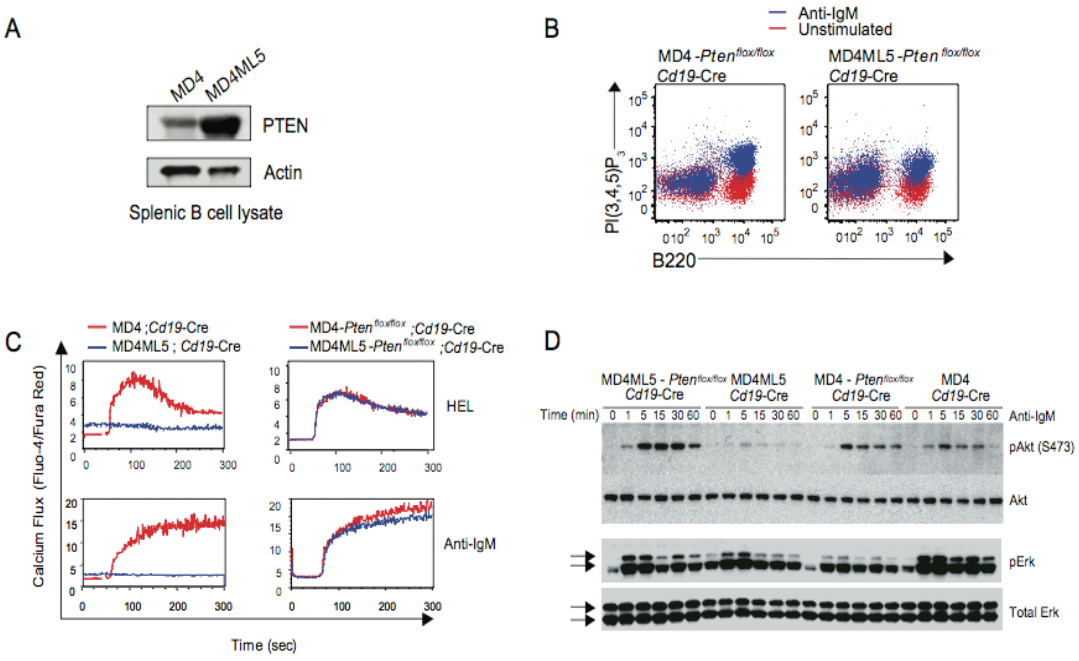


**Figure 1-2**: **PTEN protein level is increased in anergic B cells and PI3kinase signaling is recovered in PTEN-deficient B cells.** A) Purified B cells from MD4 and MD4ML5 mice were lysed and immunoblotted with anti-PTEN or anti-actin. B) Splenic cells from MD4PTEN$^{flox/flox}$ and MD4ML5PTEN$^{flox/flox}$ mice were stimulated with anti-IgM F(ab')$_2$ (blue) or left unstimulated (red) for 5 min. Cells were fixed, permeabilized and stained with antibodies against B220 and PI(3,4,5)$P_3$ and analyzed by flow cytometry. C) Purified splenic B cells from MD4, MD4ML5, MD4PTEN$^{flox/flox}$ and MD4ML5PTEN$^{flox/flox}$ mice were stimulated with 10 µg/ml HEL (upper panels) or 10 µg/ml anti-IgM F(ab')$_2$ (lower panels), and $Ca^{++}$ flux was measured by Fluo-4(530 nm)/Fura Red(685 nm) emission ratiometry. MD4 and MD4PTEN$^{flox/flox}$ cells are depicted in red, while MD4ML5 and MD4ML5PTEN$^{flox/flox}$ cells are depicted in blue. Figure 2C was contributed by Chris DelNagro D) Purified MD4, MD4ML5, MD4PTEN$^{flox/flox}$ and MD4ML5PTEN$^{flox/flox}$ splenic B cells were stimulated with anti-IgM F(ab')$_2$ for the indicated times, and cell lysates were immunoblotted with antibodies against phosphorylated Akt (S473), total Akt, phosphorylated Erk and total Erk.

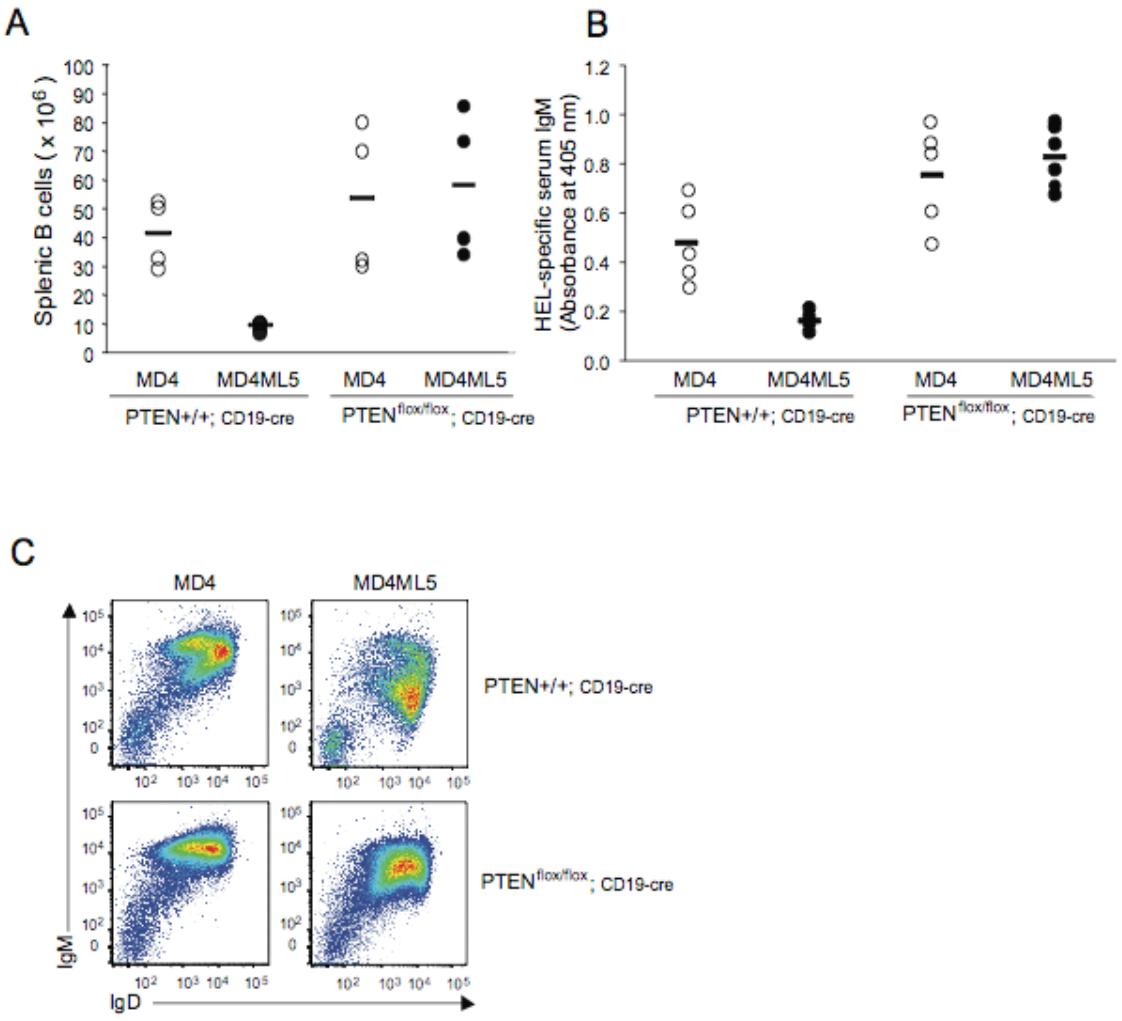


**Figure 1-3: MD4ML5 PTEN-deficient mice do not display an anergic phenotype.**
A) Splenic B cells from MD4, MD4ML5, MD4PTEN$^{flox/flox}$ and MD4ML5PTEN$^{flox/flox}$ mice were enumerated. B) HEL-specific serum IgM levels from MD4, MD4ML5, MD4PTEN$^{flox/flox}$ and MD4ML5PTEN$^{flox/flox}$ mice were determined by ELISA. C) IgM/IgD profiles of B cells from MD4, MD4ML5, MD4PTEN$^{flox/flox}$ and MD4ML5PTEN$^{flox/flox}$ mice were determined by flow cytometry.

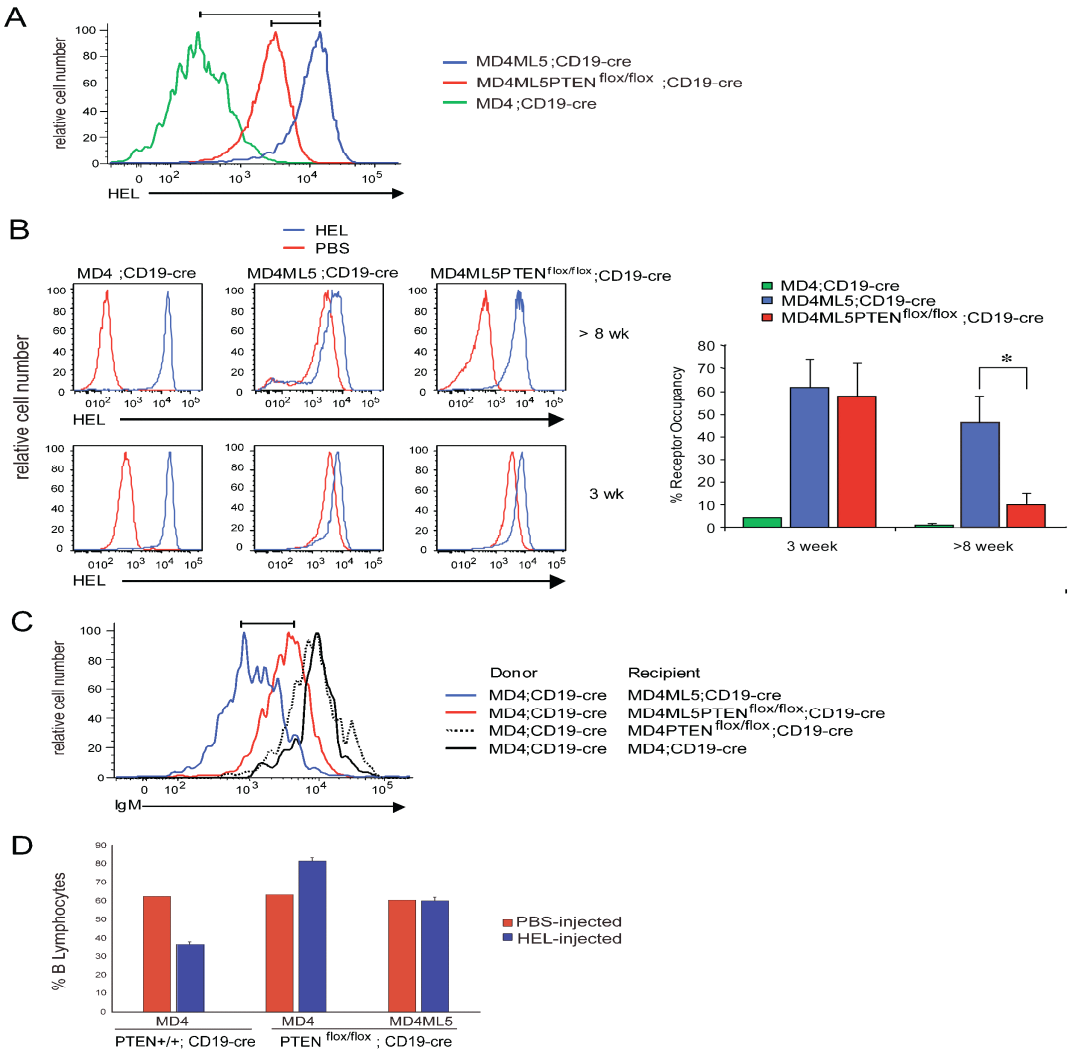


**Figure 1-4: MD4ML5 PTEN-deficient B cells exhibit low receptor occupancy.**
A) Surface HEL staining of MD4 (green), MD4ML5 (blue) and MD4ML5PTEN$^{flox/flox}$ (red) B cells was determined by flow cytometry. B) (*Upper, left panels)*, MD4, MD4ML5, and MD4ML5PTEN$^{flox/flox}$ splenic cells from adult mice (> 8 weeks old) and (lower, left panels) young mice (3 weeks old) were incubated in 20 µg/ml HEL (blue) or PBS (red). Surface HEL was detected using polyclonal antibody against HEL and measured by flow cytometry. *Right panel*, Percent receptor occupancy was determined from the ratio of HEL staining intensity of PBS-incubated cells to HEL-incubated cells. The asterisk (*) indicates a p value of < 0.05. C) MD4 B cells were CFSE-labelled and equal cell numbers were transferred into MD4ML5 (blue), MD4ML5PTEN$^{flox/flox}$ (red), MD4PTEN$^{flox/flox}$ (dotted) and MD4 (black) recipient mice by tail vein injection. After 24 hr, recipient splenic cells were harvested, stained with anti-B220 and anti-IgM. CFSE+ donor B cells were gated, and surface IgM was analyzed by flow cytometry. D). MD4, MD4PTEN$^{flox/flox}$ and MD4ML5PTEN$^{flox/flox}$ mice were injected with 1 mg of HEL (blue), 3 mice per group or PBS (red), one mouse per group. Splenic cells were isolated at 48 hr post-injection, enumerated and examined for expression of B220 by flow cytometry. Histograms represent B220 gated cells. Figure 1-4D was contributed by Matthew Cato.

A

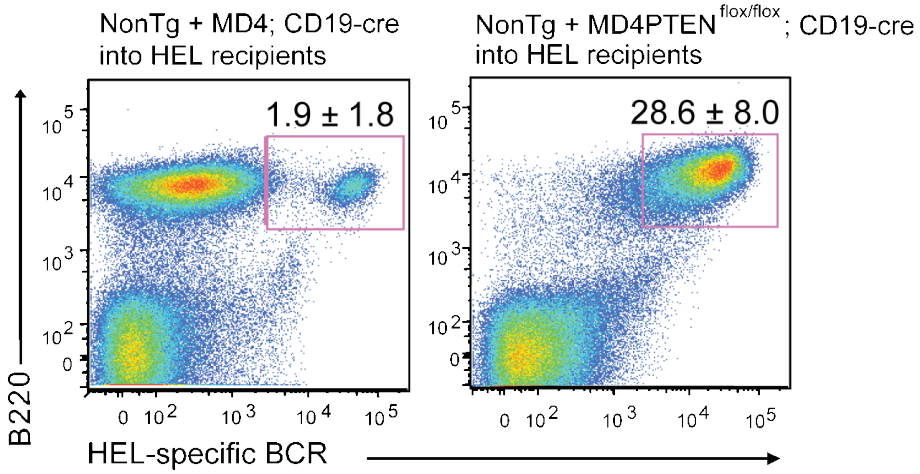


B

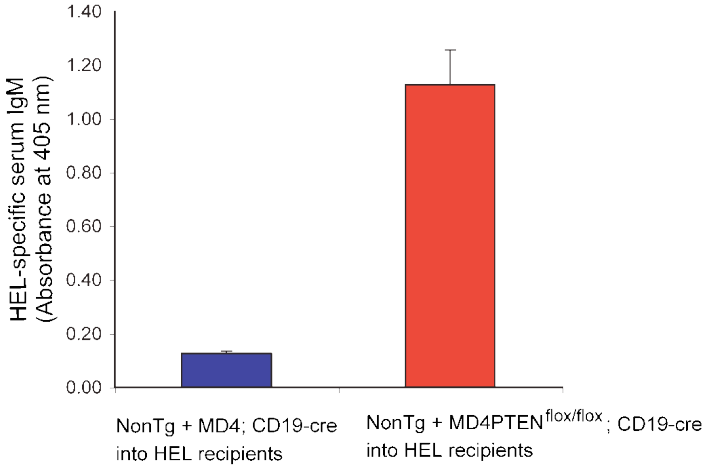


**Figure 1-5: Bone marrow reconstitution.** A. Reconstitution with mixed bone marrow HSCs consisting of Non-Tg wildtype (20%) plus either MD4 (80%, left panel) or MD4PTENflox/flox (80%, right panel) in ML5 recipients (n=3 for each group). The frequencies of HEL-specific B cells were determined after 12 weeks of reconstitution. Figure 5A was contributed by Matthew Cato. B) Sera from bone marrow chimeric recipient animals were analyzed for HEL-specific IgM by ELISA. Absorbances are depicted in the bar graph. Each bar represents the average of 3 chimeric mice.

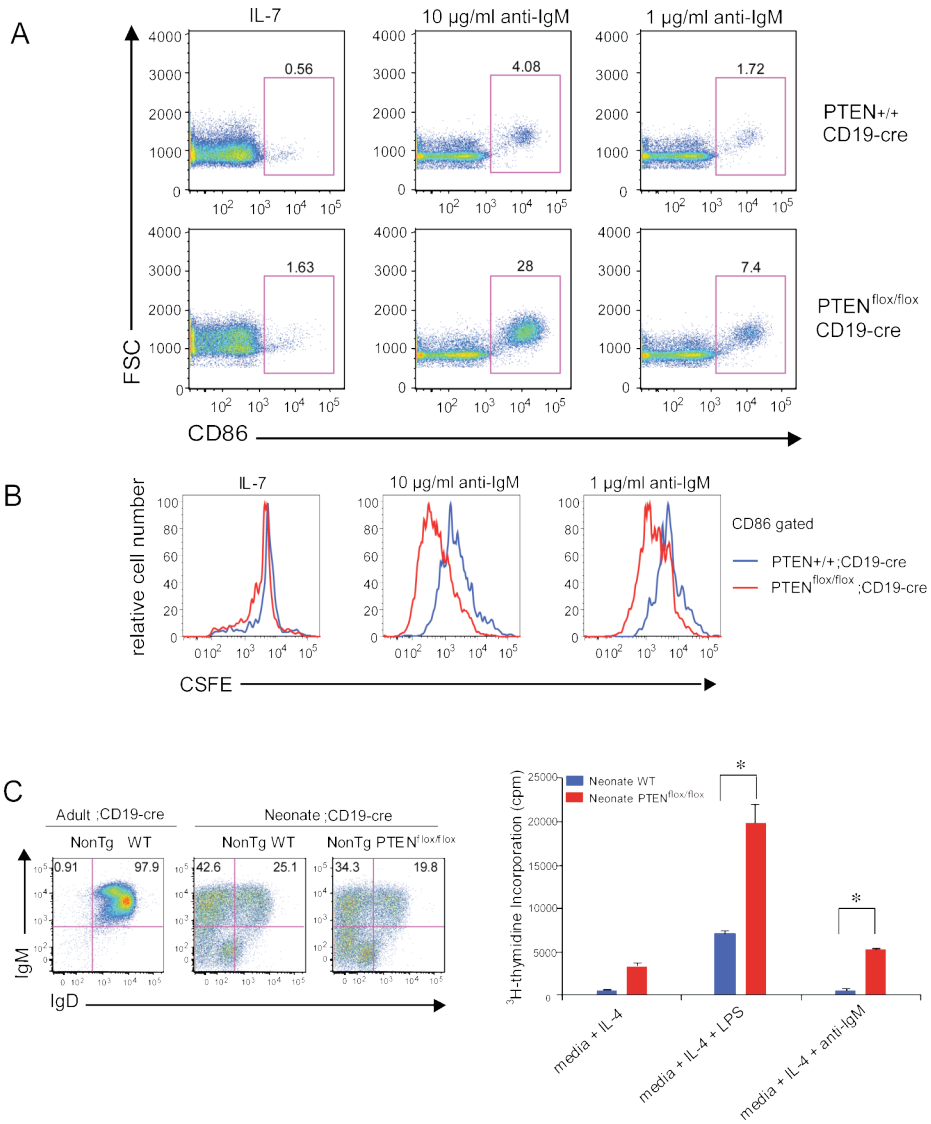


**Figure 1-6: Negative selection is impaired in MD4ML5 PTEN-deficient mice**

A) Non-transgenic wildtype and PTEN-deficient bone marrow B cells were purified, and cells were cultured in rIL-7 for 6 days. Cells were labeled with CFSE, and cultured with 10 µg/ml or 1 µg/ml anti-IgM F(ab')$_2$ or 10 ng/ml rIL-7 for 3 days. Cells were collected, stained for B220, 7AAD and CD86. 7AAD-, B220+ cells were gated. B) CD86+ cells above were stained with CFSE and the degree of proliferation was assessed in CD86-gated subsets. Figures A and B were contributed by Hart Dengler. C) *Left panel*, IgM/IgD profiles of splenic B cells from adult wildtype, neonate wildtype and neonate PTEN-deficient non-transgenic mice were analyzed by flow cytometry. *Right panel*, splenic B cells from a 5 day old non-transgenic wildtype neonatal mouse (blue) and a 5 day old non-transgenic PTEN-deficient neonatal mouse (red) were harvested and cultured in IL-4 alone or in IL-4 plus either LPS or anti-IgM F(ab)'$_2$ in a 96-well plate. After 48 hr in culture, 1 µCi of $^3$H-thymidine was added to each well, and triplicate wells were harvested 16 hr later. Proliferation was measured by scintillation counting. This is a representative of two experiments. Asterisks (*) indicate a p value of $< 0.05$.

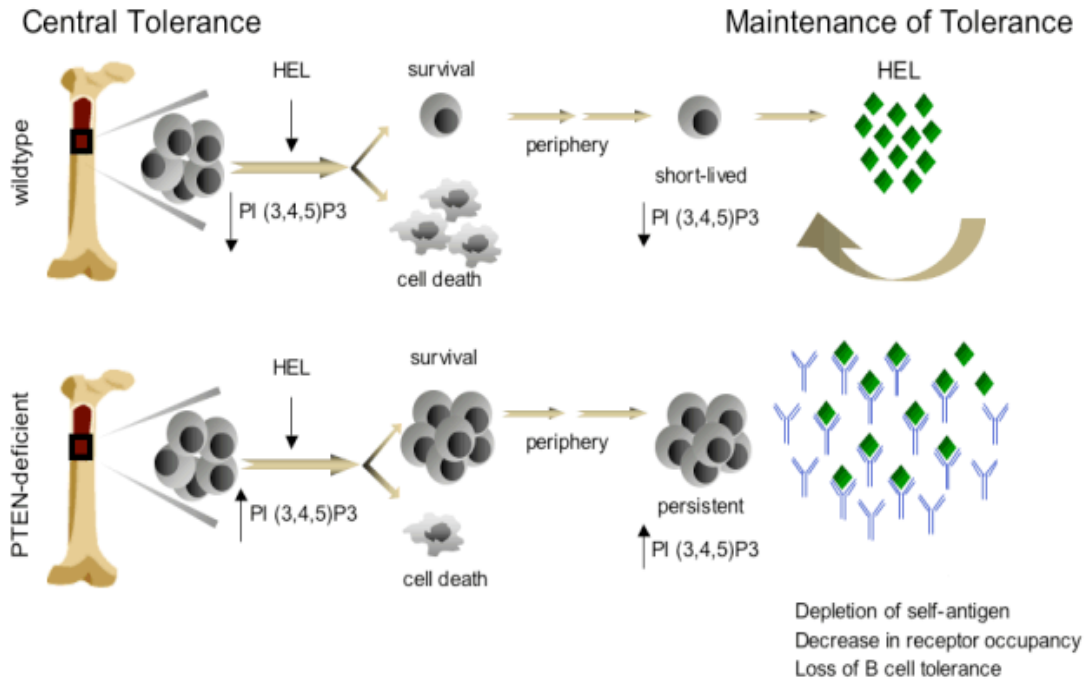


**Figure 1-7: Model depicting the impact of PTEN loss in central and peripheral tolerance**. Dysregulation of PIP3 activation leads to survival and persistence of self-reactive B cells.

Supplementary Figure 1A

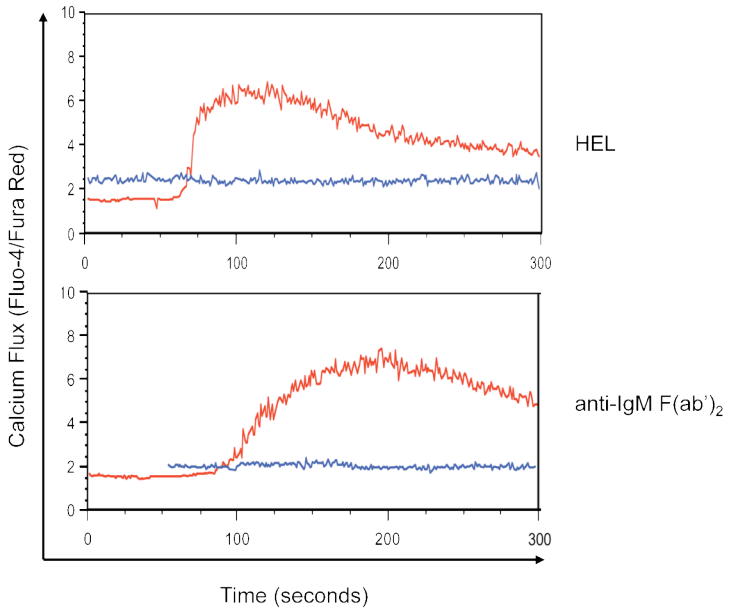


Supplementary Figure 1B


**Supplementary Figure 1-1: PI3Kinase signaling is reduced in MD4ML5 mice.** A) Purified splenic MD4 and MD4ML5 B cells were stimulated with 1 μg/ml hen egg lysozyme (upper panel) or 1 μg/ml anti-IgM F(ab')$_2$ (lower panel). Calcium flux was measured by fluorescence ratiometry. Supplementary Figure 1-1A was contributed by Chris DelNagro. B) Purified splenic MD4 and MD4ML5 B cells were stimulated with 15 μg/ml anti-kappa for the indicated time points. Cells were lysed and immunoblotted for phosphorylated Akt (S473) and actin.

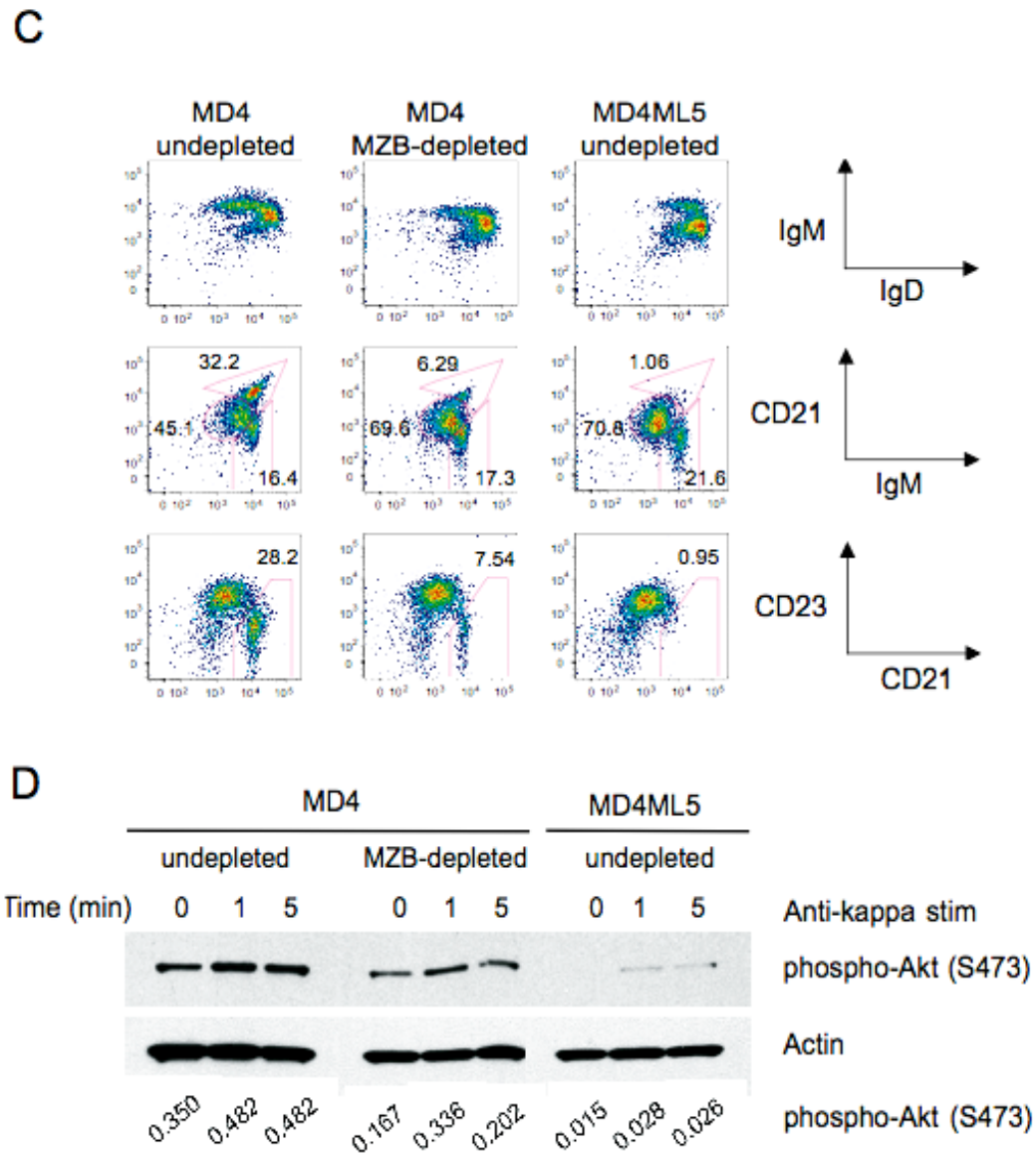


**Supplementary Figure 1-1 continued: PI3Kinase signaling is reduced in MD4ML5 mice.** C) Splenic B cells were purified by negative selection using anti-CD43-conjugated magnetic beads. Purified B cells were subsequently incubated in anti-CD9-biotin. After washing, cells were incubated in anti-biotin-conjugated magnetic beads. CD9-negative population was collected. The marginal zone compartments of pre- and post-depletion fractions were analyzed by flow cytometry. D. Pre- and post-MZ depleted fractions were stimulated with 15 μg/ml anti-kappa for 0, 1 and 5 min. Cells were lysed and immunoblotted for phosphorylated Akt (S473) and actin. Densitometric units were normalized against actin and normalized phosphorylated Akt readings are indicated below each lane.

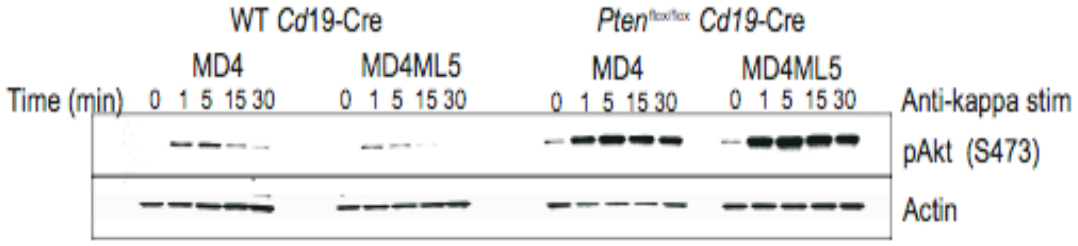


**Supplementary Figure 1-2: PI3kinase signaling is enhanced in the absence of PTEN.** Purified splenic MD4, MD4ML5, MD4PTEN$^{flox/flox}$, and MD4ML5PTEN$^{flox/flox}$ B cells were stimulated with 15 μg/ml anti-kappa for the indicated time points and immunoblotted for phosphorylated Akt (S473) and actin.

Supplementary Figure 3A

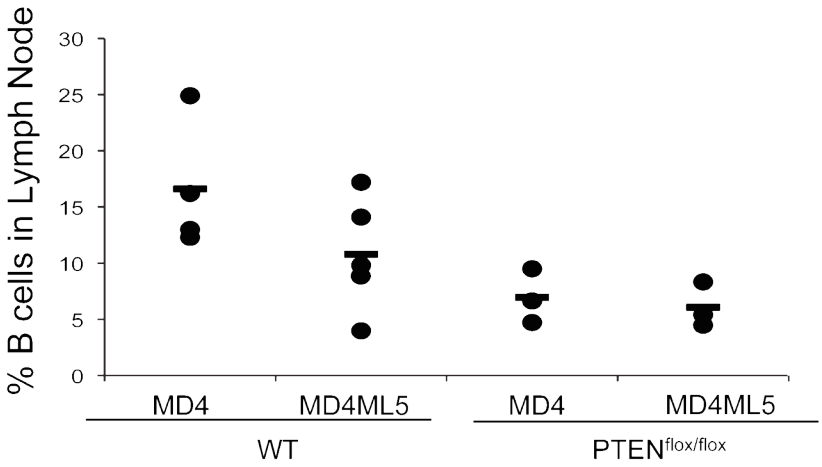


Supplementary Figure 3B

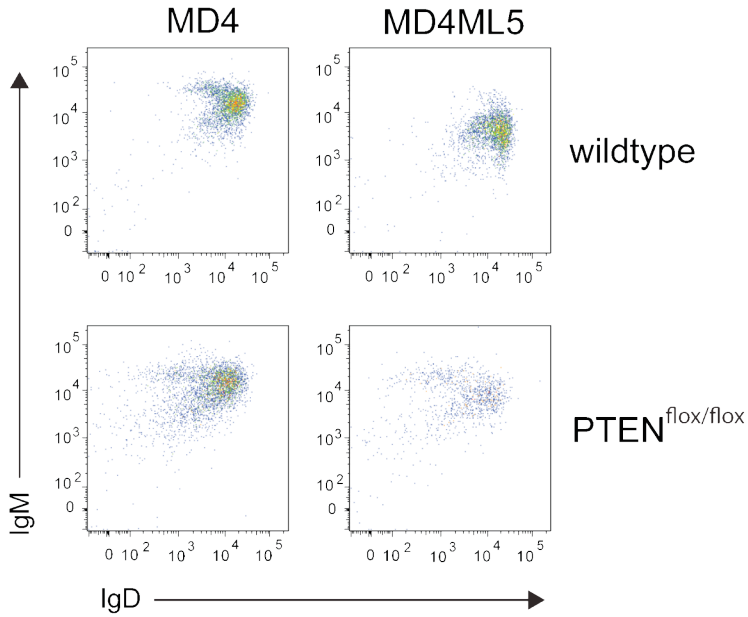


**Supplementary Figure 1-3: Low B cellularity in the lymph nodes of PTEN-deficient animals and restored IgM/IgD profiles in the PTEN-deficient MD4ML5 mice:** A) Inguinal lymph nodes were isolated from MD4, MD4ML5, MD4PTEN$^{flox/flox}$ and MD4ML5PTEN$^{flox/flox}$ mice. Lymph node B cells were quantified by B220 staining and flow cytometry. B) IgM/IgD profiles of MD4, MD4ML5, MD4PTEN$^{flox/flox}$ and MD4ML5PTEN$^{flox/flox}$ lymph node B cells were analyzed by flow cytometry.

Supplementary Figure 4

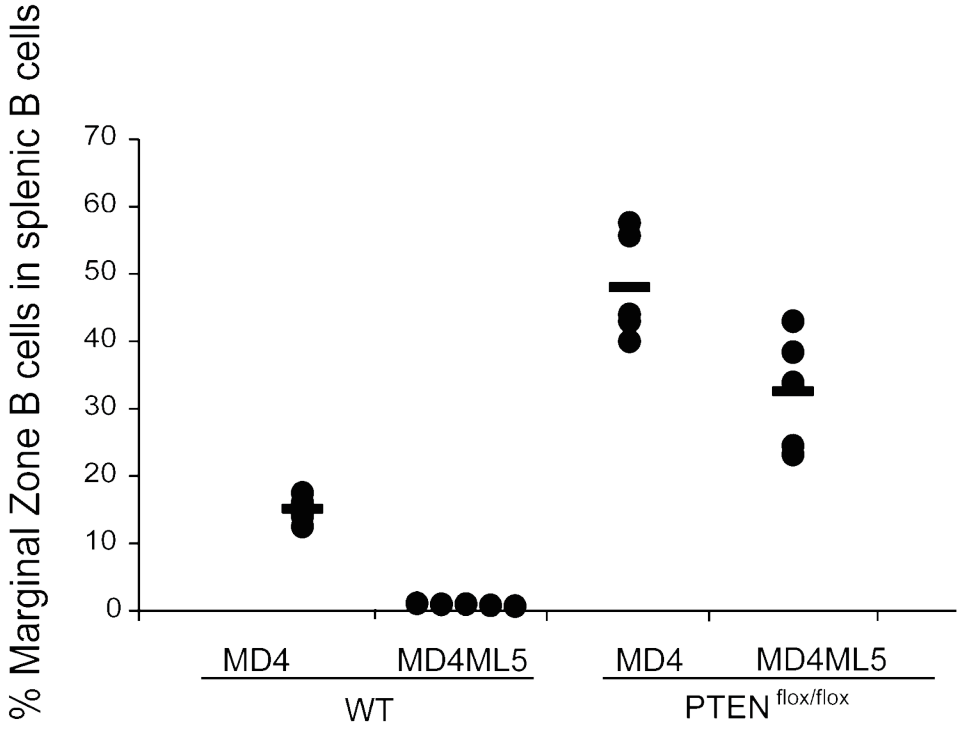


**Supplementary Figure 1-4: Marginal zone B cell compartment is restored in PTEN deficient MD4ML5 mice.** Splenic cells were isolated from MD4, MD4ML5, MD4PTEN$^{flox/flox}$ and MD4ML5PTEN$^{flox/flox}$ mice. Marginal zone B cells were quantified by B220, CD23, CD21 and IgM staining and flow cytometry.

# CHAPTER 2

## CD98hc facilitates B cell proliferation and adaptive humoral immunity

### 2.1 – Introduction

Adaptive immunity is a vertebrate specialization that requires the selective proliferation of antigen-specific lymphocytes (1, 2). The CD98 heavy chain (CD98hc; also called 4F2hc; A000262), encoded by *Slc3a2*, is a vertebrate membrane protein whose expression is much higher in proliferating lymphocytes (3). Originally described 25 years ago as a lymphocyte-activation antigen (3), the function of CD98hc in the immune system has remained obscure. CD98 has two distinct functions: facilitating amino acid transport (4, 5) and mediating integrin signaling (6, 7). The 80-kilodalton CD98hc is covalently linked to one of several 40-kilodalton light chains, which function as amino acid transporters (4, 5). Transport of leucine and isoleucine is mediated by the CD98 heterodimer (4, 5); these amino acids are important regulators of the mTOR pathway, which governs nutrient-regulated lymphocyte function (8, 9). CD98hc also interacts with certain integrin β-subunits to mediate signaling events that control cell migration, survival and proliferation (7). CD98hc is first found in primitive vertebrates, coincident with the appearance of adaptive immunity (2, 10). Consequently, we hypothesized that CD98hc could be involved in the rapid lymphocyte proliferation required for effective adaptive immunity.

Here we report that CD98hc facilitates humoral immunity by supporting the rapid proliferation of B cells that is necessary for clonal expansion and subsequent differentiation into plasma cells. We deleted CD98hc in B cells by crossing mice bearing

a *lox*P-flanked (floxed) *Slc3a2* allele (*Slc3a2*$^{f/f}$) with those expressing Cre recombinase in B cells (CD19-Cre$^{+}$). The resultant *Slc3a2*$^{f/f}$ CD19-Cre$^{+}$ had normal maturation and distribution of peripheral B cells and normal morphology of secondary lymphoid organs. *Slc3a2*$^{f/f}$CD19-Cre$^{+}$ mice immunized with T cell–dependent or T cell–independent antigens had much lower antibody responses than did control *Slc3a2*$^{f/f}$ mice without CD19-Cre, because of complete suppression of B cell proliferation and plasma cell formation by CD98hc-null B cells. A mutant form of CD98hc that mediates integrin signaling but not amino acid transport supported the proliferation of CD98hc-deficient B cells; hence, the region of CD98hc that mediates integrin interaction is required for B cell proliferation and the domain that facilitates the amino acid–transport function is dispensable for this. Furthermore, mitogenic stimulation of a mixture of CD98hc-deficient and CD98hc-sufficient B cells resulted in considerable enrichment for CD98hc-sufficient cells; this finding establishes the ability of CD98hc to confer a strong selective advantage during rapid B cell proliferation. Thus, the ability of CD98hc to enable clonal expansion, which is necessary for adaptive immunity, may have favored the appearance and retention of CD98hc in vertebrates (10).

## 2.2 - Results

### 2.2.1 - B cell CD98hc is needed for antibody responses

Because germline loss of CD98hc is embryonically lethal (11), we targeted CD98hc by flanking exons 1 and 2 of *Slc3a2* with *lox*P sites that specified Cre recombinase–mediated deletion of the cytoplasmic and transmembrane region of CD98hc (Supplementary Figure 2-1a), thus leading to complete loss of CD98hc expression (12). We crossed *Slc3a2*f/f mice with mice bearing Cre recombinase under control of the endogenous B cell–specific *Cd19* locus (13). The resulting *Slc3a2*f/fCD19-Cre+ mice had specific deletion of CD98hc in B lymphocytes beginning at the transition from pro–B cell to pre–B cell, when CD19 expression is first induced (14). In the splenic B cell compartment, 70–90% of cells lacked CD98hc (Fig. 2-1a), and we did not detect any deletion in T cells or monocytes-macrophages (Fig. 2-1b), consistent with the efficiency and specificity of CD19-Cre–mediated recombination (13). B cells from *Slc3a2*$^{flf}$ littermates lacking CD19-Cre (*Slc3a2*$^{f/f}$CD19-Cre$^{-}$ mice) were uniformly positive for CD98hc (Fig. 2-1a).

To assess whether CD98hc is important for the secretion of antibodies by B cells, we measured circulating immunoglobulin in *Slc3a2*$^{f/f}$CD19-Cre$^{+}$ and *Slc3a2*$^{f/f}$CD19-Cre$^{-}$ mice. Whereas basal circulating concentrations of immunoglobulin M (IgM) were not significantly lower ($P$>0.05) in naive *Slc3a2*$^{f/f}$CD19-Cre$^{+}$ mice, we noted significantly less ($P$<0.025) class-switched IgG in these mice (Supplementary Figure 2-1b). Furthermore, after challenge with T cell–independent antigen in PBS (Fig. 2-2a) or T cell–dependent antigen in complete Freund's adjuvant (CFA; Fig. 2-2b), we noted much lower antigen-specific IgM and IgG concentrations in *Slc3a2*$^{f/f}$CD19-Cre$^{+}$ mice than in

*Slc3a2*$^{f/f}$CD19-Cre$^{-}$ mice. This defect was not specific to Toll-like receptor signals, because we obtained similar results after immunization with T cell–dependent antigens in adjuvant lacking microbial components (incomplete Freund's adjuvant; Fig. 2-2c). In addition, this correlated with the 'gene dosage' of *Slc3a2*; *Slc3a2*$^{f/-}$CD19-Cre$^{+}$ mice had a more severe defect than did *Slc3a2*$^{f/+}$CD19-Cre$^{+}$ mice (Supplementary Figure 2-2). Thus, B cell CD98hc is important for mounting specific antibody responses to antigenic challenge.

CD98hc is involved in integrin signaling, and integrins are involved in the localization and distribution of B cells subsets (15, 16). In addition, CD98hc is important for integrin-mediated migration of mesenchymal cells (7). To test whether loss or misdistribution of B cell subsets could explain the impaired antibody production of *Slc3a2*f/fCD19-Cre+ mice, we examined lymphoid tissue for the presence and localization of B cell subsets. Despite the involvement of CD98hc in adhesive signaling and amino acid transport (6, 7, 17), CD98hc-deficient follicular B cells, marginal zone B cells, transitional B cells and peritoneal B1 cells were present in normal percentages in the periphery; in addition, pro–B cells, pre–B cells, immature B cells, and mature B cells were present in normal proportions in the bone marrow (Fig. 2-3a). Similarly, we detected no significant difference in the absolute numbers of these subsets in *Slc3a2*f/fCD19-Cre+ versus *Slc3a2*f/fCD19-Cre$^{-}$ mice ($P > 0.05$; Supplementary Figure 2-3). *Slc3a2*$^{f/f}$CD19-Cre$^{+}$ mice also had normal splenic architecture, as follicular B cells segregated with intact marginal zones, and *Slc3a2*$^{f/f}$CD19-Cre$^{-}$ and *Slc3a2*$^{f/f}$CD19-Cre$^{+}$ mice had similar numbers of germinal centers (Fig. 2-3b). Finally, we detected no differences between naive *Slc3a2*$^{f/f}$CD19-Cre$^{-}$ and *Slc3a2*$^{f/f}$CD19-Cre$^{+}$ mice in terms of

formed elements of the blood (Supplementary Figure 2-4) or the concentration of circulating natural IgM (Fig. 2-3c). Thus, CD98hc is not required for the formation of mature B cells or their ability to populate secondary lymphoid organs.

### 2.2.2 - B cell CD98hc is necessary for plasma cell formation

B cells differentiate into antibody-secreting plasma cells after antigenic challenge, which suggests that a requirement for CD98hc in plasma cell formation might explain the lower humoral immune responses of *Slc3a2*f/fCD19-Cre+ mice. To test that idea, we purified resting splenic B cells from *Slc3a2*f/fCD19-Cre+ mice, depleted the population of any B cells expressing CD98hc and stimulated the remaining population with lipopolysaccharide (LPS) to induce the formation of plasma cells. B cells from *Slc3a2*f/fCD19-Cre+ mice were defective both in class switching (Fig. 2-4a) and in development into CD138+ plasma cells (Fig. 2-4b). This phenotype bears similarities to that of $\beta_1$ integrin–deficient B cells (16). The few plasma cells formed by *Slc3a2*f/fCD19-Cre+ B cells expressed CD98hc (Supplementary Figure 2-5), which indicated that they were the progeny of a few remaining CD98hc-expressing cells that had escaped Cre-mediated recombination and *in vitro* depletion. Indeed, when we omitted the step of *in vitro* depletion of CD98hc-expressing cells, the 10–20% of B cells that expressed CD98hc in *Slc3a2*$^{f/f}$CD19-Cre$^{+}$ mice generated near normal percentages of plasma cells *in vitro* (Supplementary Figures 2-6 and 2-7).

Consistent with the defective formation of antibody-secreting plasma cells, B cells from *Slc3a2*$^{f/f}$CD19-Cre$^{+}$ mice also had impaired antibody secretion after LPS stimulation *in vitro* (Fig. 2-4c). As shown by enzyme-linked immunospot assay,

*Slc3a2*$^{f/f}$CD19-Cre$^{+}$ mice immunized with a T cell–dependent antigen also had fewer cells that secreted antigen-specific antibody immediately after isolation than did immunized *Slc3a2*$^{f/f}$CD19-Cre$^{-}$ mice (Fig. 2-4d). These data collectively show that without CD98hc, B cells are considerably impaired in their ability to form plasma cells.

### 2.2.3 - CD98hc is required for rapid B cell proliferation

Differentiation into plasma cells is preceded by many rounds of proliferation, which leads to larger numbers of antigen-specific B cells (18); class switching is also independently regulated by cell division (19). Published reports using blocking or crosslinking antibody suggest that CD98hc is involved in the proliferation of T cells (20, 21) and keratinocytes (22). To assess the function of CD98hc in B cell proliferation, we purified CD98hc-deficient or CD98hc-sufficient resting splenic B cells from *Slc3a2*$^{f/f}$CD19-Cre$^{+}$ or *Slc3a2*$^{f/f}$CD19-Cre$^{-}$ mice, respectively, labeled them with the intracellular dye CFSE, stimulated them with B cell mitogens and measured their proliferation by flow cytometry asessing dye dilution. By 5 d after stimulation, B cells from *Slc3a2*$^{f/f}$CD19-Cre$^{-}$ mice had divided five to eight times, as shown by discrete populations of daughter cells with exponential dilution of fluorescence (Fig. 2-5a). In contrast, B cells from *Slc3a2*$^{f/f}$CD19-Cre$^{+}$ littermates showed minimal division in response to the B cell antigen receptor–crosslinking agent antibody to IgM (anti-IgM), provided alone or together with interleukin 4 (IL-4) or anti-CD40; we obtained similar data by directly counting viable cells (Supplementary Figure 2-8). A few cells from *Slc3a2*$^{f/f}$CD19-Cre$^{+}$ mice did undergo one to two divisions in response to stimulation with a high dose of LPS (Fig. 2-5a). However, those divided cells expressed CD98hc

(Fig. 2-5b), which suggests that they had escaped Cre-mediated deletion of *Slc3a2*. Thus, CD98hc is necessary for the rapid proliferation of mature B cells in response to antigen or other mitogenic signals. In the absence of stimulation, the lack of CD98hc did not appreciably alter the viability of cultured B cells (Supplementary Figure 2-8), which suggests that the low CD98 expression in the resting state is not required for B cell survival. Thus, CD98hc is crucial for the rapid B cell population expansion and plasma cell formation in response to external stimuli that drive adaptive humoral immunity.

CD98hc has two well-documented biochemical functions. First, it interacts with certain integrin β-subunits to mediate integrin signaling (6, 23) and therefore influences adhesion-induced signaling events such as activation of the kinases $pp125^{FAK}$, PI(3)K and Akt and the adhesion molecule $p130^{CAS}$, which control cell proliferation (7). In addition, by associating with CD98 light chains such as Lat-1, CD98hc facilitates the transport of amino acids such as leucine and isoleucine (4, 5). These amino acids are important regulators of mTOR24, a critical 'node' in a signaling pathway that controls immune responses (8, 9). Chimeric constructs in which portions of CD98hc are replaced with portions of CD69, another type II transmembrane protein, allow distinct separation of these two CD98hc functions17 (Fig. 2-6a). We used such chimeras to identify the mechanism whereby CD98hc enables B cell proliferation.

To study the function of these chimeras in primary B cells, we infected bone marrow from *Slc3a2*$^{f/f}$CD19-Cre$^{+}$ mice with retrovirus containing bicistronic mRNA encoding either human CD98hc or a human CD98-CD69 chimera followed by an internal ribosomal entry site and a cassette encoding green fluorescent protein (GFP). We used these transduced bone marrow cells to reconstitute lethally irradiated recipient mice to

create mice in which B cells that developed and continued to express a human CD98-CD69 chimera were marked by GFP fluorescence (Fig. 2-6a and Supplementary Figures 2-9 and 2-10a). Staining with an antibody specific for mouse CD98hc enabled us to identify B cells that lacked mouse CD98hc but expressed retrovirus-encoded human CD98hc chimeras; these cells were present in the blood beginning as early as 3 weeks after bone marrow transfer. Furthermore, all B cells that expressed GFP also stained for either human CD98hc or CD69 (Supplementary Figure 2-10b). At 6 weeks after bone marrow transfer, we purified resting CD98hc-null mouse splenic B cells, labeled them with the membrane dye DiD to monitor proliferation and stimulated them with LPS. Then, 4 d later, we analyzed proliferation by means of flow cytometry assessing dye dilution (Fig. 2-6b). We found proliferation of B cells reconstituted with full-length human CD98hc or with the integrin-interacting chimera C98T98E69 (consisting of the cytoplasmic (C) domain of CD98hc, the transmembrane (T) domain of CD98hc and the extracellular (E) domain of CD69). In contrast, the C98T69E98 chimera, which interacts with Lat-1 and mediates isoleucine transport but does not interact with integrins, failed to reconstitute proliferation. Thus, the integrin-signaling portion of CD98hc is necessary and sufficient for the proliferation of mature B cells.

**2.2.4 - Loss of CD98hc inhibits integrin-dependent events**

Integrin ligation leads to signals that result in cell spreading and migration (25). In addition, integrins act in synergy with certain tyrosine kinase receptors to prolong and sustain activation of the mitogen-activated protein kinase Erk1/2, which promotes cell proliferation (26) by downregulating cyclin-dependent kinase inhibitors (27) and

facilitating progression through the G1 phase of the cell cycle (28, 29). B cells from *Slc3a2*$^{f/f}$CD19-Cre$^{+}$ mice had less phosphorylation of Erk1/2 at 17 hr after BCR ligation (Fig. 2-7a). In contrast, early activation (<1 h) of the kinases Erk1/2, Akt and Syk was intact in B cells lacking CD98hc (Supplementary Figures 2-11a–c), as was the expression of activation markers (Supplementary Figure 2-11d). However, coincident with a failure to sustain Erk1/2 activation, *Slc3a2*$^{f/f}$CD19-Cre$^{+}$ B cells showed impaired downregulation of the cyclin-dependent kinase inhibitor p27 (Fig. 2-7b), consistent with the observed lack of proliferation. Thus, the absence of CD98hc selectively impairs sustained activation of Erk1/2 after BCR ligation, an event known to depend on integrins in other cell types.

To directly assess the effect of CD98hc deficiency in B cells on another integrin-dependent function, we used a B cell adhesion and spreading assay (30, 31). Activated B cells from *Slc3a2*$^{f/f}$CD19-Cre$^{+}$ mice failed to spread after direct antibody-mediated ligation of the integrin $\alpha_L\beta_2$ (LFA-1; Fig. 2-7c). In contrast, CD98hc-bearing B cells from their *Slc3a2*$^{f/f}$CD19-Cre$^{-}$ littermates spread extensively, as shown by their twofold larger cell area and perimeter relative to that of the CD98hc-deficient B cells. In sum, these data point to the potential importance of integrin signaling in B cell proliferation.

As an initial test of that idea, we analyzed responses to cross-linking of the B cell antigen receptor on B cells from mice engineered to lack all leukocyte integrins (32). Even though some of these B cells expressed a small quantity of integrin $\beta_1$, they showed less proliferation in response to BCR ligation (Supplementary Figure 2-12), which provides direct evidence of the involvement of integrins in B cell proliferation. The occurrence of some proliferation of these B cells raises the possibility that the loss of

amino acid transport resulting from CD98hc deficiency may also contribute to the more profound defect in proliferation of CD98hc-deficient B cells.

**2.2.5 - CD98hc confers a selective advantage on B cells**

During T cell–dependent responses, antigen-specific B cell populations expand in germinal centers in competition for limited antigen (33). The experiments reported above indicated that CD98hc conferred a strong selective advantage during B cell population expansion *in vitro*. To measure that advantage *in vivo*, we immunized *Slc3a2*f/fCD19-Cre+ mice with trinitrophenyl–keyhole limpet hemocyanin (TNP-KLH), a T cell–dependent antigen, and analyzed CD98hc expression on splenic B cell subsets. In this experiment, CD98hc was present on less than 10% of resting splenic B cell subsets (Fig. 2-8a). However, during the germinal center response, B cells undergo a proliferative burst and are selected for the ability to bind antigen with high affinity. At this stage, the percentage of CD98hc-expressing cells in the *Slc3a2*f/fCD19-Cre+ mice increased from less than 10% to 40% (Fig. 2-8a). Furthermore, after class switching, over 99% of plasma cells in *Slc3a2*f/fCD19-Cre+ mice had detectable surface expression of CD98hc (Fig. 2-8a). Thus, there were no detectable CD98-null plasma cells in *Slc3a2*f/fCD19-Cre+ mice; these observations are consistent with our *in vitro* finding that CD98hc was required for the rapid proliferation of mature B cells and subsequent formation of plasma cells.

*Slc3a2*$^{f/f}$CD19-Cre$^{+}$ mice had considerably fewer germinal center B cells and plasma cells than *Slc3a2*$^{f/f}$CD19-Cre$^{-}$ mice had at 1 week after immunization (data not shown), probably because they had far fewer CD98hc-expressing precursor cells able to

proliferate in germinal centers and form plasma cells. However, at 2–3 weeks after immunization, titers of antibodies specific for TNP-KLH in *Slc3a2*$^{f/f}$CD19-Cre$^{+}$ mice were similar to those in *Slc3a2*$^{f/f}$CD19-Cre$^{-}$ mice, probably because of germinal center selection for the few pre-existing CD98hc-expressing antigen-specific B cells (Supplementary Figure 2-13). This strong selection for CD98hc-expressing B cells can thus account for the relatively modestly lower basal serum IgG concentrations in *Slc3a2*$^{f/f}$CD19-Cre$^{+}$ mice. Immunohistochemical staining for CD98hc in spleens of immunized mice confirmed that, in contrast to the surrounding follicular B cells, germinal center B cells in *Slc3a2*$^{f/f}$CD19-Cre$^{+}$ mice expressed CD98hc (Fig. 2-8b). *In vitro* analysis of B cells purified from *Slc3a2*$^{f/f}$CD19-Cre$^{+}$ mice without depletion of CD98-expressing cells provided further confirmation of the strong selective advantage conferred by CD98hc; after 4 d in culture, 99% of plasma cells expressed CD98hc (Fig. 2-8c).

CD98hc is upregulated 20- to 30-fold after B cell activation, and we have shown here that CD98hc was required for B cells to proliferate and to differentiate into plasma cells. Hence, we propose that upregulation of CD98hc can serve as a checkpoint in the progression to humoral immunity. Consequently, the expression and function of CD98hc are potential targets for the modulation of antibody responses.

**2.3 - Discussion**

CD98hc was one of the earliest lymphocyte activation antigens described (3), yet its function in the immune response has remained obscure. Although studies in which T cells were treated with anti-CD98hc *in vitro (*20, 21, 34) have suggested that CD98hc is involved in T cell activation, the function of CD98hc in lymphocytes *in vivo* has remained unknown. Here we have shown that CD98hc is absolutely required for the rapid B cell clonal proliferation necessary for their subsequent differentiation into antibody-secreting plasma cells. Consequently, higher CD98hc expression provides antigen-stimulated B cells with a profound selective advantage.

The linkage of the integrin-binding function of CD98hc to B cell proliferation suggests a new paradigm for the function of integrin signaling in lymphocytes. In addition to functioning in hematopoiesis, trafficking and the formation of immune synapses (16, 35, 36, 37, 38, 39), our work has indicated that integrin signaling is involved in clonal proliferation during immune responses. CD98hc serves two cellular functions; the first is amino acid transport, through interaction with one of several CD98 light chains (4, 5). The extracellular domain of CD98hc is responsible for this function, and reconstitution with a chimeric protein containing this domain of CD98hc was not sufficient to restore the proliferation of CD98-null B cells. The second main function of CD98hc is mediating integrin signaling (6, 7). The transmembrane and cytoplasmic domains of CD98hc are necessary for interaction with integrin β-subunits, which leads to $pp125^{FAK}$-dependent activation of Akt by PI(3)K and $p130^{CAS}$-mediated activation of the small GTPase Rac (7). Reconstitution with a chimeric protein that contained only the

transmembrane and cytoplasmic portions of CD98hc was sufficient to restore the proliferation of CD98hc-null B cells.

Integrins can act together with immunoreceptors, using similar 'downstream' signaling proteins, to promote lymphocyte proliferation and activation (40). Thus, our findings establish a nexus of CD98hc-dependent integrin and immunoreceptor signaling pathways that regulate the proliferation of lymphocytes. CD98hc could function by allowing integrins to lower the threshold for cellular activation (41) by efficiently organizing components of the immunological synapse; however, we found that CD98hc was not required for early activation events. Instead, our data support a mechanism whereby CD98h-mediated integrin signals can extend the kinetics of immunoreceptor signals (42) to the point of driving cell division and clonal expansion.

Integrins drive fibroblast proliferation by sustaining Erk activation. Without integrin-mediated adhesion, growth factor signals are transient and are unable to downregulate cyclin-dependent kinase inhibitors such as p27, and cells fail to exit the G1 phase of the cell cycle (26, 28, 29). Our data have indicated that a similar mechanism is operative in B cells. CD98hc-deficient B cells were able to generate early B cell antigen receptor signals but could not sustain late Erk1/2 signaling or downregulate p27 and failed to divide. The inability of CD98hc-deficient B cells to spread on integrin-specific antibodies confirmed the integrin signaling defect of CD98hc-deficient B cells. Published work using supported lipid bilayers or plate-bound antibodies (30) to study the formation of immunological synapses has shown that B cells spread rapidly after activation of the B cell antigen receptor in an integrin-dependent way (30, 43); we have now shown that this spreading is CD98hc dependent. Thus, CD98hc could promote

integrin-dependent changes in cell shape that might stabilize interactions with antigen-bearing cells.

One implication of our work relates to the origin of the adaptive immune system. CD98hc orthologs first appeared in primitive vertebrates (10), as did sequences in integrin β-cytoplasmic domains that permit CD98hc to interact with integrins (44). The coincidence of those events with the appearance of adaptive immunity (2, 10) suggests that the survival advantage conferred by adaptive immunity was among the factors that favored the maintenance of CD98hc and its ability to mediate integrin signaling. CD98hc is overexpressed in many cancers and mediates tumorigenesis (7, 45, 46, 47). In particular, published work has emphasized the importance of integrin signaling (25) in the development and maintenance of epithelial cancers (48, 49) and of CD98hc in potentiating the growth of cancer cells (7, 47). Thus, the appearance of CD98hc in vertebrates, which enabled an adaptive immune response, may have led to greater susceptibility to cancer.

## 2.4 - Methods

### 2.4.1 - Mice

Mice with floxed *Slc3a2* were generated by flanking of exons 1 and 2, which encode the transmembrane portion of CD98hc, with *lox*P sites (12). The neomycin-selection cassette used to select embryonic stem cell clones positive for a floxed *Slc3a2* allele was flanked by Flp sites and thus was excised when mice with floxed *Slc3a2* were bred with human β-actin FLPe deleter mice (Jackson Laboratories). *Slc3a2*$^{f/f}$CD19-Cre$^{+}$ mice were the result of crossing *Slc3a2*$^{f/f}$ with the CD19-Cre$^{+}$ strain (13). *Slc3a2*$^{f/+}$CD19-Cre$^{+}$ offspring were identified by PCR and were backcrossed with *Slc3a2*$^{f/f}$ mice to create mice heterozygous for CD19-Cre and homozygous for the *Slc3a2* floxed allele (*Slc3a2*$^{f/f}$CD19-Cre$^{-}$). This littermate comparison was used wherever possible. For Supplementary Figures 2-2 and 2-4, the offspring of *Slc3a2*$^{+/-}$ × *Slc3a2*$^{f/f}$CD19-Cre$^{+}$ matings were used. All mice were housed at the University of California San Diego animal facility, and all experiments were approved by the Institutional Animal Care and Use Committee. 'Pan-integrin'-deficient mice were generated as described (32). Integrins were ablated by crossing of *Itgb1*$^{flf}$, *Itgav*$^{flf}$, *Itgb2*$^{-/-}$ or *Itgb7*$^{-/-}$ mice (deficient in integrin $\beta_1$, $\alpha_V$, $\beta_2$ or $\beta_7$, respectively) with mice carrying an Mx1-Cre transgene. Cre expression in hematopoietic cells was induced by intraperitoneal injection of 250 μg polyinosinic-polycytidylic acid (Amersham Biosciences); 8 d later, mice were used for B cell–proliferation assays.

**2.4.2 - Flow cytometry of B cell subsets**

Bone marrow cells were prepared by dissection of femur and tibia bones from adult *Slc3a2*$^{f/f}$CD19-Cre$^{+}$ mice (10–20 weeks of age) and flushing with media with a 23-gauge needle. After two passages through the 23-gauge needle, erythrocytes were lysed for 8 min at 25 °C with ammonium chloride–potassium bicarbonate lysis buffer (Biowhittaker). Splenic single-cell suspensions were prepared by dissociation of whole spleens with a 7-ml tissue grinder (Kontes) and lysis of erythrocytes as described for bone marrow. Cells from peritoneal lavage were isolated from adult mice by flushing of the peritoneum with 10 ml complete medium (RPMI medium and 10% (vol/vol) FBS, supplemented with L-glutamine, penicillin and streptomycin) in batches of 1–2 ml. After being counted, bone marrow, spleen, or peritoneal cells were stained in 100 μl staining buffer (0.5% (wt/vol) BSA in PBS) containing fluorochrome-conjugated antibody to mouse B220 (RA3-6B2), IgM (II/41), CD21 (7G6), CD23 (B3B4), CD98hc (RL388), GL7 (GL7), CD138 (281-2) or Fas (Jo2) at optimal concentrations (all from BD Biosciences). After incubation of cells on ice for 30–45 min, followed by three washes in staining buffer, subsets were analyzed by flow cytometry with a FACSAria or FACSCalibur (BD Biosciences).

**2.4 3 - Immunohistochemistry**

For analysis of CD98 selection after immunization, adult *Slc3a2*$^{f/f}$CD19-Cre$^{+}$ mice and littermate control (*Slc3a2*$^{f/f}$CD19-Cre$^{-}$) mice were immunized intraperitoneally with 100 μg TNP-KLH (Biosearch) emulsified in CFA (250 μl). Then, 7 d later, spleens were embedded in Tissue-Tek optimum cutting temperature compound (Sakura Finetek

USA) and were frozen at -80 °C. Sections 8 μm in thickness were mounted on microscope slides, were fixed for 10 min in cold acetone, were blocked for 1 h with blocking buffer (0.5% (wt/vol) BSA in PBS), and were stained for 1 h at 25 °C with fluorescein isothiocyanate–conjugated peanut agglutinin (FL-1071; Vector Labs) and anti-B220 (BRA3-6B2), anti-CD5 (53-7.3), anti-CD3 (145-2C11) or anti-CD98 (RL388; all from BD Biosciences) or anti-MOMA-1 (MOMA-1; BaChem). After being washed with PBS containing 0.5% (vol/vol) Tween, sections were covered with Gel/Mount (Biomeda) and were sealed with glass coverslips. Images were acquired with Zeiss Axiocam M1 microscope (Zeiss) and Slidebook software (Intelligent Imaging Innovations).

**2.4.4 - Antibody analysis**

For antigen-specific antibody responses, adult *Slc3a2*$^{f/f}$CD19-Cre$^{+}$ and control littermate *Slc3a2*$^{f/f}$CD19-Cre$^{-}$ mice were injected intraperitoneally with 50 μg TNP-LPS (Sigma) in 250 μl PBS (T cell–independent antigen) or 100 μg TNP-KLH (Biosearch) emulsified in 250 μl CFA (T cell–dependent antigen). Blood serum was collected by centrifugation of tail vein blood (100–200 μl with a solution of 1–2 mM EDTA as an anticoagulant) before and 1, 2 and 3 weeks after immunization. Concentrations of TNP-specific antibody in blood sera were assessed by direct enzyme-linked immunosorbent assay (ELISA) with TNP-ovalbumin as the coating antigen and alkaline phosphatase–conjugated polyclonal anti–mouse IgG (A4312; Sigma), polyclonal anti–mouse IgM (A7784; Sigma) or monoclonal anti–mouse IgG3 (R40-82; BD Biosciences) as the detection antibody. Because of inconsistencies in commercially available anti-TNP

standards, the ELISA data in Figure 2-2 and Supplementary Figure 2-13 were quantified by multiplication of the absorbance 'reading out' of three to four dilutions of sample that was in the linear portion of the assay with the dilution factor to obtain the values presented. Concentrations of circulating IgG and IgM from naive mice and from *in vitro* splenic B cell stimulations were measured by sandwich ELISA with polyclonal anti–mouse IgG (715-005-150) or anti–mouse IgM (115-006-020; both from Jackson Immunoresearch), the detection antibodies described for the direct ELISA and standard curves obtained with purified polyclonal IgG or IgM.

### 2.4.5 - *In vitro* proliferation and differentiation of resting B cells

Resting B cells (defined as $CD43^-$) were purified from spleen cell suspensions of *Slc3a2*$^{f/f}$CD19-$Cre^+$, 'pan-integrin'-deficient or wild-type control mice by depletion of $CD43^+$ cells (and depletion of $CD98hc^+$ B cells for *Slc3a2*$^{f/f}$CD19-$Cre^+$ mice or depletion of $\beta_1$ integrin–positive cells for 'pan-integrin'-deficient mice) with B cell magnetic beads (Dynal). Purity was routinely 95–98%, as assessed by staining with anti-B220 (RA3-6B2) or anti-CD43 (eBioR2-60) and flow cytometry. Resting B cells were plated in 48-well plates at a density of $4 \times 10^5$ cells per well and were stimulated for 3–5 d with Ultrapure LPS (20 μg/ml; InVivoGen), $F(ab')_2$ goat anti–mouse IgM (30 μg/ml; Jackson Immunoresearch), anti-CD40 (2 μg/ml; 3/23; BD Biosciences) or recombinant mouse IL-4 (50 ng/ml; Peprotech). Unstimulated resting cells were cultured with medium alone. Staining with anti-CD138 (DL-101; eBioscience), anti-IgG3 (R40-82; BD Biosciences) and anti-B220 (RA3-6B2; eBioscience) and flow cytometry were used to assess class switching and differentiation into plasma cells. For measurement of proliferation,

purified resting B cells were labeled with 2 μM CFSE (carboxyfluorescein diacetate succinimidyl ester; Molecular Probes) and were analyzed by flow cytometry at 3–5 d for dilution of fluorescence (cell division). Because the extent of CFSE labeling varied among samples, unstimulated cells were also assessed (Supplementary Figure 2-12). For some differentiation or proliferation experiments, cells were also stained with anti-CD98 (RL388; eBioscience). Propidium iodide exclusion and automated counting by flow cytometry were used for analysis of the expansion of cell populations. In this *in vitro* culture system, many cells die or are lost during collecting or staining and a smaller subset divides rapidly.

**2.4.6 - Retroviral infection of mouse bone marrow and transplantation into recipient mice**

The bone marrow transplant protocol was from S. Rowland in the lab of R. Pelanda. Donor mice were treated intraperitoneally with 5-fluorouracil (Adrucil; Sicor Pharmaceuticals) in 200 μl PBS at a dose of 4 μg per mouse. Then, 3 d later, EcoPack 293 packaging cells (Imgenex) were transfected with pCl-Eco (Imgenex) and one of four retroviral constructs (C98T98E98, C98T69E98, C98T98E69 or C69T69E69, on a backbone of MSCV-IRES-GFP) (50), followed by culture for 48 h. On day 4, donor mice were killed and bone marrow was cultured overnight in complete medium containing IL-3 (25 ng/ml), IL-6 (50 ng/ml) and stem cell factor (50 ng/ml; all from Peprotech). Viral supernatants were collected from packaging cells on day 5 and were used to 'spin-infect' bone marrow on days 5 and 6 for 90 min at 1,000*g* and at 25 °C. Bone marrow cells were collected on day 7 and were injected intravenously at a dose of

$2.5 \times 10^5$ cells in 100 μl PBS per mouse. Small samples were retained and were stained with antibody to Sca-1 (D7; eBioscience), a marker of stem cells. In all samples, 24–29% of Sca-$1^+$ populations were $GFP^+$ before injection. At 6–8 weeks after transplantation, resting B cells deficient in mouse CD98hc were purified from spleens of recipient mice, then were labeled and were stimulated with LPS. Proliferation and plasma cell differentiation was assessed as described above but with DiD (1,1'-dioctadecyl-3,3,3',3'-tetramethylindodicarbocyanine; Molecular Probes), which emits in a range distinct from that of GFP.

**Acknowledegement**

Chapter 2 of this dissertation is based on the manuscript that has been published in the journal, *Nature Immunology* (Cantor J, Browne CD, Ruppert R, Féral CC, Fässler R, Rickert RC, Ginsberg MH. CD98hc facilitates B cell proliferation and adaptive humoral immunity. Nature Immunology. 2009 Apr;10(4):412-9). Contents of this chapter are presented as it may appear in the publication but supplemented with unpublished figures. Cecille D. Browne is the second author of this paper. The primary author is Joseph Cantor and the other contributing authors are Raphael Ruppert, Chloé Féral, Reinhard Fässler, Robert Rickert and Mark Ginsberg.

## 2.5 - References


1. Burnet, F.M. The Clonal Selection Theory of Acquired Immunity 49–68 (Cambridge University Press, Cambridge, 1959).

2. Cooper, M.D. & Alder, M.N. The evolution of adaptive immune systems. Cell 124, 815–822 (2006).

3. Kehrl, J.H. & Fauci, A.S. Identification, purification, and characterization of antigen-activated and antigen-specific human B lymphocytes. Trans. Assoc. Am. Physicians 96, 182–187 (1983).

4. Bertran, J. *et al*. Stimulation of system $y^+$-like amino acid transport by the heavy chain of human 4F2 surface antigen in *Xenopus laevis* oocytes. Proc. Natl. Acad. Sci. USA 89, 5606–5610 (1992).

5. Torrents, D. *et al*. Identification and characterization of a membrane protein ($y^+$L amino acid transporter-1) that associates with 4F2hc to encode the amino acid transport activity $y^+$L. A candidate gene for lysinuric protein intolerance. J. Biol. Chem. 273, 32437–32445 (1998).

6. Fenczik, C.A., Sethi, T., Ramos, J.W., Hughes, P.E. & Ginsberg, M.H. Complementation of dominant suppression implicates CD98 in integrin activation. Nature 390, 81–85 (1997).

7. Feral, C.C. *et al*. CD98hc (SLC3A2) mediates integrin signaling. Proc. Natl. Acad. Sci. USA 102, 355–360 (2005).

8. Abraham, R.T. Mammalian target of rapamycin: immunosuppressive drugs uncover a novel pathway of cytokine receptor signaling. Curr. Opin. Immunol. 10, 330–336 (1998).

9. Mondino, A. & Mueller, D.L. mTOR at the crossroads of T cell proliferation and tolerance. Semin. Immunol. 19, 162–172 (2007).

10. Uinuk-Ool, T. *et al*. Lamprey lymphocyte-like cells express homologs of genes involved in immunologically relevant activities of mammalian lymphocytes. Proc. Natl. Acad. Sci. USA 99, 14356–14361 (2002).

11. Tsumura, H. *et al*. The targeted disruption of the CD98 gene results in embryonic lethality. Biochem. Biophys. Res. Commun. 308, 847–851 (2003).

12. Feral, C.C. *et al*. CD98hc (SLC3A2) participates in fibronectin matrix assembly by mediating integrin signaling. J. Cell Biol. 178, 701–711 (2007).

13. Rickert, R.C., Roes, J. & Rajewsky, K. B lymphocyte-specific, Cre-mediated mutagenesis in mice. Nucleic Acids Res. 25, 1317–1318 (1997).

14. Otero, D.C. & Rickert, R.C. CD19 function in early and late B cell development. II. CD19 facilitates the pro-B/pre-B transition. J. Immunol. 171, 5921–5930 (2003).

15. Brakebusch, C. *et al*. Beta1 integrin is not essential for hematopoiesis but is necessary for the T cell-dependent IgM antibody response. Immunity 16, 465–477 (2002).

16. Lu, T.T. & Cyster, J.G. Integrin-mediated long-term B cell retention in the splenic marginal zone. Science 297, 409–412 (2002).

17. Fenczik, C.A. *et al*. Distinct domains of CD98hc regulate integrins and amino acid transport. J. Biol. Chem. 276, 8746–8752 (2001).

18. Tangye, S.G. & Hodgkin, P.D. Divide and conquer: the importance of cell division in regulating B-cell responses. Immunology 112, 509–520 (2004).

19. Hasbold, J., Corcoran, L.M., Tarlinton, D.M., Tangye, S.G. & Hodgkin, P.D. Evidence from the generation of immunoglobulin G–secreting cells that stochastic mechanisms regulate lymphocyte differentiation. Nat. Immunol. 5, 55–63 (2004).

20. Freidman, A.W., Diaz, L.A., Jr., Moore, S., Schaller, J. & Fox, D.A. The human 4F2 antigen: evidence for cryptic and noncryptic epitopes and for a role of 4F2 in human T lymphocyte activation. Cell. Immunol. 154, 253–263 (1994).

21. Diaz, L.A., Jr. *et al*. Monocyte-dependent regulation of T lymphocyte activation through CD98. Int. Immunol. 9, 1221–1231 (1997).

22. Fernandez-Herrera, J., Sanchez-Madrid, F. & Diez, A.G. Differential expression of the 4F2 activation antigen on human follicular epithelium in hair cycle. J. Invest. Dermatol. 92, 247–250 (1989).

23. Zent, R. *et al*. Class- and splice variant-specific association of CD98 with integrin beta cytoplasmic domains. J. Biol. Chem. 275, 5059–5064 (2000).

24. Proud, C.G. Amino acids and mTOR signalling in anabolic function. Biochem. Soc. Trans. 35, 1187–1190 (2007).

25. Hynes, R.O. Integrins: bidirectional, allosteric signaling machines. Cell 110, 673–687 (2002).

26. Schwartz, M.A. & Assoian, R.K. Integrins and cell proliferation: regulation of cyclin-dependent kinases via cytoplasmic signaling pathways. J. Cell Sci. 114, 2553–2560 (2001).

27. Motti, M.L. *et al*. Loss of p27 expression through RAS →BRAF →MAP kinase-dependent pathway in human thyroid carcinomas. Cell Cycle 6, 2817–2825 (2007).

28. Assoian, R.K. & Schwartz, M.A. Coordinate signaling by integrins and receptor tyrosine kinases in the regulation of G1 phase cell-cycle progression. Curr. Opin. Genet. Dev. 11, 48–53 (2001).

29. Walker, J.L. & Assoian, R.K. Integrin-dependent signal transduction regulating cyclin D1 expression and G1 phase cell cycle progression. Cancer Metastasis Rev. 24, 383–393 (2005).

30. Lin, K.B. *et al*. The rap GTPases regulate B cell morphology, immune-synapse formation, and signaling by particulate B cell receptor ligands. Immunity 28, 75–87 (2008).

31. Arana, E. *et al*. Activation of the small GTPase Rac2 via the B cell receptor regulates B cell adhesion and immunological-synapse formation. Immunity 28, 88–99 (2008).

32. Lammermann, T. *et al*. Rapid leukocyte migration by integrin-independent flowing and squeezing. Nature 453, 51–55 (2008).

33. Wolniak, K.L., Shinall, S.M. & Waldschmidt, T.J. The germinal center response. Crit. Rev. Immunol. 24, 39–65 (2004).

34. Warren, A.P. *et al*. Convergence between CD98 and integrin-mediated T-lymphocyte co-stimulation. Immunology 99, 62–68 (2000).

35. Shimizu, Y., Rose, D.M. & Ginsberg, M.H. Integrins in the immune system. Adv. Immunol. 72, 325–380 (1999).

36. Sims, T.N. & Dustin, M.L. The immunological synapse: integrins take the stage. Immunol. Rev. 186, 100–117 (2002).

37. Cyster, J.G. Homing of antibody secreting cells. Immunol. Rev. 194, 48–60 (2003).

38. Lo, C.G., Lu, T.T. & Cyster, J.G. Integrin-dependence of lymphocyte entry into the splenic white pulp. J. Exp. Med. 197, 353–361 (2003).

39. Rose, D.M., Alon, R. & Ginsberg, M.H. Integrin modulation and signaling in leukocyte adhesion and migration. Immunol. Rev. 218, 126–134 (2007).

40. Abram, C.L. & Lowell, C.A. Convergence of immunoreceptor and integrin signaling. Immunol. Rev. 218, 29–44 (2007).

41. Batista, F.D. *et al*. The role of integrins and coreceptors in refining thresholds for B-cell responses. Immunol. Rev. 218, 197–213 (2007).

42. Roovers, K., Davey, G., Zhu, X., Bottazzi, M.E. & Assoian, R.K. Alpha5beta1 integrin controls cyclin D1 expression by sustaining mitogen-activated protein kinase activity in growth factor-treated cells. Mol. Biol. Cell 10, 3197–3204 (1999).

43. Fleire, S.J. *et al*. B cell ligand discrimination through a spreading and contraction response. Science 312, 738–741 (2006).

44. Prager, G.W., Feral, C.C., Kim, C., Han, J. & Ginsberg, M. H. CD98hc (SLC3a2) interaction with the integrin β subunit cytoplasmic domain mediates adhesive signaling. J. Biol. Chem. 282, 24477–24484 (2007).

45. Esteban, F. *et al*. Relationship of 4F2 antigen with local growth and metastatic potential of squamous cell carcinoma of the larynx. Cancer 66, 1493–1498 (1990).

46. Hara, K., Kudoh, H., Enomoto, T., Hashimoto, Y. & Masuko, T. Malignant transformation of NIH3T3 cells by overexpression of early lymphocyte activation antigen CD98. Biochem. Biophys. Res. Commun. 262, 720–725 (1999).

47. Henderson, N.C. *et al*. CD98hc (SLC3A2) interaction with β1 integrins is required for transformation. J. Biol. Chem. 279, 54731–54741 (2004).

48. White, D.E. *et al*. Targeted disruption of β1-integrin in a transgenic mouse model of human breast cancer reveals an essential role in mammary tumor induction. Cancer Cell 6, 159–170 (2004).

49. Kass, L., Erler, J.T., Dembo, M. & Weaver, V.M. Mammary epithelial cell: influence of extracellular matrix composition and organization during development and tumorigenesis. Int. J. Biochem. Cell Biol. 39, 1987–1994 (2007).

50. Van Parijs, L. *et al*. Uncoupling IL-2 signals that regulate T cell proliferation, survival, and Fas-mediated activation-induced cell death. Immunity 11, 281–288 (1999).

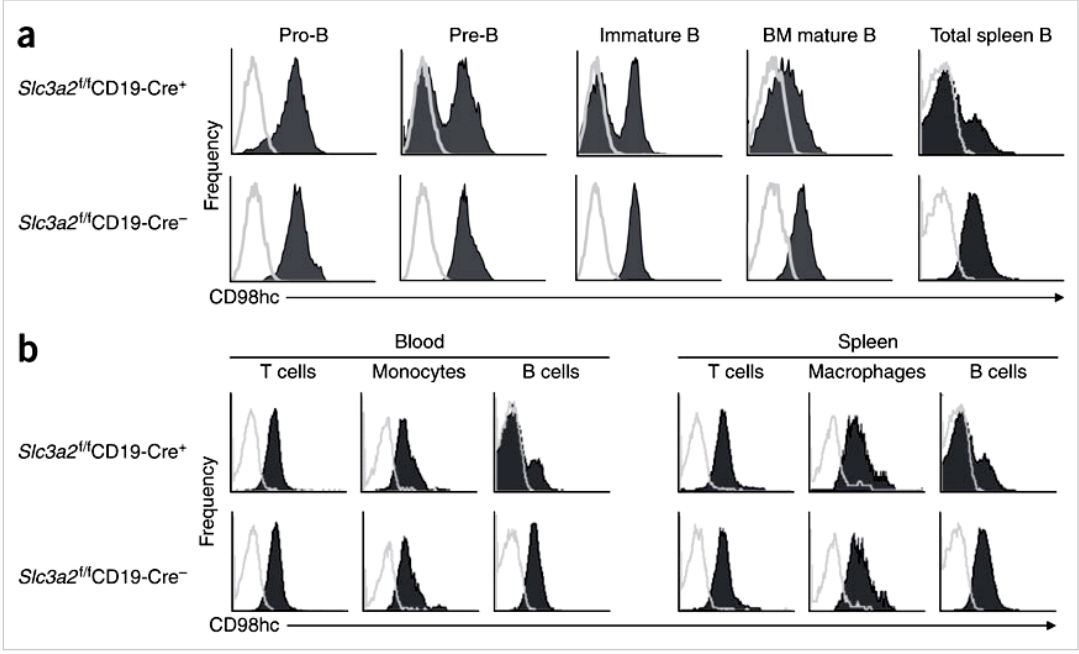


**Figure 2-1: Deletion of CD98hc in Slc3a2f/fCD19-Cre+ mice.** (a) CD98hc expression (filled histograms) and staining with isotype-matched control antibody (open histograms) in bone marrow cells isolated from adult *Slc3a2*$^{f/f}$CD19-Cre$^{+}$ and control *Slc3a2*$^{f/f}$CD19-Cre$^{-}$ mice and measured at various stages of B cell maturation. BM, bone marrow. Data are from an experiment repeated once. (b) Flow cytometry of CD98hc expression (filled histograms) and staining with isotype-matched control antibody (open histograms) on T cells (CD3$^{+}$), monocytes or macrophages (CD11b$^{+}$B220$^{-}$) and B cells (B220$^{+}$) among peripheral blood and spleen cells from *Slc3a2*$^{f/f}$CD19-Cre$^{+}$ and control *Slc3a2*$^{f/f}$CD19-Cre$^{-}$ mice, prepared by lysis of erythrocytes. Data are from one mouse of each genotype in an experiment repeated once (*n* = 4 mice per group for each).

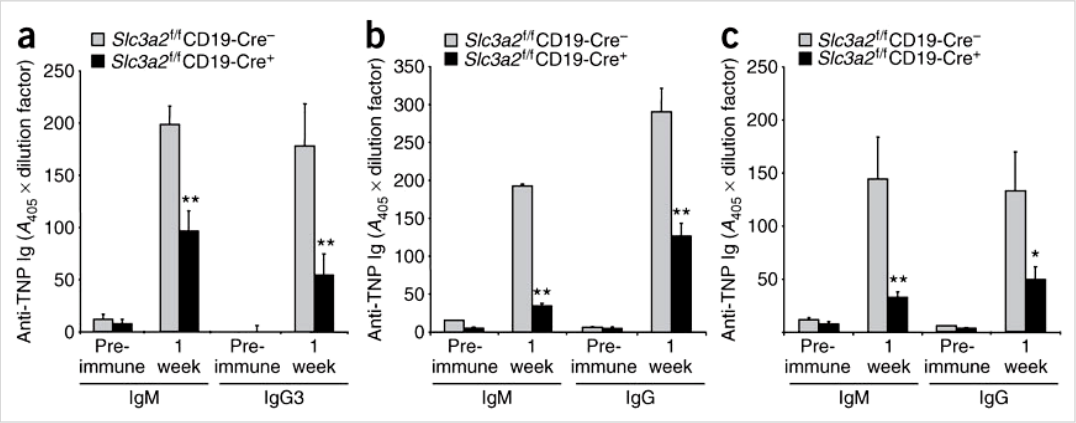


**Figure 2-2: Impaired antibody responses in *Slc3a2*$^{f/f}$CD19-Cre$^{+}$ mice.** (a) Direct ELISA of anti-TNP IgM or anti-TNP IgG3 in the serum of adult *Slc3a2*$^{f/f}$CD19-Cre$^{+}$ and control *Slc3a2*$^{f/f}$CD19-Cre$^{-}$ mice 8–12 weeks of age, immunized with 50 μg TNP-LPS (T cell–independent antigen) in PBS; serum is from blood obtained before immunization (Pre-immune) and 1 week after immunization. (b,c) Direct ELISA of anti-TNP IgM and anti-TNP IgG in the serum of *Slc3a2*$^{f/f}$CD19-Cre$^{+}$ and control *Slc3a2*$^{f/f}$CD19-Cre$^{-}$ mice immunized with 100 μg TNP-KLH (T cell–dependent antigen) in CFA (b) or incomplete Freund's adjuvant (c). $A_{405}$, absorbance at 405 nm. $^{*}$, $P = 0.057$ and $^{**}$, $P < 0.025$ (two-tailed *t*-test). Data are from an experiment repeated once (error bars, s.e.m. of five mice per group). Figure 2-2 was contributed by Joseph Cantor.

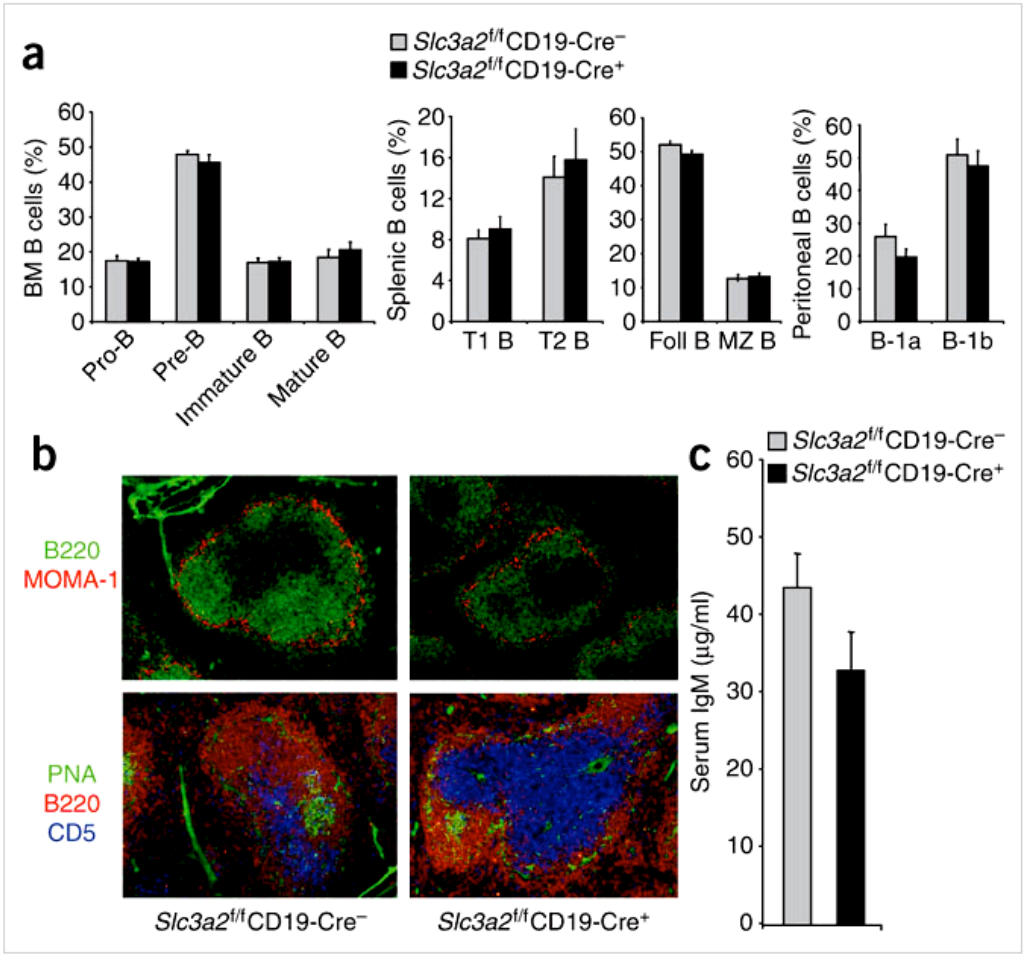


**Figure 2-3: Normal B cell distribution and natural antibody concentrations in *Slc3a2*$^{f/f}$CD19-Cre$^{+}$ mice.** (a) Flow cytometry of B cell subsets from the spleen, bone marrow and peritoneum of adult *Slc3a2*$^{f/f}$CD19-Cre$^{+}$ and control *Slc3a2*$^{f/f}$CD19-Cre$^{-}$ mice 8–12 weeks of age. Foll, follicular; MZ, marginal zone. Data are from an experiment repeated once with similar results (error bars, s.e.m. of four mice per group). (b) Secondary lymphoid architecture of frozen spleen sections from *Slc3a2*$^{f/f}$CD19-Cre$^{+}$ and littermate control *Slc3a2*$^{f/f}$CD19-Cre$^{-}$ mice, stained to detect B220$^{+}$ B cells, metallophilic macrophages that outline the marginal zone (MOMA-1$^{+}$), T cells (CD5$^{+}$) and germinal center B cells (positive for binding of peanut agglutinin (PNA)). Original magnification, × 10. Results are representative of three experiments. (c) Sandwich ELISA of total natural IgM in the serum of naive adult *Slc3a2*$^{f/f}$CD19-Cre$^{+}$ and control *Slc3a2*$^{f/f}$CD19-Cre$^{-}$ mice 8–12 weeks of age. $P = 0.11$ (two-tailed *t*-test). Data are from one experiment (error bars, s.e.m. of 30 mice per group). Figure 2-2c was contributed by Joseph Cantor.

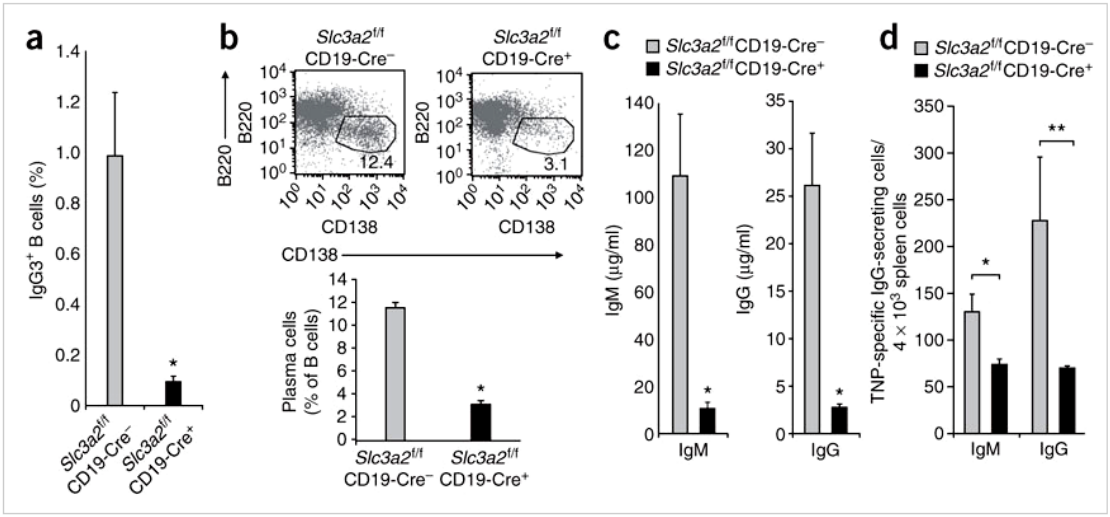


**Figure 2-4: Defective formation of plasma cells in *Slc3a2*$^{f/f}$CD19-Cre$^{+}$ mice.** (a,b) Flow cytometry of surface IgG3 (a) and CD138 (syndecan-1, a plasma cell marker; b) on splenic B cells (CD43$^{-}$ and CD98hc deficient) purified from *Slc3a2*$^{f/f}$CD19-Cre$^{+}$ and littermate control *Slc3a2*$^{f/f}$CD19-Cre$^{-}$ mice and cultured for 5 d with LPS. Graphs present IgG3$^{+}$ or CD138$^{+}$ B220$^{lo}$ cells among total B cells. Numbers adjacent to outlined areas (b, top) indicate percent B220$^{lo}$CD138$^{+}$ cells. $^{*}$, $P < 0.025$ (two-tailed *t*-test). Data are from an experiment with one mouse or an experiment repeated once with similar results (error bars, s.e.m. of three mice per group). (c) Sandwich ELISA of total IgM and IgG in supernatants of B cells stimulated for 4 d with LPS. $^{*}$, $P < 0.05$ (two-tailed *t*-test). Data are from an experiment repeated once with similar results (error bars, s.e.m. of four mice per group). (d) TNP-specific IgG–secreting plasma cells among splenocytes obtained from *Slc3a2*$^{f/f}$CD19-Cre$^{+}$ and control mice 1 week after immunization with TNP-KLH in CFA, then cultured for 2–3 h on TNP-coated polyvinylidene difluoride–membrane 96-well plates, followed by washing to remove cells and incubation with horseradish peroxidase–conjugated anti-IgG (secondary antibody); 3-amino-9-ethyl carbazole substrate was used to develop red spots. $^{*}$, $P = 0.05$ and $^{**}$, $P = 0.08$ (two tailed *t*-test). Data are from an experiment repeated once (error bars, s.e.m. of four mice per group). Figure 2-4 was contributed by Joseph Cantor.

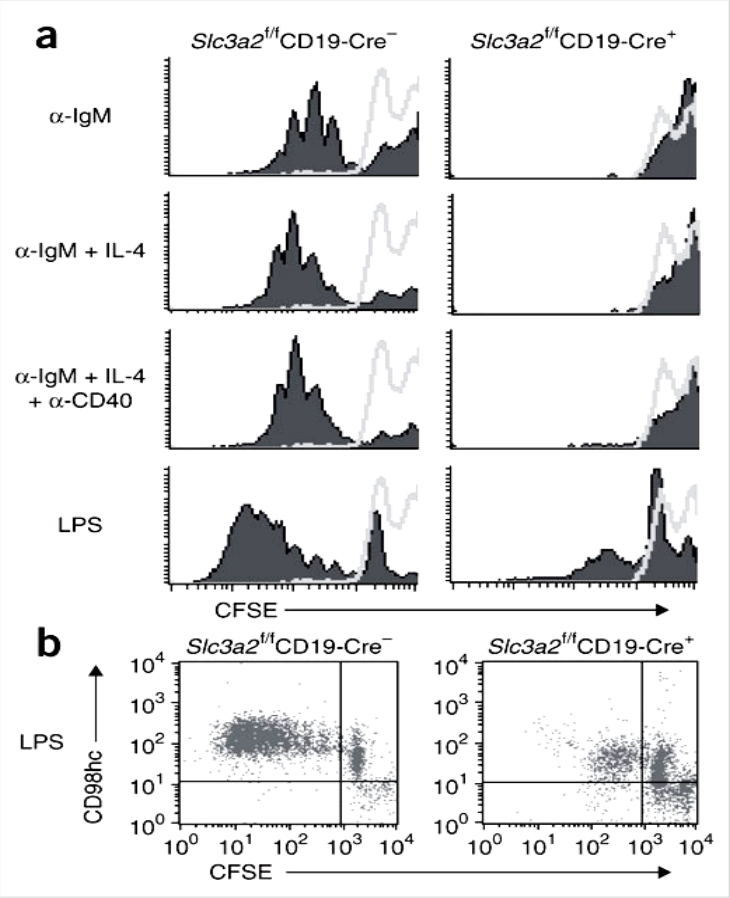


**Figure 2-5: Proliferation of splenic B cells from *Slc3a2*$^{f/f}$CD19-Cre$^{+}$ mice.** (a) Flow cytometry of the proliferation of B cells (CD43 and CD98 deficient) purified from splenocytes of *Slc3a2*$^{f/f}$CD19-Cre$^{+}$ and littermate control *Slc3a2*$^{f/f}$CD19-Cre$^{-}$ mice 8–12 weeks of age, then labeled with CFSE and left unstimulated (resting cells; open histograms) or cultured with various stimuli (left margin) for 5 d at a density of 4 ×10$^{5}$ cells per well in 48-well plates (filled histograms), assessed by CFSE dilution. α-, anti-. Data are from one mouse in one experiment (representative of three mice of each genotype), repeated twice with additional mice. (b) Two-parameter flow cytometry of CD98hc expression on CFSE$^{lo}$ (dividing) and CFSE$^{hi}$ (nondividing) cells after stimulation with LPS. Data are from an experiment repeated once. Figure 2-5 was contributed by Joseph Cantor.

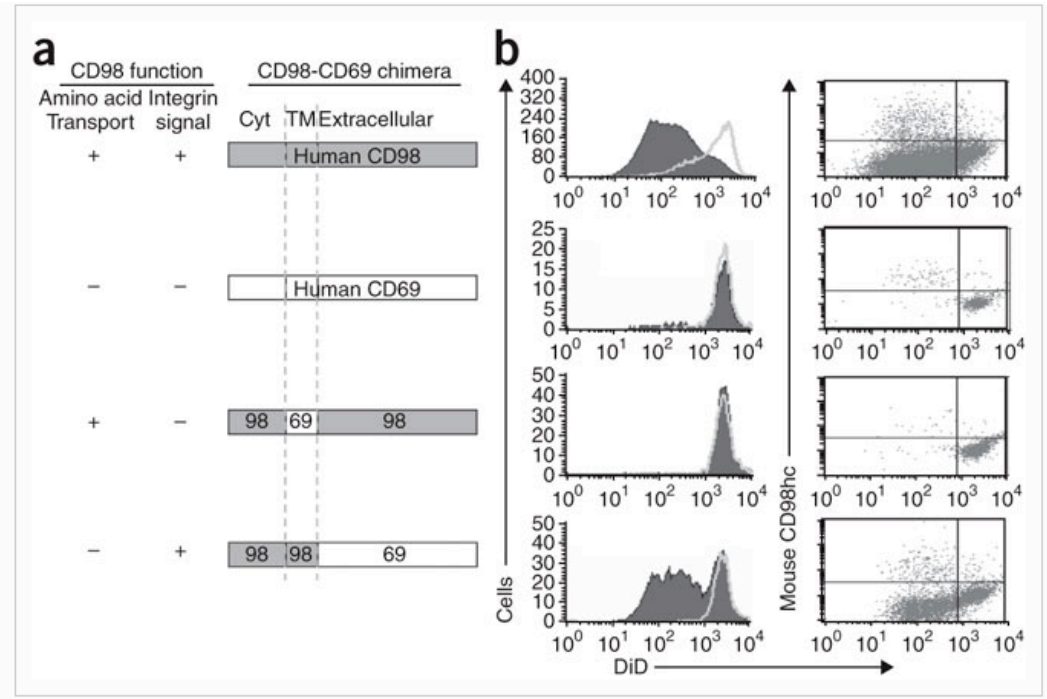


**Figure 2-6: Mechanism by which CD98hc enables B cell proliferation.** (a) CD98-CD69 chimeric constructs encoded by retroviruses. Cyt, cytoplasmic domain; TM, transmembrane domain; 98, CD98; 69, CD69. (b) Two-parameter flow cytometry to assess the proliferation of B cells ($CD43^-$ and mouse $CD98hc^-$) purified from splenocytes of recipient mice 6–8 weeks after transplantation of bone marrow cells infected with the retroviruses at left (in a), then labeled with DiD and left unstimulated (open histograms) or cultured with LPS (at a density of $3.5 \times 10^5$ cells per well in a 48-well plate; filled histograms), measured as DiD dilution; fewer dots (right) indicate lack of proliferation. Data are from an experiment repeated twice. Figure 2-6 was contributed by Joseph Cantor.

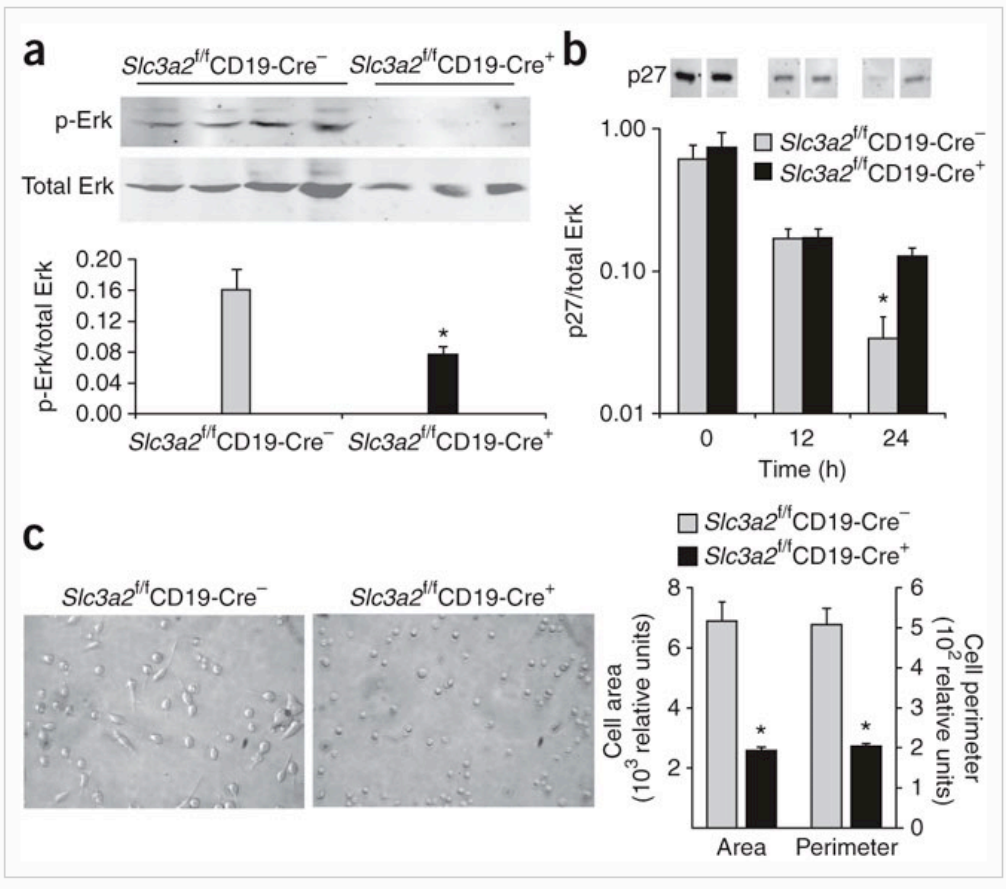


**Figure 2-7: Integrin signaling defects in B cells lacking CD98hc.** (a) Immunoblot analysis (top) of Erk1/2 phosphorylation (p-Erk) in B cells ($CD43^{-}CD98^{-}$) purified from splenocytes of *Slc3a2*$^{f/f}$CD19-Cre$^{+}$ mice ($n$ = 4) and littermate control *Slc3a2*$^{f/f}$CD19-Cre$^{-}$ mice ($n$ = 3) 8–12 weeks of age and stimulated for 17 h with anti-IgM (30 μg/ml) and IL-4 (15 ng/ml), then immediately washed with ice-cold PBS and lysed. Faint bands are present in the *Slc3a2*$^{f/f}$CD19-Cre$^{+}$ lanes. Each lane represents one mouse. (b) Immunoblot analysis (top) of p27 in B cells purified from *Slc3a2*$^{f/f}$CD19-Cre$^{+}$ or littermate control *Slc3a2*$^{f/f}$CD19-Cre$^{-}$ mice and stimulated for 0, 12 or 24 h with anti-IgM and IL-4, then washed and lysed (intervening bands are omitted for clarity). Below (a,b), staining of phosphorylated Erk1/2 (a) or p27 (b) normalized to that of total Erk. Data in a,b are from an experiment repeated once (error bars, s.e.m. of three mice per group). (c) Integrin-dependent spreading of B cells purified from *Slc3a2*$^{f/f}$CD19-Cre$^{+}$ mice (right) or littermate control *Slc3a2*$^{f/f}$CD19-Cre$^{-}$ mice (left), then stimulated for 24 h with anti-CD40 and IL-4 and plated for 16 h on anti-LFA-1. Original magnification, ×40. Data are from an experiment repeated once (error bars, s.e.m. of 30 cells per group). $^{*}$, $P < 0.015$ (two-tailed $t$-test). Figure 2-7 was contributed by Joseph Cantor.

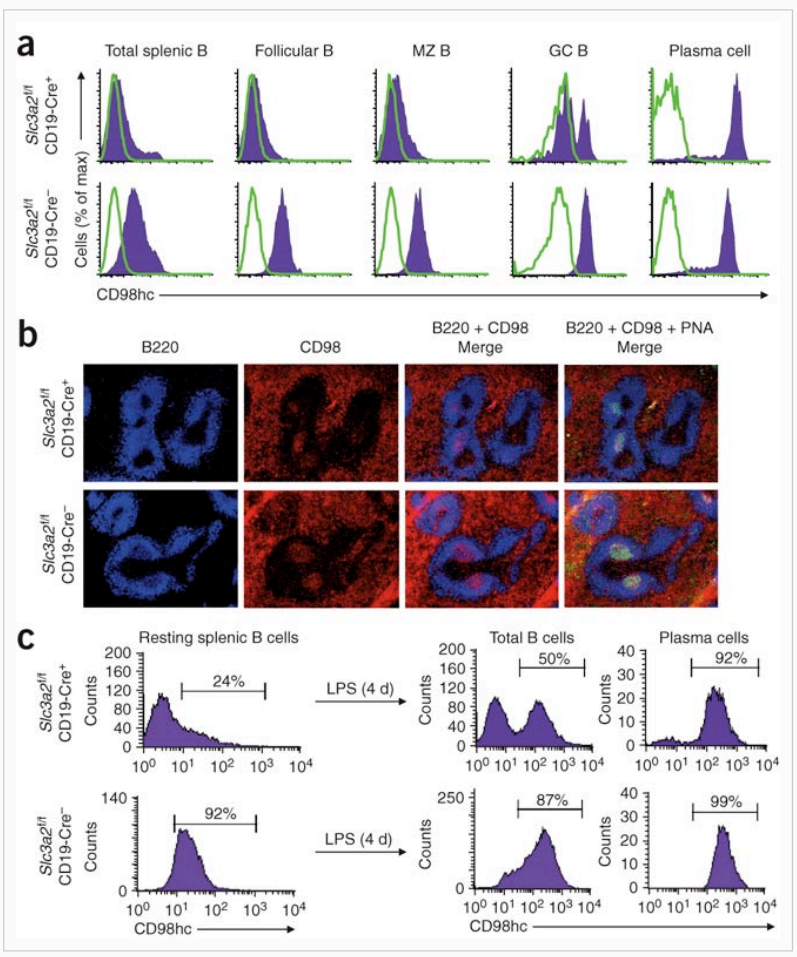


**Figure 2-8: Selection for CD98hc$^+$ B cells during activation.** (a) Flow cytometry of *in vivo* CD98hc expression (filled histograms) on B cells isolated from spleens of *Slc3a2*$^{f/f}$CD19-Cre$^+$ and control *Slc3a2*$^{f/f}$CD19-Cre$^-$ mice immunized with the T cell–dependent antigen TNP-KLH in CFA (one half of each spleen is used here). Open histograms, isotype-matched control antibody. max, maximum. (b) Microscopy of frozen sections of the remaining halves of the spleens in a, stained for B220 and CD98hc to assess selection of CD98hc$^+$ B cells *in vivo*; germinal centers were verified by staining with peanut agglutinin. Original magnification, ×10. Data in a,b are from one representative mouse of each genotype in an experiment repeated once ($n$ = 3 mice per group). (c) Flow cytometry of CD98hc expression on splenic B cells purified from *Slc3a2*$^{f/f}$CD19-Cre$^+$ mice without depletion of CD98hc$^+$ cells or from control *Slc3a2*$^{f/f}$CD19-Cre$^-$ mice, assessed before (resting; left) and after (right) culture for 4 d with LPS, and stained for B220, CD98hc and CD138 (plasma cell marker) to assess selection of CD98hc$^+$ B cells *in vitro*. Numbers above bracketed lines indicate percent CD98hc$^+$ cells. Data are from one mouse in an experiment repeated twice ($n$ = 3 mice per group. Figure 2-8c was contributed by Joseph Cantor.

**Supplementary Data:**

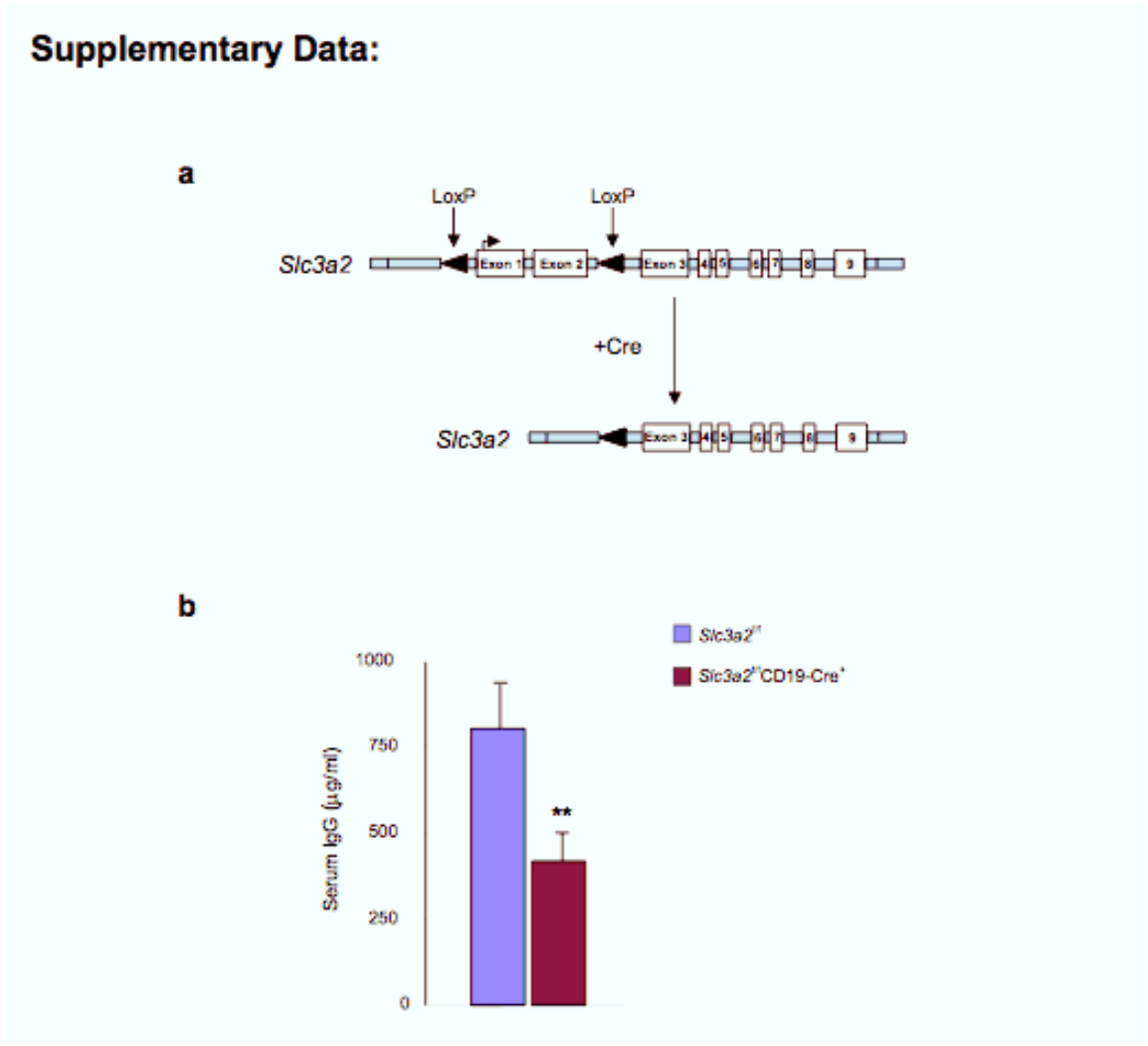


**Supplementary Figure 2-1: Conditional genetic targeting of Slc3a2 and Circulating IgG in *Slc3a2f/f*CD19- Cre+ mice. (a)** Conditional genetic targeting of Slc3a2. Using homologous recombination in ES cells, a targeting vector encoding portion of the *Slc3a2* gene locus containing the start codon and loxP sites flanking exons 1 and 2 replaced the endogenous gene segment. Exposure to Cre recombinase excised the start codon and exons 1 and 2, which encode the cytoplasmic and transmembrane portions of CD98hc, resulting in loss of CD98hc expression. **(b)** Circulating IgG in *Slc3a2f/f*CD19-Cre+ mice. Naïve adult (8-12 wk-old) *Slc3a2f/f*CD19-Cre+ and littermate control mice were bled and serum analyzed by sandwich ELISA for total Ig. Error bars represent s.e.m. from 30 mice per group (***P* = 0.017)**.** Supplementary Figure 2-1 was contributed by Joseph Cantor.

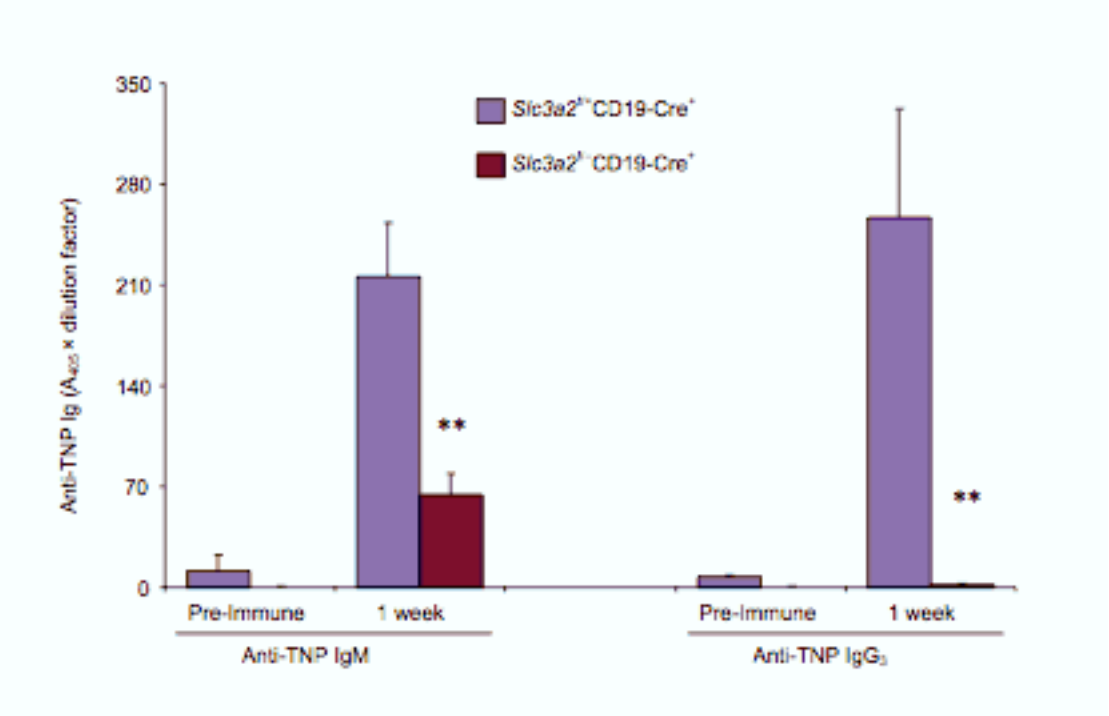


**Supplementary Figure 2-2: Humoral responses in Slc3a2f/+CD19-Cre+ vs. Slc3a2f/-CD19-Cre+ mice.** (a) Antibody response. To control for potential effects of one versus two endogenous Cd19 alleles, and for Cre- mediated toxicity, adult (8-12 wk old) Slc3a2f/+CD19-Cre+ and Slc3a2f/-CD19-Cre+ littermate mice were immunized with 50 µg of a T cell-independent antigen, TNP-LPS, in PBS. Mice were bled before immunization (pre-immune) and at one wk after immunization to obtain serum, which was analyzed for anti- TNP IgM or anti-TNP IgG3 by direct ELISA. Error bars represent s.e.m. from 3 mice for each group (**P < 0.025). This experiment was performed once. Supplementary Figure 2-2 was contributed by Joseph Cantor.

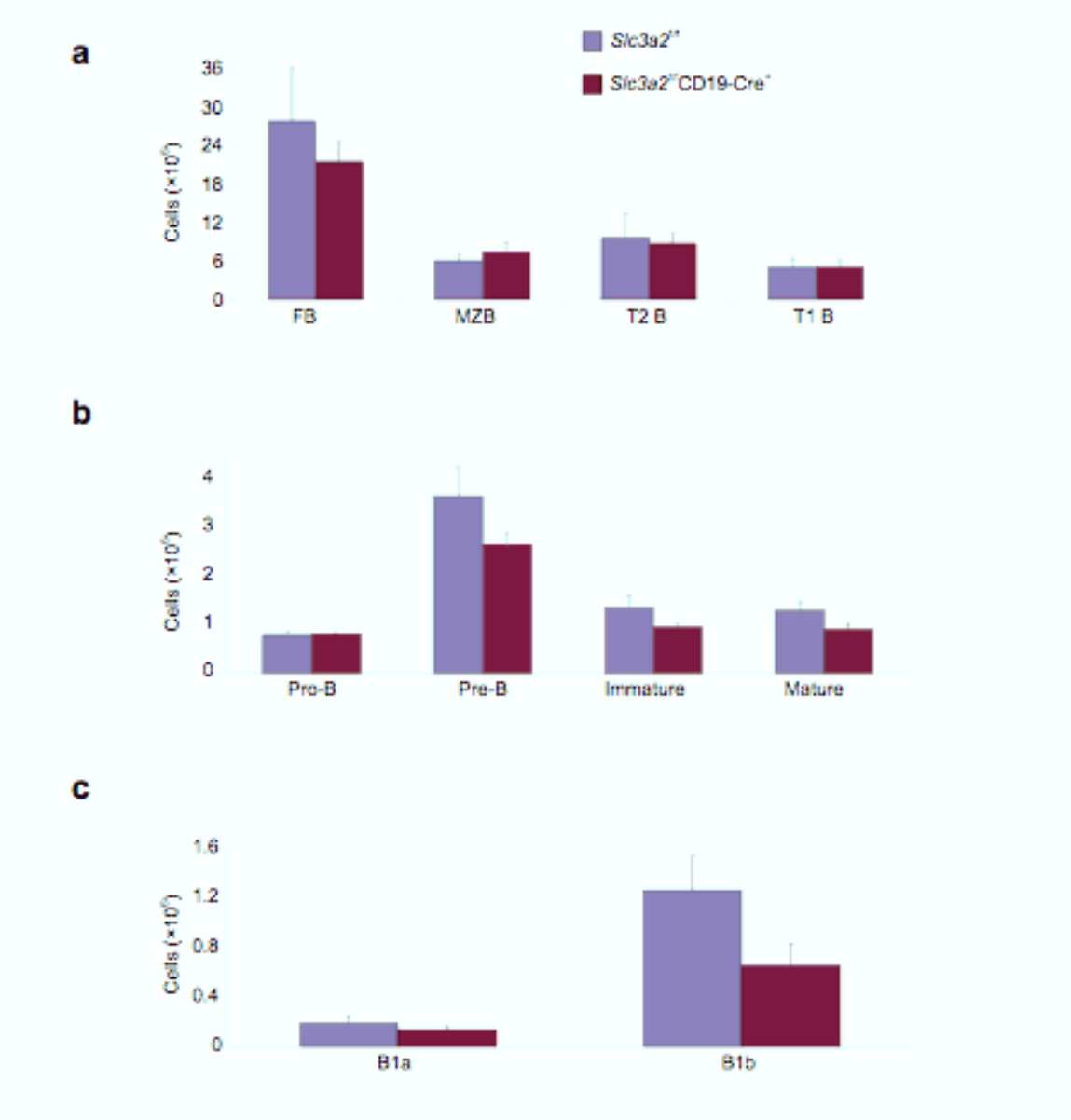


**Supplementary Figure 2-3. Absolute numbers of B cells in various subsets in Slc3a2f/fCD19-Cre+ mice.** Indicated subsets in the spleen (a), BM (b), and peritoneal lavage (c) from adult (8-12 wk old) Slc3a2f/fCD19-Cre+ or control mice were analyzed by flow cytometry. Frequency and total tissue cell number were used to derive total numbers for each subset. Error bars show s.e.m. from 4 mice per group.; experiment was repeated. Small differences in means for each subset are insignificant ($P > 0.05$). FB, follicular B; MZB, marginal zone B; T2, Transitional 2 B; T1, Transitional 1 B.

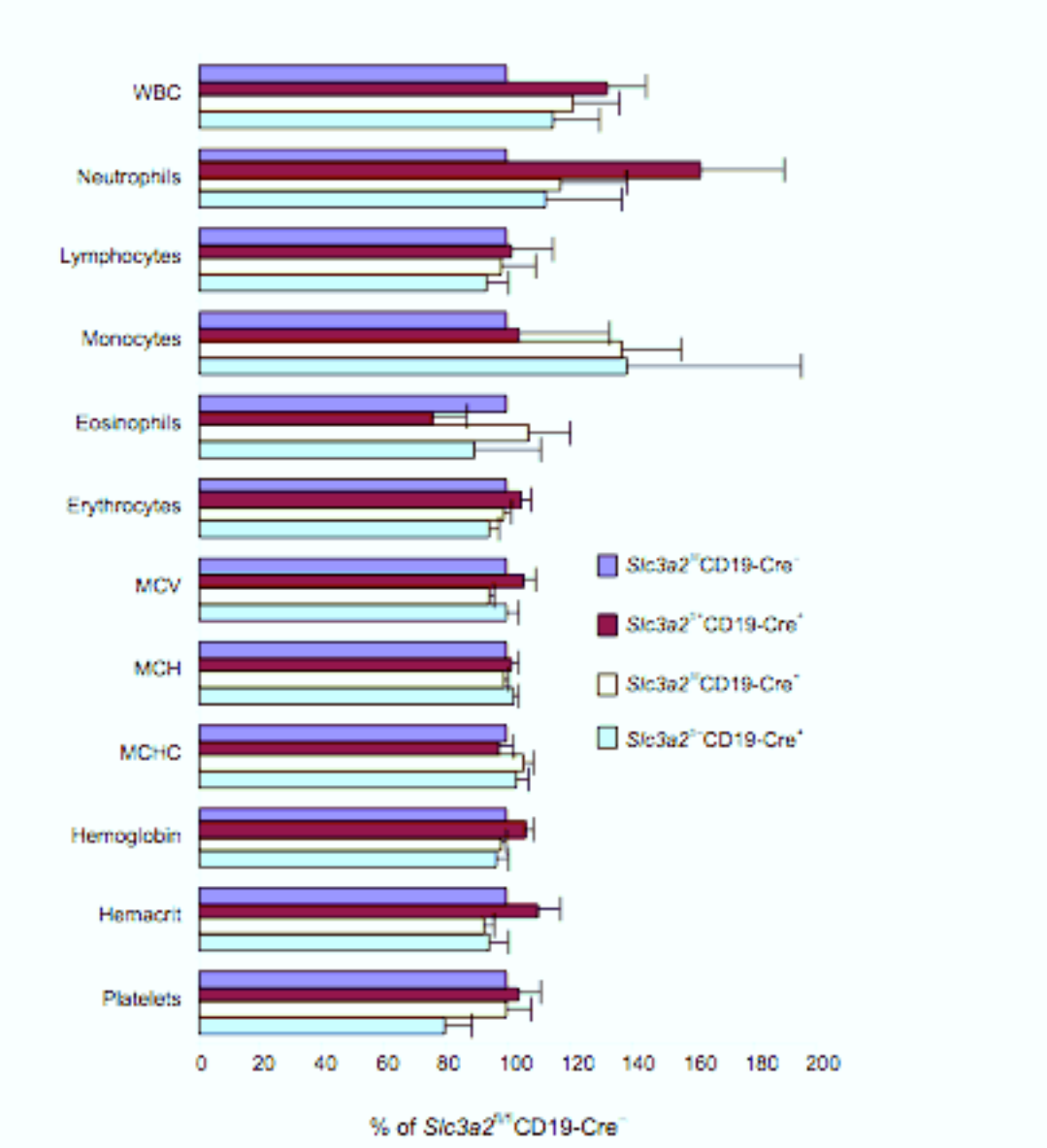


**Supplementary Figure 2-4: Blood analysis of *Slc3a2f/f*CD19-Cre+ mice.** Adult (8-16 wk old) mice of the indicated genotypes were bled and analyzed for a variety of white blood cell populations as well as standard blood parameters such as hematocrit, hemoglobin, and platelets. No statistically significant differences were apparent with *n*=5-6 mice per group. Supplementary Figure 2-4 was contributed by Joseph Cantor.

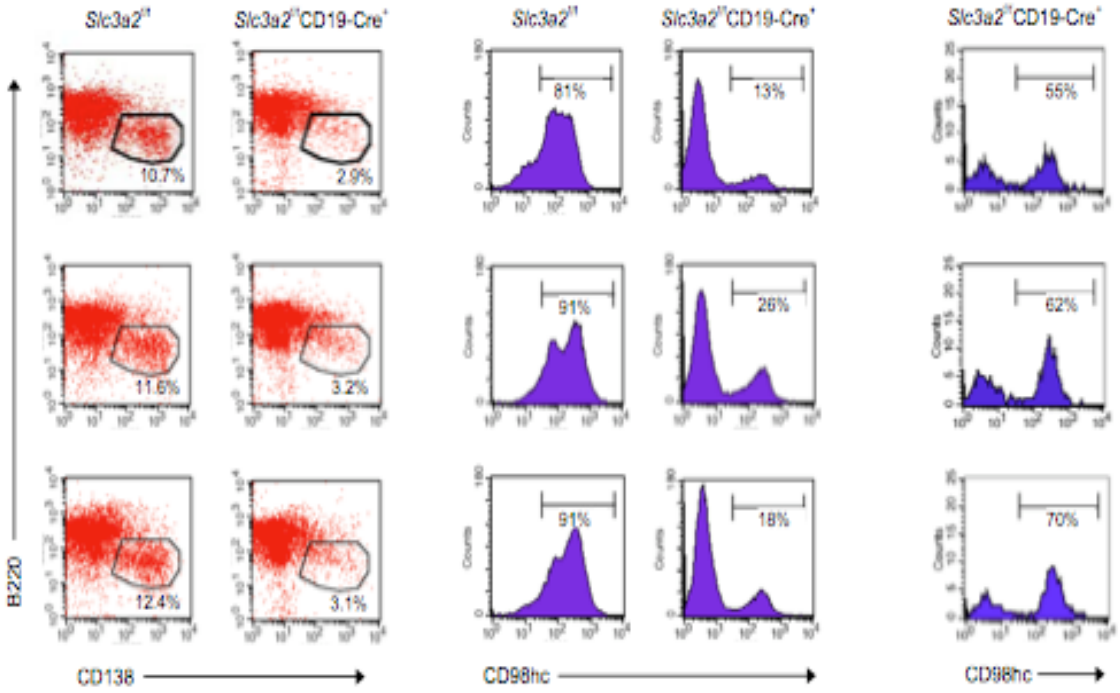


**Supplementary Figure 2-5: Differentiation to plasma cells *in vitro* using CD98hc-depletion.** Resting splenic B cells (CD43–CD98hc–) were purified using CD98hc depletion from *Slc3a2f/f*CD19-Cre+ or littermate control mice, cultured with LPS for 5 days, stained for B220, CD98hc, or CD138 (Syndecan-1, a plasma cell marker), and analyzed by flow cytometry. Each dot plot depicts cells from one mouse after 5 days stimulation with LPS. The middle set of histograms is CD98hc staining on stimulated total B cells, while the right histograms shows % of CD98+ cells within the *Slc3a2f/f*CD19-Cre+ plasma cell population. Experiment was repeated once. Supplementary Figure 2-5 was contributed by Joseph Cantor.

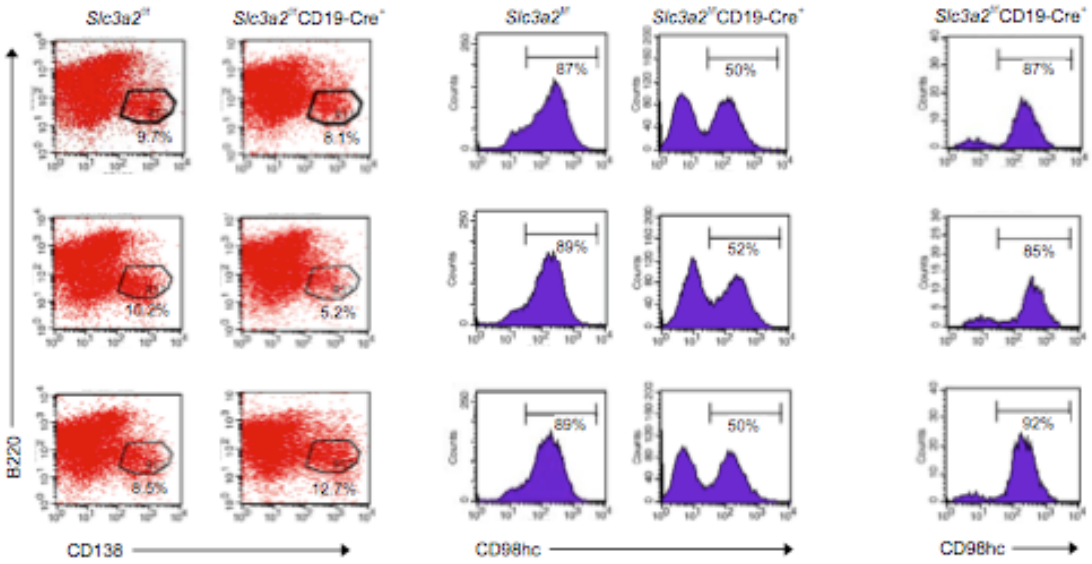


**Supplementary Figure 2-6: Differentiation to plasma cells *in vitro* without CD98hc-depletion.** Resting splenic B cells (CD43–) were purified from *Slc3a2f/f*CD19-Cre+ or littermate control mice, cultured with LPS for 5 days, stained for B220, CD98hc, or CD138 (Syndecan-1, a plasma cell marker), and analyzed by flow cytometry. Each dot plot depicts cells from one mouse after 5 days stimulation with LPS. The middle set of histograms is CD98hc staining on stimulated total B cells, while the right histograms shows % of CD98+ cells within the *Slc3a2f/f*CD19-Cre+ plasma cell population. Supplementary Figure 2-6 was contributed by Joseph Cantor.

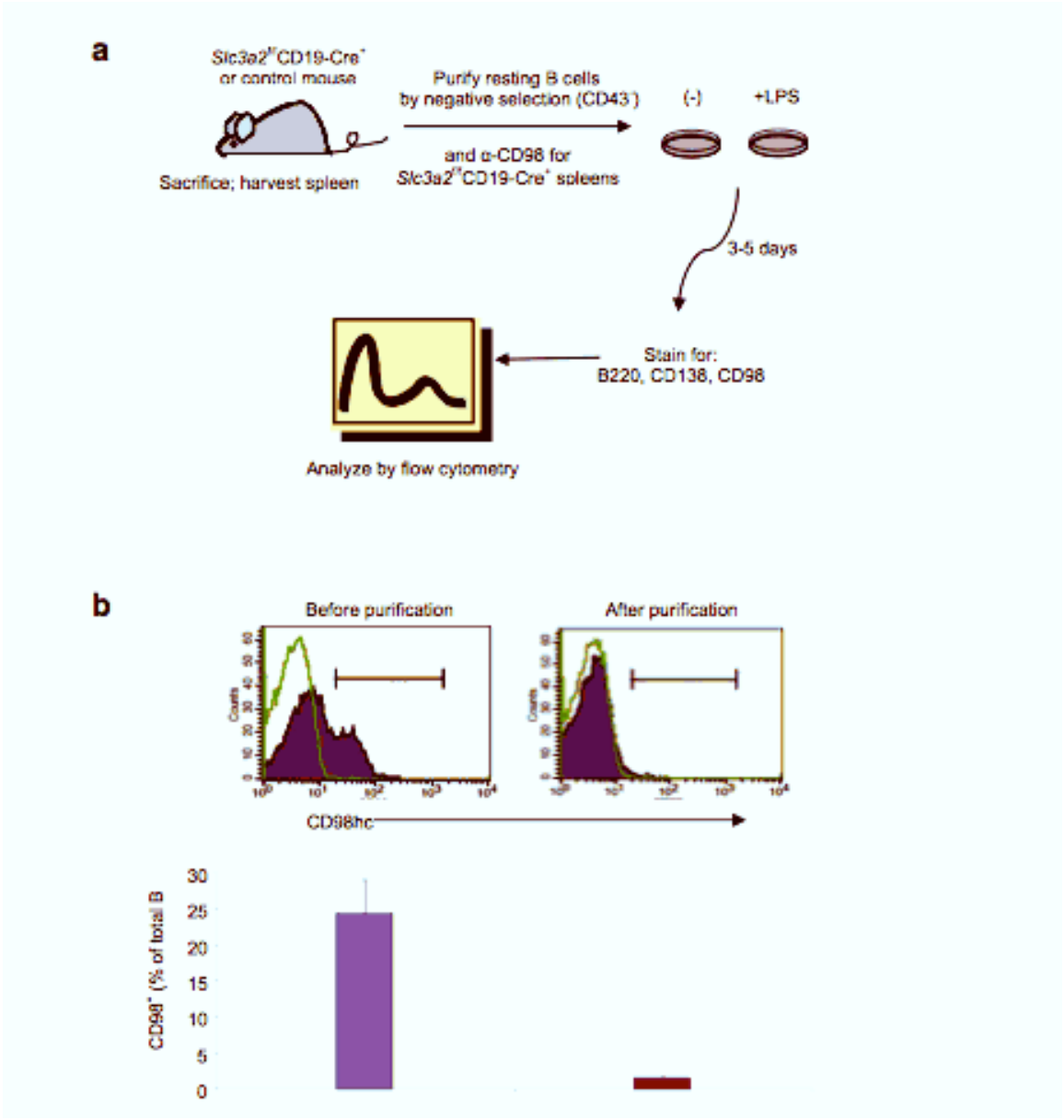


**Supplementary Figure 2-7: Purification of CD98hc-deficient B cells. (a) Purification and depletion protocol.** Resting B cells (CD43–) were purified from splenocytes of 8-16 wk-old Slc3a2f/fCD19-Cre+ and littermate control mice by negative depletion of CD43+ cells using magnetic beads. After purification, B cells were incubated, with or without LPS, for 3-5 days in vitro before staining for plasma cell formation or CFSE dilution analysis by flow cytometry. (b) Depletion efficiency. For Slc3a2f/fCD19-Cre+ (depicted in this figure), anti-CD98hc was included in the purification to deplete the approximately 25% of B cells that expressed CD98hc; <2% CD98hc+ cells remained after depletion. Representative histograms are gated on B220+ cells before and after depletion, and the bar graph below summarizes data from 3 mice from each group. Experiment was repeated three times. Supplementary Figure 2-7 was contributed by Joseph Cantor.

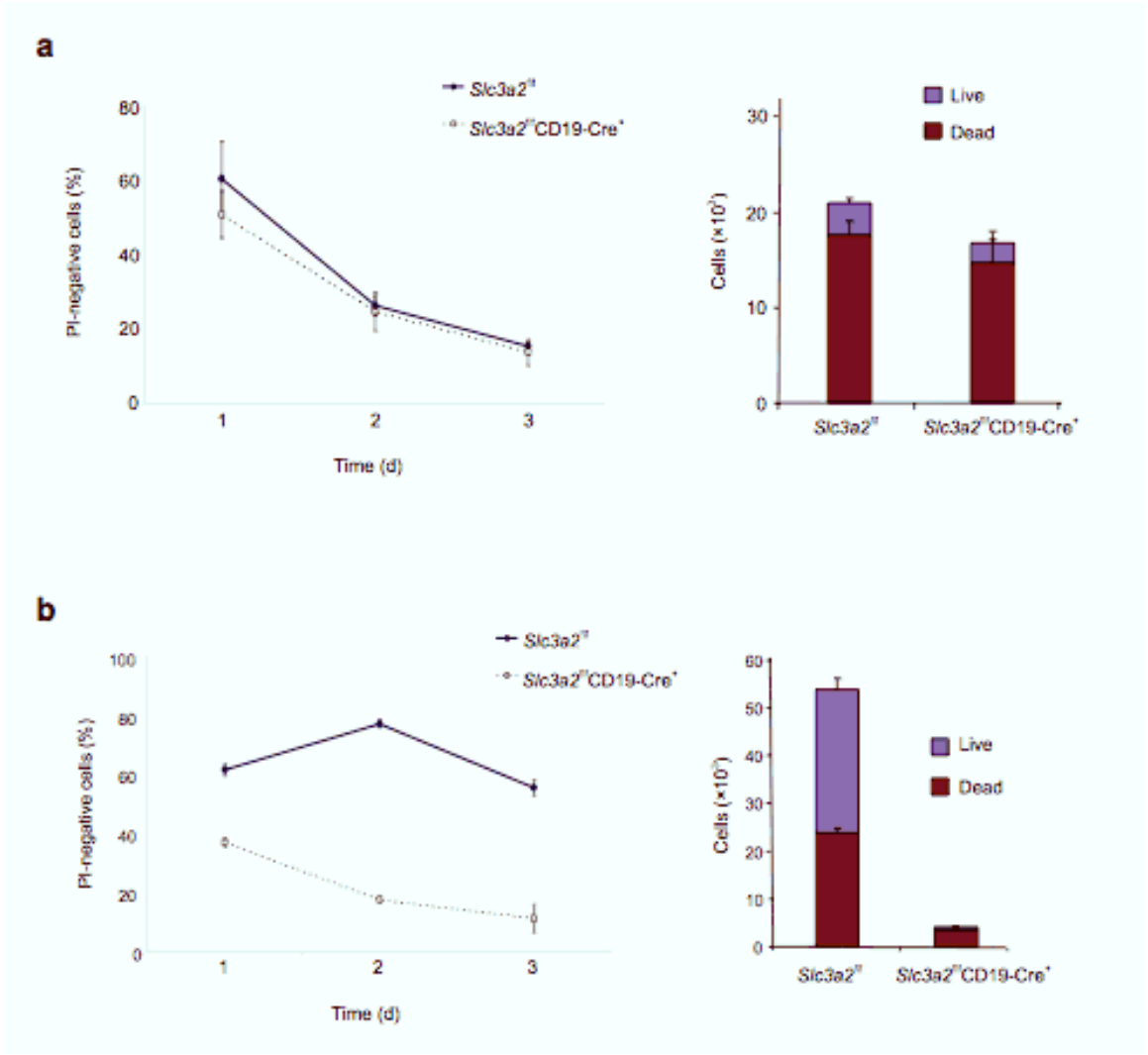


**Supplementary Figure 2-8: Survival and proliferation of splenic B cells from Slc3a2f/fCD19-Cre+ mice**. Resting B cells (CD43—) were purified from splenic single-cell suspensions from 8-12 wk-old Slc3a2f/fCD19- Cre+ or littermate control mice. 400,000 B cells were cultured per well in a 48-well plate with anti-IgM (30 µg/ml) and IL-4 (50 ng/ml) (b) or were left unstimulated (a). Cells were harvested at 1, 2, or 3 days and stained by propidium iodide to mark dead cells. At day 3, total cell number and number of dead and live cells was also determined (bar graphs); please note different scales for unstimulated vs. stimulated cells at 3 days. Error bars indicate s.e.m. from 3 mice for each group. Experiment was repeated once. Supplementary Figure 2-8 was contributed by Joseph Cantor.

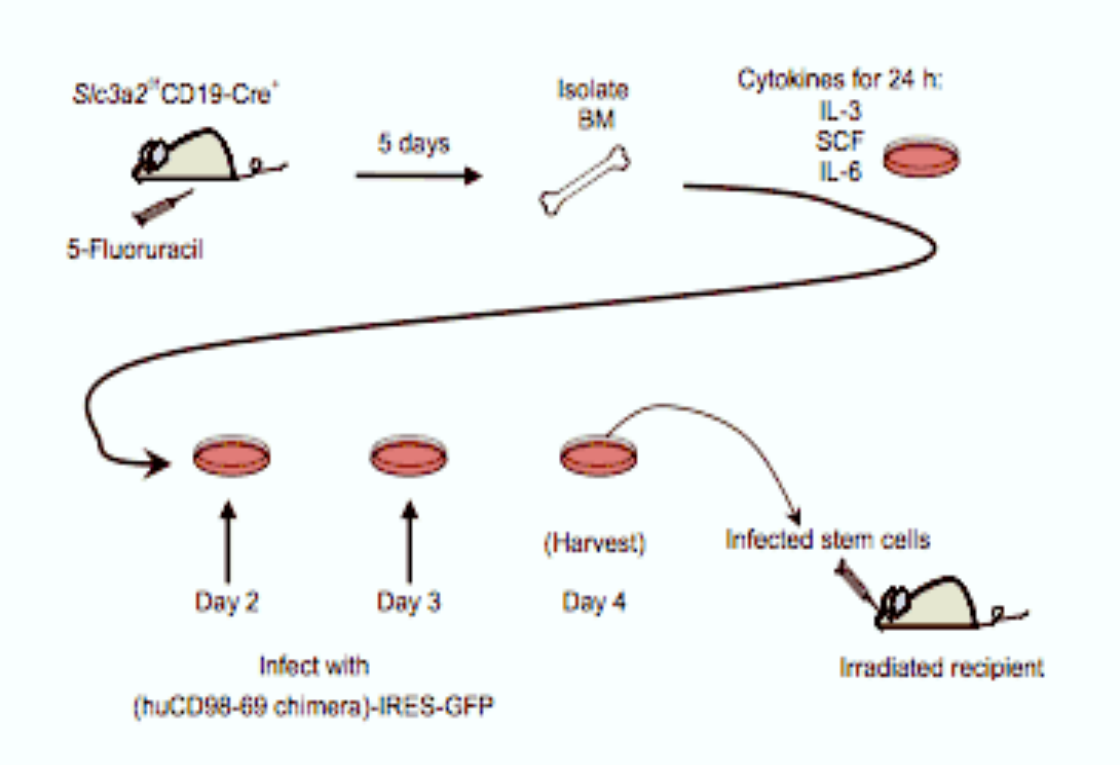


**Supplementary Figure 2-9: Protocol for generating primary B cells lacking one or both functions of CD98**. Stem cell-enriched BM isolated from adult Slc3a2f/fCD19-Cre+ mice pretreated with 5-Fluorouracil was repeatedly infected with retrovirus in the presence of IL-3, IL-6 and SCF. On day 4 after BM isolation, cells were harvested and injected into lethally irradiated recipient mice i.v. (n=3-5 per group). Supplementary Figure 2-9 was contributed by Joseph Cantor.

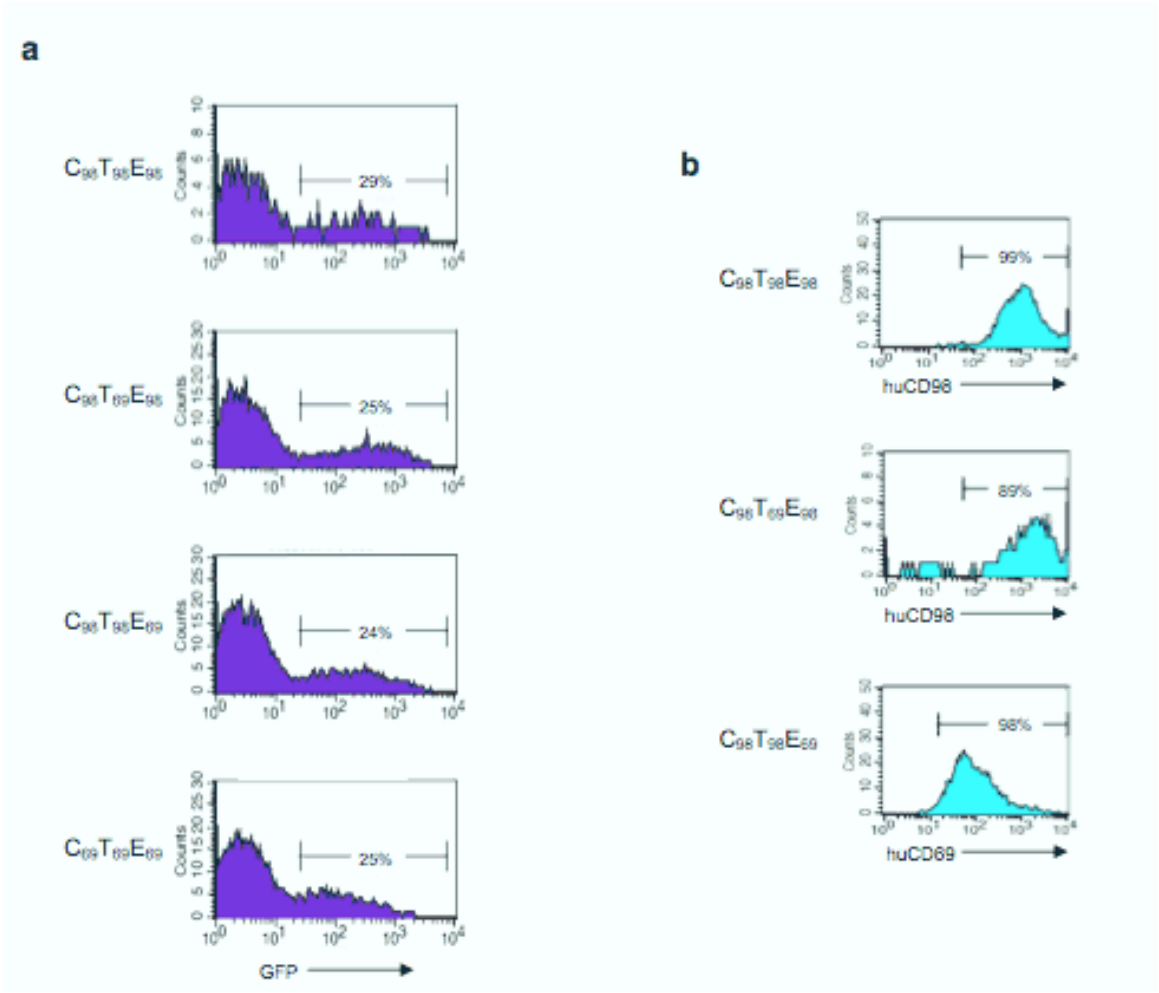


**<u>Supplementary Figure 2-10: Expression of human CD98-69 chimeras</u>**. **(a)** Efficiency of retroviral infection of stem cells. Before injection into irradiated recipient mice, BM cells infected on two successive days with indicated CD98-69chimera-IRES-GFP retroviruses were stained for the stem cell marker Sca-1, and analyzed for GFP expression by flow cytometry. Histograms are gated on stem cells (Sca-1+); percentages are % GFP+ **(b)** Chimera expression. Purified (CD43—mCD98—) B cells from irradiated mice that had been reconstitued with CD98-69chimera-IRES-GFP retrovirus-infected BM were stained for human CD98hc or CD69 to assess chimera expression by GFP+ cells. Histograms are gated on GFP+ cells; numbers indicate % of GFP% cells that express chimera. Experiment was repeated twice. Supplementary Figure 2-10 was contributed by Joseph Cantor.

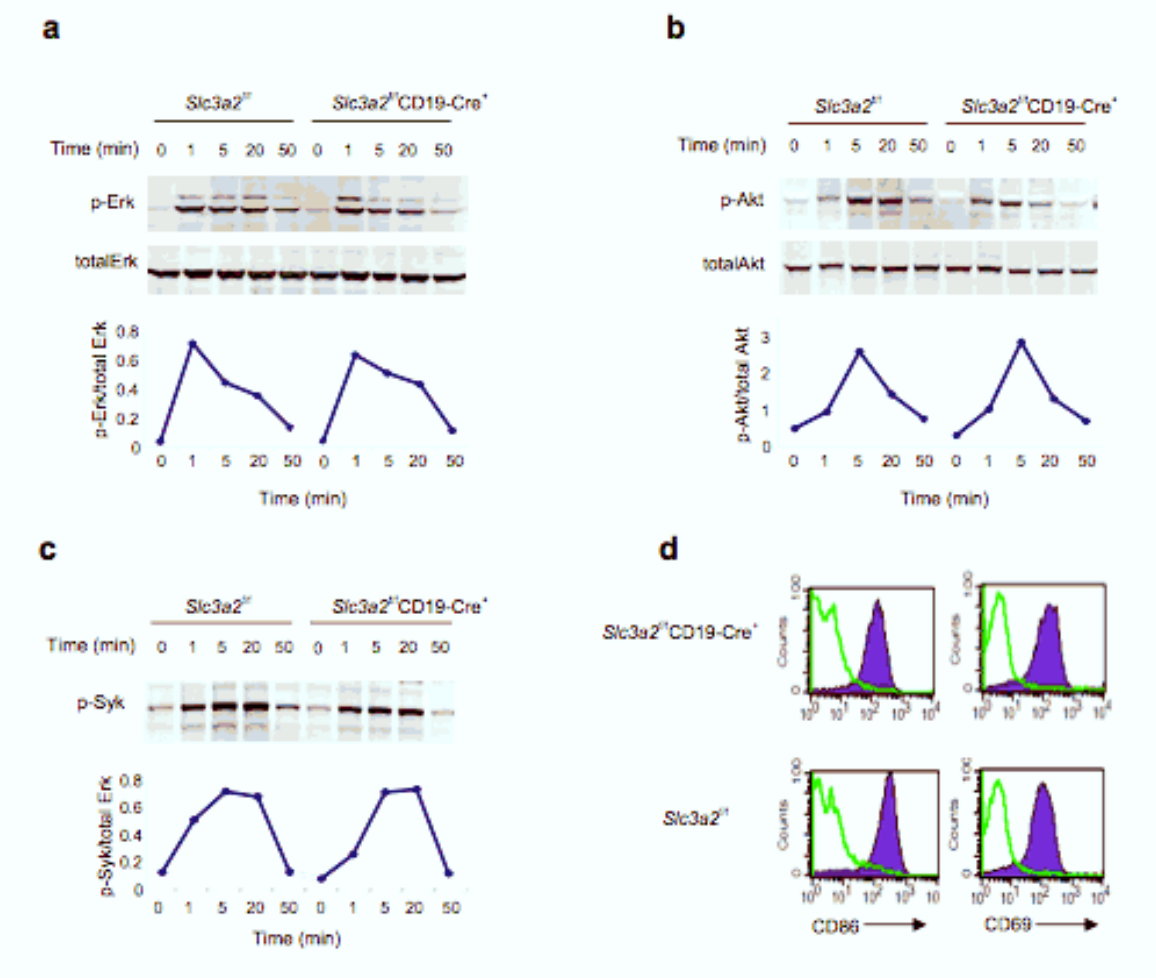


**Supplementary Figure 2-11: Early BCR signaling and activation in B cells lacking CD98hc.** **(a-c)** BCR signaling. Resting B cells (CD43—CD98—) were purified from splenocytes of 8-12 wk-old *Slc3a2f/f*CD19-Cre+ or littermate control mice and were stimulated with anti-IgM (10 ug/ml) and IL-4 (15 ng/ml) for 0-50 min. Cells were then immediatedly washed with ice-cold buffer, lysed, and phosphorylation of Erk1/2 (**a**), Akt (**b**), and Syk (**c**) were measured by immunoblotting. Plots below each lane show quantified staining density normalized to total Erk, Akt or Syk over time. This experiment was repeated 2 additional times with similar results. **(d)** B cell activation. Purified B cells from *Slc3a2f/f*CD19-Cre+ or littermate control mice were stimulated for 24 h with anti-IgM (30 ug/ml) and expression of the early activation markers CD86 and CD69 was measured by flow cytometry. Filled histograms show anti-IgM-stimulated cells, open histograms show unstimulated cells. Experiments in (**a-d**) were repeated once. Supplementary Figure 2-11 was contributed by Joseph Cantor.

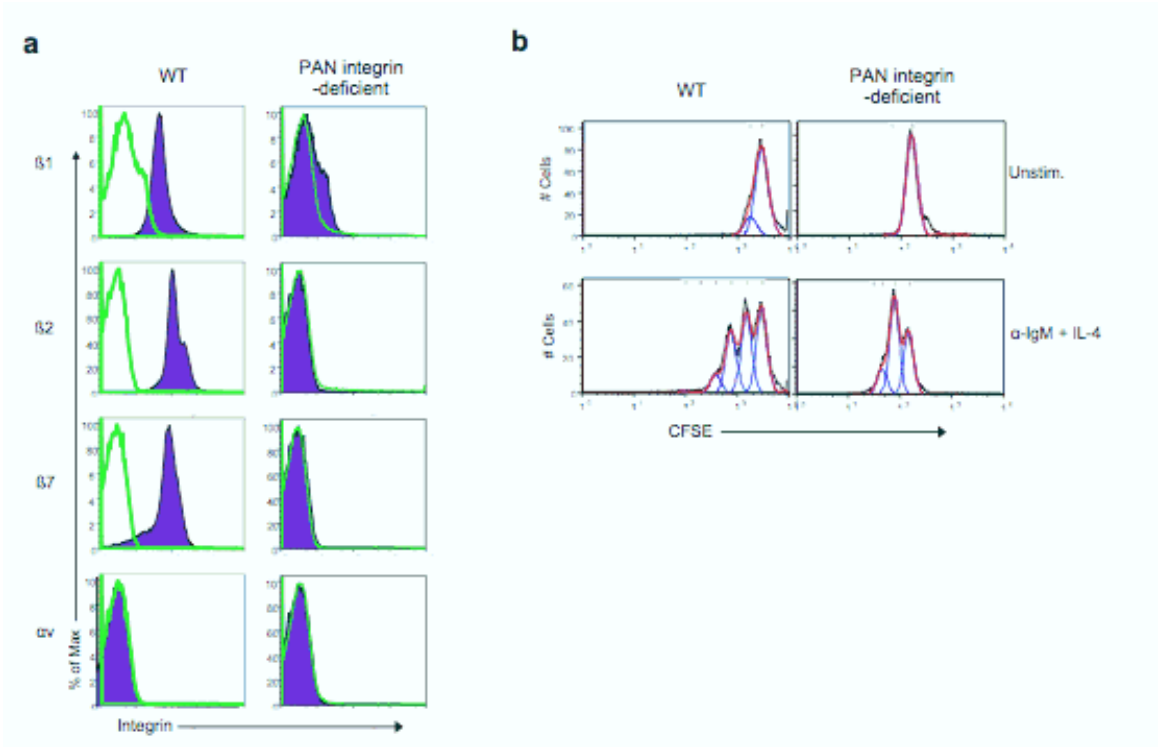


**Supplementary Figure 2-12: Pan integrin-deficient B cell proliferation. (a) Integrin expression *ex vivo*.** Resting B cells (CD43–) were purified from splenocytes of adult pan integrin-deficient mice (*Itgb1*flf, *Itgav*flf, *Itbg2*–/–, *Itgb7*–/–, mx1-CRE+, poly IC treated) or littermate control mice and were depleted of residual integrin-β1+ B cells in the case of the pan integrin-deficient B cells. Integrin expression on purified mature B cells was measured by flow cytometry after staining with specific antibodies. **(b)** B cell proliferation. Purified B cells from pan integrin-deficient mice or littermate control mice were labeled with CFSE and stimulated for 3 days with anti-IgM and IL-4. Cell division as measured by dilution of CFSE was assessed by flow cytometry. Histograms have been arranged to allow comparison with unstimulated cells, as CFSE labelling varied between samples. Data represents two experiments. Supplementary Figure 2-12 was contributed by R. Ruppert.

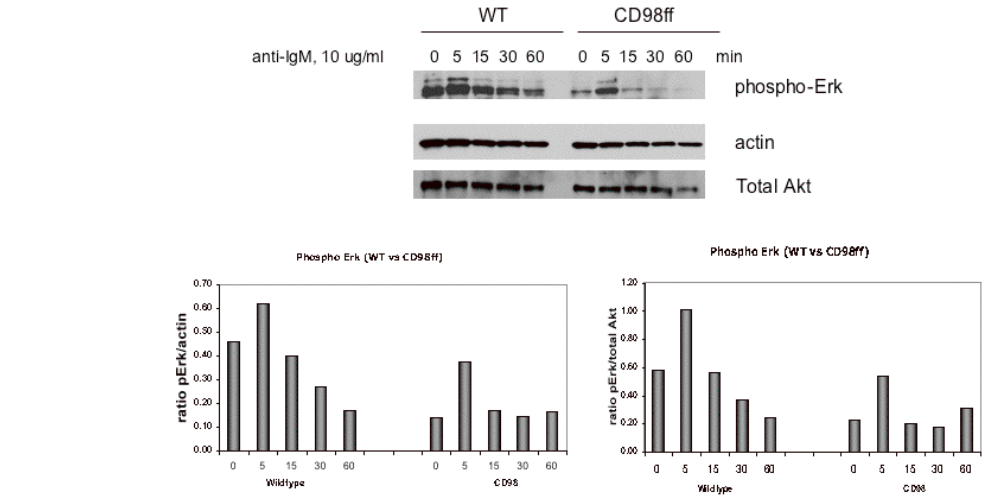


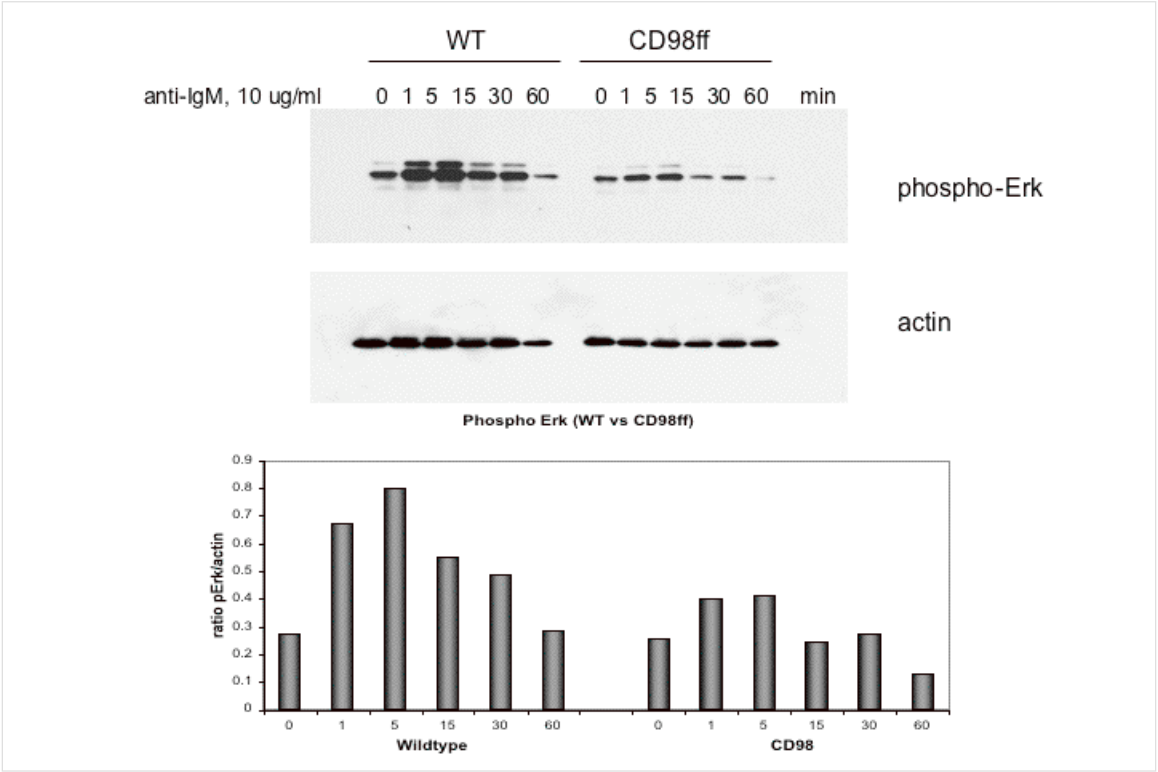


**Supplementary Figure 2-13: Erk phosphorylation is inhibited in uncultured splenic cells in the absence of IL-4 upon stimulation with anti-IgM.** Splenic B cells were purified from wildtype and CD98ff mice and immediately stimulated with anti-IgM for the indicated times. Cells were lysed and immunoblotted with anti-phospho-Erk, total actin and total Akt. Two experiments are shown.

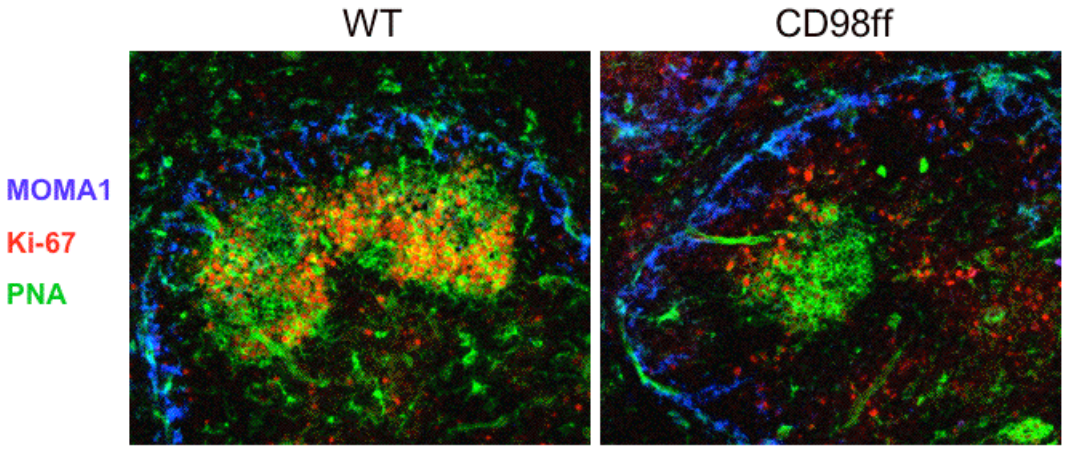


**Supplementary Figure 2-14**: **B cell proliferation is reduced in CD98ff mice upon immunization with with LPS**. Splenic sections from LPS-immunized mice were stained for Ki67 (proliferation) and PNA (germinal center). MOMA-1 shows the border between marginal zone and follicular B cells. This figure shows reduced proliferation in the absence of CD98.

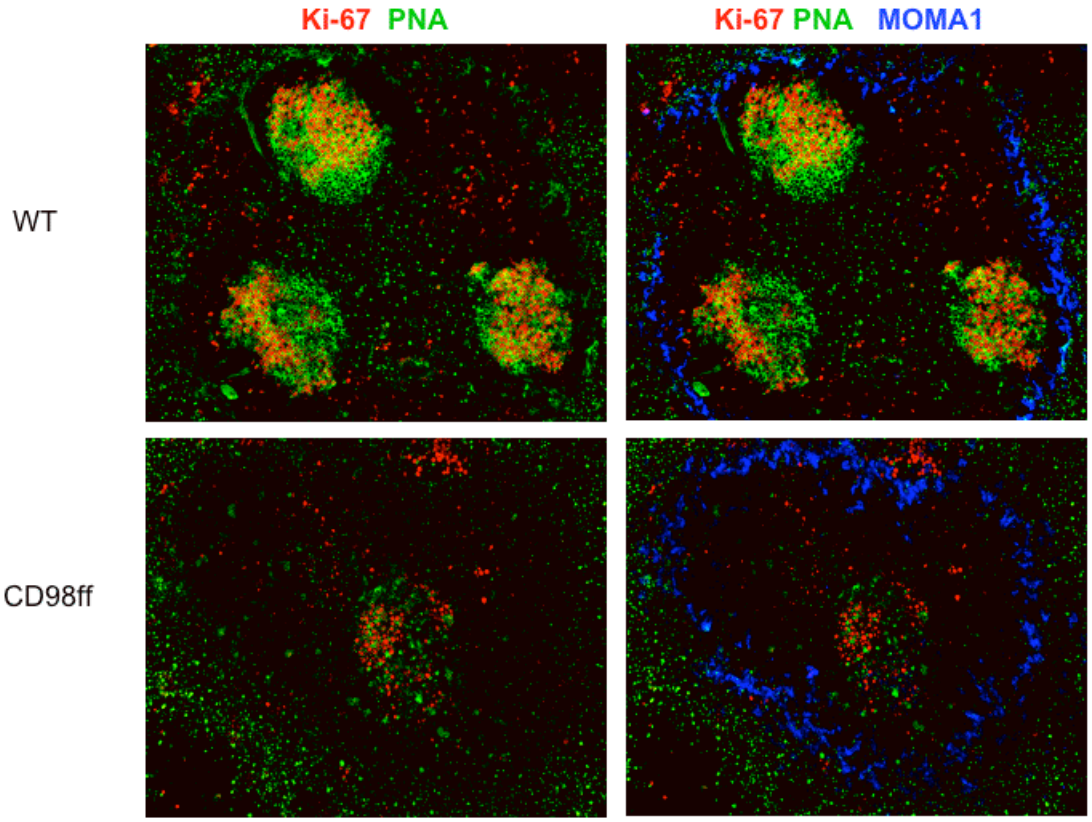


**Supplementary Figure 2-15**: **B cell proliferation is reduced in CD98ff mice upon immunization with with NP-KLH.** Splenic sections from NP-KLH-immunized mice were stained for Ki67 (proliferation) and PNA (germinal center). MOMA-1 shows the border between marginal zone and follicular B cells. This figure shows reduced germinal center B cells and poor proliferation in the absence of CD98.

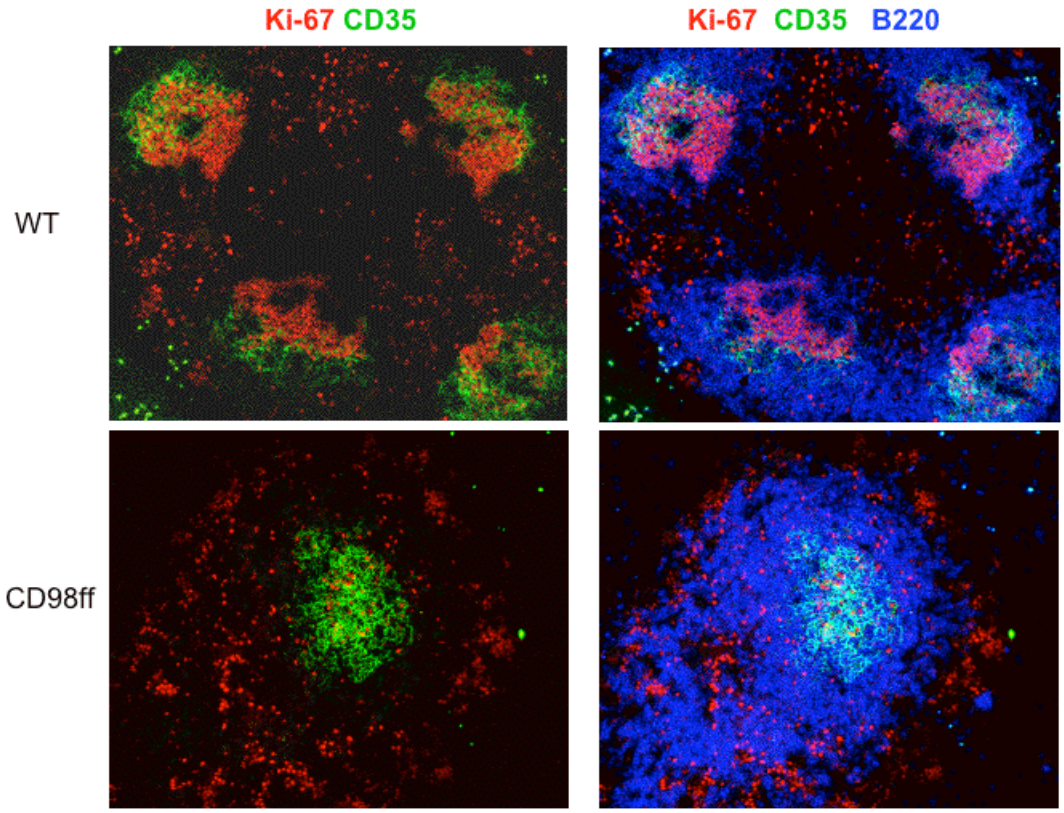


**Supplementary Figure 2-16**: **B cell proliferation is reduced in CD98ff mice upon immunization with with NP-KLH.** Splenic sections from NP-KLH-immunized mice were stained for Ki67 (proliferation), B220 and CD35.

# CHAPTER 3

## SHEP1 and B cell motility

### 3.1 - Introduction

B cell movement is a requirement for B cell development, differentiation and function. Chemokines such as BLC and SDF1α choreograph adhesion, de-adhesion and forward movement of B cells depending on environmental and developmental contexts (1-4). Lipid mediators such as sphingosine-1-phosphate have also been shown to direct B cell movement (5, 6). In consideration of the number of chemokines, lipids mediators, ligands, receptors, environmental and developmental cues that dictate motility, it is not surprising that sophisticated programs of intracellular events are in place in B cells ready to respond to diverse scenarios. Research in cell signaling effecting adhesion, polarization and migration has grown over the years, yet many open questions remain.

Two major types of receptors that can trigger migration and adhesion in B cells are chemokine receptors and the Edg (endothelial differentiation gene) family of receptors. The chemokine receptor family consists of 18 distinct members in mammals (7). Chemokine receptors have a 7-transmembrane structure that couples to G-proteins for signal transduction. Edg receptor family members also couple to G-proteins when bound by lysophospholipids, such as lysophosphatidic acid (LPA) and sphingosine 1-phosphate (S1P) (8). Edg receptors are G protein-coupled receptors consisting of a short, acidic N-terminal end, a 7-transmembrane domain and an intracellular C-terminus containing serine and threonine residues (8). G-proteins link to the C-terminal end of the chemokine receptors following ligand engagement. G-proteins heterotrimerize when

GTP-loaded (active state). G-proteins activate phospholipase C (PLC), which then cleaves phosphatidylinositol (4, 5) -bisphosphate (PIP2) to form the two second messenger molecules called inositol triphosphate (IP3) and diacylglycerol (DAG). IP3 triggers calcium mobilization while DAG activates protein kinase C (PKC) (9).

Other players downstream of chemokine receptors are small GTPases, which are 20-29 kDa proteins that contain guanosine triphosphate binding domains (10). Small GTPases are activated by the removal of bound GDP and the loading of GTP, and this exchange is facilitated by guanine nucleotide exchange factors (GEF). In the activated conformation, GTPases bind effector molecules. GTPs on GTPases are hydrolyzed by GTPase-activating proteins (GAPs). Conversion of GTP to GDP represents the 'off switch', after which the GTPase can no longer bind effector molecules. This on and off cycle of small GTPases is therefore controlled by GEFs and GAPs (10). The interplay of GTPAses, GEFs and GAPs has been shown to be essential in B cell differentiation. C3G (Crk SH3-domain-binding guanine-nucleotide releasing factor) is a GEF known to activate Rap1 and requires the adaptor molecule CrkL (11). The loss of a GAP known as signal-induced proliferation-associated gene1 (SPA1) in mice results in selective memory responses (12). SPA1-deficient B cells reveal an accumulation of Rap1-GTP (13) indicating a requirement for GAP in the hydrolysis of Rap-GTP. Moreover, Rap1A-deficient lymphocytes have impaired integrin-mediated cell adhesion (14).

Interestingly, many molecular lesions affecting GTPases, GAPs and GEFs lead to a loss of marginal zone compartment. This is most likely due to the fact that marginal zone B cells are residents of the marginal zone niche and their recruitment and maintenance in this niche specifically requires integrin activation (15, 16). For example,

the loss of Rap1B leads to a loss in marginal zone B cells (17,18). Deletion in mice of DOCK2, a key adaptor molecule downstream of chemokine-mediated Rac activation, resulted in the loss of chemotactic responses and MZB cells (19). Lsc, a rhoGEF has been shown to be important in immune responses to T-independent (TI) and T-Dependent (TD) antigens and the formation of the marginal zone (20). Pyk2, a tyrosine kinase involved in cytoskeletal rearrangements and B cell migration, has been found to be a downstream effector of BCR, CXCR5 and S1P receptor signaling (21-23). Crk-associated substrate lymphocyte-specific protein, CasL, has been shown to be important in MZB cell maintenance and its loss impaired lymphocyte trafficking (24).

SHEP1, or SH2 domain containing Eph receptor binding protein 1, also known as CHAT, or Cas-Hef1 Associated Signal Transducer, share the same family as NSP1 and BCAR3/AND34, all of which contain an SH2 domain linked to a GEF or GEF-like domain (25). SHEP1 isoforms are SHEP1α (long), SHEP1β, SHEP1γ and SHEP1δ and the expression of these variants can be tissue specific (25). The SHEP1 gene consists of 15 exons with alternative splicing occurring among the first six exons (25). Aside from an SH2 domain, SHEP1 also contains a proline/serine rich domain and a guanine nucleotide exchange factor-like domain (Fig 3-1); however, the catalytic activity of the GEF-like domain has not been demonstrated. The C-terminal domain has also been shown to bind Ras and Rap (26).

Regelman and coworkers have implicated SHEP1 in T cell migration (27). The authors showed that the loss of SHEP1 negatively affected Rap1 activation following SDF1α stimulation. Therefore, Rap1 activation may be dependent upon SHEP1 and CasL association (27). How SHEP1 is mechanistically involved in B cell motility is not

known. Since B cell differentiation also depends on migration and adhesion, the loss of SHEP1 in B cells is predicted to interfere with these processes.

To investigate the role of SHEP1 in B cells, we established a conditional *SHEP1*-deficient mouse in which SHEP1 deletion is driven by the B cell-specific CD19 promoter. We found that *SHEP1*$^{flox/flox}$ *CD19cre* mice mount normal immune responses to T-independent and T-dependent antigens. We found however, that *SHEP1*$^{flox/flox}$ *CD19cre* have a markedly reduced marginal zone B cell compartment. SHEP1-deficient B cells have defects in cell migration and spreading. Mechanistically, we found that signaling events following BCR activation, such as calcium flux and Akt and Erk activation, were intact. However, Rac activation is severely diminished in the absence of SHEP1 downstream of both the BCR and S1P receptor. We also found that SHEP1 constitutively binds CasL and that SHEP1-deficient B cells show a reduced level of the p115 molecular form of CasL, suggesting an inability of CasL to become serine phosphorylated downstream of BCR and S1P stimulation. Tyrosine 787 of SHEP1$\alpha$ corresponds to tyrosine 635 of SHEP1$\beta$, which has been shown to be an important residue for p130Cas binding (28, 29). There is an ongoing effort in our lab to test our hypothesis that the interaction between SHEP1 and CasL via this tyrosine residue is important for B cell integrin activation and for the formation of the marginal zone.

## 3.2 - Results

### 3.2.1 - SHEP1 is expressed in B cells and SHEP1$^{-/-}$ mice have a reduced marginal zone B cell compartment.

The long isoform of SHEP1, SHEP1α, has been shown to be expressed in T cells (27). However, SHEP1α expression in B cells has not been investigated. To determine if SHEP1α is expressed in B cells, purified splenic B cells from wildtype and SHEP1$^{-/-}$ mice were lysed and probed by Western blot using antibodies specific to the SH2 domain of SHEP1. We found that SHEP1α is expressed in B cells as shown by the presence of a 115 kDa band present in wildtype B cell lysates and absent in SHEP1$^{-/-}$ B cells (Fig 3-2A). Analysis of the immunological compartments of the SHEP1$^{-/-}$ mice revealed that pre/pro (IgM-, IgD-), immature (IgM+, IgD-) and recirculating mature (IgM+, IgD+) B cell compartments in the bone marrow were comparable to wildtype controls (Fig 3-2B). CD4/CD8 double positive T cells in the thymus of SHEP1$^{-/-}$ mice were comparable to wildtype controls (Fig 3-2C). In the lymph node, the frequencies of B cells, CD4 and CD8 positive T cells, and CD11b+ macrophages were also comparable to wildtype controls (Fig 3-2D). In the blood, B220+ B cell frequencies were found to be elevated in the SHEP1$^{-/-}$ (Fig 3-2E, upper left panels), which may be indicative of a defect in B cell homing. B cell IgM and IgD receptor profiles, as well as T cell CD4/CD8 single positive populations in the blood of SHEP1$^{-/-}$ were comparable to control (Fig 3-2E, lower right panels). In the spleen, overall B cell (B220+), T cell (CD5+) and macrophage (CD11b+) populations were also comparable to control (Fig 3-2F top panels). Analysis of B cell subcompartments in the spleen revealed a 2.4-fold reduction in the gated compartment comprised of marginal zone B and marginal zone precursor B cells, represented by the

IgMhi, CD21hi gated population (Fig 3-2F, middle left panels). The marginal zone population based on another gating strategy (CD23lo, CD21hi) was reduced 10-fold (Fig 3-2F, lower left panels). There were no differences in T cell subpopulations (Fig 3-2F, middle right panels) and neither in basal germinal center population (FAS+) (Fig 3-2F, lower right panels). The microarchitecture of the spleen of SHEP1$^{-/-}$ mice, analyzed by immunofluorescent staining, was also found to be disrupted, with a loss of the IgMhi B cell population identifying the marginal zone B cells at the periphery of follicles (Fig 3-2G).

The marginal zone is comprised of stromal cells, macrophages and B cells. At this point, it is unclear whether the loss of the marginal zone is intrinsic to B cells or due to the loss of SHEP1 in other resident cells. To determine if the observed loss of the marginal zone is intrinsic to B cells, *SHEP1$^{flox/flox}$* mice were bred with *CD19cre* mice to obtain mice with a B cell-specific deletion of SHEP1. Deletion of SHEP1$\alpha$ was verified by Western blot showing the absence of SHEP1 in purified B cell lysates and the presence of SHEP1 in the fraction containing T cells and macrophages (Fig 3-3A). Immunological compartments of *SHEP1$^{flox/flox}$CD19cre* mice were analyzed by flow cytometry. In the blood, the frequencies of B cells were elevated in the *SHEP1$^{flox/flox}$CD19cre* mice and moderately elevated in the *SHEP1$^{flox/+}$CD19cre* mice compared to wildtype (Fig 3-3B, top panel and 3-3D). This is consistent with what was observed in the SHEP1$^{-/-}$, further supporting the possibility of defective homing of SHEP1-deficient B cells. In the bone marrow, the immature B, pre/pro B and mature B cell numbers were comparable with control mice (Fig 3-3B, lower right panel and 3-3C). In the spleen, overall B cell, T cell and macrophage numbers were found to be

comparable to wildtype (Fig 3-3B, lower left panel). Analysis of B cell subcompartments in the spleen revealed a 6.7-fold reduction in the mature marginal zone and marginal zone precursor B cell compartments (CD21hi, IgMhi) in *SHEP1*$^{flox/flox}$*CD19cre* mice (Fig 3-3E) by CD21/IgM staining. This result was confirmed by CD23/CD21 staining which shows a 4.7-fold decrease in the marginal zone compartment (Fig 3-3F). Immunofluorescent staining of splenic sections with B220 (green) for B cells and MOMA-1 (red) for metallophilic macrophages (which line the marginal sinus and delineate the follicular B cells and the marginal zone B cells) confirmed the loss of the marginal zone compartment (Fig 3-3G). To address the possibility that MZB cells may have altered their CD23/CD21 expression and are mislocalized in the spleen, B cells were stained with other markers, such as CD1d and CD9, shown to be highly expressed in marginal zone B cells. These additional markers confirmed the loss of marginal zone B cells in *SHEP1*$^{flox/flox}$*CD19cre* mice (Fig 3-3H). The *SHEP1*$^{flox/flox}$ mice were also bred with the *Ig-α cre* mice to achieve deletion of SHEP1 at the earliest pro-B cell stage in development (47). Bone marrow and lymph node B and macrophage compartments in these animals were also found to be normal (data not shown). Upon analysis of splenic B cells in *SHEP1*$^{flox/flox}$ *Ig-α cre* mice, we found that the marginal zone compartment in these animals was also reduced (Fig 3-4).

Marginal zone B cells have been shown to interact with resident marginal zone macrophages in the marginal zone niche and this interaction is important for the retention of marginal zone B cells in the marginal zone (30-32). To determine if the loss of marginal zone B cells is accompanied by a loss of marginal zone macrophages, splenic sections were stained with MARCO, a marker expressed by marginal zone resident

macrophages and with MOMA-1. We found that the marginal zone macrophage population was intact in the absence of marginal zone B cells (Fig 3-5). Thus, the loss of resident B cells is not due to loss of co-resident macrophages.

The cell differentiation stage just prior to the marginal zone stage is the marginal zone precursor stage (MZP). To determine if the loss of marginal zone B cells is due to the specific loss of marginal zone precursor B cells, this population (CD23hi, CD21hi, IgMhi) was analyzed. While 27.1% of the gated marginal zone plus marginal zone precursor (MZ+MZP) B cell compartment in the wildtype was MZP, 59.5% of the gated MZ+MZP compartment in the *SHEP1*$^{flox/flox}$*CD19cre* mice was MZP (Fig 3-6A, upper left panels). The bar graph (Fig 3-6A, right panel) shows the average of three animals. The MZP population was also analyzed in *SHEP1*$^{flox/flox}$ *Ig-alpha cre* mice and we found a similar trend (Fig 3-6A, lower panels). Further analysis of absolute MZP numbers (data not shown) revealed no statistically significant difference between *SHEP1*$^{flox/flox}$*CD19cre* and control mice, indicating that the high MZP frequency in *SHEP1*$^{flox/flox}$*CD19cre* mice was due to a difference in ratios between MZ and MZP populations. These findings indicate that SHEP1-deficient B cells differentiate normally up to the MZP stage and but fail to be recruited and/or retained in the marginal zone. The presence of MZP B cells in the spleens of both *SHEP1*$^{flox/flox}$*CD19cre* and control mice are evident in splenic sections stained with CD23 and CD21 antibodies (Fig 3-6B). Follicular B cells are CD23hi, CD21lo, while marginal zone B cells are CD23lo, CD21hi and marginal zone precursor cells are CD23hi and CD21hi. Dual staining of CD21 and CD23 would represent the marginal zone precursor cells. Thus, SHEP1 may be involved in the differentiation of

MZB cells, which may be linked to the ability of MZB cell precursors to migrate to the marginal zone niche.

### 3.2.2 - SHEP1-deficient mice produce normal T-independent and T-dependent immune responses.

To determine the immune responses of SHEP1$^{flox/flox}$/CD19cre mice to TD and TI antigens, SHEP1$^{flox/flox}$/CD19*cre* and wildtype mice were immunized with T-independent antigen, nitrophenyl-conjugated FICOLL (NP-FICOLL) and T-dependent antigen, nitrophenyl-conjugated keyhole limpet hemocyanin (NP-KLH). Immune responses to NP-FICOLL (Fig 3-7) and NP-KLH (Fig 3-8) were comparable. *SHEP1$^{flox/flox}$CD19cre* mice were also immunized with a heat-inactivated strain of *Streptococcus pneumoniae* (R36A). In response to these bacterial cells, the antibodies predominantly produced are directed to the phosphorylcholine (Pc) determinant on the cell wall. Marginal zone B cells have been shown to have specificity towards Pc. The immune response to R36A, measured by ELISA, appeared to be normal (Fig 3-9A). However, flow cytometric analyses of B cell compartments of the immunized SHEP1$^{flox/flox}$/CD19*cre* mice showed an increase in germinal center B cells (GL7hi, FAShi) (Fig 3-9B, bottom panels), plasma cells (IgDlo, Syndecan-1hi) (Fig 3-9B, top and middle panels), and switched B cells (data not shown).

### 3.2.3 - SHEP1-deficiency leads to impaired B cell migration.

To investigate the mechanistic role of SHEP1 in B cells, we assessed the ability of SHEP1-deficient B cells to migrate towards BLC/CXCL13, a critical B cell chemokine

(2) and towards sphingosine-1-phosphate (S1P), a lipid present in blood, which had been shown to be critical in chemoattracting B cells to the marginal zone niche (5). Using a transwell migration assay, we found that *SHEP1*$^{flox/flox}$*CD19cre* B cells migrated poorly towards S1P (Fig 3-10A). However, this decrease may be due to the loss of the marginal zone population, which specifically responds to S1P. Therefore, it would be helpful to perform a modified version of the *in vitro* migration assay, in which migrant cells will be analyzed by flow cytometry for specific B cell subpopulations. Migration towards BLC was also reduced with SHEP1$^{flox/flox}$/CD19*cre* B cells. Both follicular and marginal zone B cells have been shown to respond to BLC; therefore the observed 50% reduction in migration towards BLC further supports the possibility that SHEP1 plays a role in cell signaling leading to successful cell migration (Fig 3-10B, left panel). The observed reduction in migration towards BLC was not due to a decrease in the BLC receptor, CXCR5, which we found to be higher in SHEP1-deficient B cells (Fig 10B, right panels).

B cells have been shown to spread upon BCR engagement. Cell spreading is a qualitative measure of adhesion and actin polymerization. The ability of B cells to spread on anti-IgM-coated slides was assessed after 24 hr of culture. We found that *SHEP1*$^{flox/flox}$*CD19cre* B cells initially showed the ability to spread (data not shown); however, after 24 hr, the degree of cell spreading diminished (Fig 3-10C).

To determine if defective migration and cell spreading were due to the inability of these cells to activate integrins, B cells were stimulated with anti-IgM F(ab')$_2$ and then allowed to bind VCAM-Fc and ICAM-Fc. VCAM/ICAM binding was detected by flow cytometry using anti-Fc conjugated antibodies. SHEP1-deficient B cells can inducibly bind integrin ligands upon BCR stimulation; however, this binding appeared to be poorly

maintained by follicular B cells (Fig 3-11A, upper panel). Analysis of the marginal zone B cells reveal constitutively active integrins and this is consistent with the observation by Lu and Cyster that marginal zone B cells have elevated integrin expression (46). We found that MZB cells downmodulate integrin activity upon stimulation. We also found that the kinetics of integrin 'inactivation' was faster in SHEP1$^{flox/flox}$-CD19*cre* B cells (Fig 3-11A, lower panel). The levels of total integrin expression, detected by anti-LFA and anti-VLA antibodies were comparable between SHEP1$^{flox/flox}$-CD19*cre* B cells and wildtype cells in both follicular and marginal zone B cell compartments (Fig 3-11B). Actin polymerization was also measured by staining BCR-stimulated cells with phalloidin. We determined a basal loss of polymerized actin in SHEP1$^{flox/flox}$-CD19*cre* B cells (Fig 3-11C). These results suggest that SHEP1 may be mediating the maintenance of integrin activation and actin remodeling both of which are critical factors effecting B cell motility.

### 3.2.4 - SHEP1-deficient B cells have reduced Rac activation upon S1P receptor stimulation and reduced Rac and Cdc42 activation in response to BCR stimulation.

B cell receptor stimulation leads to Rac and Cdc42 activation, which is important for actin remodeling. To determine if the loss of SHEP1 would impact Rac and Cdc42 activation, splenic B cells were stimulated with anti-IgM, lysed and activation of Rac and Cdc42 were determined using a GST pulldown assay. Splenic cells were also stimulated with S1P and lysed were similarly analyzed for activated Rac and Cdc42. We found that while Rac is constitutively active, Cdc42 was not. After 1 min of BCR stimulation, wildtype B cells continue to have activated Rac and were able to induce Cdc42

activation; however, *SHEP1*$^{flox/flox}$*CD19cre* B cells have markedly reduced Rac and Cdc42 activation upon stimulation of the BCR (Fig 3-12A). Upon stimulation with S1P, while Rac activation appeared to be moderately reduced, Cdc42 activation was not affected within this time course (Fig 3-12A). Stimulation of the BCR also triggers the mobilization of calcium and JNK and Erk phosphorylation, and JNK activation, in particular, is downstream of Rac activation. To determine if the loss of Rac activation leads to diminished JNK activation, wildtype and SHEP1-deficient B cells were stimulated with anti-IgM and probed for these proteins. Consistent with the reduced Rac activation, JNK activation was also reduced, but Erk activation was unaffected in SHEP1-deficient B cells (Fig 3-12B). The ability to mobilize calcium in response to BCR stimulation was intact in SHEP1-deficient B cells (Fig 3-13A). Interestingly, stimulation with BLC resulted in reduced calcium flux in SHEP1-deficient B cells (Fig 3-13B). Akt phosphorylation, determined by flow cytometry, in follicular and marginal zone compartments was unaffected in the absence SHEP1 (Fig 3-13C). Thus, SHEP1 may be playing a role only in specific signaling axes downstream of BCR or S1P receptor stimulation. It appears that SHEP1 is not involved in pathways leading to Erk and Akt activation, but it is important in Rac and Cdc42 activation downstream of BCR stimulation. It also appears that downstream of S1P receptor stimulation, SHEP1 is important in Rac activation but it may not be important in Cdc42 activation.

### 3.2.5 – Constitutive Association between CasL and SHEP1

To determine the mechanism by which SHEP1 mediates responses to S1P and BCR stimulation, we first analyzed the subcellular localization of SHEP1 by

immunofluorescence microscopy using unstimulated Bal17 cells, which is a mature B cell line. An association between SHEP1 and CasL has been previously reported in T cells (27). Bal17 cells were plated onto VCAM-coated wells overnight. After fixation and permeabilization, cells were stained with phalloidin, anti-SHEP1 and anti-CasL and analyzed by immunofluorescence microscopy. SHEP1 colocalized with the peripheral actin ring in B cells, as well as with cytoplasmic actin (Fig 3-14) suggesting the activity of SHEP1 in the vicinity of actin polymerization activity. In the basal state, CasL and actin colocalization is not apparent at the periphery, and CasL and SHEP1 colocalization is more cytoplasmic in nature (Fig 3-14). To determine if CasL and SHEP1 associate in response to S1P, Bal17 cells were stimulated with S1P, and CasL was immunoprecipitated and immunoblotted with anti-SHEP1 antisera. Interestingly, a constitutive association between SHEP1 and CasL was seen and the level of detectable CasL increased over time (Fig 3-15A). Blotting for SHEP1 showed a similar increase in SHEP1 proteins (Fig 3-15A). The concomitant increase in association of SHEP1 and CasL suggests a co-stabilization between the two molecules.

To determine the status of CasL in the absence of SHEP1, SHEP1-deficient B cells were lysed and immunoblotted for CasL. SHEP1-deficient B cells show less CasL protein than wildtype B cells (Fig 3-15B) and this reduction is not because CasL is expressed only in marginal zone B cells since we found it expressed in both follicular and marginal zone B cells (Fig 3-15C). It is also possible that this reduction is due to the loss of the hyper- phosphorylated species of CasL, which migrates slightly higher (115kDa). However, this apparent reduction in CasL band may depend on the detergent used to lyse cells. In another experiment in which RIPA lysis buffer, rather than NP-40 lysis buffer,

the difference in CasL band was no longer seen (data not shown). Additional experiments are necessary to assess the degradation of CasL in the absence of SHEP1; the use of the proteasome inhibitor may provide insight on how CasL degradation. It is possible that CasL function is perturbed in the absence of SHEP1 and this may be related to the instability of CasL. Furthermore, it is possible that the phosphorylation status of CasL requires SHEP1/CasL interaction.

Others have shown that CasL$^{-/-}$ mice have reduced marginal zone B cells. This leads us to hypothesize that the loss of marginal zone B cells in the *SHEP1$^{flox/flox}$CD19cre* mice may be due to CasL instability and overexpression of CasL may compensate for the degradation of CasL. To address this possibility, we overexpressed CasL in SHEP1-deficient bone marrow and looked for the reconstitution of the marginal zone. Bone marrow from wildtype and *SHEP1$^{flox/flox}$CD19cre* mice were transduced with CasL-expressing retrovirus. Transduced bone marrow cells were used to reconstitute irradiated *SHEP1$^{flox/flox}$-CD19cre* or wildtype mice. Mice were analyzed after 8 weeks. Fig 3-16A shows that reconstitution of irradiated wildtype or SHEP1$^{flox/flox}$CD19*cre* mice with *SHEP1$^{flox/flox}$-CD19cre* bone marrow did not reconstitute the marginal zone. To determine if overexpression of CasL rescues the marginal zone, irradiated mice that that been reconstituted with bone marrow transduced with CasL expressing retrovirus were analyzed after 8 weeks of reconstitution. Some animal deaths occurred which was not specific to any one experimental condition. At the end of the reconstitution only 1 of the experimental group of *SHEP1$^{flox/flox}$CD19cre* recipients reconstituted with *SHEP1$^{flox/flox}$CD19cre* plus CasL had survived. Interestingly, however, this mouse showed a partially restored MZB cell compartment (Fig 3-16B). Although this

experiment needs to be repeated, it suggests that the absence of SHEP1 destabilizes CasL and that CasL overexpression partially corrects the situation and in the absence of SHEP1, CasL eventually degrades. The incomplete rescue also suggests that SHEP1 may have other critical roles in the mediation of signals downstream of S1P.

### 3.2.6 - Creation of SHEP1 mutant constructs for future efforts to study SHEP1/CasL interaction and its importance for the formation of the marginal zone.

To determine if the interaction of SHEP1 with CasL is important for the formation of the marginal zone, mutant SHEP1 constructs were generated. It has been shown that a tyrosine residue in the short form of SHEP1 is critical in binding p130Cas (26, 28). The Y675E mutation but not Y675F mutation abrogated the binding of SHEP1 with p130Cas (26, 28). Since this tyrosine is also present in CasL, it is possible that this tyrosine residue is also critical for the interaction of SHEP1 with CasL and if so, this could be used as a tool in investigating the role of this interaction in the formation of the marginal zone. SHEP1 was amplified from purified B cell total cDNA and subcloned into pMIT vector. By site-directed mutagenesis, Y787E and Y787F mutant retroviral constructs have been generated (Fig 3-17). SHEP1-Y787E-pMIT, SHEP1-Y787F-pMIT and SHEP1-pMIT retroviral constructs will be used to infect bone marrow cells derived from $SHEP1^{flox/flox}$ CD19cre mice. Transduced bone marrow will be transferred into irradiated $SHEP1^{flox/flox}$ CD19cre mice. Mice will be analyzed after 8 weeks of reconstitution.

**3.3 - Discussion**

This chapter presents the observations that 1) SHEP1α is expressed in B cells; 2) SHEP1-deficient mice have a marked reduction in the marginal zone B cell compartment that has been consistently observed in SHEP1$^{-/-}$, *SHEP1$^{flox/flox}$-CD19cre* and *SHEP1$^{flox/flox}$Ig alphacre* mice; 3) SHEP1-deficient B cells are blocked at the marginal zone precursor stage; 4) SHEP1-deficient B cells have defects in migration in response to S1P and defects in cell spreading upon BCR stimulation; 5) SHEP1-deficient B cells have defects in integrin activation; and 6) SHEP1 and CasL constitutively associate, and SHEP1-deficient B cells appear to have reduced CasL signal, although it is possible that the high molecular weight form, hyper-(serine-, threonine- and tyrosine-) phosphorylated CasL (p115), may be absent, as seen in T cells (27).

The predominant expression of the long form of SHEP1 resonates with observations in T cells (27) both of which require adaptive motility in response to foreign antigens. SHEP1α contains a unique N-terminal region that is absent in shorter isoforms of SHEP1. It has been shown to position SHEP1 at the periphery of the cell (27) and myristoylation of the shorter isoform of SHEP1 led to enhanced Rap1 activation in HEK293 cells (33). When we queried the first ~200 amino acid residues of SHEP1α using the Motif Search Prosite server, we learned of five motifs present in this region, one of which is a myristoylation site at residues 21-26. It would be interesting to perform a mutagenesis study to demonstrate that these residues are in fact myristoylated (Fig 3-18A). I also wondered if this region of SHEP1α has TRP motifs, even though these motifs were not identified by the Motif Search Prosite server (34). TRP (tetratricopeptide repeat) motifs are degenerate ~34 amino acid repeats that may be mediating protein-

protein, as well as protein-lipid interactions (35). Proteins containing these repeats may act as scaffolds for assembly of multiprotein complexes (36). Furthermore, it has been reported that Rac-GTP binds TRP motifs within NADPH oxidase (37). Analyzing the first ~35 residues of SHEP1α, I found a pattern of residues that appear to follow the consensus sequence of TRP repeats shown in Fig 3-18B (35). Thus, as a scaffolding protein, SHEP1α may be specially designed for complex assembly. Whether or not the GEF-like domain of SHEP1 has an exchange function and which GTPase is using SHEP1 as a GEF remains to be determined. The impairment of Rac activation implies that SHEP1 indirectly or directly promotes Rac activation. Another NSP family member, AND-34, has been shown to promote Cdc42 and Rac1 activation (45). This function may or may not be independent of its association with CasL.

The observation that the major B cell compartment affected by the loss of SHEP1 is the marginal zone B cell compartment implies its involvement in integrin regulation, which has been shown to be a requirement for marginal zone B cells to settle and be maintained in the marginal zone niche (16). Indeed we find that integrin activation is reduced in SHEP1-deficient B cells. This is consistent with the phenotypic losses of the marginal zone upon deletion of molecules regulating integrins (11,21). The fact that the marginal zone B cell precursors are not significantly affected in the absence of SHEP1 suggests that a critical migratory event is required specifically for the differentiation of these precursors into mature marginal zone B cells. Others have already shown that sphingosine-1-phosphate receptor 3 is the predominant receptor responsible for the recruitment of marginal zone B cells to the niche (5). Thus it is intriguing that SHEP1 plays a role downstream of S1P engagement. Given that S1P influences other B cell

activities such as the egress of B cells out of lymph nodes, the homing of plasma cells to secondary lymphoid organs or the trafficking of peritoneal B cells (38-41) we predict that these responses would also be perturbed.

Interestingly, the fact that the immune responses to TI antigen were intact could indicate that marginal zone precursor B cells are responding, as it has been shown by others (42). Early B cell development is intact, suggesting that SHEP1 may not be mediating movements in the bone marrow. It is unclear why SHEP1-deficient B cells are able to localize to the follicles, create germinal centers and yet exhibit reduced migration to BLC, the major chemokine that chemoattracts B cells to the follicles and a chemokine that is involved the movements within the germinal center B cell compartment (43). It is possible that other chemokines are compensating for these movements such as SLC (44). The higher frequencies of germinal center B cells in response *Streptococcus pneumoniae* that germinal center B cells have difficulties leaving the germinal center and this exit may be sphingosine-1-phosphate mediated akin to the egress of B cells out of lymph nodes. Immunization with pathogens to which a physically intact marginal zone is necessary, such as *Borrelia burgdorferi* might show a defect in SHEP1-deficient mice (45).

The observed increase in B cells in the blood was initially thought to be due to the release of marginal zone B cells into the blood, however, when blood B cells were analyzed for CD23/CD21 marginal zone B cell markers, both wild-type and *SHEP1*$^{flox/flox}$*CD19cre* mice were similarly negative for marginal B cells (data not shown). Thus, it is possible that some relocalize to another niche, such as lymph nodes, thymus, etc. with concomitant revision of surface markers such that identification of these cells will prove to be difficult.

Mechanistically, SHEP1 may also be involved downstream of both BCR and S1P receptor signaling. We observed that the absence of SHEP1 does not affect the calcium, Akt and Erk pathways. However, the absence of SHEP1 affected Rac activation and JNK activation, which strongly suggests a participation of SHEP1 in integrin activation and actin polymerization. SHEP1 was found to interact with CasL, and this result is consistent with the finding that another family member, AND-34, binds CasL in B cells (45). Our observation that the overexpression of CasL results in a partial rescue of the marginal zone suggests that CasL or its hyper-phosphorylated species may be sensitive to degradation and that the association with SHEP1 prolongs its half-life. This is consistent with the observed loss of marginal zone B cells in CasL-deficient mice (24) by Seo et al. who also communicated to us an intermediate marginal zone phenotype in CasL heterozygotes (unpublished data).

Ongoing experiments address the following pertinent questions: 1) Will the loss of SHEP1/CasL interaction lead to an absence of the marginal zone. To answer this, we have created SHEP1 tyrosine mutant Y787E, which has been shown to prevent p130Cas binding and CasL binding (27, 28); 2) Is SHEP1 or CasL tyrosine phosphorylated and is CasL serine phosphorylated upon BCR, S1P, SDF1$\alpha$ and BLC stimulations? This will be investigated using the B cell line Bal17 and by immunoprecipitation of SHEP1 or CasL. It would also be interesting to determine if SHEP1 has guanine nucleotide exchange activity. It will also be helpful to identify other molecules that require SHEP1. In a preliminary immunoprecipitation experiment, SHEP1 has been shown to pull down several tyrosine phosphorylated proteins (data not shown), but these may not all be driven by SH2 to phosphotyrosine interactions. It will be interesting to identify these proteins,

which were 250, 180, 150, 100, 60, 55 and 50 kDa in sizes; possible candidates representing these bands are DOCK2, CasL, SKAP or IAP (integrin associated protein). Understanding the biology of SHEP1 will require analysis of all associating molecules in response to relevant stimuli.

Fig 3-19A and Fig 3-19B present paradigms for the involvement of SHEP1 in BCR and S1P receptor signaling, respectively. In Fig 3-19B, BCR signaling may be triggering Rap activation upstream of SHEP1 based on a preliminary experiment showing Rap1 activation in the absence of SHEP1 (data not shown). However, it is possible that SHEP1 helps the binding of Rap to RapL leading to integrin activation. In addition, SHEP1 may be important for CasL serine phosphorylation either through the maintenance/stabilization of the p115 CasL species or the recruitment of serine kinases. The serine kinase targeting CasL is not known. Nevertheless, the serine-phosphorylation of CasL may be important for its interaction with Crk and subsequently, the recruitment of C3G and DOCK2 leading to Rac activation. S1P receptor signaling may utilize similar pathways, although BCR signaling in the absence of SHEP1 affected both Rac and Cdc42 activation, while S1P receptor signaling in the absence of SHEP1 did not affect Cdc42 within the time course used in the experiment. It is possible that Cdc42 activation downstream of S1P does not require SHEP1 (Fig 3-19A).

In summary, these studies underscores the fact that B cell movement, depending on the stimuli, environmental context, developmental/differentiation stage, are addressed by a distinct team of molecular players. When considering the potential utility of SHEP1 for dynamically organizing molecular players mediating chemotactic responses, a deeper understanding of this molecule would help elucidate chemotactic signaling processes

including actin remodeling, integrin activation and integrin downstream signaling pathways. Overall, the current study corroborates what has been observed in T cells and opens new avenues for understanding the biology of SHEP1 in B cells.

## 3.4 – Methods

### 3.4.1 - Mice

*SHEP1*$^{flox/flox}$ mice have loxP sites flanking exon 7 of *SHEP1*. Coexpression of cre recombinase results in the recombination of these loxP sites and the subsequent deletion of exon 7. *SHEP1*$^{flox/flox}$ mice were crossed with *CD19cre* mice (in which cre recombinase expression is driven by the CD19 promoter that turns on at the preB cell stage) to generate *SHEP1*$^{flox/flox}$*CD19cre* mice. *SHEP1*$^{flox/flox}$ mice were also crossed with *Ig-alpha cre* mice (in which cre recombinase expression is induced at the earliest preB cell stage) to generate *SHEP1*$^{flox/flox}$*Ig alpha cre* mice. Mice were genotyped by PCR amplification of genomic DNA from tail samples. Neonatal mice used were 5 day old and adult mice used were 8-16 weeks old. All animals were maintained in a pathogen free animal facility at The Burnham Institute for Medical Research (La Jolla, CA).

### 3.4.2 - Cloning and mutagenesis

Splenic B cells from B6 mice were purified using CD43 MACS beads and purity of 95% was verified by flow cytometry. RNA was isolated from B cells using Nucleospin RNAII kit (Macherey-Nagel, Germany). Total cDNA was prepared using the MMLV Reverse Transcriptase cDNA Advantage Kit (Clontech, Temecula, CA). The following primers were used to amplify SHEP1 (AF168364) from total cDNA: Forward SKC F3: CCA CAT GCT AGC AAA CCA GAG and Reverse SKC R1: ATC TCC GGG GTC ACA GCT CGC. An approximately 2.9 kb band was purified using Qiagen MinElute Gel extraction kit (Qiagen). This band was confirmed by internal primers for SHEP1. Plasmids were purified using Macherey-Nagel plasmid purification kit. For

mutagenesis, SHEP1 plasmid was mutagenized using primers: for Y787E mutation (Forward sequence, ACCACGGGGGCCTCGAACACA and Reverse sequence, CAGCGTTGGTGTGTTCGAGGC) and for Y787F mutation (SHEP1 Y787F Forward Sequence, ACC ACG GGG GCC TCT TCC ACA CCA ACG CTG and SHEP1 Y787F Reverse Sequence, CAG CGT TGG TGT GGA AGA GGC CCC CGT GGT). Mutant clones were sequenced for confirmation.

### 3.4.3 - Cells and stimulation reagents

WEHI and Bal17 cells were grown in complete RPMI medium. Stimulations, S1P (Biomol International), BLC (RD Systems), anti-IgM F(ab')$_2$ (Zymed Laboratories, S. San Francisco, CA).

### 3.4.4 - Western Blot

One to ten million cells were washed with PBS and stimulated with 10 μg/mL goat anti-mouse IgM F(ab')$_2$ for the indicated times at 37°C. Cell pellets were lysed on ice for 30 min in either RIPA lysis buffer (50 mM Tris-HCl pH 7.4, 150 mM NaCl, 2 mM EDTA, 1% NP-40, 0.1% SDS) or NP-40 lysis buffer (20 mM Tris-HCl pH 7.5, 1% NP-40, 10% glycerol, 10 mM NaCl, 1 mM EDTA) plus protease inhibitors (2 μg/ml leupeptin, 2 mM PMSF, 2 μg/ml aprotinin and 1 mM sodium orthovanadate). Lysates were electrophoresed using 12% acrylamide SDS gels and transferred onto nitrocellulose paper. Antibodies to SHEP1 were generated in the laboratory of Dr. Elena Pasquale (The Burnham Institute for Medical Research). Antibody against CasL was from Rockland Immunological. Anbodies to Akt, phospho-Akt, Erk, phospho-Erk, actin and

phosphotyrosine were from Cell Signaling Technology, Inc. (Danvers, MA). Protein bands were revealed with HRP-labeled donkey anti-mouse or anti-rabbit antibodies and developed with a chemiluminescence kit (Amersham Biosciences, Piscataway, NJ).

### 3.4.5 - Flow Cytometry

Spleens were excised and red blood cells were depleted from cell suspensions using hypotonic ammonium chloride. One million cells were resuspended in FACS buffer (PBS, 1% FBS and 0.01% sodium azide) and incubated with the following conjugated antibodies from BD Biosciences Pharmingen (San Diego, CA): IgM-APC, IgD-PE, B220-APC-Cy7, and CD11b-PE-Cy7, CD23, CD21, AA4.1. Samples were washed once with FACS buffer and read using FACSCanto flow cytometer (BD Biosciences, San Jose, CA). Samples were analyzed using FlowJo software (Treestar, Ashland, OR). For SHEP1 and CasL intracellular staining, cells were fixed in 2% formaldehyde for 10 min at 37°C, permeabilized and stained with anti-SHEP1 or isotype control, with anti-CasL or isotype control, with phalloidin-FITC and DAPI.

### 3.4.6 - Serum ELISA

Serum samples were collected by retroorbital bleeding. 96-well high binding capacity plates were coated with 10 μg/ml NP3-BSA or NP30-BSA for 24 hr at 4°C. Plates were blocked for 20 min at RT with blocking buffer (0.5% BSA in PBS). Serum samples were serially diluted (beginning at 1:200) in blocking buffer, and incubated in coated wells for 2 hr at RT. Plates were washed and incubated with alkaline phosphatase-conjugated anti-mouse IgM or anti-mouse IgG for 1 hr at RT. Phosphatase

substrate (Sigma, St. Louis, MO) was added to wells, and $A_{405}$ was measured using BioTek Elx808 colorimetric plate reader (BioTek Instruments, Winooski, VT).

### 3.4.7 - Immunization

Mice were intra-peritoneally immunized with NP-KLH (in alum), NP-FICOLL (in alum) and intravenously with R36A (generously provided by Dr. Kearney). Mice were bled retro-orbitally. Spleen, bone marrow and lymph nodes were harvested and analyzed by flow cytometry as previously described.

### 3.4.8 - Histology

Spleens were embedded in Tissue-Tek O.C.T. compound (Sakura Finetek U.S.A., Torrance, CA) and frozen at -80°C. Eight μm sections were mounted on microscope slides, fixed for 10 min in cold acetone, blocked for 1 hr with block buffer (0.5% BSA in PBS) and stained with antibodies from BD Biosciences for 1 hr at RT (B220-FITC, IgM-APC, CD4-FITC, CD3-PE, CD11b-PE, MOMA1-biotin and PNA-FITC). Sections were washed with PBS + 0.5% Tween and incubated with Streptavidin-Cy3 (Invitrogen, Carlsbad, CA) or Streptavidin-Cy5 (Jackson Immunoresearch Labs, West Grove, PA) for 30 min at RT. After washing with PBS + 0.5% Tween, sections were covered with Gel/Mount (Biomeda Corp, Foster City, CA) and sealed with glass coverslips. Images were acquired using Zeiss Axiocam M1 microscope (Zeiss, Thornwood, NY) and Slidebook software (Intelligent Imaging Innovations, Denver, CO).

### 3.4.9 - Calcium Flux

Two million B cells were resuspended in 250 µl media (DMEM, 10 mM HEPES and 2.5% FBS). Four µl Fura Red, 2 µl Fluo-4 and 2µl pluronic acid (Invitrogen Molecular Probes) were added to 1 ml of media. An equal volume of dye mix was added to each cell suspension. Cells were incubated for 45 min at 37ºC in the dark. Stained cells were read for 1 min to obtain a baseline on the flow cytometer, and then stimulated with 10 µg/ml anti-IgM $F(ab')_2$. Calcium flux was measured by Fluo-4 (530 nm)/Fura Red (685 nm) emission ratiometry for 5 min. See Appendix I for a more detailed calcium flux protocol.

### 3.4.10 – Migration

For migration assay, purified B cells were plated onto chamber wells of a Transwell plate (Corning, 5.0 µm in diameter, 24 well plate) containing in media containing the S1P, BLC and SDF1α in the bottom wells. Cells were allowed to migrate for 4-8 hr at 37ºC. Migrant cells are enumerated by flow cytometry.

### 3.4.11 – Cell spreading assay

Twenty four - well culture plates were coated with ICAM, VCAM, anti-IgM $F(ab')_2$ or BSA overnight at 4ºC and blocked with 2% BSA for 3 hrs at RT. Purified splenic B cells were cultured in each well at $10^5$ cells in a volume of 500 µl of media with or without S1P, BLC or SDF1α. After 24 hrs incubation at 37ºC, cells were analyzed by microscopy for spreading. Cells that are morphologically elongated (not rounded) are counted and divided by the total cells in the field.

**Acknowledgement**

Chapter 3 of this dissertation includes work on the role of SHEP1 in B cell differentiation and function. Content of this chapter is being prepared for submission for publication. Cecille will be the primary author of this paper. Supporting authors include Yann Wellez, Melanie Hoefer, Suresh Chintalapati, Matthew Cato, Derek Ostertag, Elena Pasquale and Robert Rickert.

## 3.5 – References


1. Kehrl, J.H., I.Y. Hwang, and C. Park, Chemoattract receptor signaling and its role in lymphocyte motility and trafficking. Curr Top Microbiol Immunol, 2009. **334**: p. 107-27.

2. Forster, R., A.E. Mattis, E. Kremmer, E. Wolf, G. Brem, and M. Lipp, A putative chemokine receptor, BLR1, directs B cell migration to defined lymphoid organs and specific anatomic compartments of the spleen. Cell, 1996. **87**(6): p. 1037-47.

3. Forster, R., A.E. Mattis, E. Kremmer, E. Wolf, G. Brem, and M. Lipp, A putative chemokine receptor, BLR1, directs B cell migration to defined lymphoid organs and specific anatomic compartments of the spleen. Cell, 1996. **87**(6): p. 1037-47.

4. Ansel, K.M., V.N. Ngo, P.L. Hyman, S.A. Luther, R. Forster, J.D. Sedgwick, J.L. Browning, M. Lipp, and J.G. Cyster, A chemokine-driven positive feedback loop organizes lymphoid follicles. Nature, 2000. **406**(6793): p. 309-14.

5. Cinamon, G., M. Matloubian, M.J. Lesneski, Y. Xu, C. Low, T. Lu, R.L. Proia, and J.G. Cyster, Sphingosine 1-phosphate receptor 1 promotes B cell localization in the splenic marginal zone. Nat Immunol, 2004. **5**(7): p. 713-20.

6. Vora, K.A., et al., Sphingosine 1-phosphate receptor agonist FTY720-phosphate causes marginal zone B cell displacement. J Leukoc Biol, 2005. **78**(2): p. 471-80.

7. Zlotnik, A., O. Yoshie, and H. Nomiyama, The chemokine and chemokine receptor superfamilies and their molecular evolution. Genome Biol, 2006. **7**(12): p. 243.

8. Sanchez, T. and T. Hla, Structural and functional characteristics of S1P receptors. J Cell Biochem, 2004. **92**(5): p. 913-22.

9. Hubbard, K.B. and J.R. Hepler, Cell signalling diversity of the Gqalpha family of heterotrimeric G proteins. Cell Signal, 2006. **18**(2): p. 135-50.

10. Scheele, J.S., R.E. Marks, and G.R. Boss, Signaling by small GTPases in the immune system. Immunol Rev, 2007. **218**: p. 92-101.

11. Shi, S., M. Noda, and H. Kitayama, Rap1 mutants with increased affinity for the guanine-nucleotide exchange factor C3G. Oncogene, 2004. **23**(54): p. 8711-9.

12. Ishida, D., H. Yang, K. Masuda, K. Uesugi, H. Kawamoto, M. Hattori, and N. Minato, Antigen-driven T cell anergy and defective memory T cell response via deregulated Rap1 activation in SPA-1-deficient mice. Proc Natl Acad Sci U S A, 2003. **100**(19): p. 10919-24.

13. Kurachi, H., Y. Wada, N. Tsukamoto, M. Maeda, H. Kubota, M. Hattori, K. Iwai, and N. Minato, Human SPA-1 gene product selectively expressed in lymphoid tissues is a specific GTPase-activating protein for Rap1 and Rap2. Segregate expression profiles from a rap1GAP gene product. J Biol Chem, 1997. **272**(44): p. 28081-8.

14. Tsukamoto, N., M. Hattori, H. Yang, J.L. Bos, and N. Minato, Rap1 GTPase-activating protein SPA-1 negatively regulates cell adhesion. J Biol Chem, 1999. **274**(26): p. 18463-9.

15. Lo, C.G., T.T. Lu, and J.G. Cyster, Integrin-dependence of lymphocyte entry into the splenic white pulp. J Exp Med, 2003. **197**(3): p. 353-61.

16. Lu, T.T. and J.G. Cyster, Integrin-mediated long-term B cell retention in the splenic marginal zone. Science, 2002. **297**(5580): p. 409-12.

Allen, C.D., K.M. Ansel, C. Low, R. Lesley, H. Tamamura, N. Fujii, and J.G. Cyster, Germinal center dark and light zone organization is mediated by CXCR4 and CXCR5. Nat Immunol, 2004. **5**(9): p. 943-52.

17. Duchniewicz, M., T. Zemojtel, M. Kolanczyk, S. Grossmann, J.S. Scheele, and F.J. Zwartkruis, Rap1A-deficient T and B cells show impaired integrin-mediated cell adhesion. Mol Cell Biol, 2006. **26**(2): p. 643-53.

18. Chen, Y., M. Yu, A. Podd, R. Wen, M. Chrzanowska-Wodnicka, G.C. White, and D. Wang, A critical role of Rap1b in B-cell trafficking and marginal zone B-cell development. Blood, 2008. **111**(9): p. 4627-36.

19. Fukui, Y., et al., Haematopoietic cell-specific CDM family protein DOCK2 is essential for lymphocyte migration. Nature, 2001. **412**(6849): p. 826-31.

20. Girkontaite, I., K. Missy, V. Sakk, A. Harenberg, K. Tedford, T. Potzel, K. Pfeffer, and K.D. Fischer, Lsc is required for marginal zone B cells, regulation of lymphocyte motility and immune responses. Nat Immunol, 2001. **2**(9): p. 855-62.

21. Guinamard, R., M. Okigaki, J. Schlessinger, and J.V. Ravetch, Absence of marginal zone B cells in Pyk-2-deficient mice defines their role in the humoral response. Nat Immunol, 2000. **1**(1): p. 31-6.

22. Tse, K.W., M. Dang-Lawson, R.L. Lee, D. Vong, A. Bulic, L. Buckbinder, and M.R. Gold, B cell receptor-induced phosphorylation of Pyk2 and focal adhesion kinase involves integrins and the Rap GTPases and is required for B cell spreading. J Biol Chem, 2009. **284**(34): p. 22865-77.

23. Durand, C.A., J. Westendorf, K.W. Tse, and M.R. Gold, The Rap GTPases mediate CXCL13- and sphingosine1-phosphate-induced chemotaxis, adhesion, and Pyk2 tyrosine phosphorylation in B lymphocytes. Eur J Immunol, 2006. **36**(8): p. 2235-49.

24. Seo, S., et al., Crk-associated substrate lymphocyte type is required for lymphocyte trafficking and marginal zone B cell maintenance. J Immunol, 2005. **175**(6): p. 3492-501.

25. Vervoort, V.S., S. Roselli, R.G. Oshima, and E.B. Pasquale, Splice variants and expression patterns of SHEP1, BCAR3 and NSP1, a gene family involved in integrin and receptor tyrosine kinase signaling. Gene, 2007. **391**(1-2): p. 161-70.

26. Dodelet, V.C., C. Pazzagli, A.H. Zisch, C.A. Hauser, and E.B. Pasquale, A novel signaling intermediate, SHEP1, directly couples Eph receptors to R-Ras and Rap1A. J Biol Chem, 1999. **274**(45): p. 31941-6.

27. Regelmann, A.G., N.M. Danzl, C. Wanjalla, and K. Alexandropoulos, The hematopoietic isoform of Cas-Hef1-associated signal transducer regulates chemokine-induced inside-out signaling and T cell trafficking. Immunity, 2006. **25**(6): p. 907-18.

28. Dail, M., M.S. Kalo, J.A. Seddon, J.F. Cote, K. Vuori, and E.B. Pasquale, SHEP1 function in cell migration is impaired by a single amino acid mutation that disrupts association with the scaffolding protein cas but not with Ras GTPases. J Biol Chem, 2004. **279**(40): p. 41892-902.

29. Derunes, C., et al., Molecular determinants for interaction of SHEP1 with Cas localize to a highly solvent-protected region in the complex. FEBS Lett, 2006. **580**(1): p. 175-8.

30. Dingjan, G.M., A. Maas, M.C. Nawijn, L. Smit, J.S. Voerman, F. Grosveld, and R.W. Hendriks, Severe B cell deficiency and disrupted splenic architecture in transgenic mice expressing the E41K mutated form of Bruton's tyrosine kinase. Embo J, 1998. **17**(18): p. 5309-20.

31. Nolte, M.A., R. Arens, M. Kraus, M.H. van Oers, G. Kraal, R.A. van Lier, and R.E. Mebius, B cells are crucial for both development and maintenance of the splenic marginal zone. J Immunol, 2004. **172**(6): p. 3620-7.

32. Karlsson, M.C., R. Guinamard, S. Bolland, M. Sankala, R.M. Steinman, and J.V. Ravetch, Macrophages control the retention and trafficking of B lymphocytes in the splenic marginal zone. J Exp Med, 2003. **198**(2): p. 333-40.

33. Sakakibara, A., S. Hattori, S. Nakamura, and T. Katagiri, A novel hematopoietic adaptor protein, Chat-H, positively regulates T cell receptor-mediated interleukin-2 production by Jurkat cells. J Biol Chem, 2003. **278**(8): p. 6012-7.

34. Sigrist C.J.A., Cerutti L., Hulo N., Gattiker A., Falquet L., Pagni M., Bairoch A., Bucher P. PROSITE: a documented database using patterns and profiles as motif descriptors. Brief Bioinform. 3:265-274(2002).

35. Blatch, G.L. and M. Lassle, The tetratricopeptide repeat: a structural motif mediating protein-protein interactions. Bioessays, 1999. **21**(11): p. 932-9.

36. Ponting, C.C. and C. Phillips, Rapsyn's knobs and holes: eight tetratrico peptide repeats. Biochem J, 1996. **314 ( Pt 3)**: p. 1053-4.

37. Lapouge, K., S.J. Smith, P.A. Walker, S.J. Gamblin, S.J. Smerdon, and K. Rittinger, Structure of the TPR domain of p67phox in complex with Rac.GTP. Mol Cell, 2000. **6**(4): p. 899-907.2.

38. Kabashima, K., N.M. Haynes, Y. Xu, S.L. Nutt, M.L. Allende, R.L. Proia, and J.G. Cyster, Plasma cell S1P1 expression determines secondary lymphoid organ retention versus bone marrow tropism. J Exp Med, 2006. **203**(12): p. 2683-90.

39. Matloubian, M., C.G. Lo, G. Cinamon, M.J. Lesneski, Y. Xu, V. Brinkmann, M.L. Allende, R.L. Proia, and J.G. Cyster, Lymphocyte egress from thymus and peripheral lymphoid organs is dependent on S1P receptor 1. Nature, 2004. **427**(6972): p. 355-60.

40. Kunisawa, J., M. Gohda, Y. Kurashima, I. Ishikawa, M. Higuchi, and H. Kiyono, Sphingosine 1-phosphate-dependent trafficking of peritoneal B cells requires functional NFkappaB-inducing kinase in stromal cells. Blood, 2008. **111**(9): p. 4646-52.

41. Wang, J.H., et al., Marginal zone precursor B cells as cellular agents for type I IFN-promoted antigen transport in autoimmunity. J Immunol, 2010. **184**(1): p. 442-51.

42. Allen CD, Ansel KM, Low C, Lesley R, Tamamura H, Fujii N, Cyster JG.Germinal center dark and light zone organization is mediated by CXCR4 and CXCR5. Nat Immunol. 2004 Sep;5(9):943-52.

43. Bowman, E.P., J.J. Campbell, D. Soler, Z. Dong, N. Manlongat, D. Picarella, R.R. Hardy, and E.C. Butcher, Developmental switches in chemokine response profiles during B cell differentiation and maturation. J Exp Med, 2000. **191**(8): p. 1303-18.

44. Belperron, A.A., C.M. Dailey, C.J. Booth, and L.K. Bockenstedt, Marginal zone B-cell depletion impairs murine host defense against Borrelia burgdorferi infection. Infect Immun, 2007. **75**(7): p. 3354-60.

45. Cai, D., K.N. Felekkis, R.I. Near, G.M. O'Neill, J.M. van Seventer, E.A. Golemis, and A. Lerner, The GDP exchange factor AND-34 is expressed in B cells, associates with HEF1, and activates Cdc42. J Immunol, 2003. **170**(2): p. 969-78.

46. Lu TT, Cyster JG. Integrin-mediated long-term B cell retention in the splenic marginal zone. Science, 2002. **297**(5580):409-12.

47. E. Hobeika, S. Thiemann, B. Storch, H. Jumaa, P. J. Nielsen, R. Pelanda, and M. Reth. Testing gene function early in the B cell lineage in mb1-cre mice. Proc Natl Acad Sci U S A. 2006. **103**(37): 13789–13794.

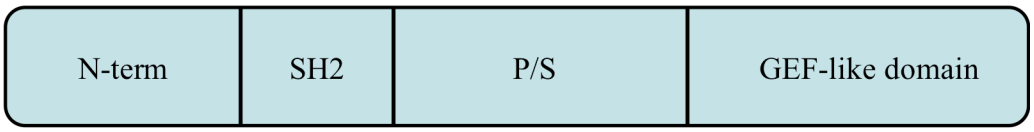


**Figure 3-1: Molecular domains of SHEP1.** SHEP1 consists of an N-terminal region, an SH2 domain, a proline/serine rich domain and a Guanine Nucleotide Exchange Factor-like domain.

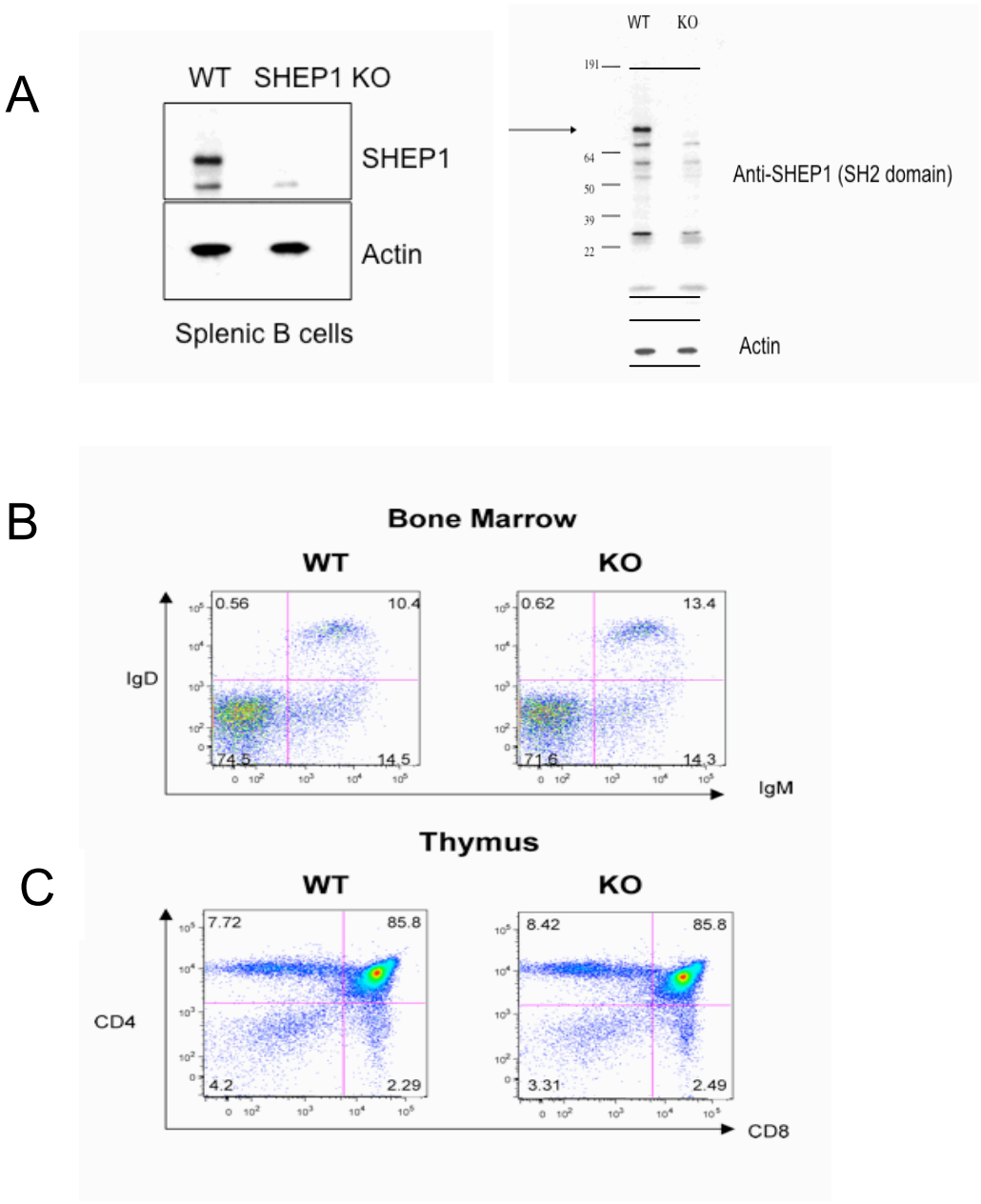


**Figure 3-2: SHEP1 expression in B cells; B cell compartments in SHEP1$^{-/-}$ mice.** A) Purified splenic B cells from SHEP1$^{-/-}$ (SHEP1 KO) and wildtype mice were lysed and probed with anti-SHEP1 antibodies specific for the SH2 domain of SHEP1 or with actin. B) Flow cytometric analysis of bone marrow, CD43-,B220+ gated: Mature B cells are IgD+IgM+, immature B cells are IgD-, IgM+ and pro/pre -B cells are IgD-, IgM-. C) Flow cytometric analysis of thymic T cells.

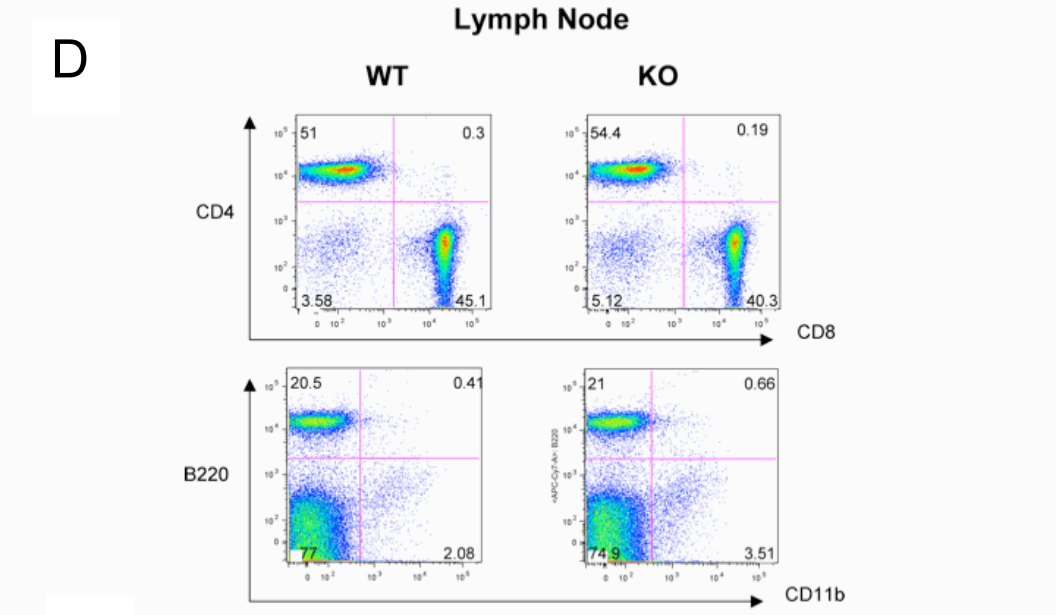


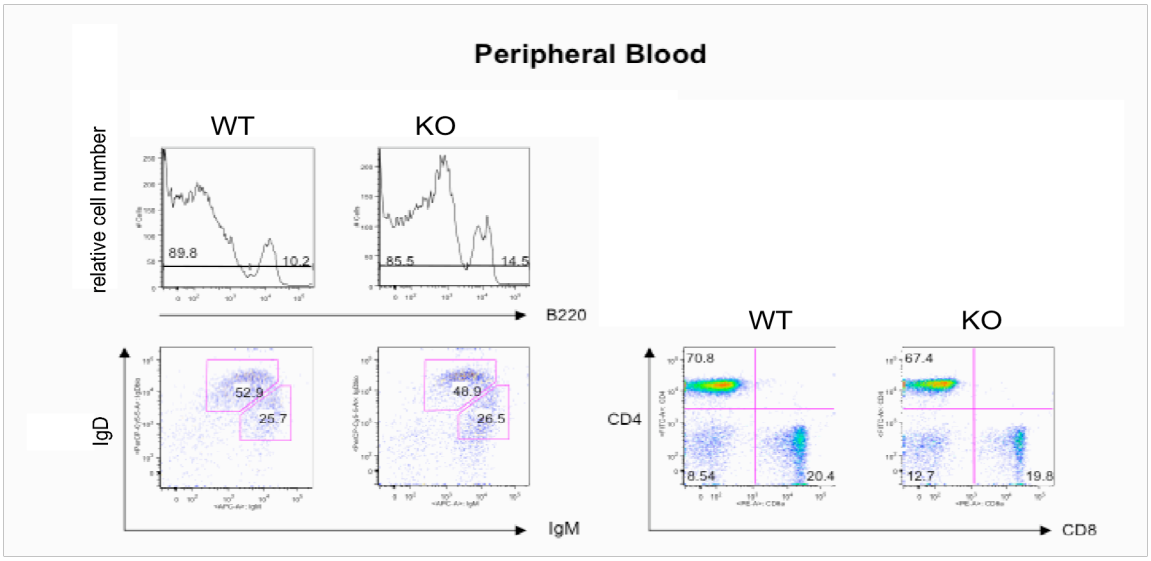


**Figure 3-2 continued: SHEP1 expression in B cells; B cell compartments in SHEP1 KO mice.** D) Flow cytometric analysis of lymph nodes. Top panels are lymph node T cells: CD4 single positive and CD8 single positive. Lower panels are live gated: B220+ (B cells) and CD11b (macrophages) and E) Flow cytometric analysis of blood. Upper left panels are histograms showing the B220+ population. Lower left panels are B220 gated cells, IgD/IgM profiles. Lower right panels show the CD4+, CD8+ Tcell subcompartments.

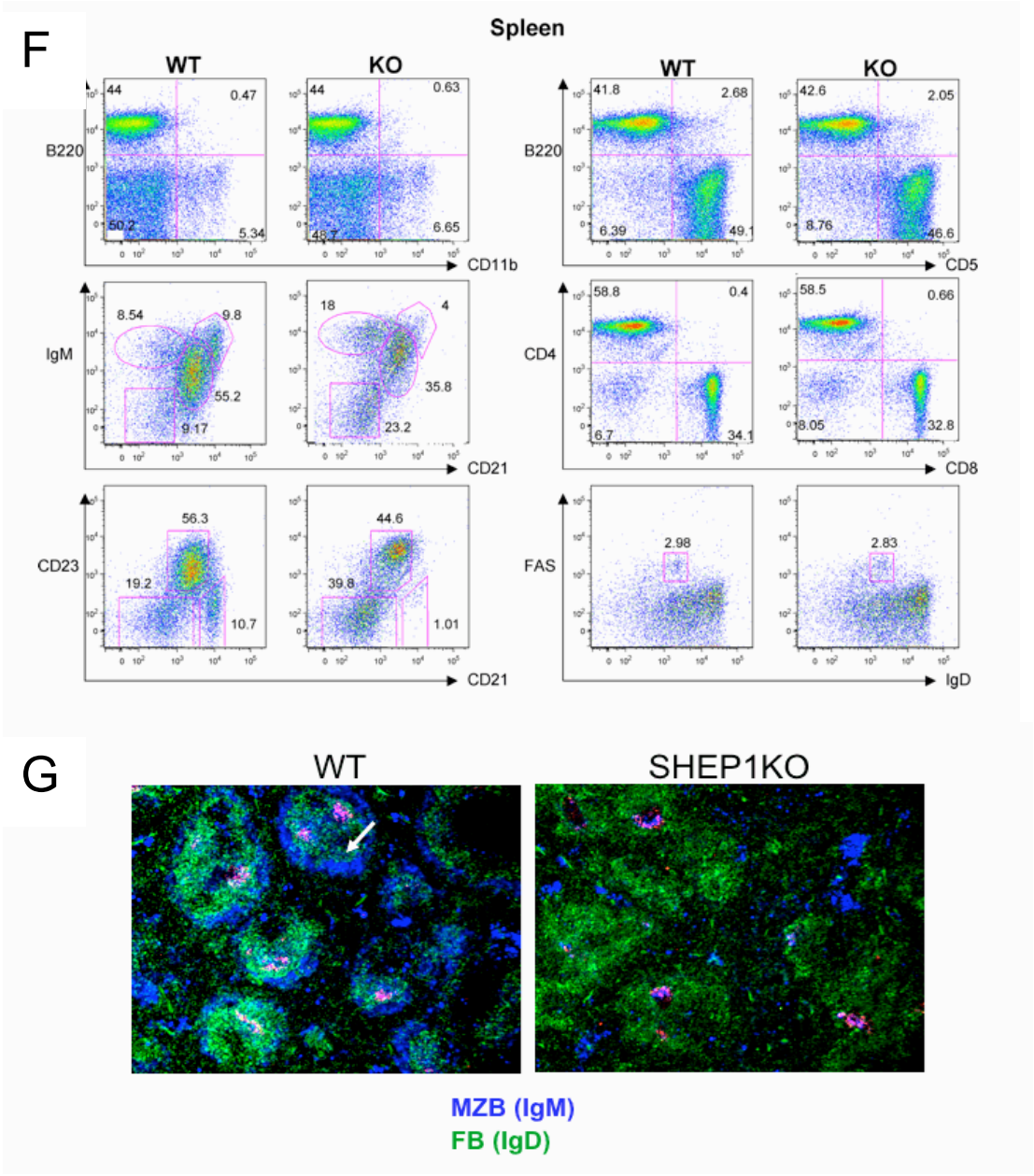


**Figure 3-2 continued: SHEP1 expression in B cells; B cell compartments in SHEP1 KO mice.** F) Flow cytometric analysis of the spleen. Top left panels: B220+ and CD11b+ cells, middle left panels: (B220-gated) transitional T1/T2 cells are IgMhi CD21-, marginal zone and marginal zone precursor B cells are IgMhi and CD21hi, follicular B cells are IgM lo, CD21lo. Lower left panel: (B220-gated) Marginal zone B cells are CD21hi, CD23 low and follicular B cells are CD21lo, CD23hi. Top right panel: (live gated) B220+ cells and CD5+ cells. Middle right panel: CD4/CD8 T cell populations. Lower right panel: FAS+, IgDlo are germinal center B cells. G) Immunofluorescent staining of splenic sections showing marginal zone B cells (blue) and follicular B cells (green).

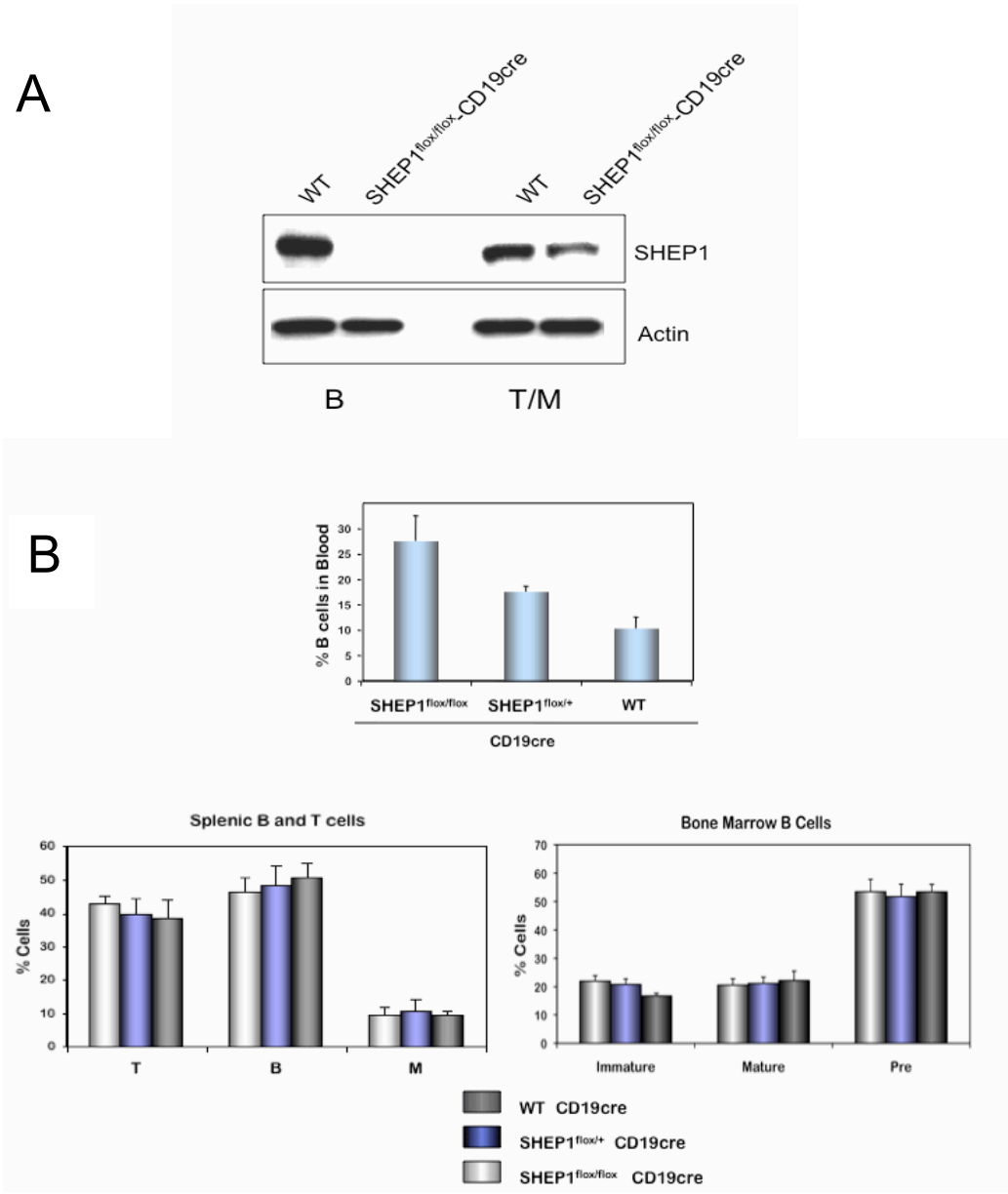


**Figure 3-3: SHEP1 expression in B and non-B cells; B cell compartments in SHEP1$^{flox/flox}$CD19cre mice.** A) Western blot analysis of purified B cells derived from SHEP1$^{flox/flox}$-CD19cre and wildtype mice (which are SHEP1++, CD19cre) and of the purified fraction containing T cells and macrophages. Lysates were immunoblotted with anti-SHEP1 (anti-SH2 domain) and actin. B) Summary of flow cytometric analysis of B cell compartments in blood (top panel), splenic B, T, and macrophage compartment (lower left panel) and immature, mature and pre/pro B cells in the bone marrow (lower right panel). Three mice per group were analyzed.

C

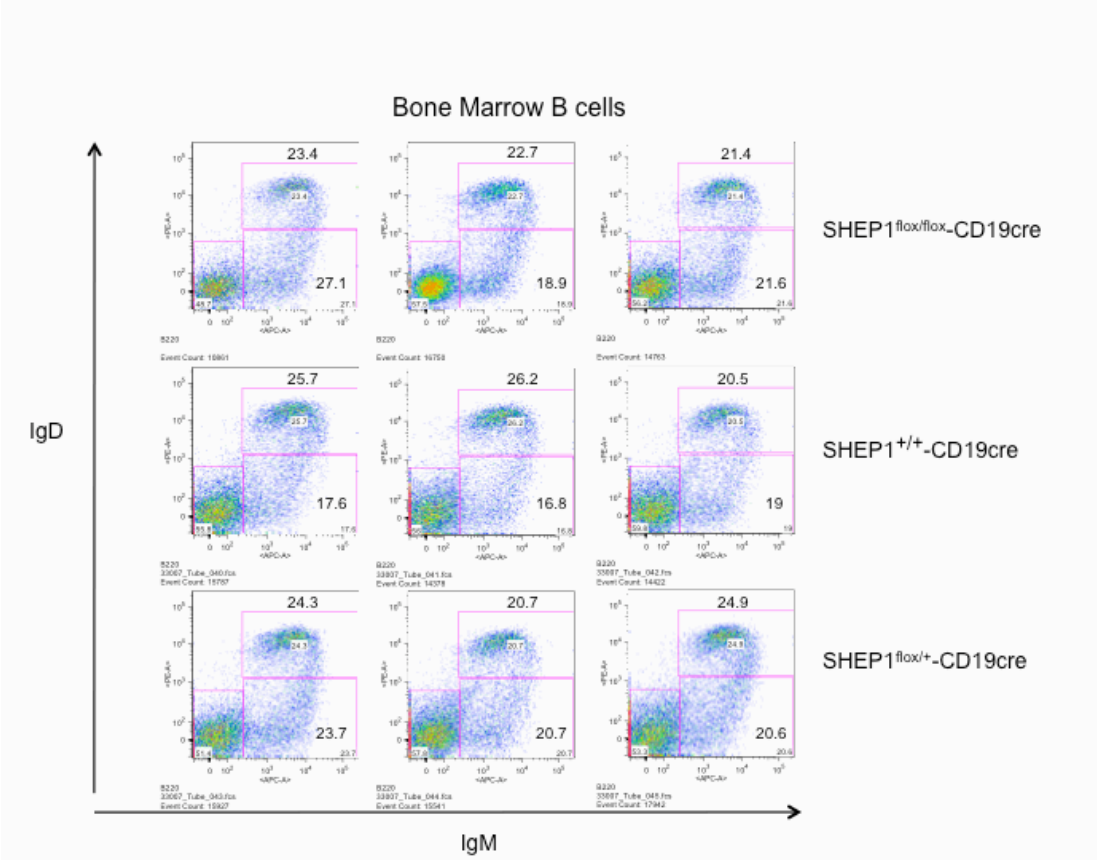


**Figure 3-3 continued: SHEP1 expression in B and non-B cells; B cell compartments in SHEP1$^{flox/flox}$-CD19cre mice.** C) Flow cytometric analysis of B cell compartments in the bone marrow.

D

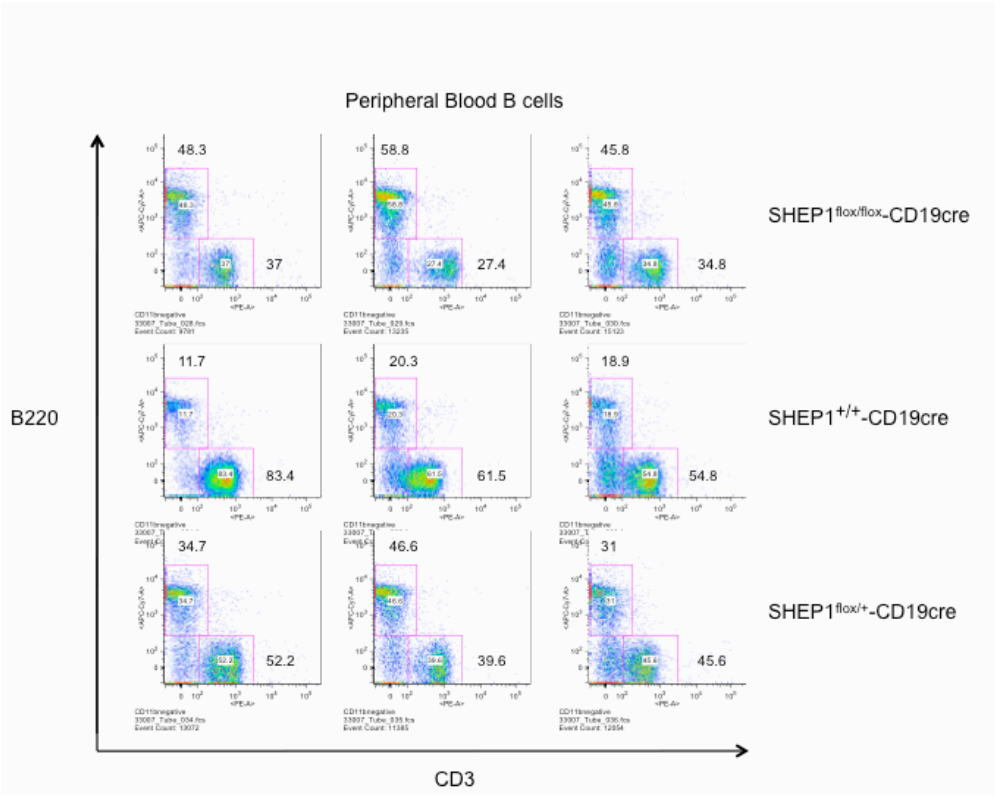


**Figure 3-3 continued: SHEP1 expression in B and non-B cells; B cell compartments in SHEP1$^{flox/flox}$CD19cre mice.** D) Flow cytometric analysis of B and T cell compartments in the blood.

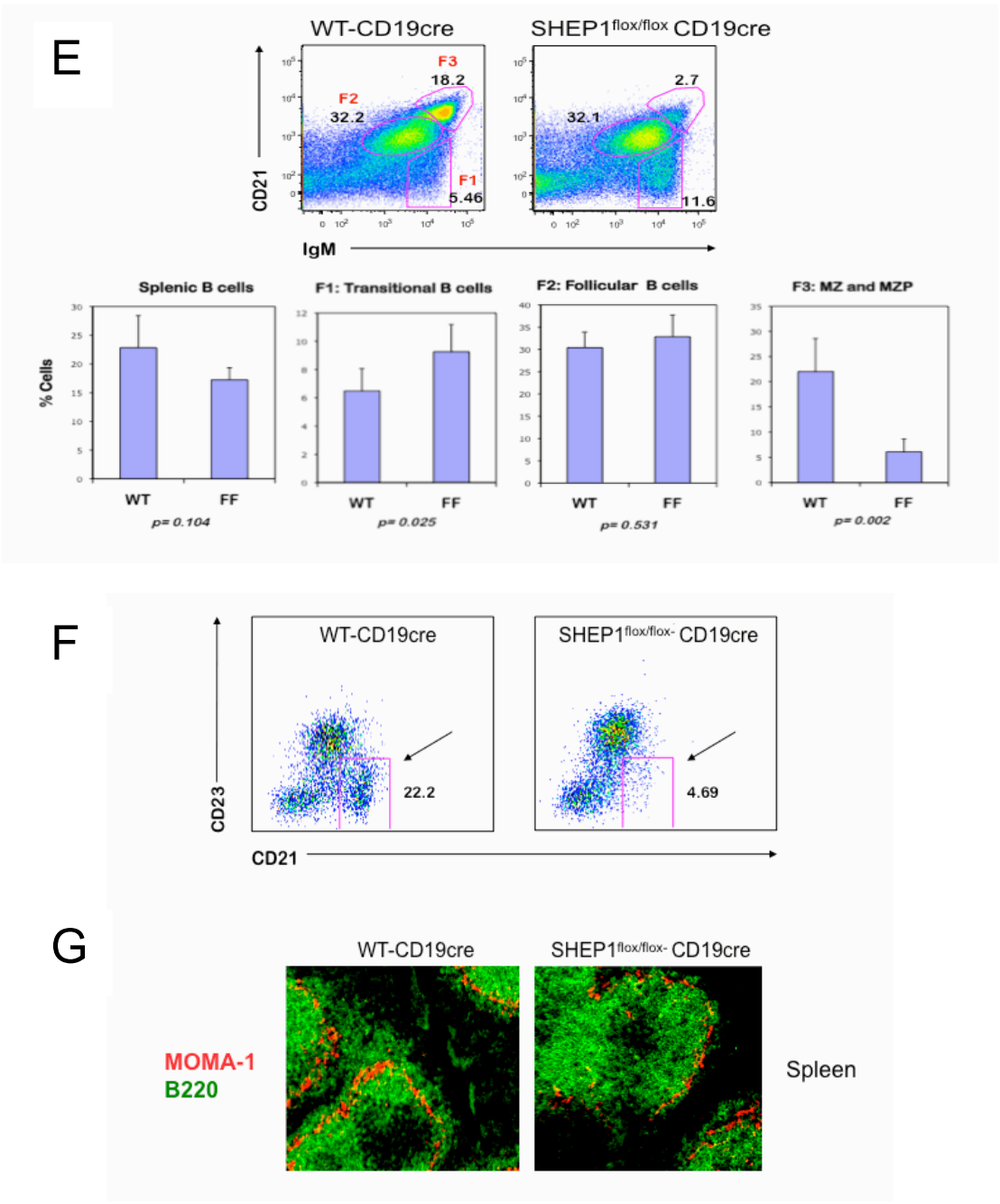


**Figure 3-3 continued: SHEP1 expression in B and non-B cells; B cell compartments in SHEP1$^{flox/flox}$CD19cre mice.** E) Flow cytometric analysis of B cell gated population. Top panel: F1 (transitional T1/T2 cells), F2 (follicular B cells), F3 (marginal zone and marginal zone precursor B cells). Lower panel: summary histograms of B cell subpopulations (average of 3 mice per group). P values are indicated below histograms. F) Flow cytometric analysis of the marginal zone B cell compartment by CD23/CD21 staining and G) histological examination of the same animals is depicted in the lower panels. Marginal zone B cells B220+ (green), located exterior to the red metallophilic macrophages stained by MOMA-1 antibody (red).

H

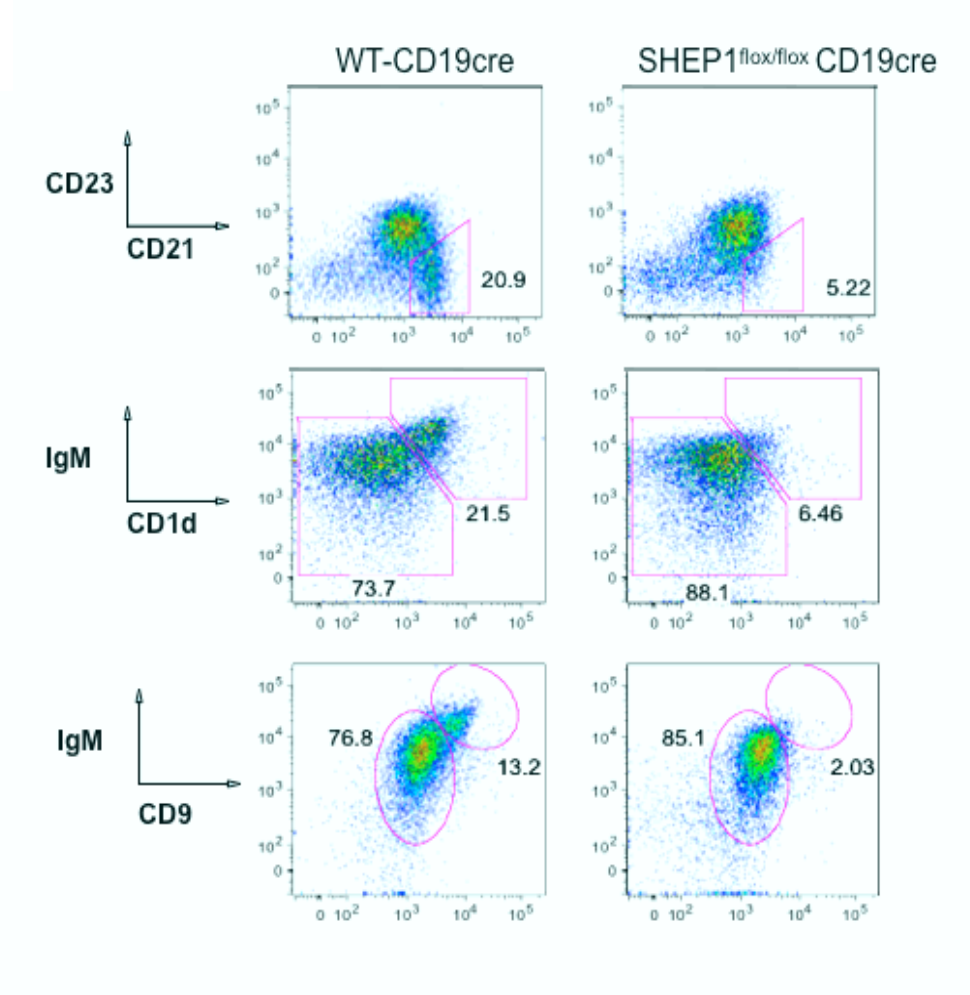


**Figure 3-3 continued: SHEP1 expression in B and non-B cells; B cell compartments in SHEP1$^{flox/flox}$CD19cre mice.** H) Flow cytometric analysis of B220-gated splenic B cells using CD9 and CD1d markers in addition to CD23 and CD21. CD1dhi, IgMhi and CD9hi, IgMhi populations representing the marginal zone B cells, are gated.

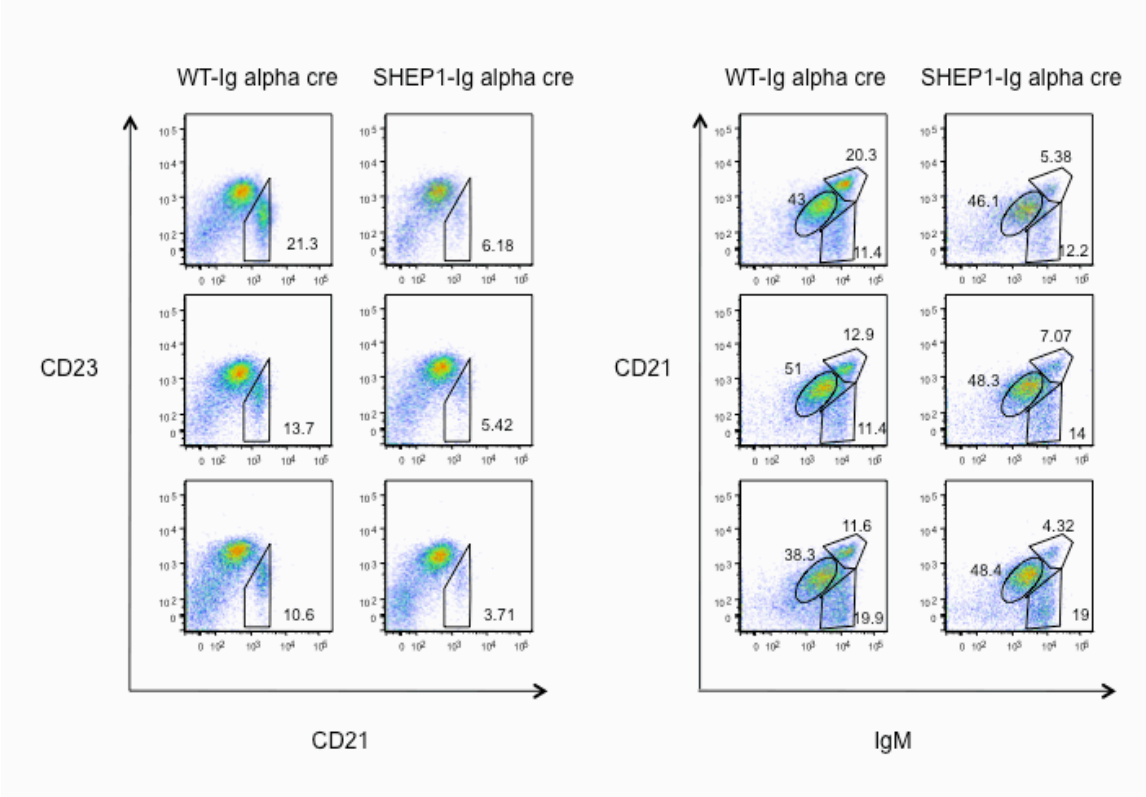


**Figure 3-4: SHEP1$^{flox/flox}$Ig alpha cre mice also exhibit a reduction in the marginal zone B cell compartment**. Left panels are flow cytometric analysis of B cells stained for CD23 and CD21 in which the marginal zone compartment is gated as shown (CD23lo and CD21hi). Right panels are flow cytometric analysis of B cells stained for CD21 and IgM in which the marginal zone/ marginal zone precursor B cell compartment is shown (CD21hi and IgMhi). Transitional B cells are CD21lo and IgMhi and follicular B cells are CD21+ and IgMlo.

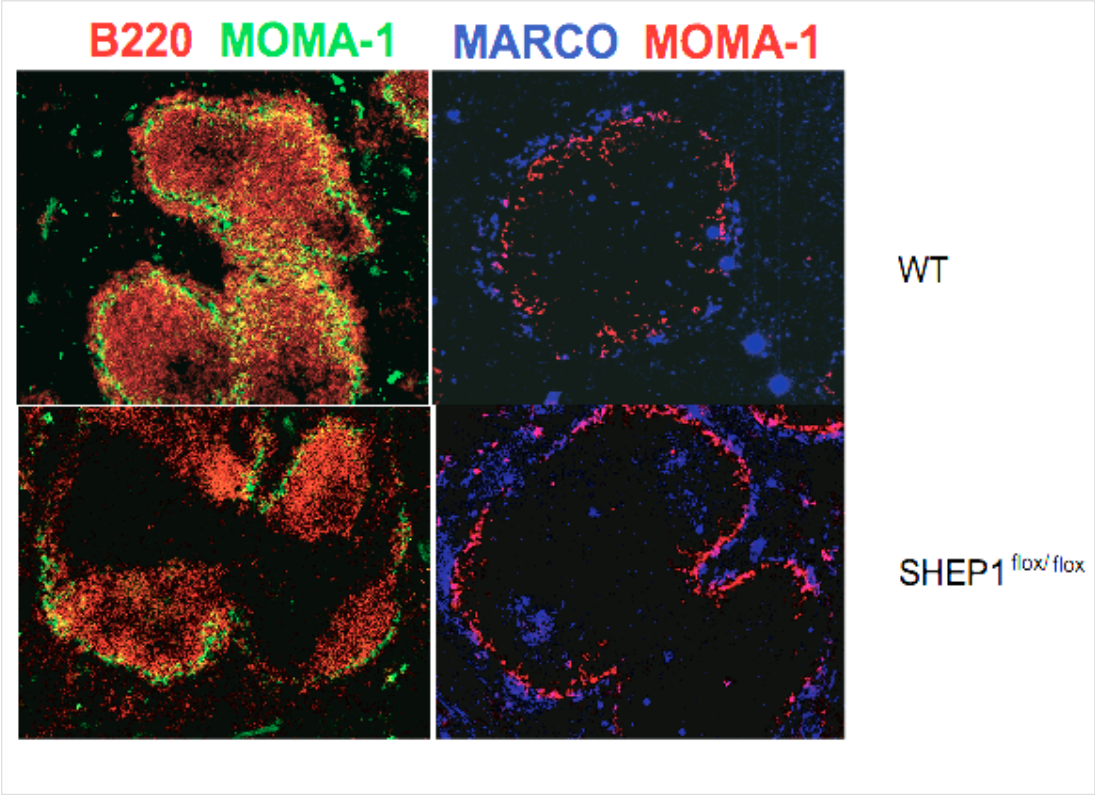


**Figure 3-5: Intact marginal zone macrophage population in the marginal zone niche of SHEP1$^{flox/flox}$ CD19cre mice.** Left: B cells are in red (B220), metallophilic macrophages in green (MOMA-1). Right: Marginal zone macrophages are stained blue (MARCO), metallophilic macrophages in red (MOMA-1).

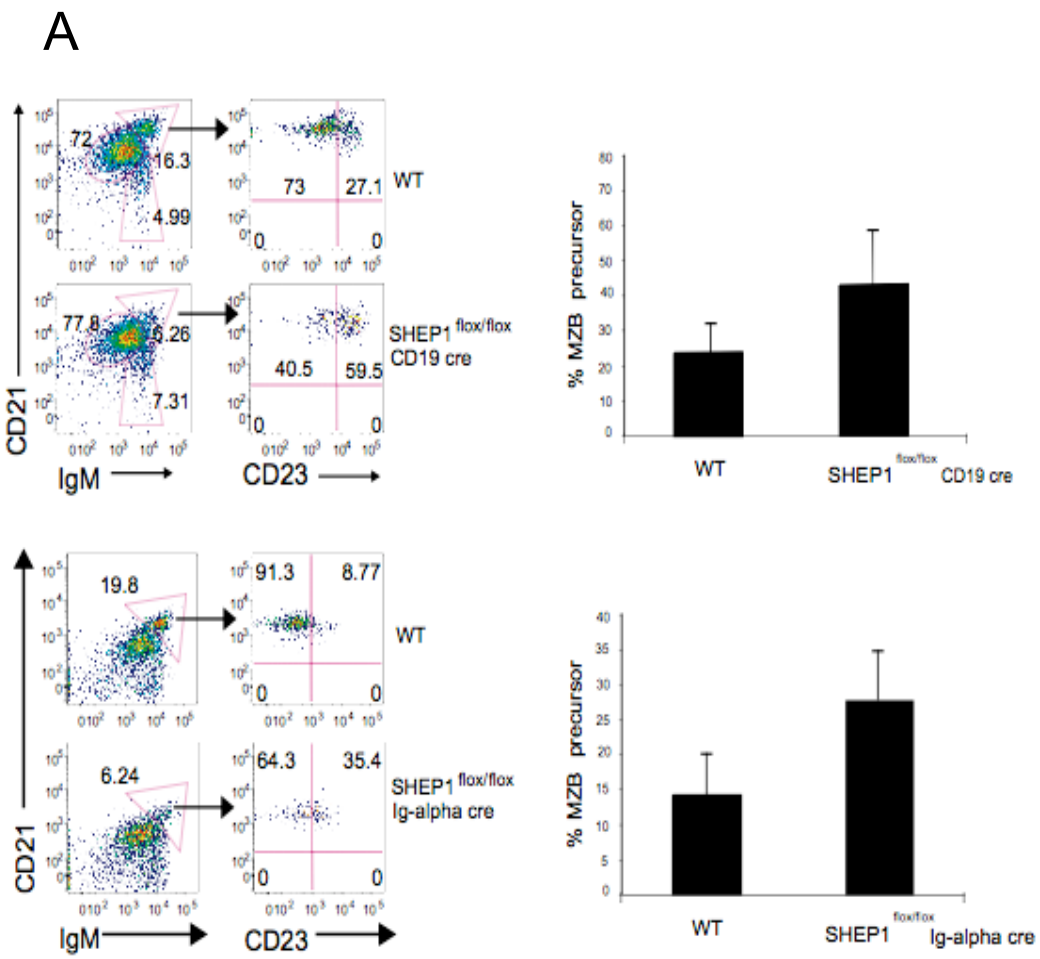


**Figure 3-6: SHEP1$^{flox/flox}$-CD19cre mice have an intact marginal zone precursor population.** A) SHEP1$^{flox/flox}$-CD19cre mice encompass an intact marginal zone precursor population identified by flow cytometry as CD23hi, IgMhi, CD21hi population.

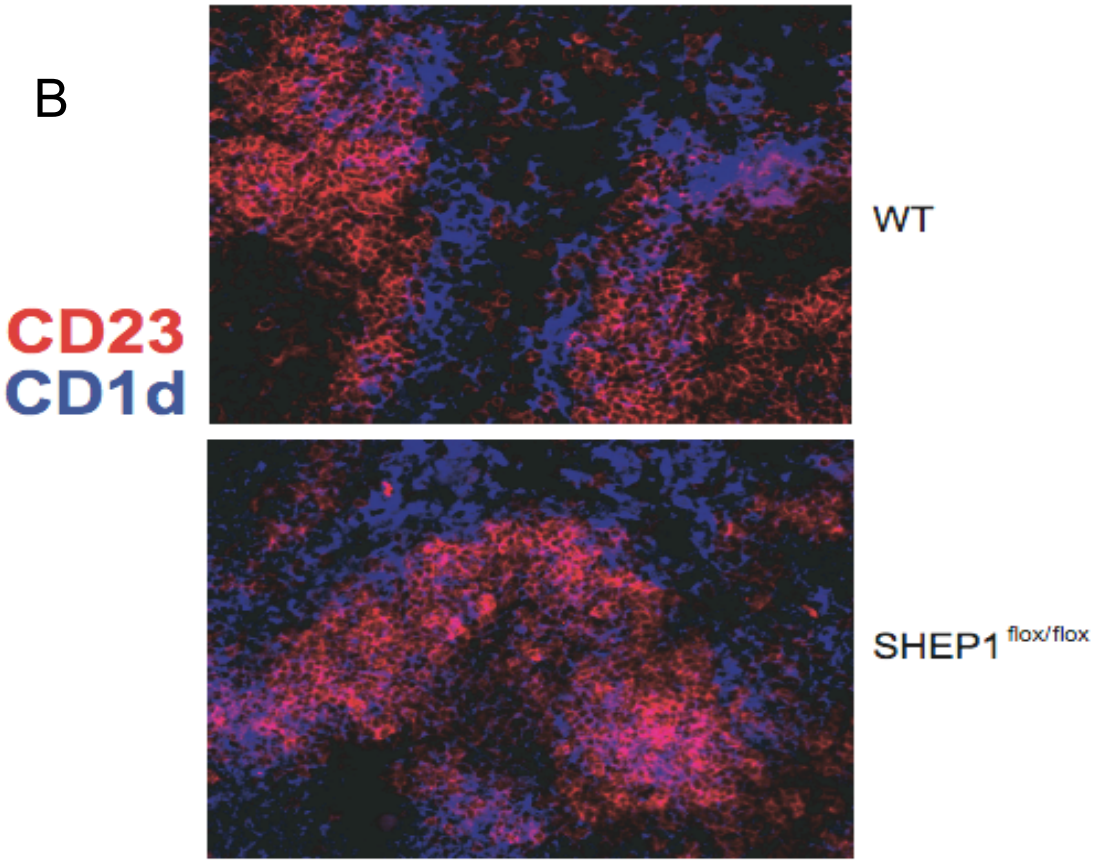


**Figure 3-6 continued: SHEP1$^{flox/flox}$-CD19cre mice have an intact Marginal Zone Precursor population.** B) Splenic cross section stained with CD23 and CD1d. CD23+CD1d+ cells represent the marginal zone precursor population and appear purple in the follicular area.

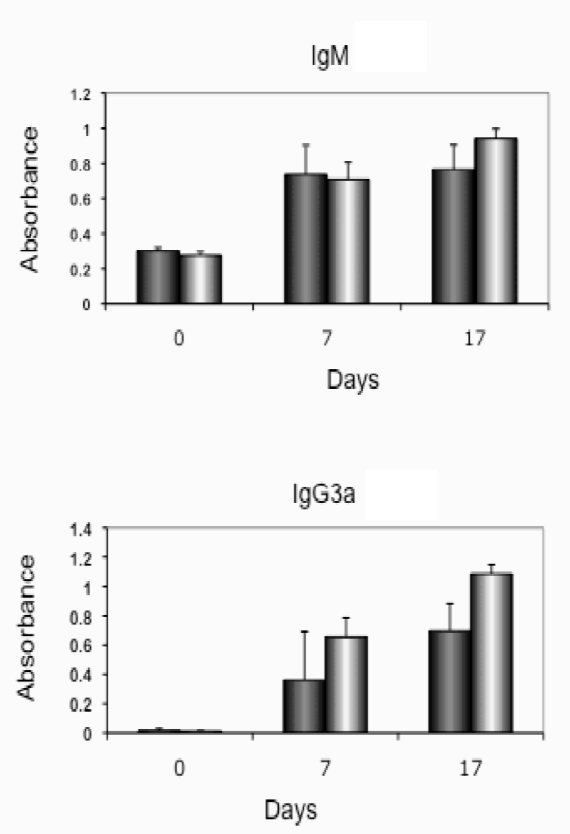


**Figure 3-7: T-independent immunization of SHEP1-deficient mice**. A) Wildtype and SHEP1$^{flox/flox}$ CD19cre mice were immunized *i.p.* with NP-FICOLL in alum and sera from immunized mice were collected on days 7 and 17. Serum samples from three mice from each group were analyzed in triplicate by ELISA using plates coated with NP-30 BSA.

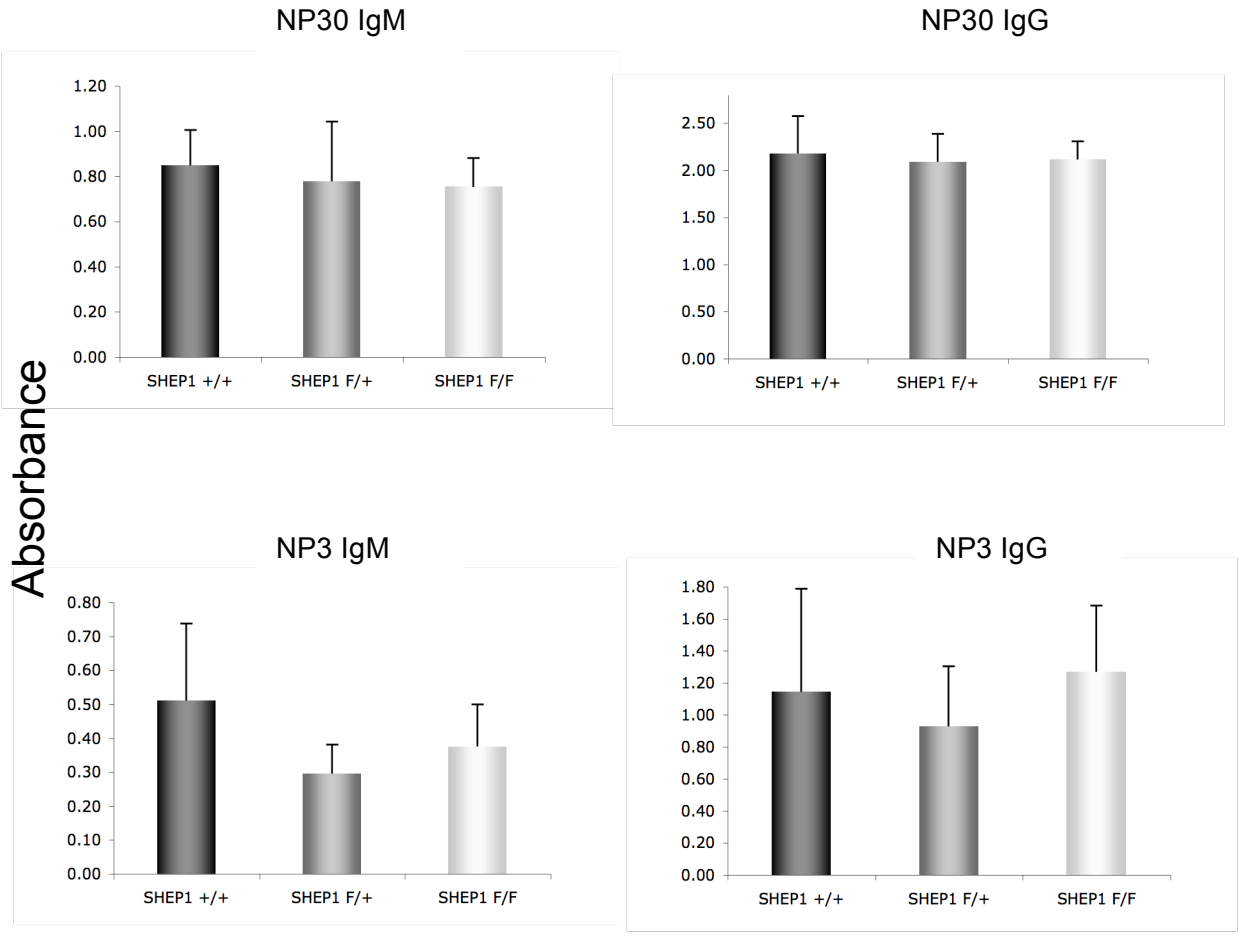


**Figure 3-8: T-dependent immunization of SHEP1-deficient mice**. Wildtype and *SHEP1*$^{flox/flox}$ *CD19cre* mice were immunized *i.p.* with NP-KLH in alum. Serum samples from three mice from each group were collected on days 7 and 14 analyzed in triplicate by ELISA. Serum anti-NP responses were analyzed by ELISA for IgM (day 7) and IgG (day 14). Serum samples were incubated in microwell plates coated with NP3-BSA or NP30-BSA. Immunoglobulins captured on NP3-coated plates are high affinity antibodies secreted by B cells that have undergone affinity maturation. Immunoglobulins captured by NP30-coated plates represent low and high affinity NP-specific immunoglobulins. Each group is represented by three mice.

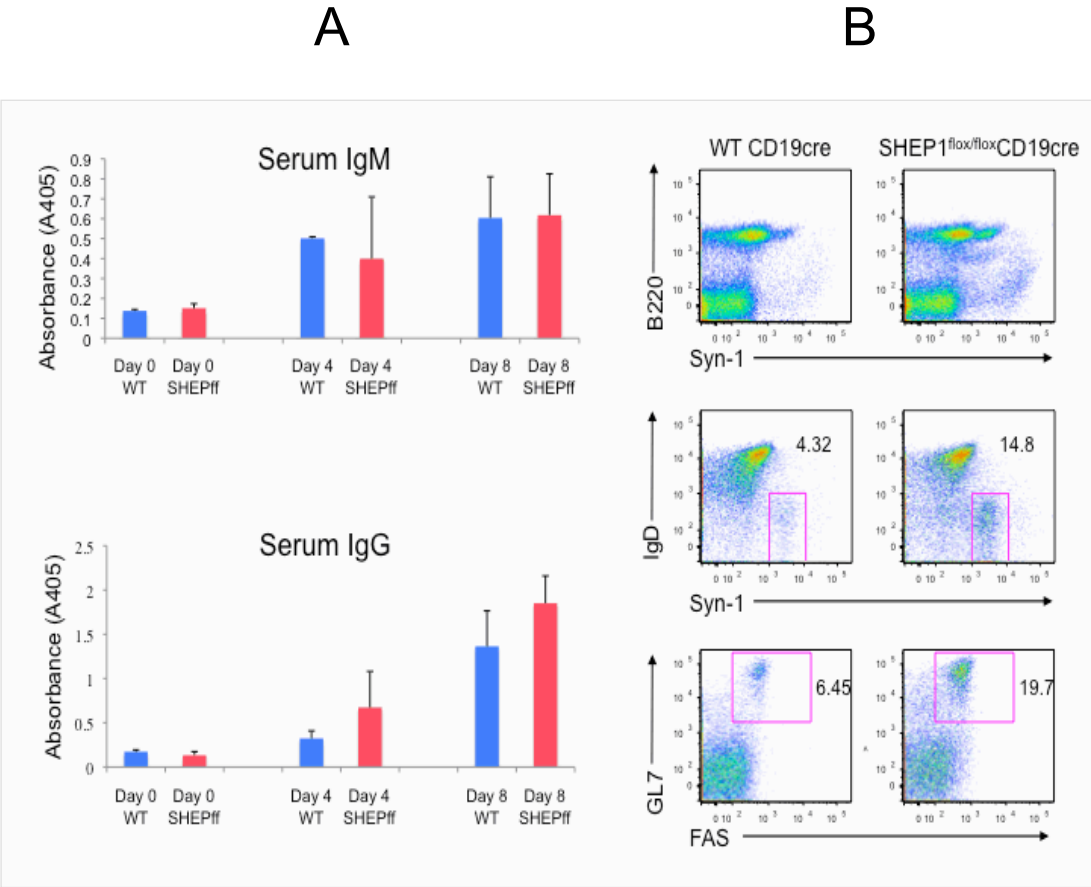


**Figure 3-9: *Streptococcus pneumonia* immunization of SHEP1-deficient mice**.
A) Wildtype and SHEP1$^{flox/flox}$ CD19cre mice were immunized *i.v.* with the R36A strain of *Streptococcus pneumoniae* and sera were collected on days 4 and 8. Serum samples from three mice from each group were analyzed in triplicate by ELISA. B) Splenic cells from immunized mice were analyzed by flow cytometry on day 8 for plasma cells (B220lo, Syn-1+ or IgDlo, Syn-1+) and for germinal center B cells (GL7+, FAS+).

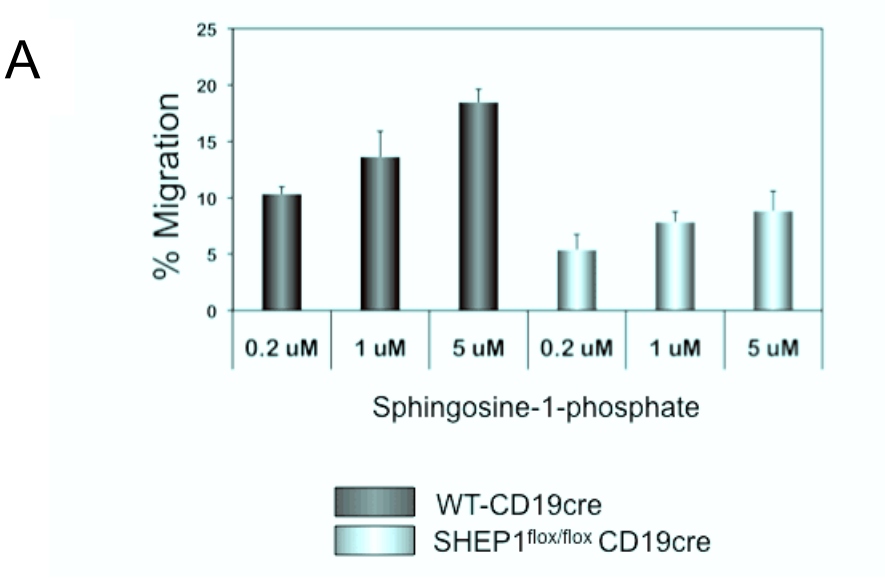


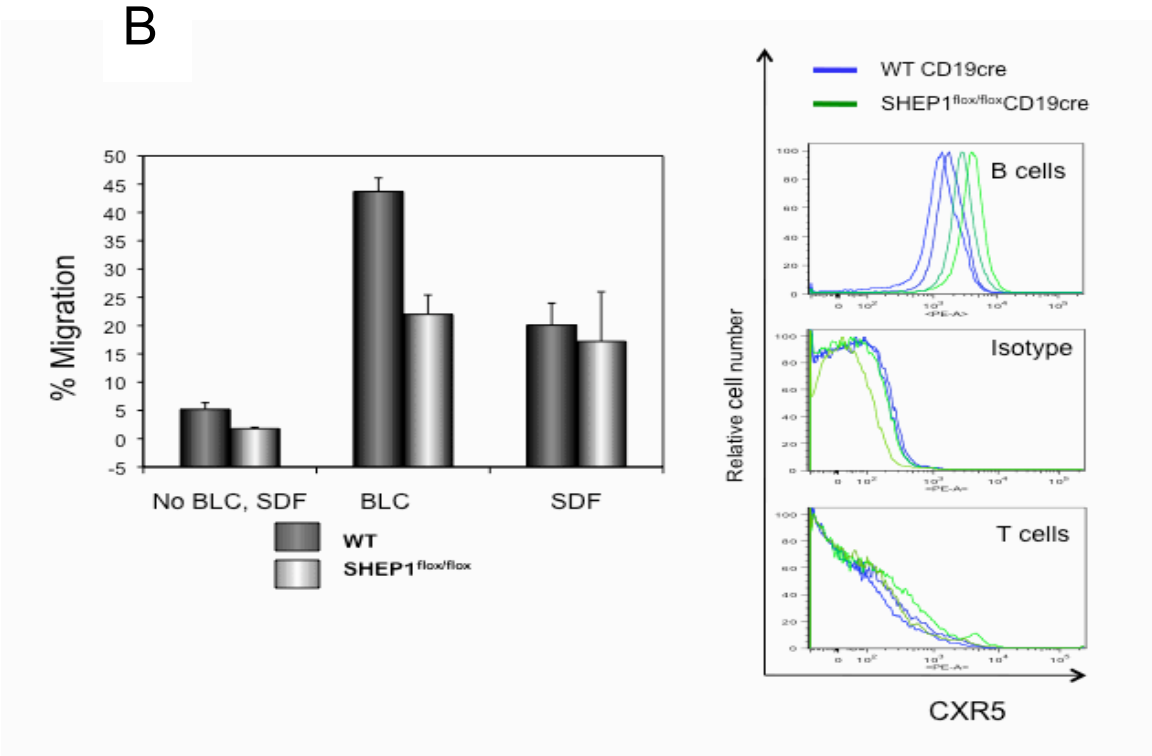


**Figure 3-10: Migration of SHEP1$^{flox/flox}$CD19cre B cells.** A) *In vitro* migration assay of purified splenic B cells in response to sphingosine-1-phosphate. Each bar represents the average of triplicate wells per group. B) Migration in respose to BLC and SDF1$\alpha$ (left panel). CXCR5 staining of B and T cells (right panel).

C

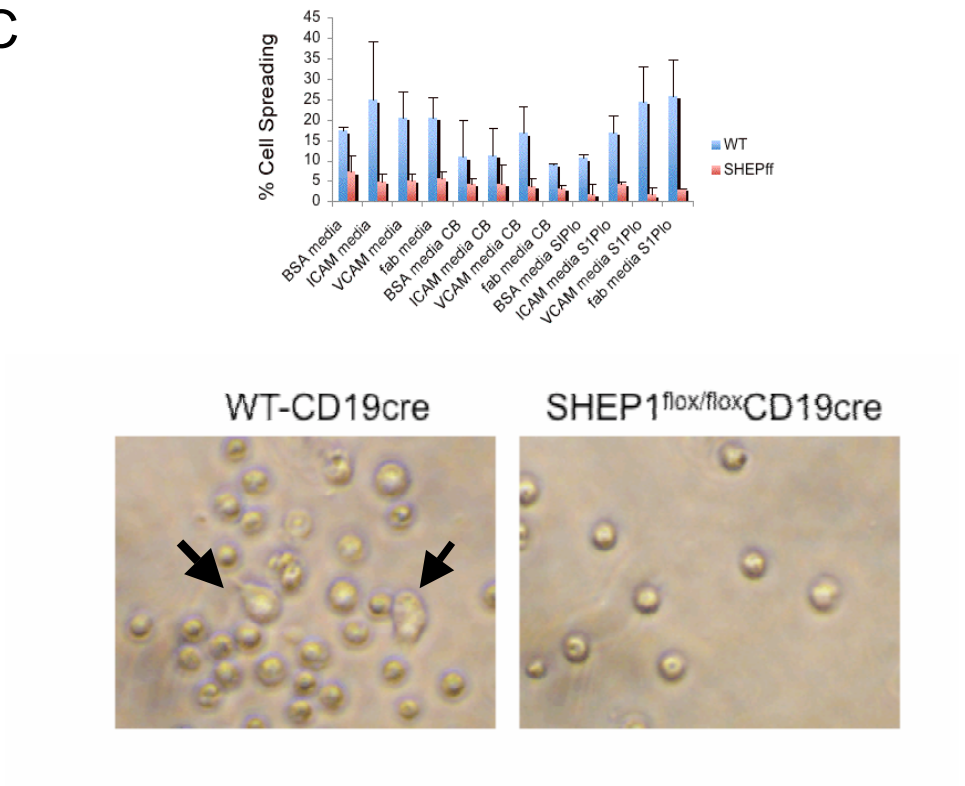


**Figure 3-10 continued: Migration of SHEP1$^{flox/flox}$CD19cre B cells.** C) Cell spreading assay of purified splenic B cells. Cells were cultured in 24 well plates coated with VCAM, ICAM, anti-IgM F(ab')$_2$ or BSA in the presence of 1 μM S1P, media alone, cytochalasin B for 24 hr. Spreading on anti-IgM F(ab')$_2$ in the presence of 1 μM S1P is shown. Quantification of cell spreading assay based on 3-5 fields per condition. The number of elongated cells (examples are pointed with black arrows) were counted and divided by the total number of cells in a given field. The average and standard deviation from 3-5 fields per condition is depicted (upper panel). Phase contrast microscopy of spreading cells (lower panel).

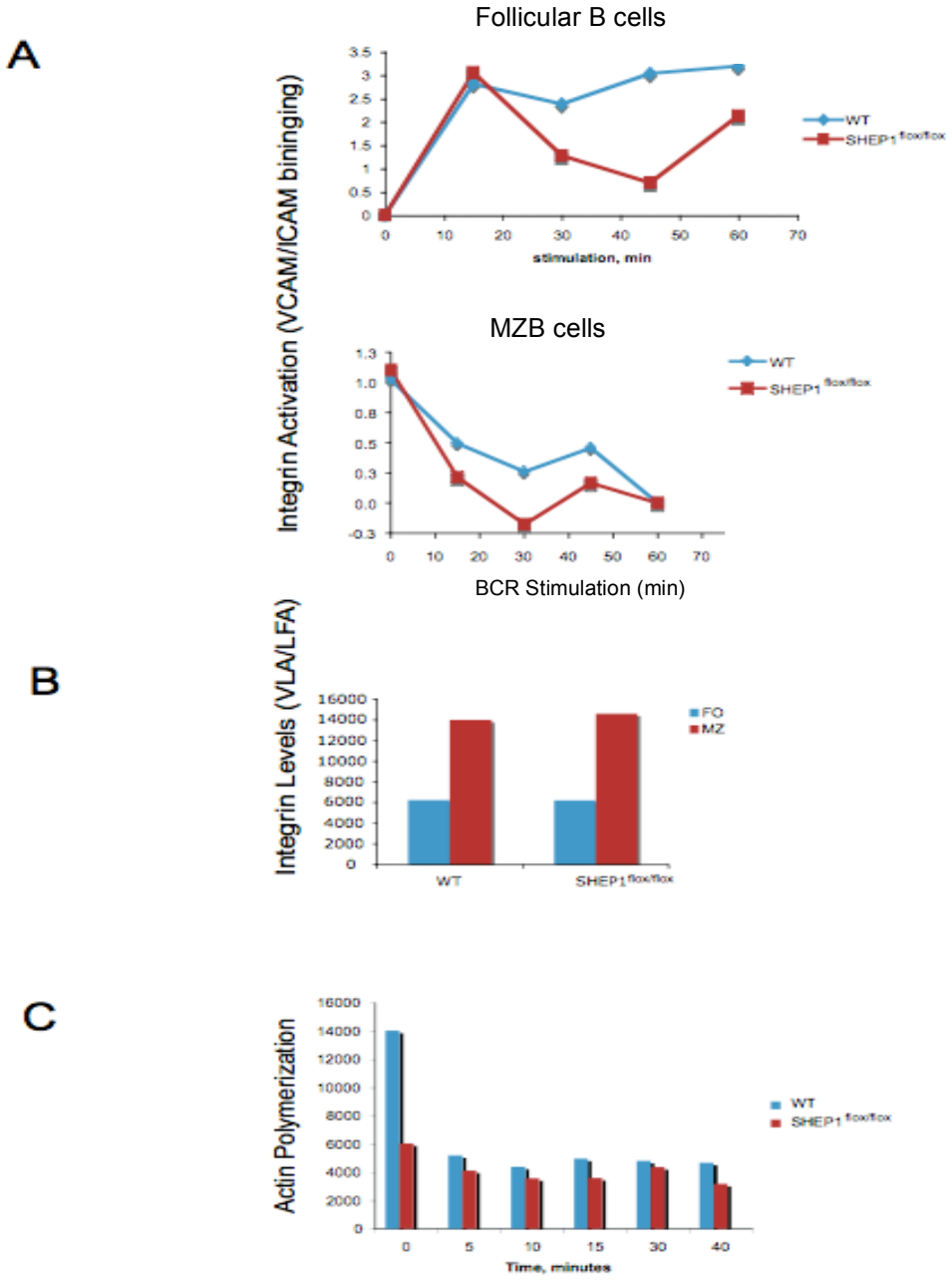


**Figure 3-11: Integrin activation and actin polymerization**: A) Purified splenic B cells from wildtype or SHEP1$^{flox/flox}$ CD19cre mice were stimulated with 10 μg/ml anti-IgM F(ab')$_2$. Cells were incubated with VCAM/ICAM-Fc. VCAM/ICAM binding was analyzed by flow cytometry. B) Purified splenic B cells from wildtype or SHEP1$^{flox/flox}$ CD19cre mice were stained for VLA/LFA integrins and marginal zone and follicular B cell compartments were gated. C) Actin polymerization was measured by flow cytometry.

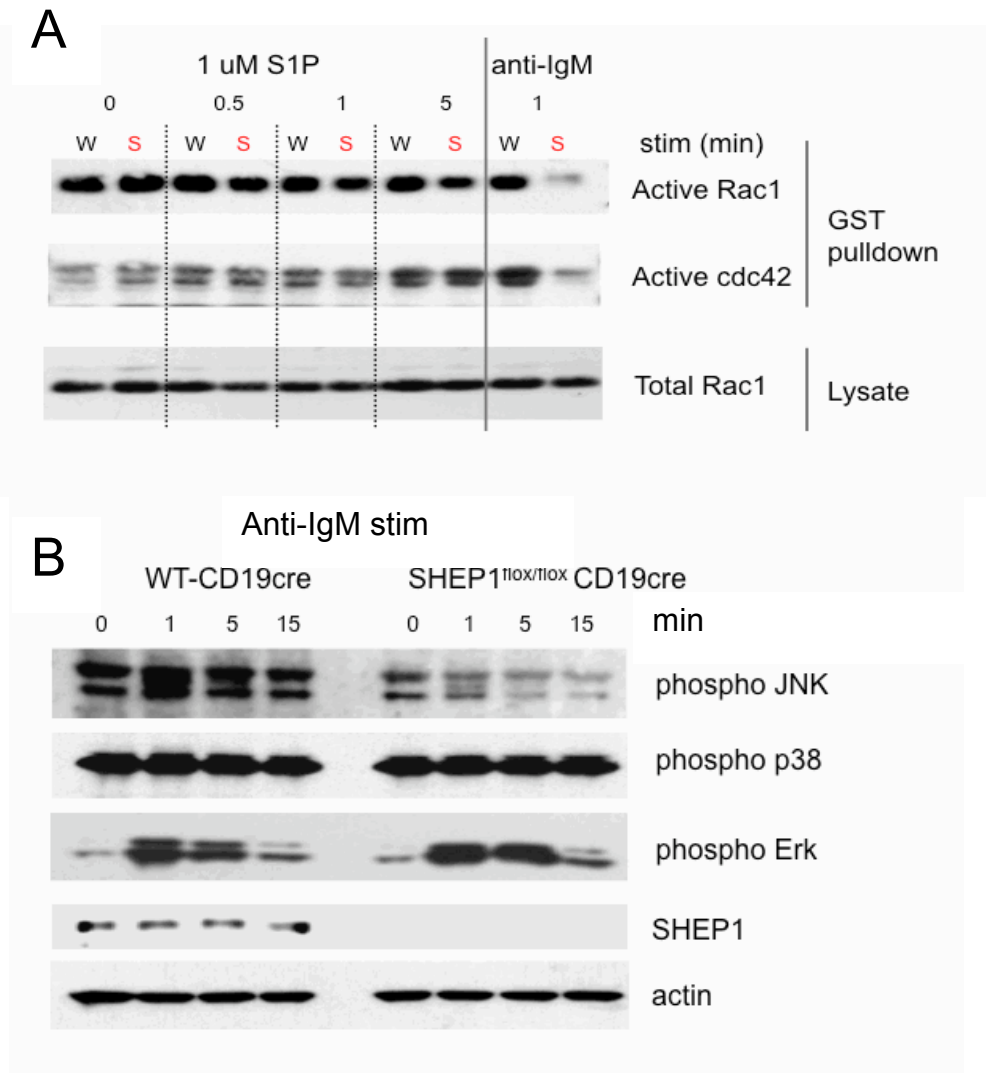


**Figure 3-12: BCR and S1P signaling**. A) Purified splenic B cells from wildtype or SHEP1$^{flox/flox}$ CD19cre mice were stimulated with 1 μM S1P or 10 μg/ml anti-IgM F(ab')$_2$. Cells were lysed and lysates were incubated with GST-conjugated GDS specific for active Rac and cdc42. Pulldowns were electrophoresed and immunoblotted for Rac1 and cdc42. Lysates were also immunoblotted for total Rac1 for loading. B) Purified splenic B cells from wildtype or SHEP1$^{flox/flox}$ CD19cre mice were stimulated with 10 μg/ml anti-IgM F(ab')$_2$, lysed and immunoblotted with antibodies to phospho-JNK, phospho-p38, phospho-Erk, SHEP1 and actin.

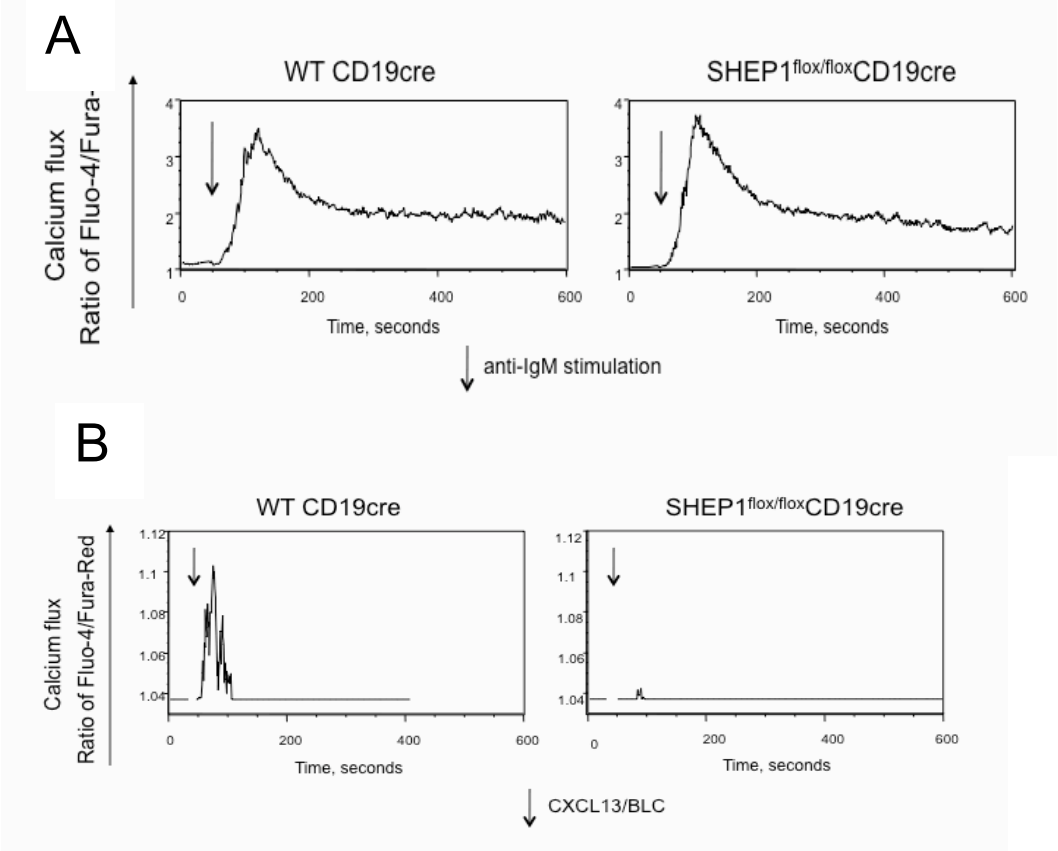


**Figure 3-13: Calcium flux and Akt activation.** A) Calcium flux in response to BCR stimulation with anti-IgM F(ab')$_2$. B) Calcium flux in response to BLC stimulation.

C

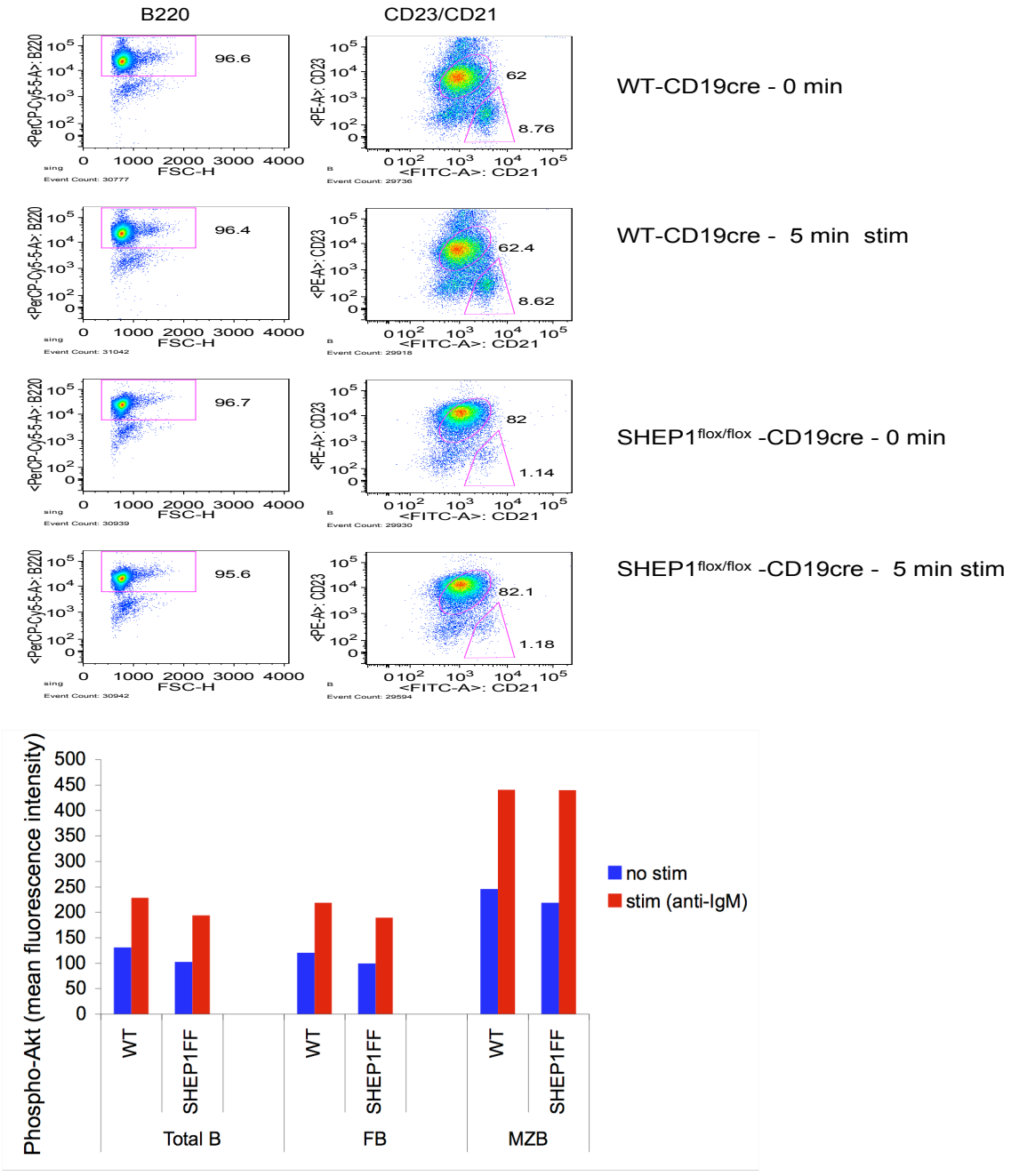


**Figure 3-13 continued: Calcium flux and Akt activation.** C) Purified splenic B cells from wildtype or SHEP1$^{flox/flox}$ CD19cre mice were stimulated with 10 μg/ml anti-IgM F(ab')$_2$ for 10 min, fixed, permeabilized and stained with anti-CD21-FITC or anti-CD21-PE and anti-B220-PerCP-Cy5.5 and with anti-phospho-Akt conjugated to AlexaFluor 647. Stained cells were analyzed by flow cytometry.

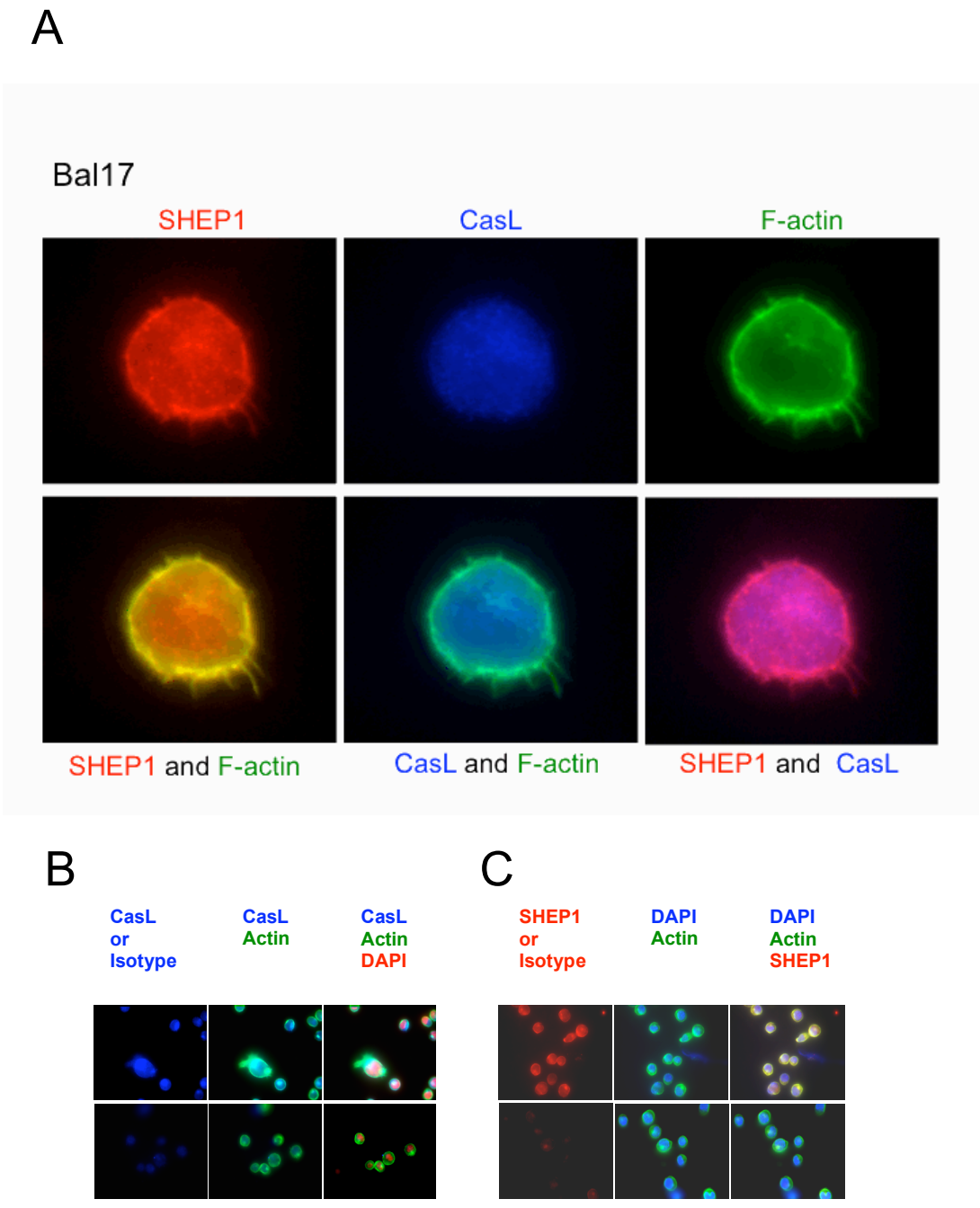


**Figure 3-14**: **SHEP1 and CasL localization**. A) Bal17 cells were placed on a slide coated with VCAM. Cells were fixed, permeabilized and stained with anti-SHEP1 (red), anti-CasL (blue) and phalloidin (F-actin, green). B) Upper row: stained with anti-CasL, phalloidin and DAPI; bottom row: stained with mouse isotype, phalloidin and DAPI. C) Upper row: stained with anti-SHEP1, phalloidin and DAPI; bottom row: stained with rabbit isotype, phalloidin and DAPI.

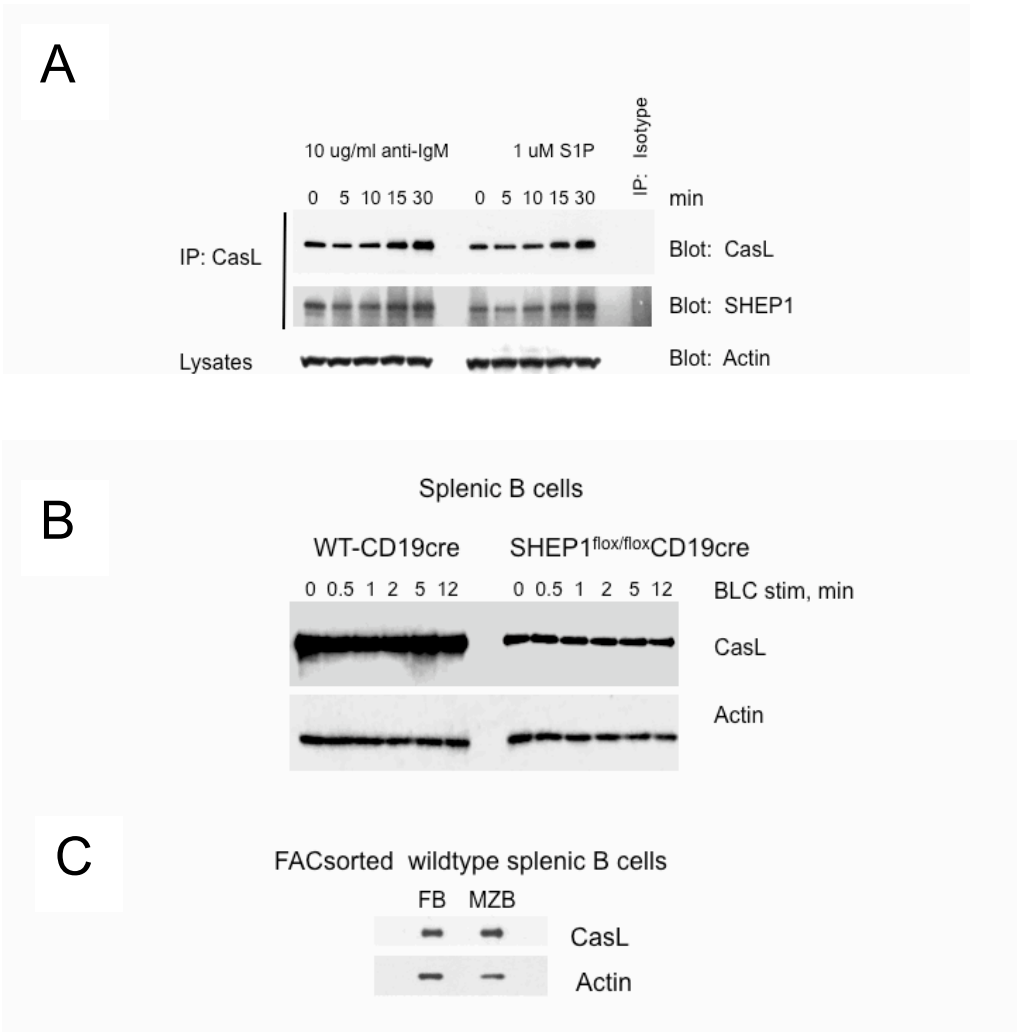


**Figure 3-15: SHEP1 and CasL association.** A) Bal17 cells were stimulated with S1P or anti-IgM and immunoprecipitated with anti-CasL and immunoblotted with anti-CasL or anti-SHEP1. B) Splenic B cells were lysed and immunoblotted with anti-CasL or actin. E) Follicular B cells and marginal zone B cells were sorted by flow cytometry. Purified fractions were lysed and blotted for CasL.

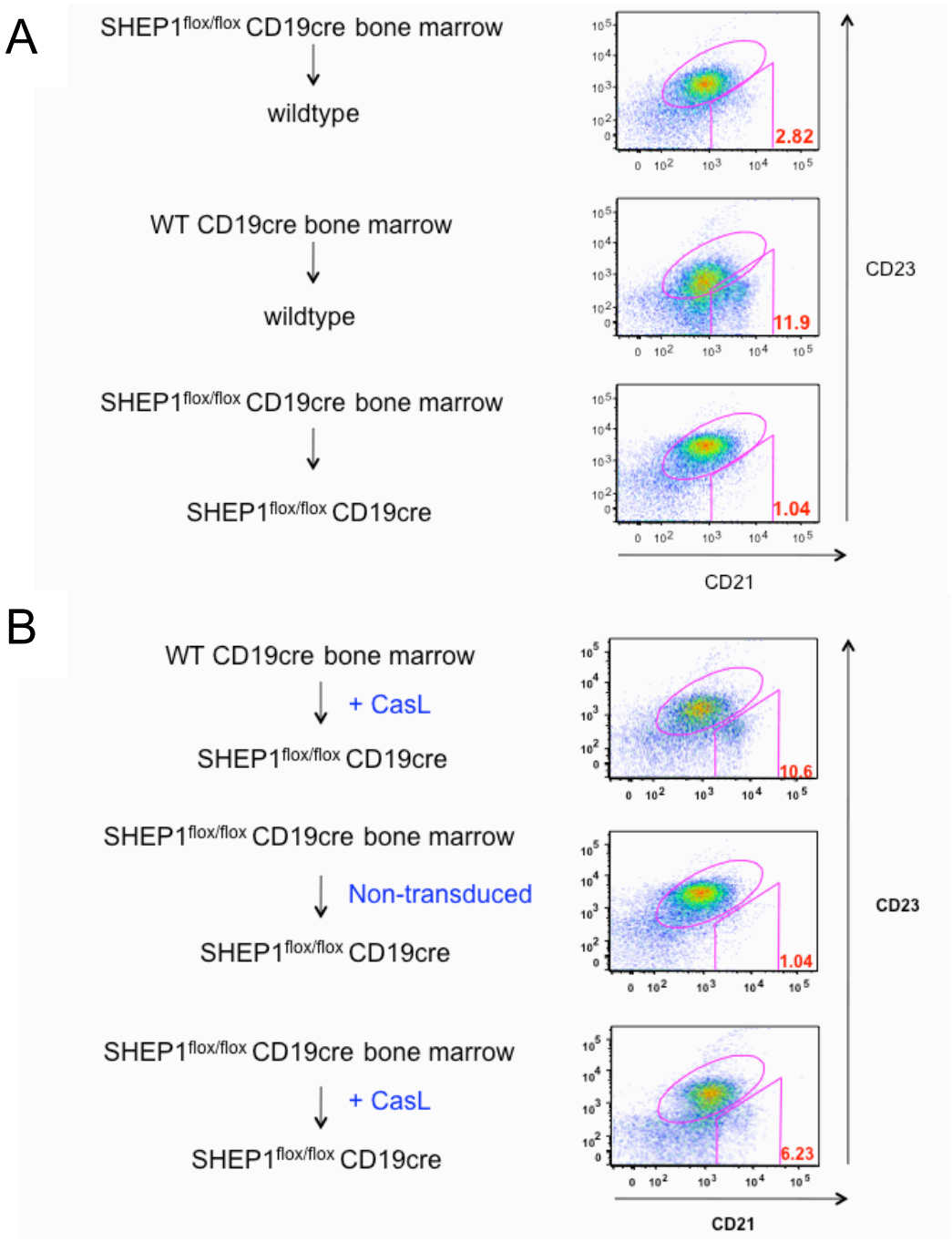


**Figure 3-16**: **Bone marrow reconstitution with CasL encoding retrovirus**. A) Bone marrow from wildtype or SHEP1$^{flox/flox}$ CD19cre mice was transferred into irradiated SHEP1$^{flox/flox}$ CD19cre or wildtype mice. Mice were analyzed after 8 weeks of reconstitution. B) Bone marrow from wildtype and SHEP1$^{flox/flox}$ CD19cre was transduced with retrovirus encoding CasL and transduced bone marrow was transferred into irradiated SHEP1$^{flox/flox}$ CD19cre mice. Mice were analyzed after 8 weeks of reconstitution.

>gi|6469330|gb|AAF13305.1|AF168364_1 SH2 domain-containing Eph receptor-binding protein SHEP1 [Mus musculus]
MTEMPKKTGRKFKFFKFKGLGSLSNLPRSFSLRRSSASASIRSCPEPDTFEATQDDMVTLPKSPPAYARS
SDMYSHMGTMPRPNIKKAQKQQAVQKAQEVSRESHLVSRRLPEPPDLEAAKEAGEGTEALLEDTAPSAVE
VDPMRELEDLTVDTEKEQVPGDVSPERTAAELEAAGDYVKFSKEKYILDSSPEKLHKELEEELKLSSTDL
RSHAWYHGRIPREVSETLVQRNGDFLIRDSLTSLGDYVLTCRWHNQALHFKINKVVVKAGESYTHIRYLF
EQESFDHVPALVRYHVGSRKAVSEQSGAIIYCPVNRTFPLRYLEASYGLSQGSSKTASPASPSGSKGSHM
KRRSITMTDGLTTDKVTRSDGCPNSTSLPHPRDSIRNCALSMDQIPDLHSPLSPISESPSSPAYSTVTRV
HAPSATPSTSAQPASPVARRSSEPQLCPGNTPKPPGESDRAPHASPSHTLCKASPSPSLSSYSDPDSGHY
CQLQPPVRGSREQAAGETPRKARGSGERQKELLENGVSDGEWGKTFTVPVVEATSSFNLATFQSQLIPKE
NRPLEVALLRKVKELLSEVDARTLARHVTKVDCLVARILGVTKEMQTLMGVRWGMELLTLPHGRQLRLDL
LERFHTMSIMLAVDILGCTGSAEERAALLHKTIQLAAELRGTMGNMFSFAAVMGALEMAQISRLEQTWMT
LRQRHTEGAILYEKKLKPFLKSLNEGKEGPPLSNTTFPHVLPFITLLECDSAPAEGPEPWGSTEHGVEVV
LAHLEAARTVAHHGGLYHTNAEVKLQGFQARPELLEVFSTEFQMRLLWGSQGANSSQAWRYEKFDKVLTA
LSHKLEPAIRSSEL

**Figure 3-17**: **Mouse SH2 domain-containing Eph receptor-binding protein SHEP1 amino acid sequence.** SHEP1$\alpha$ amino acid sequence showing the location of the tyrosine that has been mutated to phenylalanine or glutamine (red box).

A

MTEMPKKTGRKFKFFKFKGLGSLSNLPRSFSLRRSSASASIRSCPEPDTFEATQDDMVTL
PKSPPAYARSSDMYSHMGTMPRPNIKKAQKQQAVQKAQEVSRESHLVSRRLPEPPDLEAA
KEAGEGTEALLEDTAPSAVEVDPMRELEDLTVDTEKEQVPGDVSPERTAAELEAAGDYVK
FSKEKYILDSSPEKLHKELEEELKLSSTDLRSHAWYHGRIPREVSETLVQRNGDFLIRDS
LTSLGDYVLTCRWHNQALHFKINKVVVKAGESYTHIRYLF

---

**Number of found motifs: 5**

---

**PROSITE PATTERN**

| Found Motif | Position | PROSITE | Description | Related Sequences | Related Structures |
|---|---|---|---|---|---|
| PKC_PHOSPHO_SITE | 8..10<br>31..33<br>40..42<br>108..110 Detail<br>154..156<br>250..252 | PS00005 | Protein kinase C phosphorylation site. | -- | -- |
| CAMP_PHOSPHO_SITE | 33..36 Detail | PS00004 | cAMP- and cGMP-dependent protein kinase phosphorylation site. | -- | -- |
| AMIDATION | 8..11 Detail | PS00009 | Amidation site. | -- | -- |
| MYRISTYL | 21..26 Detail | PS00008 | N-myristoylation site. | -- | -- |
| CK2_PHOSPHO_SITE | 43..46<br>53..56<br>137..140<br>154..157<br>168..171 Detail<br>190..193<br>206..209<br>243..246 | PS00006 | Casein kinase II phosphorylation site. | -- | -- |

B

**MTEMPKKTGRKFKFFKFKGLGSLSNLPRSFSLRRSSAS**
**ASIRSCPEPDTFEATQDDMVTLPKSPPAYARSSDMYSHM**
**GTMPRPNIKKAQKQQAVQKAQEVSRESHLVSRRLPEPP**
**DLEAAKEAGEGTEALLEDTAPSAVEVDPMRELEDLTVDT**
**EKEQVPGDVSPERTAAELEAAGDYVKFSKEKYILDSSPE**

**Figure 3-18: N-terminal region unique to SHEP1α.** A) Motifs found using Prosite server. B) Putative TPR motif. Amino acid residues in red follow the TPR consensus sequence.

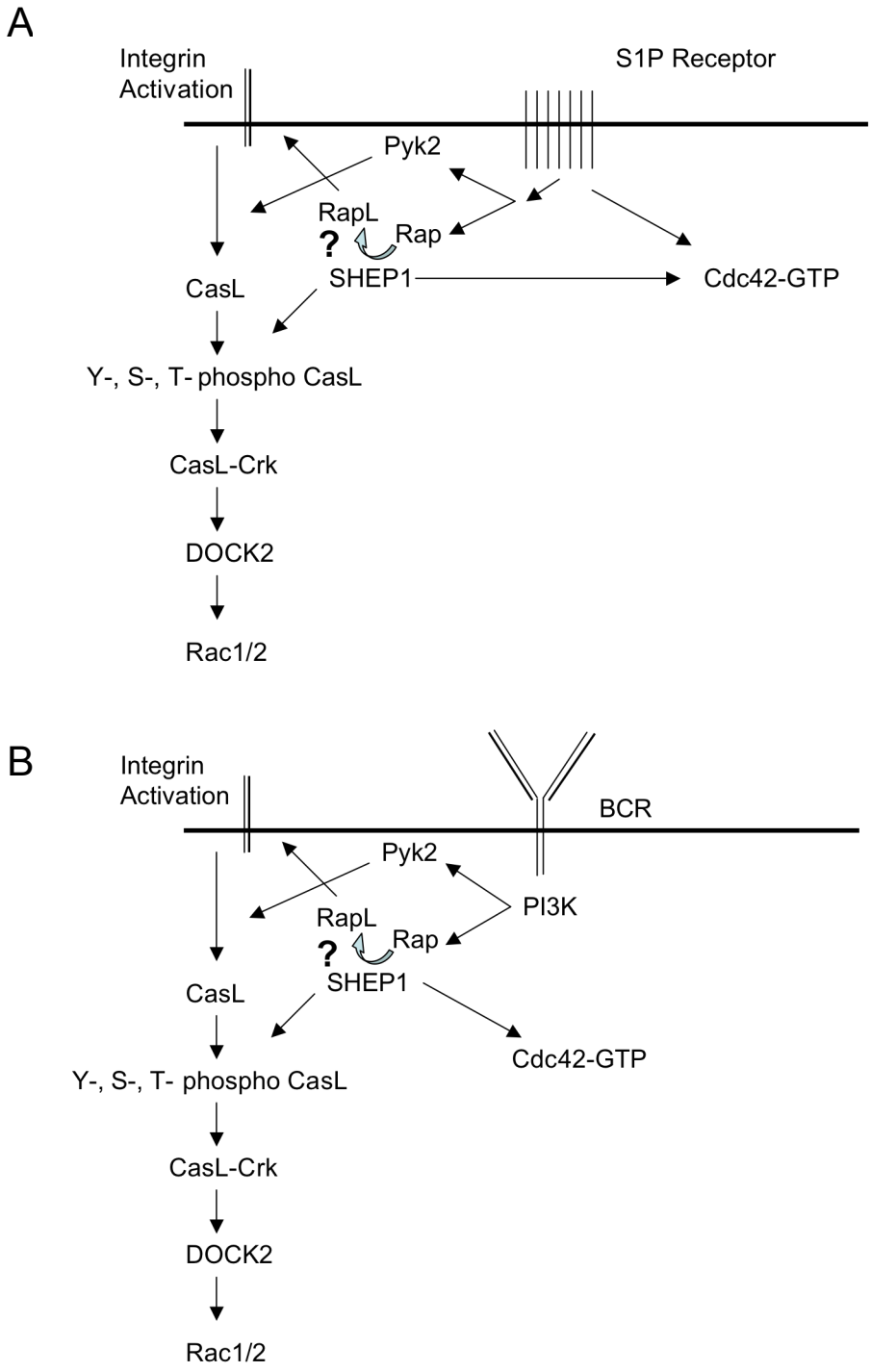


**Figure 3-19**: **Working models showing the involvement of SHEP1 downstream of S1P receptor (A) and BCR stimulation (B).**

# CHAPTER 4

## $\beta_1$ integrin and B cell differentiation and immune response

### 4.1 - Introduction

A successful immune response depends on the ability of lymphocytes to quickly access sites of injury or infection. Migration of lymphocytes is a highly regulated and complex process. The integrin family of adhesion molecules has long been established as crucial in leukocyte adhesion and trafficking in and out of a variety of tissue environments. Impairment of integrin function in mice had been linked to impaired neutrophil recruitment (1), wound healing and response to infections (2). In a study of Multiple Sclerosis-like Experimental Autoimmune Encephalomyelitis (EAE) in mice lacking the $\beta_1$ integrin in T lymphocytes, it was shown that T cells rely upon $\beta_1$ integrins to accumulate in the central nervous system (CNS) during EAE (3) and hence, targeting of the $\beta_1$ integrin, VLA-4, had been shown to reverse EAE in mice (4). Polymorphisms in $\beta_2$ integrin have also been associated with human Hirschsprung's disease–associated enterocolitis in humans (5). Thus, further understanding of integrin expression, activation and signaling as they relate to lymphocyte function would provide a platform for designing therapeutics for integrin-associated autoimmunity, inflammation and cancer.

The integrin family consists of 18 different $\alpha$ and 8 different $\beta$ subunits, which pair up to form at least 24 different $\alpha\beta$ heterodimeric receptors (6). Leukocytes express leukocyte function–associated antigen 1 (LFA-1) which is a heterodimer of $\alpha$L and $\beta$2 subunits and very late antigen 4 (VLA-4), which is a heterodimer of $\alpha$4 and $\beta$1 subunits.

LFA-1 binds intercellular adhesion molecules (ICAMs) displayed on vascular endothelial cells. VLA-4 binds vascular intercellular adhesion molecule (VCAM1). These integrins assist in slow rolling, adhesion, and transendothelial migration, and they are also involved in other cellular functions such as phagocytosis, cytokine production and proliferation (6). In the previous chapter of this thesis, the association between SHEP1 and integrin signaling underscores the importance of integrins in bridging actin cytoskeletal dynamics to ligands presented in the extracellular environment.

During B cell development and differentiation in the bone marrow, B cells reside in distinct niches depending on the ontogenic stage they are in. Residence in these niches has been shown to depend on B cell integrin interaction with the microenvironment. VLA-4 binding to VCAM1 had been shown to mediate adhesion of pre-B cells to cultures of bone marrow cells (7, 8) as well as to fibroblasts (9). VLA binding to fibronectin has been shown to be essential for the differentiation of plasma cells (10). More recently, Li et al. have shown that inhibition of the VLA/VCAM interaction led to an inability of B cells to reconstitute in α-1,6-fucosyltransferase-deficient mice (11). VLA-4 is a heterodimer $\alpha_4$ and $\beta_1$ and creation of $\alpha_4$ null mice was used as a model for VLA-4 deficiency. $\alpha_4$ null mice lack both $\alpha_4\beta_1$ and $\alpha_4\beta_7$ integrins and reveal an early block in B cell development as well stranded T cell precursors in the bone marrow (18). The loss of $\alpha_4$ also results in severe reductions of erythrocytes and myeloid cells. More recently, however, chimeric mice reconstituted with $\beta_1$-deficient bone marrow were used to investigate how the loss of $\beta_1$ would affect total hematopoiesis and immune responses (12). The authors found that the loss of $\beta_1$ in total hematopoietic cells is not important for hematopoiesis, but T cell - dependent immune responses and T cell independent (TI-

2) immune responses were affected (13). However, from this work, it was unclear whether the observed responses were intrinsic to B cells.

To determine whether the loss of $\beta_1$ integrin specifically in B cells would impact immune responses and to confirm the findings that the loss of $\beta_1$ would not affect hematopoiesis, $\beta_1^{flox//flox}$ mice were bred with Ig-$\alpha$ cre mice to produce mice in a B cell-specific deletion of $\beta_1$ integrins. We determined that bone marrow, blood, spleen and lymph node B cell numbers were normal. Immune responses of $\beta_1^{flox//flox}$ Ig-$\alpha$ cre mice to TD antigens were normal. However, upon analysis of peripheral B cell subcompartments, these mice showed a reduction in germinal center B cell frequencies and an increase in immature B cells.

## 4.2 - Results

### 4.2.1 - B cell-specific loss of $\beta_1$ integrin in $\beta_1^{flox/flox}$ -Ig-$\alpha$ cre mice.

To verify the B cell - specific loss of $\beta_1$ integrin in $\beta_1^{flox/flox}$ -Ig-$\alpha$ cre mice, splenic cells were stained for $\beta_1$ integrin or isotype control and analyzed by flow cytometry. Fig 4-1A shows the loss of $\beta_1$ integrin in the B cell-gated populations from three $\beta_1^{flox/flox}$ -Ig-$\alpha$ cre mice. Non-B cell populations (CD11b-, B220-) from $\beta_1^{flox/flox}$ -Ig-$\alpha$ cre mice express $\beta_1$, thus the deletion of $\beta_1$ is confined to B cells. Interestingly, the gated non-B cell population, which was largely comprised of T cells, from both wildtype and $\beta_1^{flox/flox}$ -Ig-$\alpha$ cre mice show two peaks for $\beta_1$ expression. It is known that $\beta_1$ expression is increased in activated T cells and recently, it has been shown that not only did *in vitro* differentiated Th1 and Th2 cells both express elevated levels of integrins, but that the

Th2 subset displayed the activated conformation of $\beta_1$ and greater adhesiveness (14). A small fraction of B220+ cells appear to have retained expression of $\beta_1$, which is indicative of an incomplete deletion of $\beta_1$. These B220+ $\beta_1$+ cells contain IgMhi and IgMlo subpopulations (Fig 4-1B).

### 4.2.2 - B cell subcompartments in $\beta_1$ integrin in $\beta_1^{flox/flox}$ -Ig-$\alpha$ cre mice are normal.

The frequencies of bone marrow splenic B cell subcompartments were analyzed by flow cytometry. We found normal frequencies in pre/pro B, immature and recirculating mature B cells in the bone marrow (data not shown), normal frequencies of T1/T2, marginal zone, marginal zone precursors and follicular B cells in the spleen (Fig 4-2). However, we observed two peaks of B220 staining intensity in the $\beta_1^{flox/flox}$ -Ig-$\alpha$ cre mice (Fig 4-2). In the lymph nodes, B cell, macrophage and T cell frequencies in the $\beta_1$ integrin in $\beta_1^{flox/flox}$ -Ig-$\alpha$ cre mice were comparable to control and the two peaks on B220 staining intensity were not seen (Fig 4-3, data not shown).

### 4.2.3 – T1 and T2, but not T3, subpopulations have reduced B220 levels.

In Fig 4-2, we found that the B220 staining intensity in the $\beta_1^{flox/flox}$ -Ig-$\alpha$ cre mice were split into B220hi and B220lo peaks, which were not seen in wildtype mice. We found that the B220lo populations were Transitional B cells. To further determine which subpopulation of transitional cells display the B220lo phenotype, splenic B cells were stained for AA4.1, a marker of immature B cells. AA4.1+ B cells were gated and T1, T2 and T3 subpopulations were analyzed in an IgM vs. CD23 plot (Fig 4-4). Frequencies of these subpopulations were found to be comparable to wildtype (Fig 4-4,

upper histogram). However, the B220lo B cell population, seen in the conditional knockout, was found to be comprised of T1 and T2 subpopulations (Fig 4-4, lower histogram). This suggests that $\beta_1$ may be necessary for the upregulation of B220 levels that could be occurring as B cells progress from the T1 to T2 to mature B cell stages.

### 4.2.4 - Immune responses to SRBC are intact but with moderately reduced GC B cell numbers.

To determine if $\beta_1$ play a specific role in the immune response, mice were immunized with SRBC and analyzed 6 days later. B, T and myeloid compartments were comparable (Fig 4-5A). Analysis of B220 staining intensity revealed a B220lo population as seen in Fig 2, although in these immunized animals, instead of a peak, we see a left shoulder on the histograms (Fig 4-5B). The T1/T2, marginal zone, marginal zone precursor and follicular B cell compartments were normal (Fig 4-5B). To determine the formation of germinal center B cells and plasma cells, splenic cells were stained for Syndecan-1, GL7 and FAS. While no significant difference was seen in plasma cell formation, the germinal center response appeared to be modestly reduced (Fig 4-5C). Class-switch-recombination (replacement of the IgH Cmu constant region with one of several IgH constant regions to change from IgM to another IgH class, such as IgG, IgE, or IgA) was analyzed by staining splenic cells with anti-IgG. We found that B cells from $\beta_1^{flox/flox}$ -Ig-$\alpha$ cre were able to class switch to IgG (Fig 4-5D).

### 4.2.5 - Immune responses to NP-KLH are intact but with moderately reduced GC B cell numbers and elevated IgM response.

To determine the immune response to the T-dependent antigen NP-KLH, mice were immunized with NP-KLH and analyzed 12 days post immunization. $\beta_1^{flox/flox}$ -Ig-$\alpha$ cre mice can undergo class switch to IgG (Fig 4-6A), however, as seen in SRBC immunization, they showed modestly reduced germinal center responses (Fig 4-6A and 4-6B). Antigen-specific immunoglobulin, measured by ELISA, was found to be comparable to control for IgG however, $\beta_1^{flox/flox}$ -Ig-$\alpha$ cre mice had an elevated IgM responses (Fig 4-6C). To determine high affinity maturation, a serum ELISA was performed using $NP_3$-BSA coated plates. Similarly, $\beta_1^{flox/flox}$ -Ig-$\alpha$ cre had normal IgG responses and elevated IgM responses (Fig 4-6D). The elevated IgM response may be related to the reduced germinal center response. Cells that are unable to differentiate into germinal center B cells are excluded from the class-switch environment and therefore differentiate into IgM-secreting plasma cells outside of this niche.

### 4.2.6 - B cell proliferation is intact in $\beta_1$ integrin in $\beta_1^{flox/flox}$ -Ig-$\alpha$ cre mice.

To determine if the loss of $\beta_1$ would impact B cell proliferation**,** purified splenic B cells were labeled with CFSE and cultured in media alone or in the presence of anti-CD40, anti-IgM and LPS with or without IL-4. After 72 hr, cells were harvested and stained for IgG and Syndecan-1. The degree of proliferation is commensurate with a reduction in CFSE staining. Fig 4-7A (media alone) shows that in the absence of stimuli, no proliferating cells and no IgG-switched cells can be seen. Fig 4-7B shows that in the presence of LPS (left panels), $\beta_1^{flox/flox}$ -Ig-$\alpha$ cre and wildtype B cells proliferated and

switched to IgG3 in a comparable manner. Fig 4-7B also shows that in the presence of LPS + IL-4 (right panels), there was comparable proliferation and switching to IgG1/2. Fig 4-7C shows comparable proliferation and switching to IgG1/2 in the presence of anti-CD40 + IL-4. Fig 4-7D and 4-7E show comparable proliferation and switching to IgG1/2 in the presence of low dose and high dose of BCR stimulation. Plasma cell formation which is apparent in anti-CD40 + IL-4 stimulation was also comparable between the two groups (Fig 4-7F). Overall, the loss of $\beta_1$ does not have a significant impact in B cell proliferation, class switch to IgG and plasma cell formation.

**4.3 – Discussion**

The initial characterization of $\beta_1^{flox/flox}$ -Ig-$\alpha$ cre mice presented in this chapter suggests that the loss of $\beta_1$ specifically in B cells 1) may lead to a delay in the upregulation of the B220 marker as cells progress through the transitional stages of development or premature release of immature B cells out of the bone marrow, 2) does not affect the differentiation of transitional, marginal zone and marginal zone precursor B cells, 3) does not impact cell proliferation, and 4) leads to a reduction in germinal center B cell numbers, which may be linked to the enhanced IgM immunoglobulin response.

Our results share some of the findings of Brakebusch et al. (13) with regards to the dispensability of $\beta_1$ in B lymphopoiesis and support the hypothesis that $\alpha$4 may be alternatively partnering with $\beta_7$ to compensate for the loss of $\beta_1$. Brakebush et al. mentioned in their paper that immature B cells express $\beta_1$ but not $\beta_7$, however, in mature B cells both are expressed. This may explain our observation of a B220lo population in the Transitional subset, a stage where $\beta_7$ cannot compensate. Our findings differ from that of Brakebusch et al. with regards to immune responses. The relative germinal center B cell numbers were consistently, but modestly reduced in the absence of $\beta_1$. Furthermore, the TD IgM response was elevated in the absence of $\beta_1$. In their system, $\beta_1$ is absent in B, T, dendritic cells and the reduced TD response they observed may be T cell related. The modest reduction in the IgM TI response is similarly difficult to interpret due to the loss of $\beta_1$ in other cell types. A TI immune response assay is yet to be accomplished in our $\beta_1^{flox/flox}$ -Ig-$\alpha$ cre mice. In our B cell intrinsic system, the elevated IgM response in conjunction with lower GC response could be suggestive of a defect in

following the migration protocol between dark and light zones within the germinal center, the migration towards the GC or the retention within the GC of mutant B cells.

The redundancy of β subunits is the most plausible rational for the lack of a severe defect in lymphopoiesis in the $\beta_1^{flox/flox}$ -Ig-α cre mice. Several studies have shown this possibility (16, 17, 18). This compels one to propose a $\beta_1/\beta_7$ double conditional mutant mice. However, the dual loss of these integrins did not affect hematopoiesis and lymphopoiesis, but immune responses had not been assessed (15).

The preliminary analyses of the role of $\beta_1$ in B cells using the $\beta_1^{flox/flox}$ -Ig-α cre mice may serve as a platform for further investigation.

## 4.4 – Methods

### 4.4.1 - Mice

Itgβ1$^{flox/flox}$ mice were purchased from The Jackson Laboratory. The strain name is B6; 129-*Itgb1*$^{tm1Efu}$ /J and the stock number is 004605. The floxed allele is genotyped using forward primer 5' cgg ctc aaa gca gag tgt cag tc 3' and the reverse primer is 5'cca caa ctt tcc cag tta gct ctc 3'. PCR conditions used are a slight modification of the one recommended by The Jackson Laboratory: 1) 94°C, 3 min 2) 94°C, 30 sec 3) 65°C, 1 min 4) 72°C, 1 min, 5) 72°C, 2 min 6) 4°C hold; steps 2-4 were repeated for 35 cycles and the expected band is approximately 280 bp for the floxed allele and 160 bp for the wildtype allele. Itgβ1$^{flox/flox}$ mice were crossed with Ig-α *cre* mice (in which cre recombinase expression is driven by the Ig-alpha promoter that turns on at the early pre-B cell stage) to generate Itgβ1$^{flox/flox}$ mice /Ig-α *cre* mice. Mice were genotyped by PCR amplification of genomic DNA from tail samples. Adult mice used were 8-20 weeks old. All animals

were maintained in a pathogen free animal facility at Sanford-Burnham Medical Research Institute.

### 4.4.2 - Flow Cytometry

Spleens were excised and red blood cells were depleted from cell suspensions using hypotonic ammonium chloride. One million cells were resuspended in FACS buffer (PBS, 1% FBS and 0.01% sodium azide) and incubated with the following conjugated antibodies from BD Biosciences Pharmingen (San Diego, CA): IgM-APC, IgD-PE, B220-APC-Cy7, and CD11b-PE-Cy7, CD23, CD21, AA4.1. Beta 1 integrin antibody was from eBioscience, clone eBioHMb1-1, catalog #13-0291-80, biotin-conjugated anti-CD29. Samples were washed once with FACS buffer and read using a FACSCanto flow cytometer (BD Biosciences, San Jose, CA). Samples were analyzed using FlowJo software (Treestar, Ashland, OR).

### 4.4.3 - Serum ELISA

Serum samples were collected by retroorbital bleeding. 96-well high binding capacity plates were coated with 10 μg/ml $NP_3$-BSA or $NP_{30}$-BSA for 24 hr at 4°C. Plates were blocked for 20 min at RT with blocking buffer (0.5% BSA in PBS). Serum samples were serially diluted (beginning at 1:200) in blocking buffer, and incubated in coated wells for 2 hr at RT. Plates were washed and incubated with alkaline phosphatase-conjugated anti-mouse or anti-mouse IgG for 1 hr at RT. Phosphatase substrate (Sigma, St. Louis, MO) was added to the wells, and $A_{405}$ was measured using a BioTek Elx808 colorimetric plate reader (BioTek Instruments, Winooski, VT).

### 4.4.4 - Immunization

Mice were intra-peritoneally immunized with 100 μg of NP-KLH (in alum) in 200 μl of PBS or 200 μl of a 10% suspension of twice-washed sheep red blood cells. Mice were bled retro-orbitally as previously described. Spleen, bone marrow and lymph nodes were harvested and analyzed by flow cytometry as previously described.

## 4.5 - References


1. T.N. Mayadas and X. Cullere, Neutrophil beta2 integrins: moderators of life or death decisions, *Trends Immunol* 26 (2005), pp. 388–395.

2. T. Peters, A. Sindrilaru and B. Hinz et al., Wound-healing defect of CD18(-/-) mice due to a decrease in TGF-beta1 and myofibroblast differentiation, EMBO J 24 (2005), pp. 3400–3410.

3. Bauer M, Brakebusch C, Coisne C, Sixt M, Wekerle H, Engelhardt B, Fässler R. Beta1 integrins differentially control extravasation of inflammatory cell subsets into the CNS during autoimmunity. Proc Natl Acad Sci U S A. 2009 Feb 10;106(6):1920-5. Epub 2009 Jan 28.

4. Kent SJ, Karlik SJ, Cannon C, Hines DK, Yednock TA, Fritz LC, Horner HC. A monoclonal antibody to alpha 4 integrin suppresses and reverses active experimental allergic encephalomyelitis. J Neuroimmunol. 1995 Apr;58(1):1-10.

5. Moore SW, Sidler D, Zaahl MG. The ITGB2 immunomodulatory gene (CD18), enterocolitis, and Hirschsprung's disease. J Pediatr Surg. 2008 Aug;43(8):1439-44.

6. Abram CL, Lowell CA. The ins and outs of leukocyte integrin signaling. Annu Rev Immunol. 2009;27:339-62.

7. Ryan DH, Nuccie BL, Abboud CN, Winslow JM. Vascular cell adhesion molecule-1 and the integrin VLA-4 mediate adhesion of human B cell precursors to cultured bone marrow adherent cells. J Clin Invest. 1991 Sep;88(3):995-1004.

8. Shen W, Bendall LJ, Gottlieb DJ, Bradstock KF. The chemokine receptor CXCR4 enhances integrin-mediated in vitro adhesion and facilitates engraftment of leukemic precursor-B cells in the bone marrow. Exp Hematol. 2001 Dec;29(12):1439-47

9. Tang J, Scott G, Ryan DH.Subpopulations of bone marrow fibroblasts support VLA-4-mediated migration of B-cell precursors. Blood. 1993 Dec 1;82(11):3415-23.

10. Roldán E, García-Pardo A, Brieva JA. VLA-4-fibronectin interaction is required for the terminal differentiation of human bone marrow cells capable of spontaneous and high rate immunoglobulin secretion. J Exp Med. 1992 Jun 1;175(6):1739-47.

11. Li W, Ishihara K, Yokota T, Nakagawa T, Koyama N, Jin J, Mizuno-Horikawa Y, Wang X, Miyoshi E, Taniguchi N, Kondo A.Reduced alpha4beta1 integrin/VCAM-1 interactions lead to impaired pre-B cell repopulation in alpha 1,6-fucosyltransferase deficient mice. Glycobiology. 2008 Jan;18(1):114-24.

12. Arroyo AG, Taverna D, Whittaker CA, Strauch UG, Bader BL, H Rayburn H, Crowley D, Parker CM and Hynes RO. In vivo roles of integrins during leukocyte development and traffic: insights from the analysis of mice chimeric for α5, αv, and α4 integrins, J. Immunol. 165 (2000), pp. 4667–4675.

13. Brakebusch C, Fillatreau S, Potocnik AJ, Bungartz G, Wilhelm P, Svensson M, Kearney P, Körner H, Gray D, Fässler R. Beta1 integrin is not essential for hematopoiesis but is necessary for the T cell-dependent IgM antibody response. Immunity. 2002 Mar;16(3):465-77.

14. Lim YC, Wakelin MW, Henault L, Goetz DJ, Yednock T, Cabañas C, Sánchez-Madrid F, Lichtman AH, Luscinskas FW. Alpha4beta1-integrin activation is necessary for high-efficiency T-cell subset interactions with VCAM-1 under flow. Microcirculation. 2000 Jun;7(3):201-14.

15. Bungartz G, Stiller S, Bauer M, Müller W, Schippers A, Wagner N, Fässler R, Brakebusch C. Adult murine hematopoiesis can proceed without beta1 and beta7 integrins. Blood. 2006 Sep 15;108(6):1857-64.

16. Marsal J, Brakebusch C, Bungartz G, Fässler R, Agace WW. beta1 integrins are not required for the maintenance of lymphocytes within intestinal epithelia. Eur J Immunol. 2005 Jun;35(6):1805-11.

17. Bungartz G, Stiller S, Bauer M, Müller W, Schippers A, Wagner N, Fässler R, Brakebusch C. Adult murine hematopoiesis can proceed without beta1 and beta7 integrins. Blood. 2006 Sep 15;108(6):1857-64.

18. Arroyo A.G., Yang J.T., Rayburn H., Hynes R.O. Differential requirements for α4 integrins during fetal and adult hematopoiesis. Cell. 1996 85 (7):997-1008.

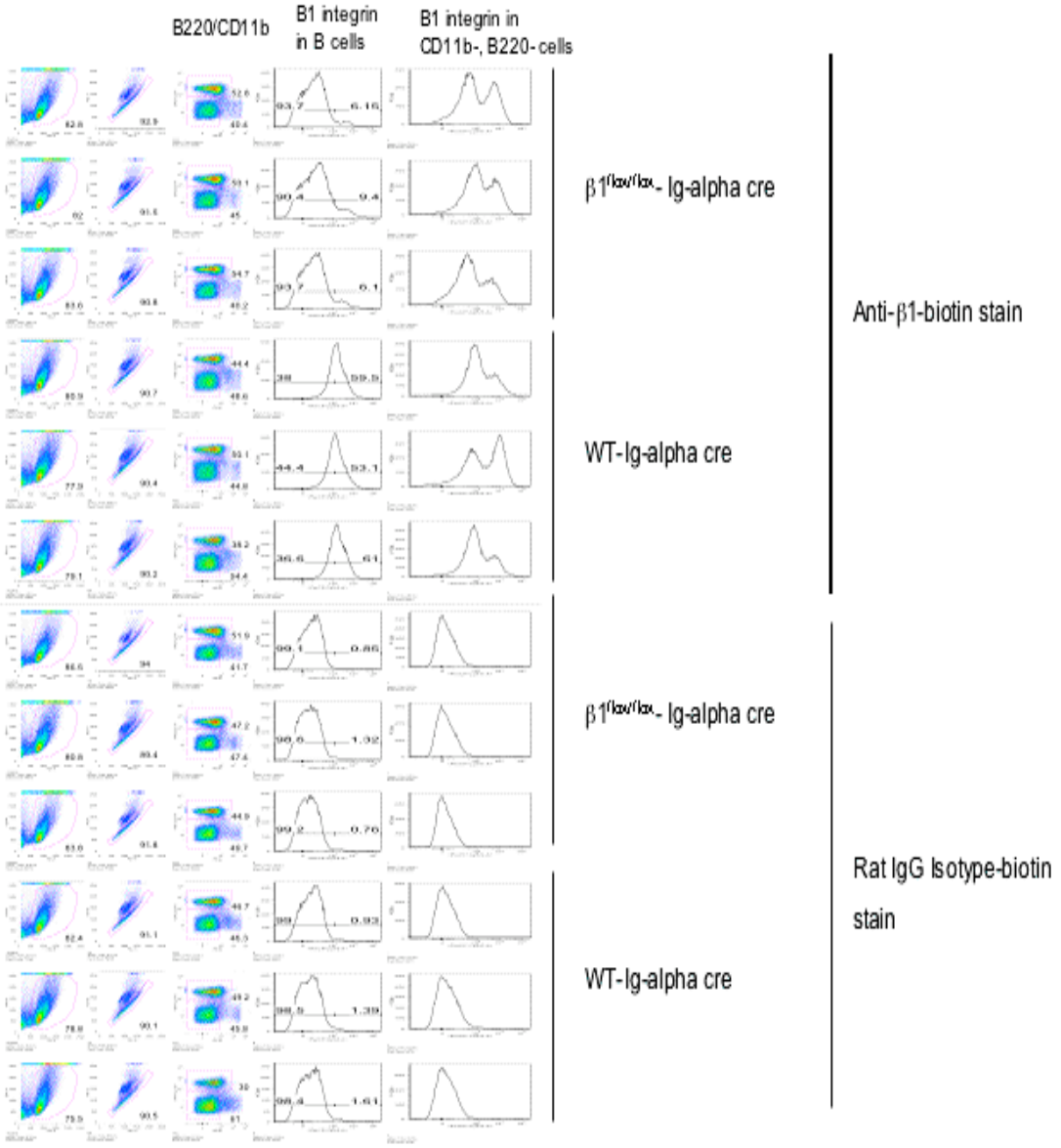


**Figure 4-1**: **B cell-specific loss of $\beta_1$ integrin in $\beta_1^{flox/flox}$ -Ig-$\alpha$ cre mice.**
A) Splenic cells from $\beta_1^{flox/flox}$-Ig-$\alpha$ cre mice were analyzed for the expression of $\beta_1$. Cells were stained with specific $\beta_1$ antibody or isotype control. Column 1 - lymphocyte gate, column 2 - single cells, column 3 - B220 versus CD11b, column 4 - histogram of $\beta_1$ expression in B220+ cells (B cells) and column 5 - $\beta_1$ expression in B220-, CD11b- cells (non B cells).

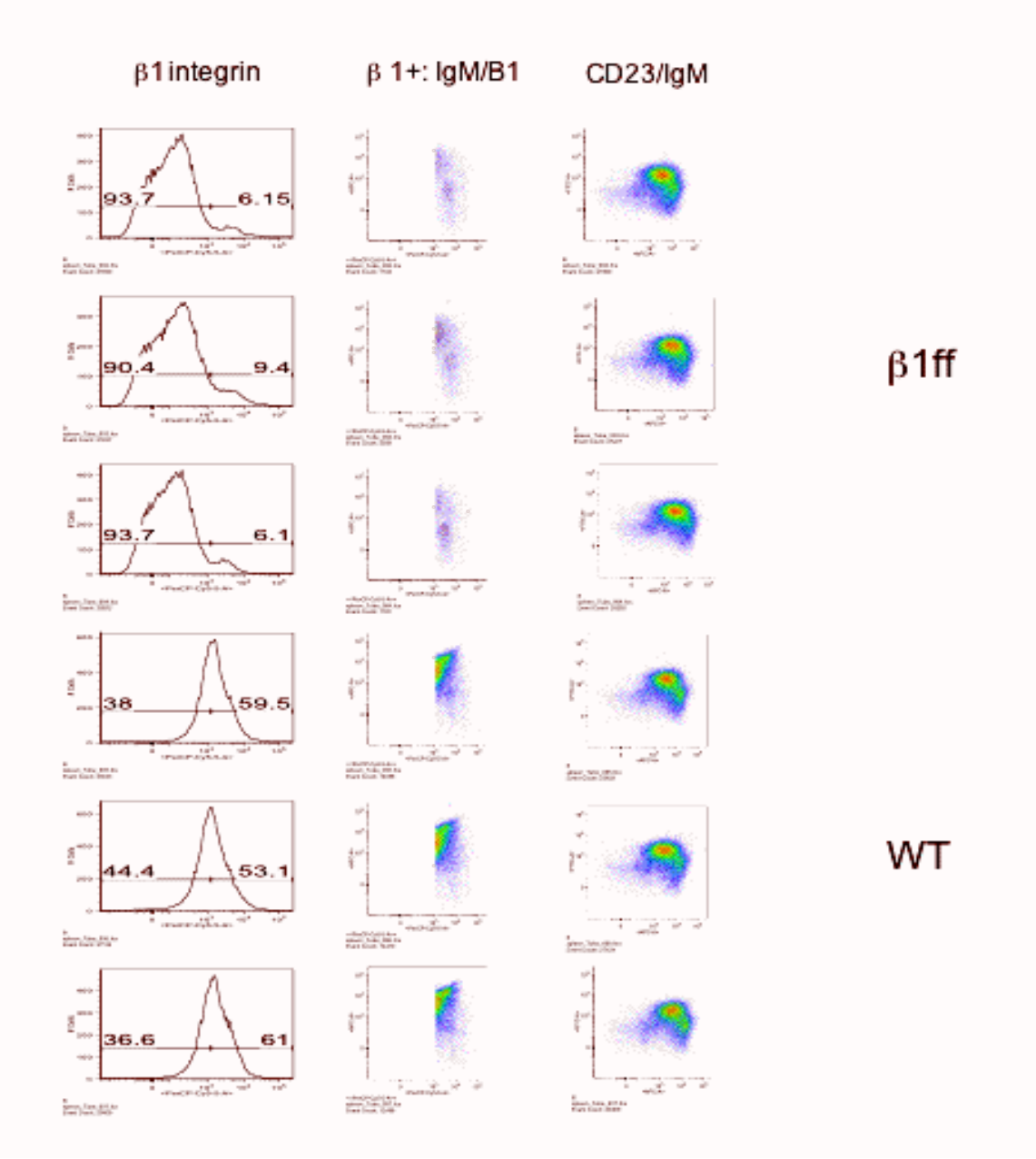


**Figure 4-1 continued**: **B cell-specific loss of $\beta_1$ integrin in $\beta_1^{flox/flox}$ -Ig-$\alpha$ cre mice.** B) $\beta_1$ expressing B cells were analyzed for IgM levels shown in column 2 as IgM (y-axis) vs. $\beta_1$ plot. Column 3 – gated B cells are depicted in a CD23 vs. IgM plot.

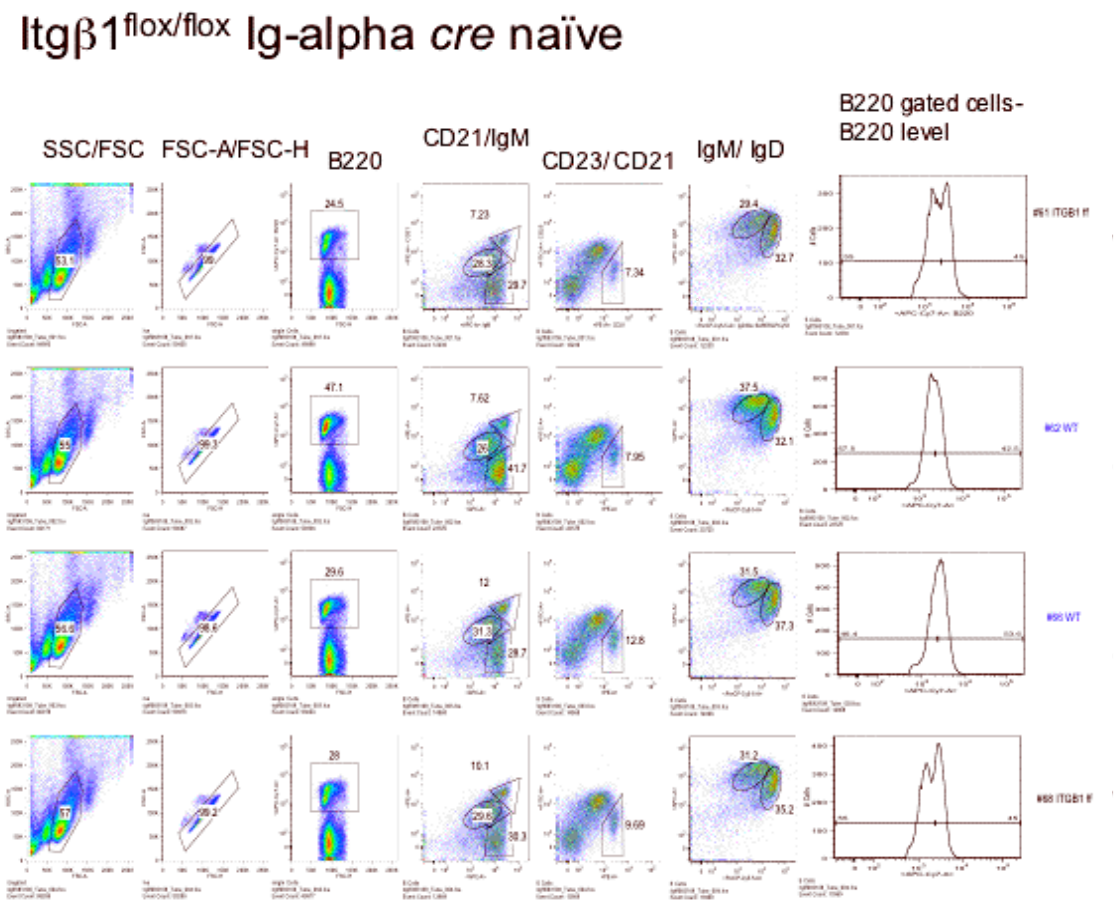


**Figure 4-2**: **B cell subcompartments in $\beta_1^{flox/flox}$-Ig-$\alpha$ cre mice spleens.** Splenic B cells from $\beta_1^{flox/flox}$-Ig-$\alpha$ cre mice were stained with CD23, CD21, IgM and IgD antibodies and analyzed by flow cytometry. CD21hiCD23- populations as well as CD21hi, IgMhi populations represent the marginal zone compartment and the marginal zone plus marginal zone precursors, respectively. Wildtype label in blue; $\beta_1^{flox/flox}$-Ig-$\alpha$ cre label in black.

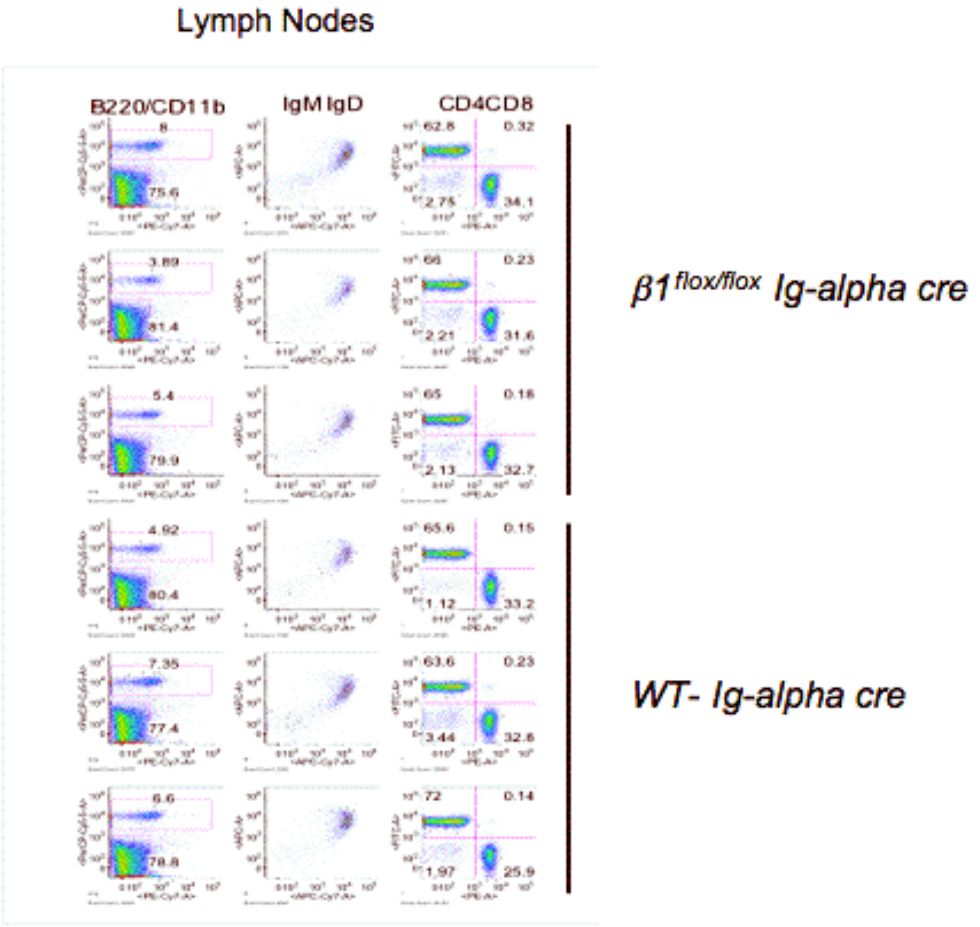


**Figure 4-3: B and T cells in $\beta_1$ integrin in $\beta_1^{flox/flox}$ -Ig-$\alpha$ cre mice lymph nodes.**
Lymph node B and T cells from $\beta_1^{flox/flox}$-Ig-alpha cre mice were stained with IgM IgD, CD4 and CD8 antibodies and analyzed by flow cytometry. The IgM/IgD profiles of B220-gated populations are shown. The CD4/CD8 profiles of B220-, CD11b- populations are shown (T cells).

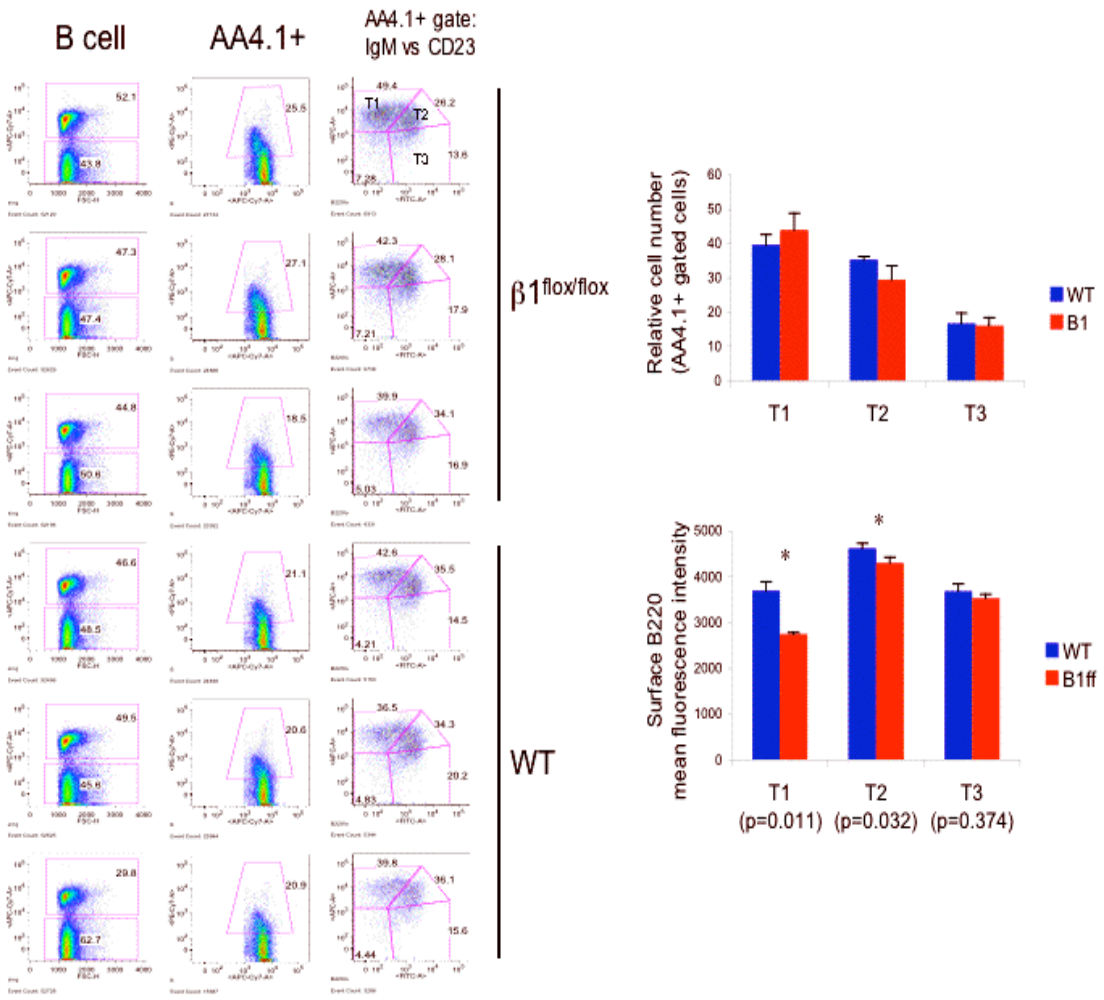


**Figure 4-4: Immature B cells in $\beta_1^{flox/flox}$ -Ig-alpha cre mice spleens.** Splenic B cells from $\beta_1^{flox/flox}$-Ig-alpha cre mice were stained with AA4.1, CD23, B220 and analyzed by flow cytometry (left panels) and the relative cells numbers as well as the mean fluorescence intensities of surface B220 were analyzed in T1, T2 and T3 subcompartments (right panel). Asterisks denote $P < 0.05$ using Student's T test.

A

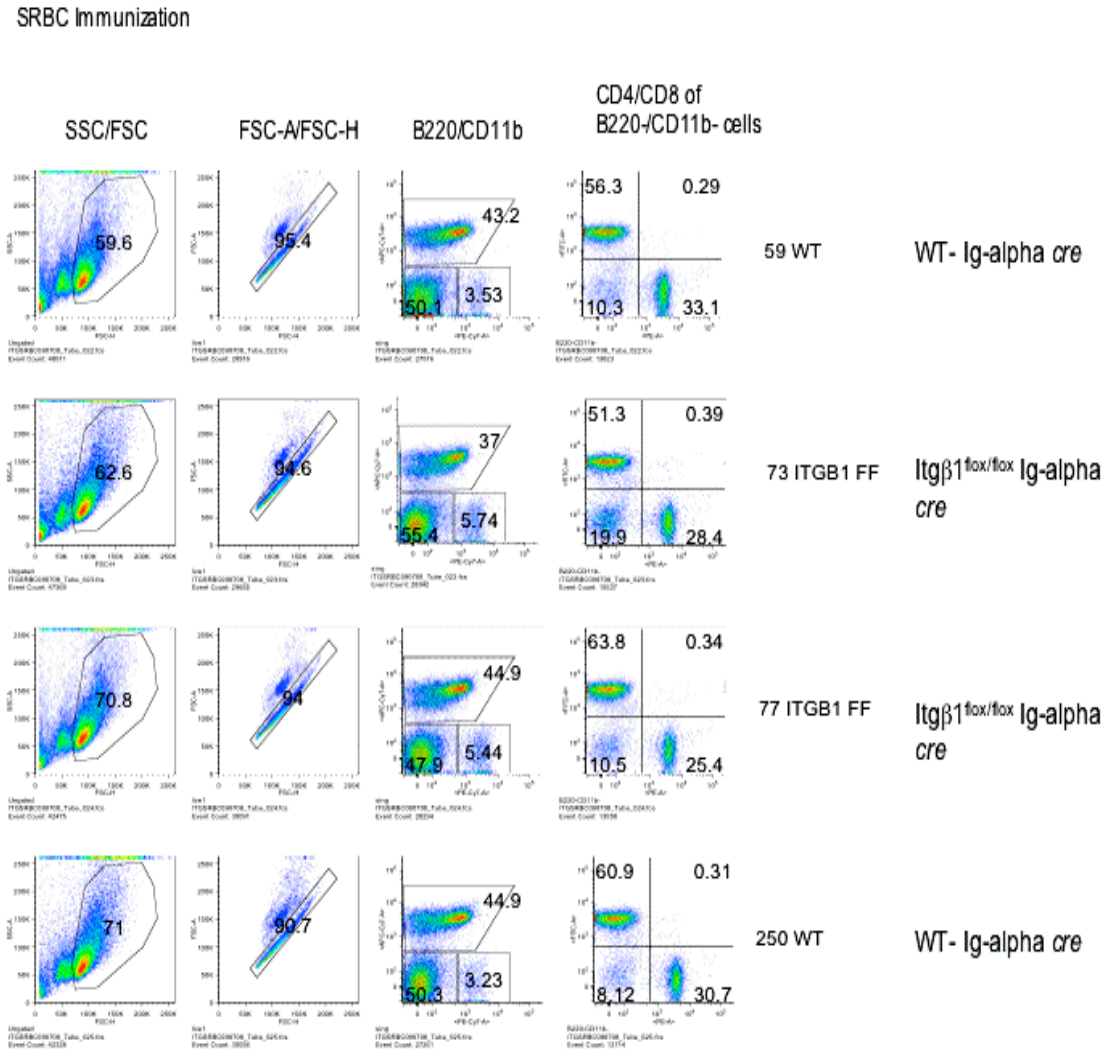


**Figure 4-5: Immune response to SRBC.** A) B, T and myeloid cell subcompartments in SRBC-immunized mice. Splenic cells from immunized mice were harvested 6 days post-immunization and stained with CD11b, CD4, CD8 and B220 antibodies and analyzed by flow cytometry.

B

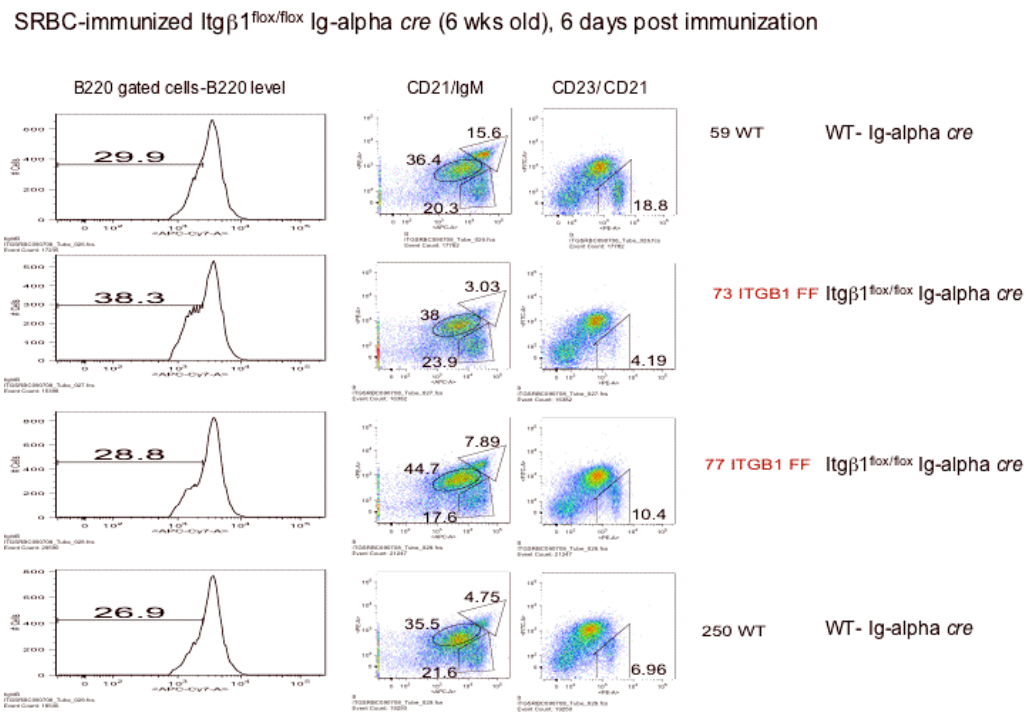


**Figure 4-5 continued: Immune response to SRBC.** B) B cell subcompartments in SRBC-immunized mice. Splenic cells from immunized mice were harvested 6 days post-immunization and stained with CD21, CD23, B220 and IgM antibodies.

C

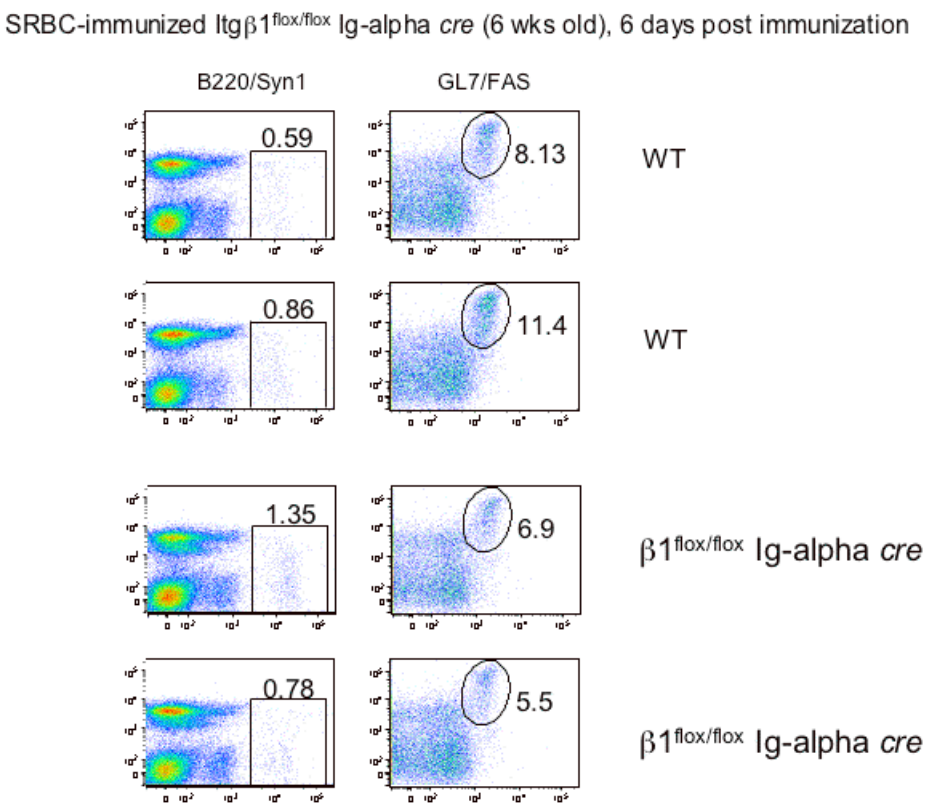


**Figure 4-5 continued: Immune response to SRBC.** C) B cell subcompartments in SRBC-immunized mice. Splenic cells from immunized mice were harvested 6 days post-immunization and stained with Syn1/CD138, FAS, B220 and GL7 antibodies.

D

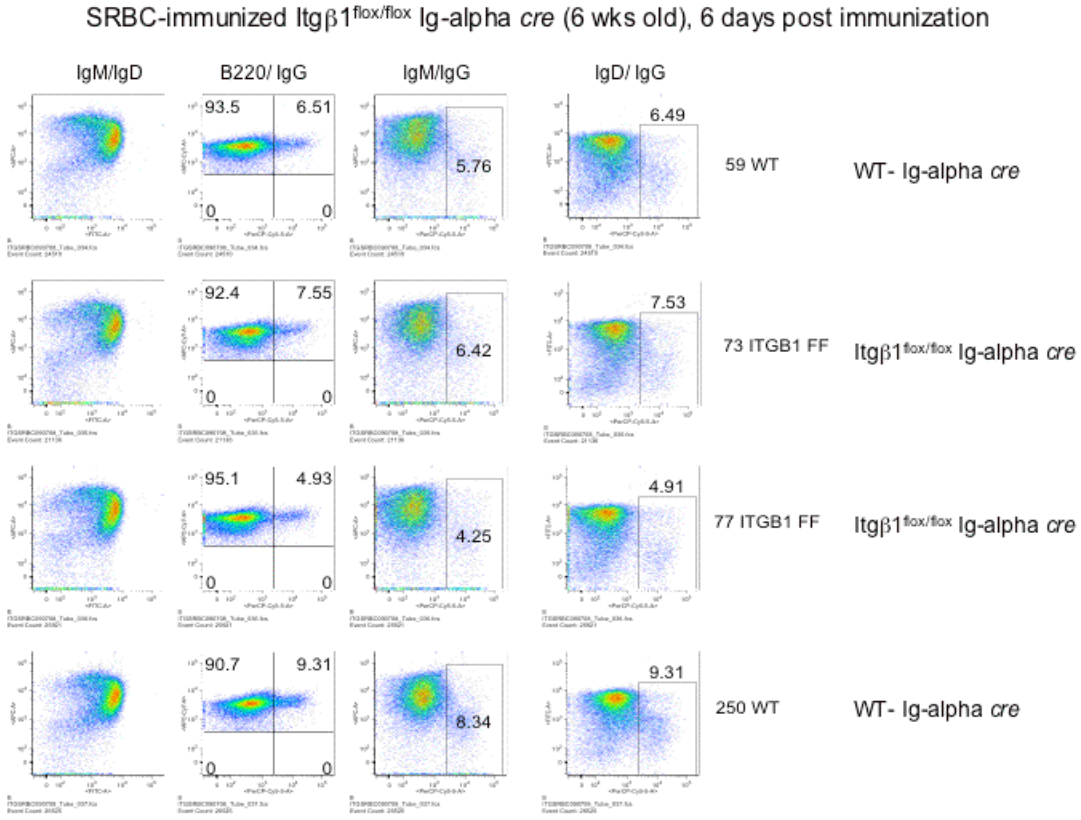


**Figure 4-5 continued: Immune response to SRBC.** D) B cell subcompartments in SRBC-immunized mice. Splenic cells from immunized mice were harvested 6 days post-immunization and stained with IgD, B220 and IgM antibodies and analyzed by flow cytometry.

A

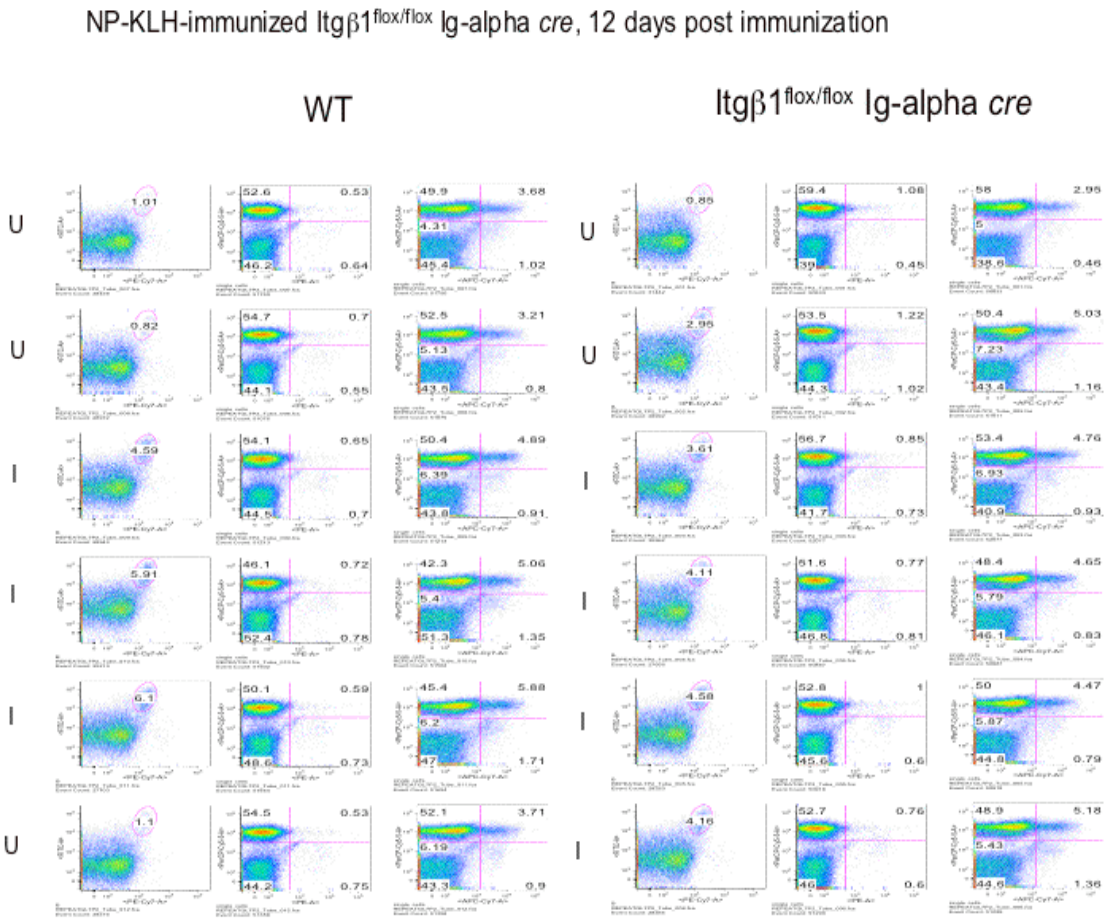


**Figure 4-6: Immune response to NP-KLH.** A) B cell subcompartments in NP-KLH-immunized mice. Splenic cells from immunized mice were harvested 12 days post-immunization and stained with B220, FAS, GL7, IgG, IgD and IgM antibodies and analyzed by flow cytometry. U = unimmunized, I = immunized

B

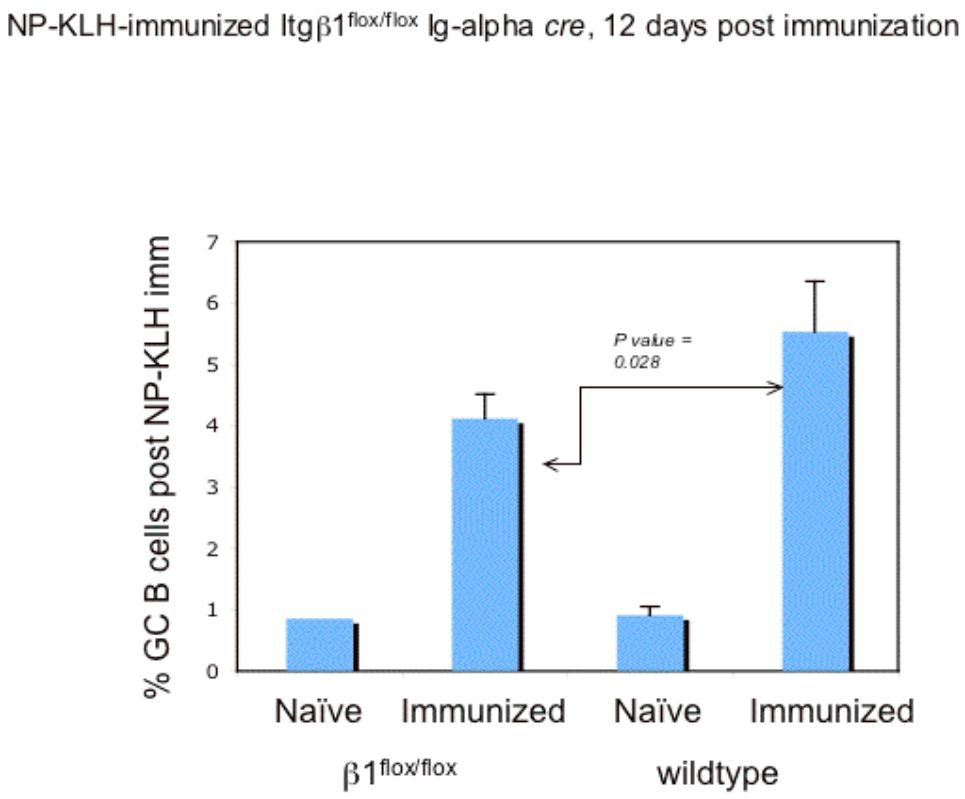


**Figure 4-6 continued: Immune response to NP-KLH.** B) The percentages of germinal center B cells based on GL7+ FAS+ splenic B cells are summarized. 2-4 animals were used in each group.

C

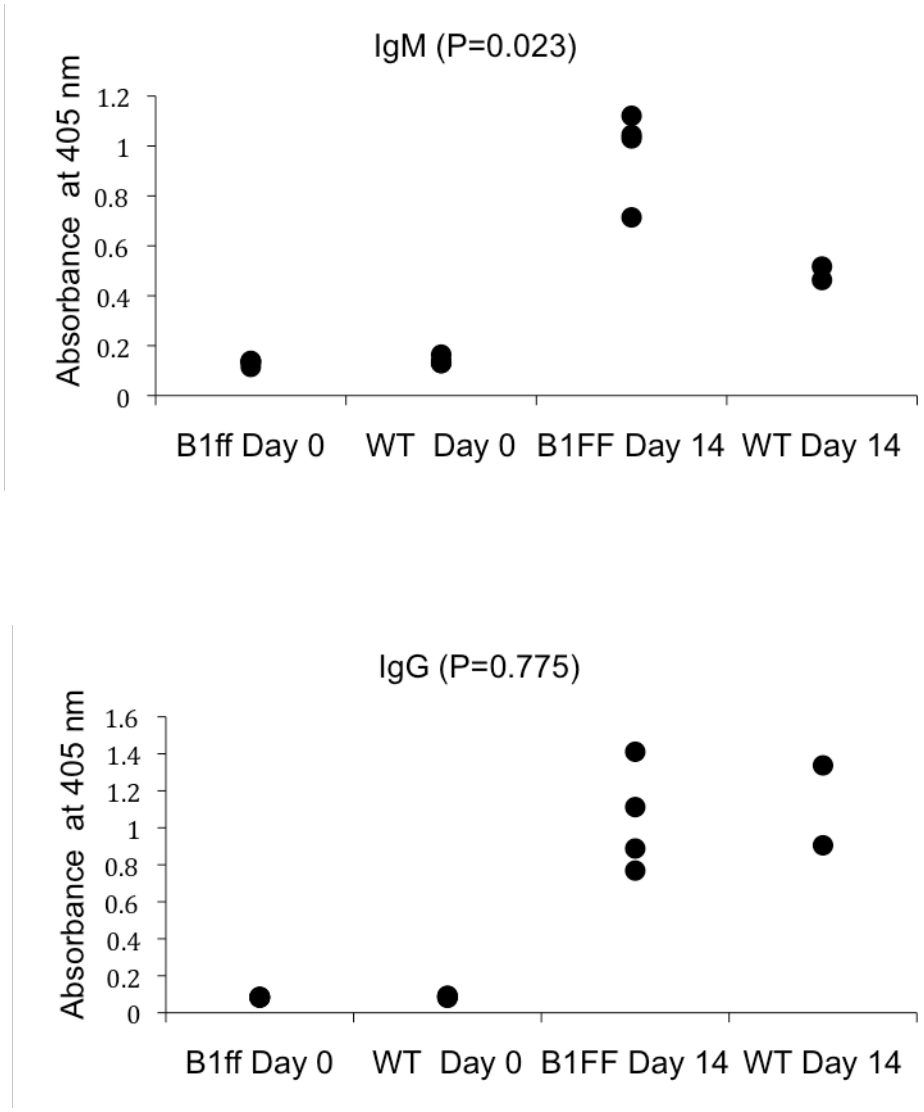


**Figure 4-6 continued: Immune response to NP-KLH.** C) ELISA of serum samples obtained 12 days post immunization. ELISA plates were coated with NP23-BSA, blocked and incubated with serum samples diluted at 1:800. IgM (upper panel) and IgG (lower panel) were detected.

D

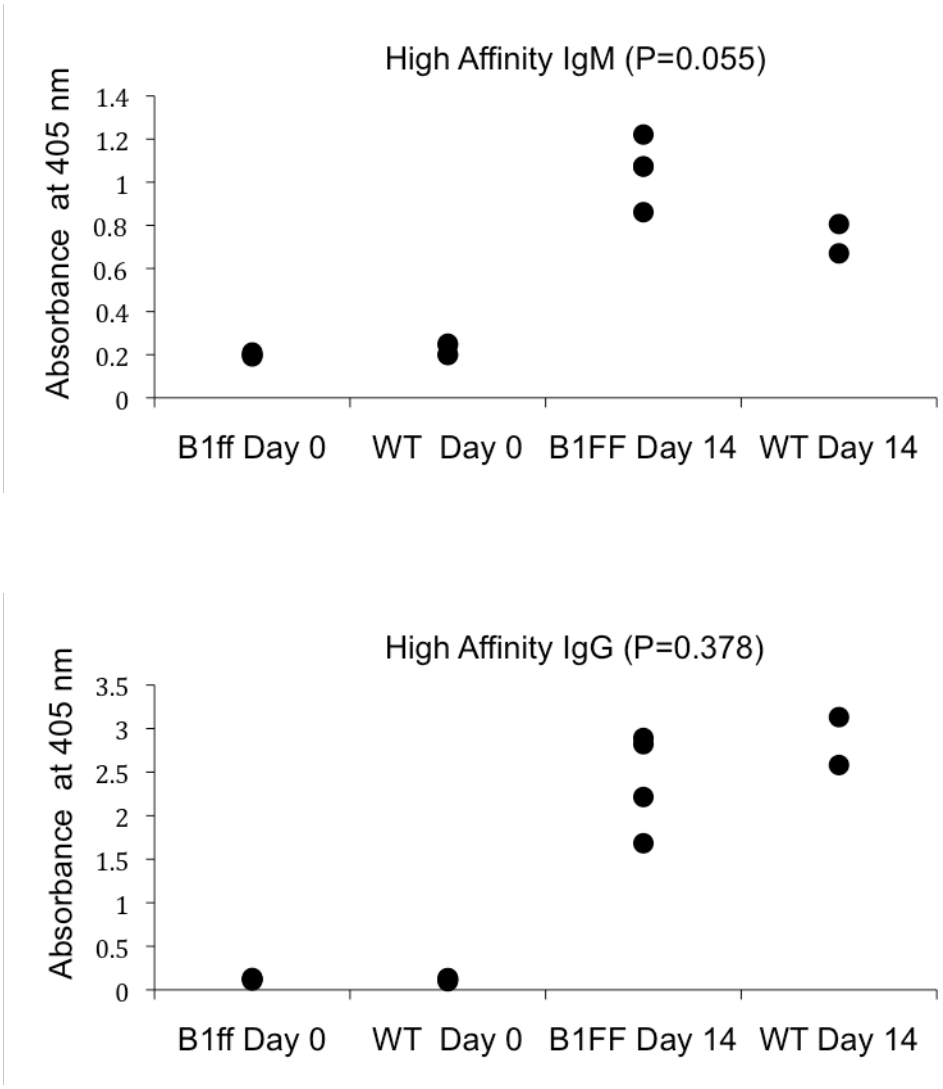


**Figure 4-6 continued: Immune response to NP-KLH.** D) Serum ELISA of serum samples obtained 12 days post immunization. ELISA plates were coated with NP3-BSA (high affinity), blocked and incubated with serum samples diluted at 1:800. IgM (upper panel) and IgG (lower panel) were detected.

A

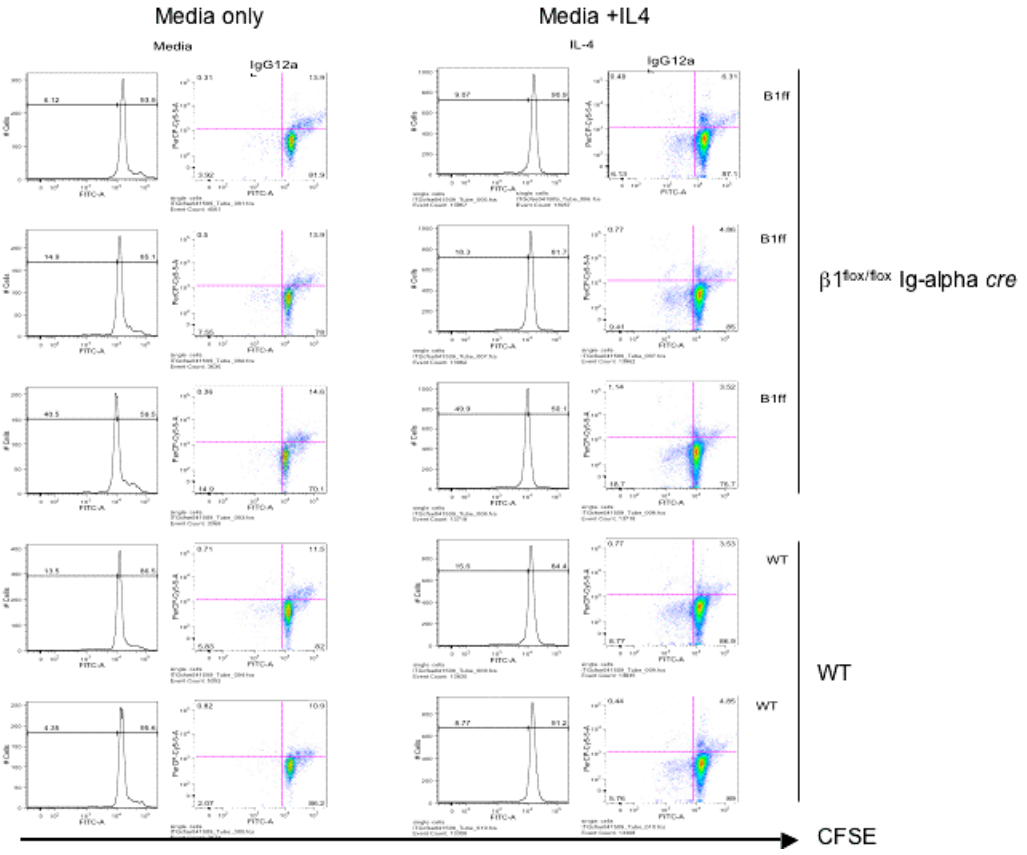


**Figure 4-7. B cell proliferation is intact in $\beta_1$ integrin in $\beta_1^{flox/flox}$ -Ig-$\alpha$ cre mice.**
*CFSE proliferation assay.* Purified splenic B cells were labeled with CFSE and cultured for 72 hr with or without anti-CD40, LPS, anti-IgM F(ab')$_2$ with or without IL-4. A) Media and Media +IL4.

B

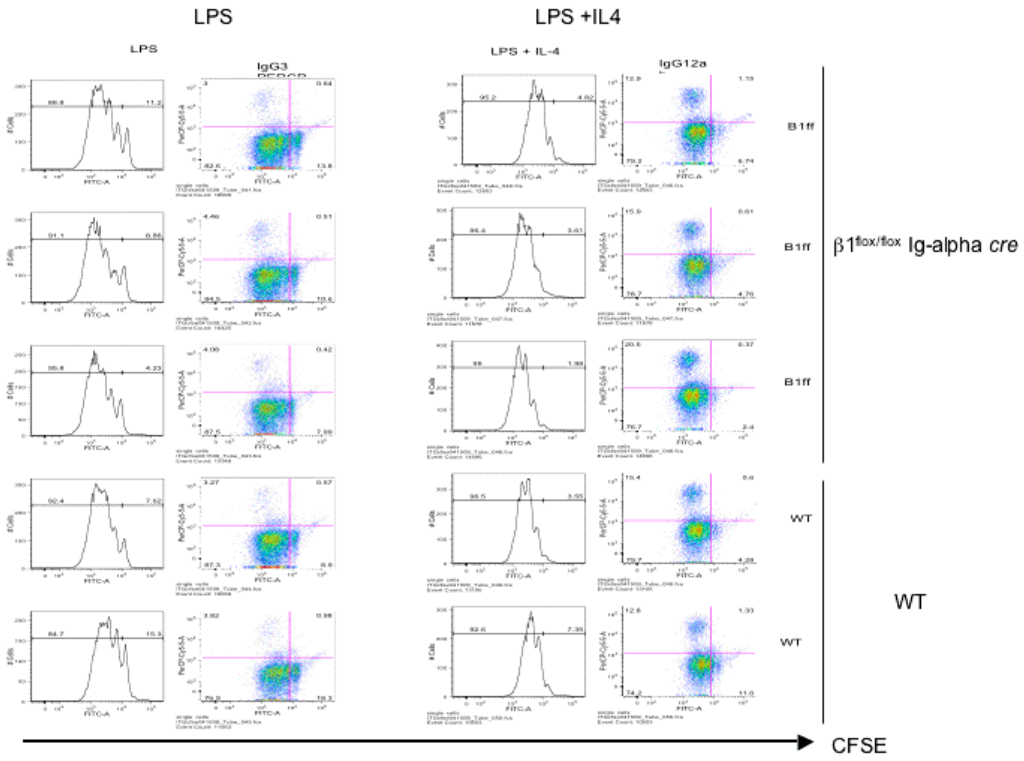


**Figure 4-7 continued: B cell proliferation is intact in $\beta_1$ integrin in $\beta_1^{flox/flox}$ -Ig-alpha cre mice.** *CFSE proliferation assay.* Purified splenic B cells were labeled with CFSE and cultured for 72 hr with or without anti-CD40, LPS, anti-IgM F(ab')$_2$ with or without IL-4. B) LPS and LPS + IL-4.

C

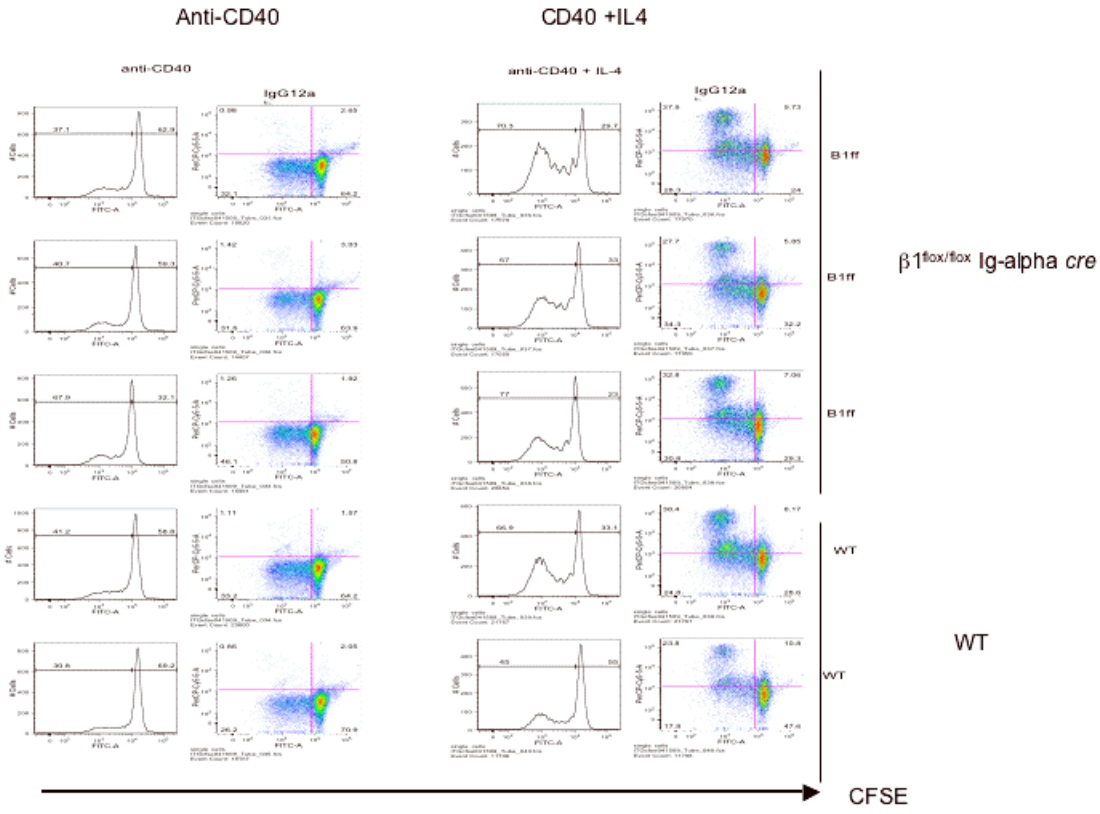


**Figure 4-7 continued: B cell proliferation is intact in $\beta_1$ integrin in $\beta_1^{flox/flox}$ -Ig-alpha cre mice.** *CFSE proliferation assay.* Purified splenic B cells were labeled with CFSE and cultured for 72 hr with or without anti-CD40, LPS, anti-IgM F(ab')$_2$ with or without IL-4. C) anti-CD40 and anti-CD40 + IL4.

D

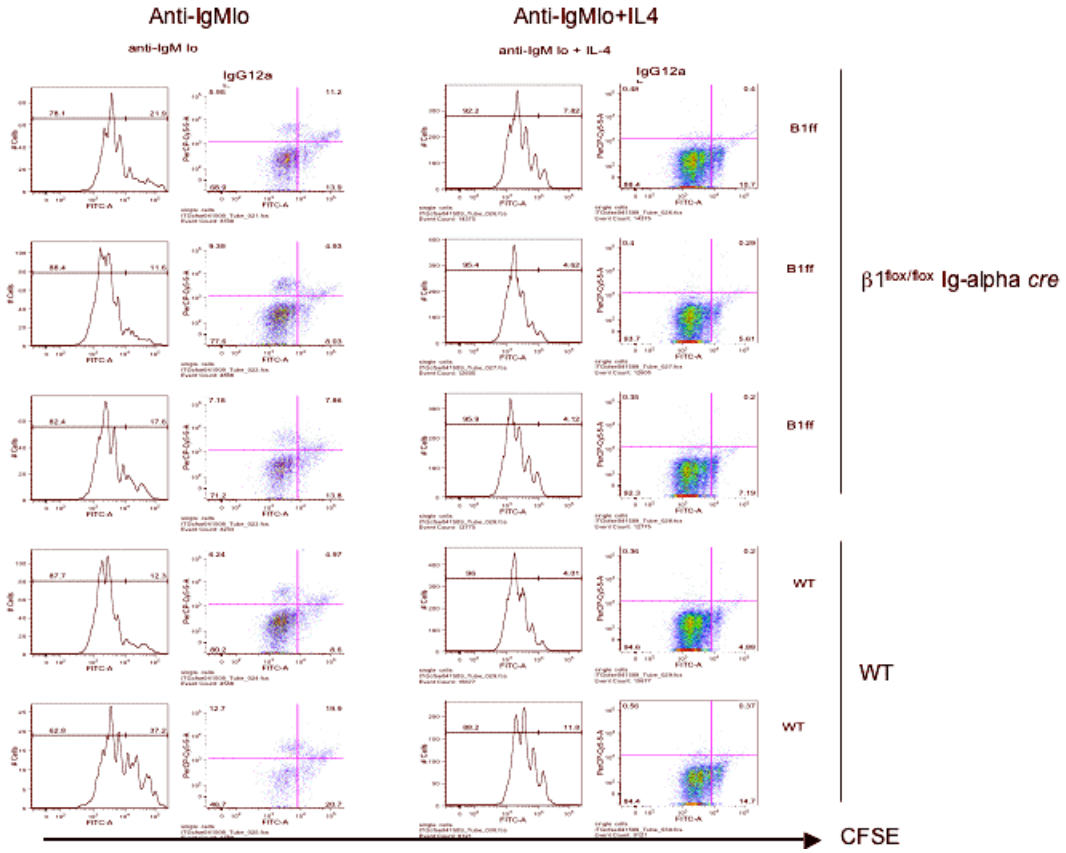


**Figure 4-7 continued: B cell proliferation is intact in $\beta_1$ integrin in $\beta_1^{flox/flox}$ -Ig-alpha cre mice.** *CFSE proliferation assay.* Purified splenic B cells were labeled with CFSE and cultured for 72 hr with or without anti-CD40, LPS, anti-IgM F(ab')$_2$ with or without IL4. D) anti-IgM lo and anti-IgM lo + IL4. Anti-IgMlo means that the concentration of anti-IgM used was 5 μg/ml.

E

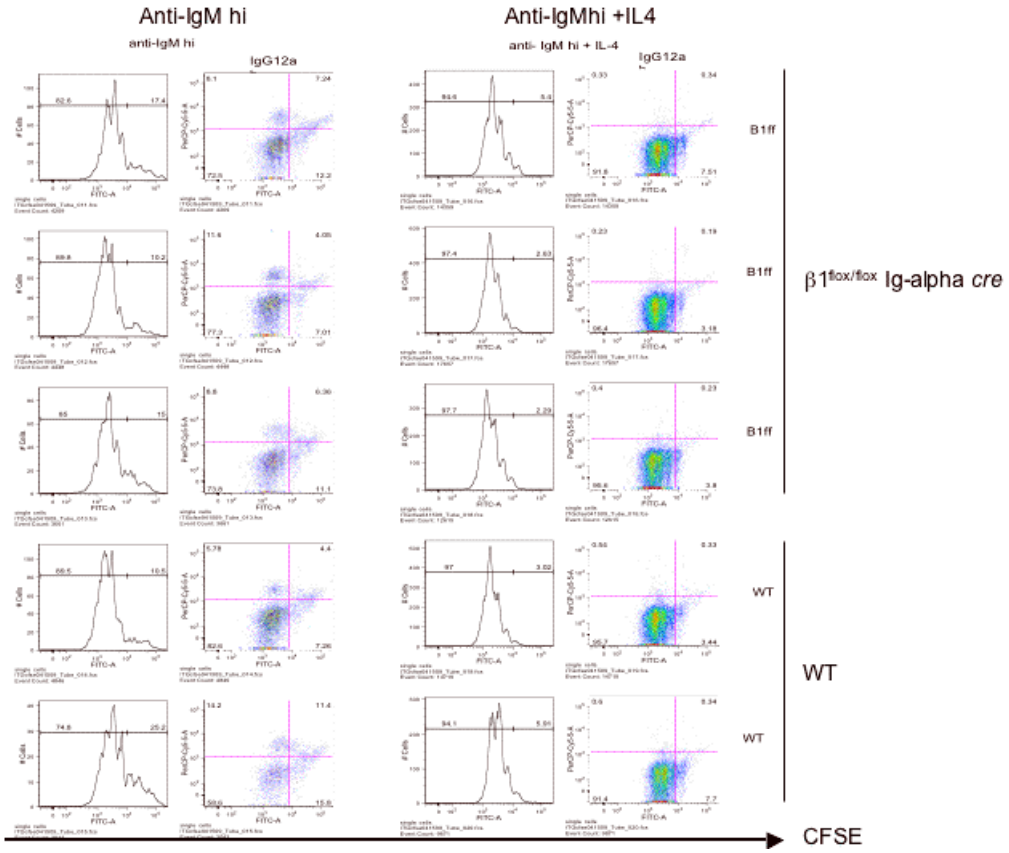


**Figure 4-7 continued: B cell proliferation is intact in $\beta_1$ integrin in $\beta_1^{flox/flox}$ –Ig alpha cre mice.** *CFSE proliferation assay.* Purified splenic B cells were labeled with CFSE and cultured for 72 hr with or without anti-CD40, LPS, anti-IgM F(ab')$_2$ with or without IL4. E) anti-IgM hi and anti-IgM hi + IL4. Anti-IgMhi means that the concentration of anti-IgM used was 20 μg/ml.

F

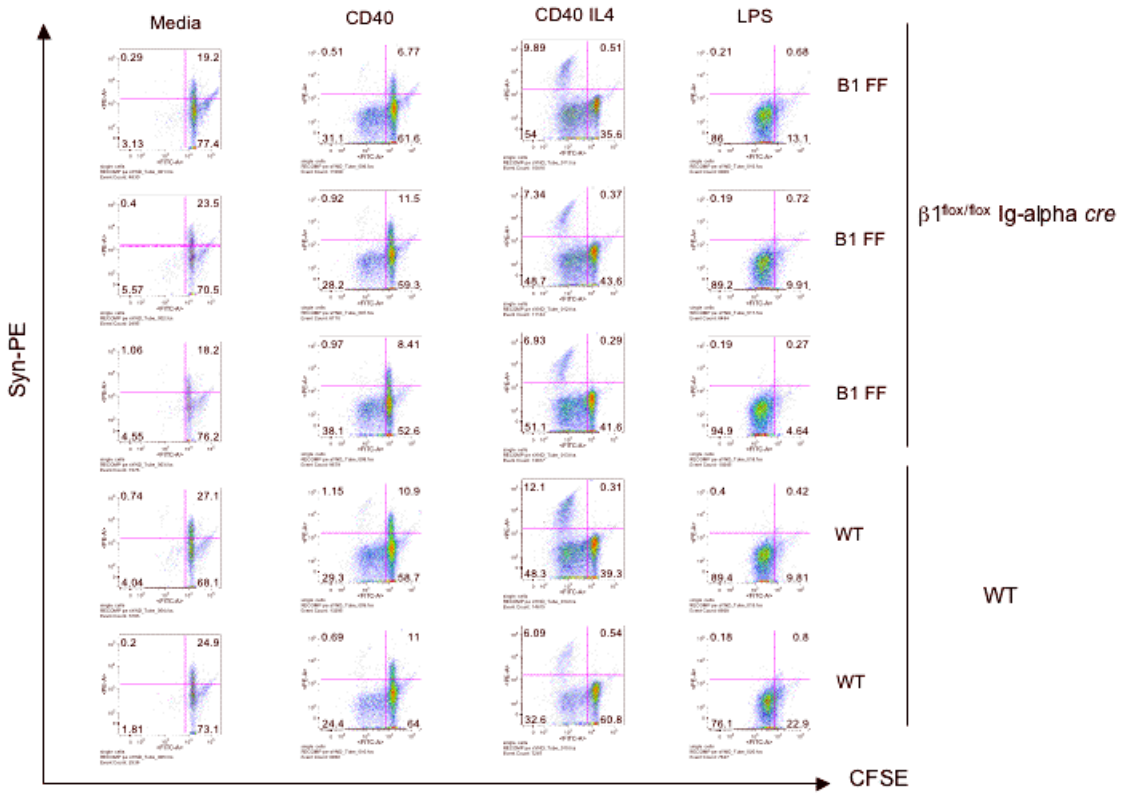


**Figure 4-7 continued: B cell proliferation is intact in $\beta_1$ integrin in $\beta_1^{flox/flox}$ –Ig alpha cre mice.** *CFSE proliferation assay.* Purified splenic B cells were labeled with CFSE and cultured for 72 hr with or without anti-CD40, LPS, anti-IgM F(ab')$_2$ with or without IL4. F) Plasma cell formation was analyzed by syndecan-1 staining.

# CHAPTER 5

## Activation of the inflammasome in gout

### 5.1 – Introduction

Gout is an auto-inflammatory arthritis that can be triggered by the sedimentation of monosodium urate crystals in articular joints and is characterized by severe pain, swelling, redness and stiffness in the affected joints. The overall prevalence of gout in the U.S. was determined to be 41 in 1000 (1). Men are at a higher risk than women for gout, and the risk increases with age for both males and females (1). The initiation and development of gout is not completely understood. Diagnostically, serum uric acid content is measured in symptomatic patients and lowering uric acid levels is one of the therapeutic goals in the management of this disease. Although hyperuricemia can promote the development of gout by increasing the likelihood of urate crystal deposition, hyperuricemia *per se* does not automatically lead to gout. This is highly suggestive of a variable ability among humans to react to crystal load. Resident macrophages are responsible for the production of potent pro-inflammatory cytokines, IL-1β and IL-6, as well as chemokines that promote the infiltration of neutrophils during crystal-induced inflammation (2). The molecular mechanism by which macrophages are induced to produce IL-1β is not completely understood. Recent studies have described the role of inflammasomes in mediating crystal-induced inflammatory responses (3, 7).

The inflammasomes are multimolecular platforms that promote the activation of pro-caspase-1, which in turn proteolytically processes pro-IL-1β into mature IL-1β. Active inflammasomes are assemblies of NLR (nucleotide-binding oligomerization domain-like receptors) family members, adaptor proteins (TUCAN/CARD-8 or ASC)

and pro-caspase-1 (4,5). The NALP3/NLRP3/cryopyrin inflammasome has been reported to be the particular assembly that mediates crystal-induced IL-1β production (3). Activation of the NALP3 inflammasome is depicted in Figure 5-1. The NALP3 inflammasome is comprised of NALP3 and adaptor proteins TUCAN/CARD8 and ASC. When activated, the macromolecular complex recruits and activates pro-caspase-1, which then proteolytically cleaves pro-ILβ thereby promoting the release of mature IL-β (5).

In 2008, Verma et al. found that a patient with familial periodic fever syndrome and with a high level of serum IL-1β carry compound SNPs in the NALP3 (Q750K) and the CARD8 (C10X) genes (6). In their population-based study, the frequencies of these alleles are 6.5% and 34%, respectively, and 4% of the population carried both mutations (6). The NALP3 (Q750K) mutation occurs in the LRR (Leucine-rich repeat) domain, the 'sensing' region of NALP3, while the CARD8 (C10X) mutation results in a premature stop codon. It is unclear how the NALP3 mutation leads to a heightened response. Does this mutation lead to a disengagement of an inhibitory component? Does his mutation lead to increased sensitivity to intracellular danger signals? Investigating this mutation using *in vitro* and *in vivo* model systems would give insight on how the NALP3 component of the NALP3 inflammasome reacts to intracellular danger signals. CARD8 has been shown to inhibit caspase-1 (8). Therefore, the loss of CARD8 as a result of the C10X mutation could lead to a heightened caspase-1 activity. Since crystal-induced IL-1β production utilizes the NALP3 inflammasome, it is possible that these activating mutations also play a role not only in familial periodic fever syndrome but also in the development of gout. The elevated IL-1β associated with these mutations suggest a hyperactive inflammasome state, therefore, understanding these mutations would

eventually provide insight as to how the NALP3 inflammasome is activated by uric acid crystals.

It has been suggested that lysosomal instability leads to the leakage of the lysosomal exopeptidase, cathepsin B, into the cytosol and that cathepsin B is 'sensed' by the components of the inflammasome leading to its immediate assembly (7). The mechanistic role of cathepsin B in the activation of the NALP3 inflammasome is not known. In the NALP3 mutation, does the need for cathepsin B no longer exists? Revealing the direct or indirect action of cathepsin B on the inflammasome assembly or components thereof is important in elucidating how the danger signals of crystals are communicated to the inflammasome and in understanding inflammasomal dysfunction, which could influence the pathogenesis of gout.

## 5.2 – Questions

This proposal centers on the following specific questions: 1) Would the Q750K mutation in NALP3 result in crystal-induced hyper-inflammatory responses *in vitro* and *in vivo*? 2) Would the loss of CARD8 result in elevated IL-1β secretion and 3) Does cathepsin B directly cleave components of the inflammasome leading to inflammasone activation?

## 5.3 – Hypotheses

This proposal presents the following hypotheses: 1) The Q750K mutation in NALP3 would lead to hyper-inflammatory responses, 2) The loss of CARD8 would lead

to hyper-inflammatory responses and 3) Cathepsin B would cleave the inhibitory component of the inflammasome.

## 5.4 - Experimental Approaches and Alternatives

### 5.4.1 - Aim 1: Preparation of mutant constructs and siRNA.

Prepare a NALP3 (Q750K) mutation construct by site directed mutagenesis and introduced mutant DNA or wildtype DNA into a GFP-encoding plasmid. This reagent will be used in Aim 2. Design or commercially obtain siRNA to CARD8. (This will mimic the loss-of-function mutation of CARD8 C10X). This reagent will be used in Aim 3. Prepare the mouse equivalent construct of the NALP3 Q750K mutation and introduce this mutant gene in a retroviral vector encoding a Thy1.1 marker. This reagent will be used in Aim 4.

### 5.4.2 - Aim 2: Determination of the functional consequences of the NALP3 (Q750K) mutation in a monocytic cell line.

Introduce GFP-NALP3 mutant construct, GFP-NALP3 wildtype construct or empty vector into the human monocytic cell line, THP1 by transfection. Sort GFP positive monocytes by flow cytometry, culture and induce differentiation into macrophages. Analyze the THP1 transfectants. Confirm GFP-NALP3 protein expression by Western blot of lysates of THP1 cells transfected with GFP-NALP3 mutant or wildtype GFP-NALP3. Stimulate transfected cells with increasing concentration of monosodium urate (MSU) crystals, similar to what Martinon et al. described (3). Stimulate cells for 6 hours. Analyze supernatants for the presence of mature IL-1β and

IL-18 by ELISA. Analyze cell extracts for the presence of pro-IL-1β and pro-IL-18. Confirm the observed levels of IL-1β by performing a transwell migration assay in which neutrophils are placed in the upper wells and pre-differentiated and MSU pre-treated THP1 cells in the bottom wells. Measure the degree of neutrophil migration towards the bottom wells. Assess cell extracts of transfected and treated cells for pro-caspase 1 and mature caspase 1 levels by Western blot. By immunoprecipitation, assess the ability of each transfectant to assemble the inflammasome upon stimulation. Using anti-GFP antibodies, pull down GFP and blot the immunoprecipitates with anti-NALP3, anti-CARD8, anti-ASC and anti-pro-caspase-1.

*Expectations and Alternatives*

The expectation is that cells transfected with NALP3 mutant will show enhanced inflammatory responses compared to wildtype GFP-NALP3 and empty GFP plasmid due to an alteration in the sensing (LRR) region of the molecule making it more sensitive to cytoplasmic signals. If this is not the case, then perhaps the elevated IL-1β in a patient with NALP3 (Q750K) plus CARD8 (C10X) mutations is largely due to the loss of CARD8.

If THP1 cells prove to be difficult to transfect, the use of HEK cells would be considered for transfections.

### 5.2.3 - Aim 3: Determination of the functional consequences of the loss of CARD8 in a monocytic cell line.

Transfect THP1 cells with siRNA targeting the CARD8 domain or with control siRNA. Confirm the loss of CARD8 expression by Western blot. Stimulate differentiated THP1 cells with increasing concentrations of MSU and assess transfectants as described in AIM 2, except for the immunoprecipitation assay to assess assembly of the inflammasome. For Aim 3, anti-NALP3 antibodies will be used to pull down NALP3 and immunoprecipitates will be blotted with anti-ASC and anti-pro-caspase 1.

*Expectations and Alternatives*

The expectation is that cells transfected with CARD8 siRNA will show enhanced inflammatory responses compared to cells transfected with control siRNA because CARD8 regulates the self-activation of pro-caspase-1 and without this regulator in the macromolecular complex, pro-caspase-1 autoactivation is uninhibited leading to an elevated pro-IL-1β processing. If this is not the case, then perhaps another adaptor molecule keeps pro-caspase-1 in check.

If THP1 cells prove to be difficult to transfect, the use of HEK cells would be considered for transfections.

### 5.2.4 - Aim 4: Determination of the functional consequences the NALP3 mutation *in vivo*.

Obtain donor NALP3 knockout mice (9) and treat these animals with 5-fluorouracil. Isolate bone marrow (enriched with HSCs) and culture. Transduce stem

cells with a NALP3 mutant-encoding retroviral vector or control retroviral vector with a Thy1.1 marker prepared in Aim 1. After 2-3 days in culture, purify Thy1.1 expressing HSCs and propagate for 2-3 days. Intravenously transfer HSCs to lethally irradiated mice. After 6-8 weeks, induce peritonitis by injecting animals with crystals as described by Martinon et al. (3). Measure serum IL-1β and IL-18 by ELISA. Perform a peritoneal lavage and analyze fluids for PMN recruitment using a neutrophil marker. Derive macrophages from these animals and analyze macrophages for pro-caspase-1 activation by Western blot.

*Expectations and Alternatives*

Reconstitution of lethally irradiated mice with bone marrow from NALP3 null mice transduced with mutant NALP3 retrovirus will reconstitute the monocytic lineage bearing the mutation in the LRR domain. The expectation is that cells transfected with NALP3 mutant will show enhanced inflammatory responses. It is possible that reconstituted animals will appear sick.

### 5.2.5 - Aim 5: Determination of potential inflammasomal targets of cathepsin B in a monocytic cell line treated with MSU.

Incubate THP1 cell cultures (differentiated cells) in media containing MSU plus the cathepsin B inhibitor, CA074, or control vehicle. Lyse the treated cells and subject cell lysates to 2D gel electrophoresis. Perform spot analysis and compare spots between inhibitor treated and untreated samples. Purify differentially displayed spots and analyze

by mass spectrometry. Determine which of these protein or protein fragments are derived from components of the NALP3 inflammasome.

*Expectations and Alternatives*

Alternatively, if a large number of spots is obtained and proves to be difficult to analyze, an isolated system can be designed. Purified NALP3, ASC and CARD8 can de directly subjected to cathepsin B activity in the presence or absence of cathepsin B inhibitor and the resulting protein fragments can be analyzed by mass spectrometry.

## 5.3 – Collaboration

The HHMI-sponsored Med-Into-Grad program is a unique and excellent program that aims to narrow the gap between basic science research and medicine. This program opened the doors for me to an arena of rheumatologic diseases and their clinical management. This program also introduced me to faculty members who may be interested in the outcome of this proposal. My graduate research experience thus far has allowed me to learn and master some of the laboratory techniques that this proposal calls for.

**Acknowledgement**

Chapter 5 of this dissertation presents a proposal written during my Howard Hughes Med-into-Grad Clinical Training in the area of Rheumatology, Allergy and Immunology under the guidance of my clinical mentors Gary S. Firestein, M.D. and Susan E. Sweeney, M.D.

## 5.4 - References


1. Wallace KL, Riedel AA, Joseph-Ridge N, Wortmann R.J. Increasing prevalence of gout and hyperuricemia over 10 years among older adults in a managed care population. J Rheumatol 2004 Aug; 31(8):1582-7.

2. Martin WJ, Walton M, Harper J. Resident macrophages initiating and driving inflammation in a monosodium urate monohydrate crystal-induced murine peritoneal model of acute gout. Arthritis Rheum. 2009 Jan; 60(1):281-9.

3. Martinon F, Pétrilli V, Mayor A, Tardivel A, Tschopp J. Gout-associated uric acid crystals activate the NALP3 inflammasome. Nature 2006 Mar; 440: 237-241.

4. Franchi L, Eigenbrod T, Muñoz-Planillo R, Nuñez G. The inflammasome: a caspase-1-activation platform that regulates immune responses and disease pathogenesis. Nature Immunol 2009 Feb; (10) 241-247.

5. Fritz JH, Ferrero RL, Philpott DJ, Girardin SE. Nod-like proteins in immunity, inflammation and disease. Nature Immunol 2006 Dec; 7: 1250 – 1257.

6. Verma D, Lerm M, Lujinder RB, Eriksson P, Soderkvist P, Sarndahl E. Gene Polymorphisms in the NALP3 inflammasomes are associated with interleukin-1 production and severe inflammasomes. Arthritis and Rheumatism 2008 Mar; (58)3: 888-894.

7. Hornung V, Bauernfeind F, Halle A, Samstad EO, Kono H, Rock KL, Fitzgerald KA, Latz E. Silica crystals and aluminum salts activate the NALP3 inflammasome through phagosomal destabilization. Nature Immunol 2008 July; (9) 8: 847 – 856.

8. Razmara M, Srinivasula SM, Wang L, Poyet JL, Geddes BJ, DiStefano PS, Bertin J, Alnemri ES. CARD-8 protein, a new CARD family member that regulates caspase-1 activation and apoptosis. J Biol Chem 2002 Apr; 277(16): 13952-8.

9. Eisenbarth SC, Colegio OR, O'Connor W, Sutterwala FS, Flavell RA. Crucial role for the Nalp3 inflammasome in the immunostimulatory properties of aluminium adjuvants. Nature 2008 June; 453, 1122-1126.

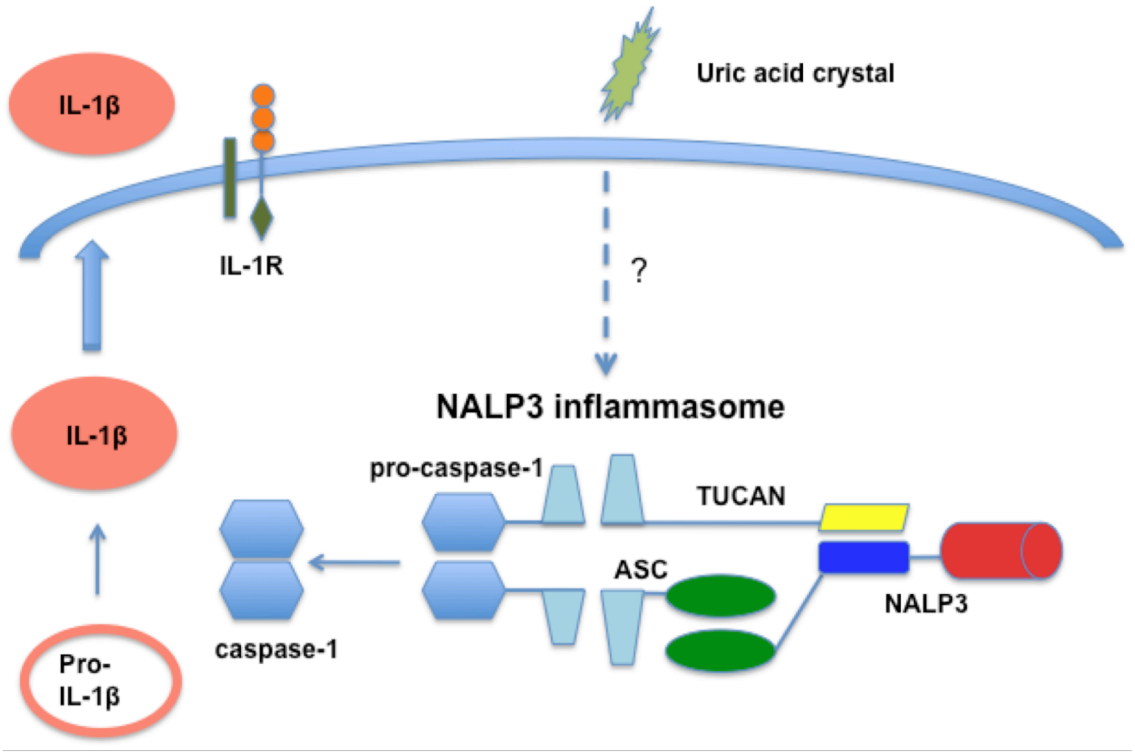


**Figure 5-1: Schematic representation of the assembly of the NALP3 inflammasome.** The NALP3 inflammasome is comprised of NALP3, a nucleotide-binding oligomerization domain-like receptor and adaptor proteins TUCAN/CARD-8 and ASC. Upon activationi, the macromolecular complex recruits and activates pro-caspase-1, which then proteolytically cleaves pro-IL-1β thereby promoting the release of mature IL-1β.

## Appendices

### I. CB Calcium Flux Protocol for B cells

1. Resuspend approximately 5 million splenic cells or purified B cells in 250 μl media (DMEM + 10 mM HEPES and 2.5% FBS). This amount of cells may be sufficient for multiple conditions/stimulations. You may need to adjust this number depending on your experiment.

2. Thaw Fura Red and Fluo-4. Thaw Pluronic acid F-127 (optional).

   Note: The two dyes above are labeled as cell permeant and therefore do not really need Pluronic acid. However, the use of pluronic acid has been reported to facilitate dye entry, eliminating any possible hydrolysis of the dyes by external esterases, and more efficient loading while maintaining cell integrity. I've used this protocol successfully with and without pluronic acid.

   Note: The Fura Red (Invitrogen/Molecular Probes # F-3020 MW = 1089.00) emits at 685 nm (PerCPCy5.5 channel). Its signal will go down when it binds calcium. The Fluo-4 (Invitrogen/Molecular Probes #F14217 MW = 1096.95) emits at 525 nm (FITC channel). Its signal will go up when it binds calcium. Adjust the intensity for each channel so that there will be room in the axes to see these shifts. The starting intensities of the two channels should be close to each other so that baseline ratio will approximate 1.

3. Prepare a 2x strength mixture of these dyes in media. Make enough volume for the number of cell samples you want to stimulate.

   Fura Red final concentration (final concentrations I've used: 5 – 20 uM; 6 μM final concentration is good.)
   Fluo-4 (final concentrations I've used: 2.4 to 5.0 μM; 3 μM final concentration is good.)
   Pluronic acid (final of 0.01 to 0.02% recommended)

   Note: The fluorescence of Fura Red tends to be weaker than Fluo 4, so it is recommended to use a higher concentration of Fura Red compared to Fluo 4 (e.g. 2:1).

   Optional: You can also prepare samples with single dyes for compensation.

4. Add 250 μl of 2x dye mix to 250 μl cell suspension. Mix.
5. Incubate cells at 37°C, 45 min in the dark (loading). (You can place tubes in a heat block set at 37°C. Cover the tubes with foil.)

6. Wash once with media, spin and resuspend in 500 μl media.
7. Let the loaded cells rest for 20 min at RT in the dark.
8. If needed (for example, if your starting material is mixed splenic cells), stain with B220 APC (or other conjugates with fluorochromes other than FITC and PerCP Cy5.5). Resuspend cells in media plus B220 APC and incubate at RT for 15 min. Wash with media. Resuspend in 500 μl media.
9. Take an aliquot of loaded cells into a tube and dilute with RT media (0.5 to 1ml) so that the suspension is about 1- 4 million cells/ml. Place the cell suspension on the cytometer and acquire. Adjust flow speed (slow or medium speed, about 400 to 2000 cells/second). Set the number of events to collect at a high number such as 1 million so that the machine does not stop collection too early. Adjust the baseline intensities for FITC and PerCPCy5.5 as described in #2.

   Keep extra loaded cells in the dark at RT, or if kept on ice, you will need to warm them up to RT before stimulation.

   Just before fluxing, make sure that stimulating reagents are ready.

   Optional: Compensate using single stains.

10. To flux, acquire and record for 30 seconds. Remove the tube from the cytometer (without stopping the acquisition/recording), quickly add stimulus to cell suspension and quickly mix. Return the tube to the cytometer and continue reading for at least 5 min. You should see a right shoulder forming when viewing the FITC channel.

    Note: For BCR stimulations, I use a final of 10 μg/ml of anti-IgM $F(ab')_2$.

    Optional: Stimulate one sample with 1 ug/ml ionomycin to establish maximum flux. Or, stimulate in the presence of a final concentration of 6-8 mM EGTA added in the media just before reading the sample to chelate extracellular calcium.

    To analyze in FlowJo (v 8.1.0), go to Platform/Derive Parameters/Define new/change. Choose parameter and function to create a new parameter for the ratio of Fluo 4/Fura Red. For example, choose 'FITC', choose 'division' then choose 'PerCPCy5.5'. Click 'Add Parameter' and then 'Done'. In the Workspace, select sample, then Click 'Kinetics'. In the kinetics window, change the y axis.

**II. VCAM-Fc/ICAM-Fc Binding Protocol for B cells**

1. Aliquot 5 million of purified B cells into tubes.
2. Resuspend in 200 ul PBS. Make 20 μg/ml anti-IgM Fab'2 (2x strength).
3. Add 200 ul of 20ug/ml anti-IgM Fab'2 starting with 60 min.
4. Wash with cold 1ml PBS. Spin.
5. Resuspend in 1:400 Fc block + the appropriate stain. For example, if the marginal zone or follicular B cells need to be compartmentalized then stain with CD21-bio first (1:100; 1800 μl) in binding buffer 30 min on ice.
6. Spin. Resuspend in 100 μl of VCAM-Fc/ICAM-Fc mix in binding buffer. Make 1800 μl of 10 μg/ml ICAM Fc and 10 μg/ml VCAM Fc mix. Save one of the 60 min tubes for PBS only control. Incubate at RT 1 hr.
7. Wash with 1 ml binding buffer.
8. Resuspend in fluorescent stains made up in binding buffer and incubate for 30 min on ice. For example, if the marginal zone or follicular B cells need to be compartmentalized, use the following stains:

    Goat anti-human Fc – PE 1:100 (1400 μl) or Isotype PE (200 μl) 1:50
    IgM – APC
    B220 – APC Cy7
    CD23 – FITC
    SA- PerCPCy5.5

Binding Buffer:
10 mM HEPES/NaOH (pH 7.4), 140 mM NaCl, 2.5 mM $CaCl_2$, 2 mM $MgCl_2$, plus 2 mM $MnCl_2$. If there is high background, reduce $MnCl_2$ concentration (to perhaps, 0.5 mM)

**III. PIP3 Staining Protocol for B cells**

1. Resuspend 5-10 million splenic cells in 100-200 µl PBS. Place cells at 37°C to equilibrate for 5 minutes. Prepare 2x concentration of stimulatory antibody or antigen (e.g. 20 µg/ml of anti-IgM antibody for a final concentration of 10 µg/ml). Place stimulant at 37°C to equilibrate for 5 minutes.
2. Place an equal volume of stimulant to cells and mix. Stimulate at 37°C for 5 minutes.
3. Add 16% paraformaldehyde to cells to a final concentration of 1.5% to stop stimulation and fix cells. Mix and fix cells at RT for 10 minutes.
4. Spin cells in a tabletop microcentrifuge at 3000 rpm for 3 min.
5. Wash with cold PBS. Spin.
6. Resuspend cells in 500 µl PBS/1% BSA/0.2% saponin to permeabilize. Incubate on ice for 10 minutes.
7. Prepare 1:100 or 1:200 dilution of biotinylated anti-PIP3 IgM antibody (Echelon Biosciences Catalog #Z-B345) or biotinylated IgM isotype in PBS/BSA/saponin. Stain cells on ice for 30 minutes.
8. Wash cells 2x with PBS/BSA/saponin.
9. Resuspend cells in PBS/BSA/saponin containing 1:100 Strepavidin-FITC + 1:100 B220-APC Cy7. Incubate in the dark on ice for 20-30 minutes.
10. Wash cells 2x with FACS buffer (PBS/1%FBS/0.01% Azide). Resuspend cells in FACS buffer.
11. Analyze cells by flow cytometry